

Optimisation of T cell receptors using *in vivo* recombination and selection

Hazim Ghani

Imperial College London

Department of Medicine

Thesis submitted for the degree of
Doctor of Philosophy

Copyright declaration:

'The copyright of this thesis rests with the author and is made available under a Creative Commons Attribution Non-Commercial No Derivatives licence. Researchers are free to copy, distribute or transmit the thesis on the condition that they attribute it, that they do not use it for commercial purposes and that they do not alter, transform or build upon it. For any reuse or redistribution, researchers must make clear to others the licence terms of this work'

Declaration of originality:

I hereby certify that this Thesis is an accurate account of my own research.

All else is duly acknowledged and appropriately referenced.

The work described here was carried out under the supervision of Professor Julian Dyson and Dr. Keith Gould and was funded by the Ministry of Education, Brunei Darussalam.

The total word count of this Thesis including references is: 61,079.

Hazim Ghani

I dedicate this Thesis to my loving family:

Haji Abdul Ghani, Noratirah, Muiz and Miza.

Your endless support and sacrifice made this all possible.

This is for you.

Abstract

The $\alpha\beta$ T cell receptor (TCR) orchestrates immunity through the recognition of peptides, derived from degraded proteins, presented on major histocompatibility complex (MHC) molecules. The remarkable ability of the receptor to respond to a vast plethora of antigens is driven by V(D)J recombination, a process which generates a highly diverse TCR repertoire by somatic gene rearrangement of coding DNA. TCR diversity is confined to three short hairpin loops on each TCR chain, called the complementarity determining region (CDR), which form the antigen-binding site. The germline-encoded CDR1 and CDR2 loops predominantly contact MHC, whereas the hypervariable CDR3 are non-germline and primarily bind to the MHC-bound peptide.

In this study, we developed a novel *in vivo* mutagenesis approach which redirects somatic gene rearrangement using V(D)J recombination machinery to diversify and optimise TCR binding. This approach involves embedding a gene recombination cassette into the peptide-binding CDR3 β region of established TCRs. A retrogenic system was employed to facilitate the *in vivo* processes necessary for gene rearrangement and thymic selection. We demonstrate that the recombination cassette can successfully induce gene rearrangement and introduce variation to the targeted CDR3 β site. Thymocytes expressing the diversified TCRs can be selected on MHC and develop into functional peripheral T cells. Subsequent exposure to cognate ligands also allowed us to identify optimised and 'immunodominant' TCRs.

In addition, we produced a novel chimeric TCR chain which comprises V α and C β domains. This TCR chain forms a heterodimer with endogenous TCR α chains to form a unique V α -V α antigen-binding surface. Thymocytes expressing this novel form of $\alpha\beta$ TCR were able to engage efficiently with both MHC classes and develop normally into functional T cells typical of a conventional repertoire. Collectively, these findings suggest that the germline CDR loops are not essential for mediating MHC recognition during MHC-restricted T cell development and function.

Acknowledgements

First and foremost, I would like to thank my supervisor Julian Dyson for his help, support and encouragement during the past four years. I greatly appreciate all that you have taught and done for me: advice, patience and perseverance through the toughest of times. I have learnt many lessons from you, not only as a scientist, but as a human being. You truly are an inspiration.

I would also like to extend my gratitude to Dr. Keith Gould for helping me grow during the early stages of my PhD. Over the past few years, Dr. Istvan Bartok has been a great friend, father figure and the person I sought for advice in the lab. There have been countless number of times when he has saved me. I would like to thank my fellow colleagues: Meriem, for teaching me the ways of the lab; Anil, for much of the help with irradiation; Greg and Heidi, for the injections; Hua, Alison and Nui, for the smallest details that proved to be largely important.

Most importantly, I would like to thank my friends and family for their support during the good and unpleasant times. My parents and my siblings have always pushed me to be the best I can be. I count myself really blessed to have such a wonderful family. In particular, I would like to thank my partner Izzati, who has always been there for me during the rollercoaster that is life. I look forward to many more great moments with you.

Lastly, I am forever indebted to His Majesty and the Bruneian Government for sponsoring my studies ever since I was a young 16-year-old. It has been a long journey. Thank you.

Table of Contents

Abstract	4
Acknowledgements	5
Table of Contents	6
List of Figures	10
List of Tables	12
Abbreviations	13
Chapter 1: Introduction	17
1.1. The immune system	17
1.2. Adaptive immunity	17
1.3. T cell subsets	18
1.4. T cell development	19
1.4.1. Thymocyte development	19
1.4.2. Thymic selection – central tolerance	21
1.4.3. CD4-CD8 T cell lineage commitment	22
1.4.4. Development of Tregs – peripheral tolerance	23
1.5. Generation of the TCR repertoire	25
1.5.1. Architecture of the TCR	25
1.5.2. Organisation of the $\alpha\beta$ TCR gene loci and potential diversity	27
1.5.3. V(D)J Recombination	28
1.5.3. Junctional diversity	31
1.6. Conventional $\alpha\beta$ TCR ligands	33
1.6.1. Structure of the Major Histocompatibility Complex	33
1.6.2. Antigen processing and presentation by MHC Class I	34
1.6.3. Antigen processing and presentation by MHC Class II	35
1.7. TCR-pMHC interactions	37
1.7.1. TCR signalling complex	37
1.7.2. Co-receptors	38
1.7.3. TCR-pMHC binding geometry	40
1.7.4. TCR cross-reactivity	41
1.8. MHC restriction	43
1.9. Therapeutic use of the $\alpha\beta$ TCR	44
1.10. Aims of the project	45
Chapter 2: Overview of the <i>in vivo</i> optimisation approach and design of the diversifying $\alpha\beta$TCR constructs	48

2.1. Introduction	48
2.2. Design of the recombination cassette	49
2.3. Design of multicistronic retroviral vectors for expression of CDR3 β diversifying $\alpha\beta$ TCRs	50
2.4. Overview of retrogenic approach	54
2.5. Results.....	56
2.5.1. Preparation of the retroviral vector containing the $\alpha\beta$ TCR (CDR3 β diversifying) constructs	56
2.5.2. Transfection of the Phoenix™ packaging cell line.....	57
2.5.3. Transduction of HSC and generation of retrogenic mice.....	59
2.6. Discussion.....	61
2.6.1. Summary	61
2.6.2. Advantages and limitations of retrogenic technology.....	61
2.6.3. Conclusions	62
Chapter 3: Characterisation of H2^d retrogenic mice expressing diversifying H2^b-restricted TCR	65
3.1. Introduction	65
3.2. Results.....	67
3.2.1. Detection of EGFP and TCR β expression in FVB/N retrogenic mice peripheral blood	67
3.2.2. Analysis of the FVB/N retrogenic mice primary lymphoid organs.....	70
3.2.3. Analysis of FVB/N retrogenic mice secondary lymphoid tissue.....	75
3.3. Discussion.....	79
3.3.1. Summary	79
3.3.2. Conclusions	81
Chapter 4: Phenotypic and sequence analysis of the T cell repertoire in H2^b retrogenic mice	83
4.1. Introduction	83
4.2. Results.....	84
4.2.1. Detection of T cell repertoire in retrogenic mice peripheral blood.....	84
4.2.2. Analysis of C57BL/6 retrogenic mice primary lymphoid organs	86
4.2.3. Analysis of C57BL/6 retrogenic mice secondary lymphoid tissue	90
4.2.4. Generation of diversity in the TCR CDR3 β using novel <i>in vivo</i> recombination cassette.....	97
4.2.5. Analysis of TCR repertoire diversity and diversified CDR3 β length and net charge	106
4.3. Discussion.....	111
4.3.1. Summary	111
4.3.2. Conclusions	114
Chapter 5: Phenotypic characterisation and functional analysis of a novel chimeric TCR chain	116
5.1. Introduction	116
5.2. Results.....	118

5.2.1. Preparation of sequencing and retroviral vectors containing the novel chimeric TCR	118
5.2.2. Analysis of recombination event leading to deletion of C α and V β domains.....	119
5.2.3. Functional characterisation of V α -C β fusion TCR chain.....	121
5.2.3.1. Phoenix™ cell transfection and generation of C57BL/6 retrogenic mice	121
5.2.3.2. Analysis of co-expression of novel TCR in normal $\alpha\beta$ T cells	122
5.2.4. Phenotypic analysis of the retrogenic mice expressing the V α -C β fusion TCR chain	125
5.2.4.1. Analysis of retrogenic mice primary lymphoid organs	125
5.2.4.2. Analysis of retrogenic mice secondary lymphoid tissue	127
5.3. Discussion.....	130
5.3.1. Summary	130
5.3.2. Conclusions	131
Chapter 6: Discussion	133
6.1. Implications of this study	134
6.1.1. Viability of the <i>in vivo</i> mutagenesis approach	134
6.1.2. Diversification profile using <i>in vivo</i> recombination cassette and its consequences.....	136
6.1.3. Limitations and improvements to the <i>in vivo</i> mutagenesis approach.....	138
6.1.4. Future perspectives	140
6.1.5. A new understanding of the mechanism underpinning MHC restriction.....	141
6.2. Concluding remarks	144
Chapter 7: Materials and Methods	146
7.1. TCR Nomenclature	146
7.2. Design of the $\alpha\beta$ TCR (CDR3 β diversifying) Sequences.....	146
7.2.1. Recombination cassette design and synthesis	146
7.2.2. Plasmid vector.....	147
7.3. Mice	147
7.4. Cell counting	148
7.5. Media and Reagents	148
7.6. Molecular Biology	149
7.6.1. DNA digestion with restriction enzymes.....	149
7.6.2. Agarose gel electrophoresis of DNA	149
7.6.3. Determination of nucleic acid concentration	150
7.6.4. DNA ligation	150
7.6.5. Bacterial transformation	150
7.6.6. Isolation of plasmid DNA.....	151
7.6.7. RNA extraction and cDNA synthesis	151
7.6.8. Polymerase Chain Reaction	152

7.6.9. Primer design and synthesis	152
7.6.10. Preparation of DNA for sequencing	153
7.6.11. DNA Sequencing.....	154
7.7. Cell culture	154
7.7.1. Maintenance of Phoenix™ ecotropic retrovirus packaging cell line.....	154
7.7.2. Lipofectamine®-based transfection of Phoenix™ cells	155
7.7.3. Transduction of murine haematopoietic stem cells (HSCs).....	155
7.7.4. Blood collection	156
7.8. Flow cytometry	156
7.8.1. Preparation of single-cell suspensions.....	156
7.8.2. Cell surface staining	156
7.8.3. MHC Dextramer™ staining.....	157
7.8.4. Multimer staining.....	158
7.8.5. Fluorescence-activated cell sorting (FACS)	158
7.8.6. Intracellular FoxP3 staining.....	158
7.9. Statistical analysis	159
7.9.1. Shannon entropy analysis	159
7.9.2. Unpaired student's t-test.....	159
Appendices	161
Appendix 1	161
Appendix 2	162
References	164

List of Figures

Figure 1.1. Schematic diagram of T cell development in the thymus.	24
Figure 1.2. Schematic representation of $\alpha\beta$ TCR structure.....	26
Figure 1.3. Generation of combinatorial diversity by V(D)J recombination.	29
Figure 1.4. The mechanism of V(D)J recombination.	32
Figure 1.5. Crystal structure of peptide bound to MHC Class I and Class II.	36
Figure 2.1. Design of the novel recombination cassette to diversify TCR.....	50
Figure 2.2. Schematic overview of the novel TCR diversifying technique.	53
Figure 2.3. Schematic overview of the generation of retrogenic mice incorporating TCR diversification.	55
Figure 2.4. Ligation and sub-cloning of Marilyn and MataHari $\alpha\beta$ TCR (CDR3 β diversifying) constructs into the pMigR1 retroviral vector.....	56
Figure 2.5. Flow cytometric analysis of EGFP reporter expression and summary of transfection efficiencies.	58
Figure 2.6. Summary of transduction efficiencies and the number of EGFP ⁺ HSCs adoptively transferred into each retrogenic mice.....	60
Figure 3.1. The fate of the TCR constructs from the retroviral vector to the creation of the T cell repertoire.	66
Figure 3.2. Flow cytometric analysis of peripheral blood from FVB/N retrogenic mice transduced with Marilyn and MataHari $\alpha\beta$ TCR (CDR3 β diversifying) constructs.	68
Figure 3.3. Progression of EGFP ⁺ TCR β ⁺ cells in the peripheral blood of FVB/N retrogenic mice.	69
Figure 3.4. Thymic size and cellularity in Marilyn and MataHari TCR (CDR3 β diversifying) FVB/N retrogenic mice.....	72
Figure 3.5. Flow cytometric analysis of thymocytes from Marilyn and MataHari TCR (CDR3 β diversifying) FVB/N retrogenic mice.....	74
Figure 3.6. Splenic size and cellularity in Marilyn and MataHari TCR (CDR3 β diversifying) FVB/N retrogenic mice.....	75
Figure 3.7. Flow cytometric analysis of Marilyn and MataHari TCR (CDR3 β diversifying) FVB/N retrogenic mice splenocytes.	76
Figure 3.8. Retention and loss in binding with specific anti-V β 6/8.3 Ab epitope.	78
Figure 4.1. Flow cytometric analysis of peripheral blood from C57BL/6 retrogenic mice transduced with Marilyn and MataHari $\alpha\beta$ TCR (CDR3 β diversifying) constructs.	85
Figure 4.2. Thymic size and cellularity in Marilyn and MataHari TCR (CDR3 β diversifying) C57BL/6 retrogenic mice.....	87
Figure 4.3. Flow cytometric analysis of Marilyn and MataHari TCR (CDR3 β diversifying) C57BL/6 retrogenic mice thymocytes.	89
Figure 4.4. Splenic size and cellularity of Marilyn and MataHari TCR (CDR3 β diversifying) C57BL/6 retrogenic mice.....	90

Figure 4.5. Flow cytometric analysis of retrogenic mice secondary lymphoid organs.	93
Figure 4.6. Retention and loss in binding with specific anti-V β 6/8.3 Ab epitope.	94
Figure 4.7. Identification of specific antigen-binding in diversified T cells.	96
Figure 4.8. Cell sorting and PCR analysis of retrogenic mice splenocytes.	98
Figure 4.9. Schematic diagram of the diversified TCR repertoire from the naïve CD4 ⁺ V β 6 ⁻ lymphocyte population from Marilyn TCR (CDR3 β diversifying) retrogenic mice (n=2).	99
Figure 4.10. Overall peptide sequence diversity of peripheral TCR repertoire generated by the <i>in vivo</i> mutagenesis approach in Marilyn and MataHari TCR (CDR3 β diversifying) retrogenic mice.	107
Figure 4.11. Analysis of the diversified CDR3 β amino acid length distribution in the Marilyn and MataHari TCR (CDR3 β diversifying) retrogenic mice.	108
Figure 4.12. Analysis of the diversified TCR repertoire CDR3 β net charge and amino acid usage in the Marilyn and MataHari TCR (CDR3 β diversifying) retrogenic mice.	110
Figure 5.1. The loss of the Marilyn V β 6 domain in Marilyn TCR (CDR3 β diversifying) retrogenic mice.	117
Figure 5.2. Amplification and sub-cloning of the complete V α -C β fusion TCR construct.	118
Figure 5.3. Comparison of the nucleotide and amino acid sequences of the Marilyn TCR α and β chains with the V α -C β fusion TCR.	120
Figure 5.4. Molecular model of V α -C β fusion TCR.	121
Figure 5.5. Flow cytometric analysis of EGFP reporter expression in transfected and transduced cells.	122
Figure 5.6. Flow cytometric analysis of transduced T cells.	124
Figure 5.7. Analysis of thymus from C57BL/6 retrogenic mice expressing the V α -C β fusion TCR chain.	126
Figure 5.8. Splenic size and cellularity in retrogenic mice expressing the V α -C β fusion TCR chain.	127
Figure 5.9. Flow cytometric analysis of retrogenic mice expressing the V α -C β fusion TCR chain.	128
Figure 5.10. Flow cytometric analysis of V α usage and FoxP3 staining in the retrogenic peripheral T lymphocytes.	129
Figure 7.1. Plasmid vector pMigR1.	147

List of Tables

Table 1.1. Number of functional TCR gene segments encoded in the human and mouse genome.	27
Table 2.1. CDR1-3 amino acid sequences in each chain of Marilyn and MataHari transgenic TCRs.	52
Table 3.1. The cohorts of FVB/N retrogenic mice generated from adoptive transfer of HSCs containing Marilyn and MataHari $\alpha\beta$ TCR (CDR3 β diversifying) constructs.	67
Table 3.2. Retention and loss in binding with specific anti-V β 6/8.3 Ab epitope.	78
Table 4.1. The cohorts of C57BL/6 retrogenic mice generated from adoptive transfer of retrovirally-transduced HSCs containing Marilyn and MataHari $\alpha\beta$ TCR (CDR3 β diversifying) constructs.	84
Table 4. 2. Summary of retention and loss in binding with specific anti-V β 6/8.3 Ab epitope compared to anti-TCR β staining in retrogenic mice splenocytes.	95
Table 4.3. Summary of specific antigen-binding in diversified T cells.	96
Table 4.4. Sequence analysis of diversified TCR repertoire in naïve CD4 ⁺ V β 6 ⁺ lymphocyte population from Marilyn TCR (CDR3 β diversifying) retrogenic mice (n=2).	100
Table 4.5. Sequence analysis of diversified TCR repertoire in naïve CD4 ⁺ lymphocyte population from MataHari TCR (CDR3 β diversifying) retrogenic mice (n=2) without antigenic challenge.	102
Table 4.6. Sequence analysis of diversified TCR repertoire in naïve CD8 ⁺ lymphocyte population from MataHari TCR (CDR3 β diversifying) retrogenic mice (n=2) without antigenic challenge.	103
Table 4.7. Sequence analysis of diversified TCR repertoire in CD4 ⁺ lymphocyte population from MataHari TCR (CDR3 β diversifying) retrogenic mice (n=2) after antigenic challenge.	104
Table 4.8. Sequence analysis of diversified TCR repertoire in CD8 ⁺ lymphocyte population from MataHari TCR (CDR3 β diversifying) retrogenic mice (n=2) after antigenic challenge.	105
Table 5.1. Comparison of the MFI of TCR β and V β 11 expressions relative to EGFP expression in transduced CD8 ⁺ and CD4 ⁺ T cells.	123
Table 7.1. List of reagents and buffers.	148
Table 7.2. General PCR programme.	152
Table 7.3. List of PCR primers.	153
Table 7.4. List of sequencing primers used.	154
Table 7.5. List of monoclonal antibodies.	157

Abbreviations

AIDS	Acquired immune deficiency syndrome
AIRE	Autoimmune regulator
Ab	Antibody
AMP	Ampicillin
APC	Allophycocyanin
APC	Antigen-presenting cells
APECED	Autoimmune polyendocrinopathy-candidiasis-ectodermal dystrophy
ATP	Adenosine triphosphate
BCR	B cell receptor
BLAST	Basic Local Alignment Search Tool
BM	Bone marrow
bp	Base pairs
BSA	Bovine serum albumin
C	Constant
C-terminus	Carboxyl-terminus
CD	Cluster of differentiation
CDR	Complementarity-determining region
CLIP	Class II-associated invariant chain peptide
CLP	Common lymphoid progenitor
CO ₂	Carbon dioxide
cTEC	Cortical thymic epithelial cell
CTLA4	Cytotoxic T lymphocyte antigen 4
D	Diversity
DC	Dendritic cell
ddH ₂ O	Double distilled water
DMSO	Dimethylsulfoxide
DN	Double negative
DNA	Deoxyribonucleic acid
DNA-PKcs	DNA-dependent protein kinase catalytic subunit
dNTP	Deoxynucleoside triphosphate
DP	Double positive
EDTA	Ethylenediaminetetraacetic acid
EGFP	Enhanced green fluorescent protein
ER	Endoplasmic reticulum
Fab	Fragment-antigen binding
FACS	Fluorescence-activated cell sorting
FasR	Fas receptor
FCS	Foetal calf serum
FITC	Fluorescein isothiocyanate
Flt-3	Fms-related tyrosine kinase 3
FOXP3	Forkhead box P3
FR	Framework region
FVB/N	Friend virus B-type susceptibility
GEM	Germline-encoded mycolyl-reactive
H2	Histocompatibility-2
HEL	Hen egg lysozyme
HEPES	N-2-hydroxyethylpiperazine-N-2-ethane sulfonic acid

HIV-1	Human immunodeficiency virus 1
HLA	Human leukocyte antigen
HMG	High mobility group
HSC	Haematopoietic stem cells
Id3	Inhibitor of DNA-binding 3
IFN- γ	Interferon-gamma
Ig	Immunoglobulin
IL	Interleukin
IMDM	Iscove's Modified Dulbecco's Medium
IMGT	ImMunoGeneTics
iNKT	Invariant natural killer T cell
i.p.	Intraperitoneal
i.v.	Intravenous
IPEX	Immunodysregulation, polyendocrinopathy, enteropathy, X-linked
IRES	Internal ribosome entry site
ITAM	Immunoreceptor tyrosine-based activation motif
J	Junctional
kg	Kilogram
LB	Luria-Bertani
Lck	Lymphocyte-specific protein tyrosine kinase
LN	Lymph node
LTR	Long-terminal repeats
MAGE	Melanoma-associated antigen
MAIT	mucosal-associated invariant T cell
MCS	Multiple cloning site
MFI	Mean fluorescent intensity
MHC	Major histocompatibility complex
mg	Milligram
ml	Millilitre
mM	Millimolar
MSCV	Murine stem cell virus
mTEC	Medullary thymic epithelial cell
N	Non-templated
N-terminus	Amino-terminus
NHEJ	Non-homologous end joining
NK	Natural killer
nm	Nanometre
nTreg	Natural regulatory T cell
ORF	Open reading frame
OVA	Ovalbumin
P	Palindromic
PAMP	Pathogen-associated molecular pattern
PBS	Phosphate buffered saline
PCR	Polymerase chain reaction
PE	Phycoerythrin
PerCP	Peridinin-chlorophyll protein
PLC	Peptide-loading complex
pMHC	Peptide-MHC complex
PRR	Pattern recognition receptor
pT α	Pre-T cell receptor alpha
pTreg	Peripheral regulatory T cell

RAG	Recombination-activating gene
RBC	Red blood cell
RNA	Ribonucleic acid
rpm	Revolutions per minute
RPMI	Roswell Park Memorial Institute
RSS	Recombination signal sequence
SCF	Stem Cell Factor
SCID	Severe combined immunodeficiency
SD	Standard deviation
SH2	Src homology 2 domain
SOC	Super optimal broth
SP	Single-positve
T	Deoxythymidine
T1D	Type 1 diabetes
TAE	Tris-Acetate-EDTA
TAP	Transporter associated with antigen processing
TdT	Terminal deoxynucleotidyl transferase
Tfh	T follicular helper cell
TGF- β	Transforming growth factor beta
TM	Transmembrane
TNF	Tumour necrosis factor
Th	T helper cell
Treg	Regulatory T cell
V	Variable
WT	Wild-type
ZAP70	Zeta chain-association protein kinase 70
β 2-m	β 2 microglobulin
μ g	Microgram
μ l	Microlitre
μ M	Micromolar
5'-FU	5'-Fluorouracil

Chapter 1

Introduction

Chapter 1: Introduction

1.1. The immune system

The immune system is a specialised network of cells and biological processes that work together to protect the organism against pathogenic events. In jawed vertebrates, the immunologic defences comprise of two distinct arms - the interdependent innate and adaptive immune responses. Both responses harness related effector mechanisms and can discriminate self from nonself, but differ primarily by their recognition strategies (Janeway et al., 2005).

Innate immunity provides an immediate host immune response to infectious agents and employs a limited number of germline-encoded pattern recognition receptors (PRR) for their detection. These receptors recognise evolutionarily conserved pathogen-associated molecular patterns (PAMP) generally found on foreign microorganisms, but not the host. The innate immune system encompasses both physical barriers, such as the skin, as well as molecular and cellular components including the complement system, natural killer cells, monocytes, macrophages and dendritic cells (Janeway & Medzhitov, 2002).

Adaptive immunity, by contrast, is composed of cells bearing highly diverse antigen receptors generated through somatic gene rearrangement and able to recognise the plethora of pathogens (Azuma, 2006; Tonegawa, 1983). The adaptive immune response is slower to respond, but has the advantage of lifelong immunological memory, which promotes a quicker and amplified response following subsequent antigenic exposure (Walker & Slifka, 2010). Adaptive immunity is mediated by antigen-specific T and B lymphocytes, which are responsible for cellular (cell-mediated) and humoral (antibody-mediated) immune responses respectively. T and B lymphocytes, and most cellular components of the immune system, originate from pluripotent haematopoietic stem cells (HSCs) in the bone marrow (BM). However, T and B cells are distinguished by their antigen receptors and sites of differentiation – T cells in thymus and B cells in BM (Janeway et al., 2005).

1.2. Adaptive immunity

The hallmark of the adaptive immune system is the ability to mount a specific immune response against virtually any foreign antigen whilst maintaining tolerance to self. In principle, this is achieved through the expression of a huge repertoire of clonally variable receptors in the T and B lymphocyte population. B cells engage with intact ligands in their native form via the membrane-bound B cell

receptor (BCR), composed of the antigen-binding immunoglobulin (Ig) associated with the invariant $Ig\alpha/\beta$ signalling complex (Harwood & Batista, 2010). Engagement of the BCR with antigen triggers B cell activation and differentiation into plasma cells capable of secreting antibodies (Ab), which are the main effectors in humoral adaptive immunity. T cells, in contrast, utilise transmembrane T cell receptors (TCR) that can only recognise antigens once they have been processed into small peptide fragments and displayed by major histocompatibility complex molecules (MHC) on the surface of antigen-presenting cells (APCs). Upon effective ligand binding, the TCR along with other accessory proteins recruit signalling molecules required for T cell activation (Smith-Garvin, Koretzky & Jordan, 2009; Rudolph, Stanfield & Wilson, 2006).

Defects involving the T and B cell populations have indeed highlighted the importance of a functional adaptive immune system (Cunningham-Rundles & Ponda, 2005). For example, severe combined immunodeficiency (SCID), is a primary immunodeficiency characterised by severely reduced numbers of functional T and B cells. This rare disease is caused by mutations in any one of ten distinct genes that are inherited in an X-linked or autosomal recessive pattern (Buckley, 2004). Infants born with SCID are susceptible to opportunistic infections after waning of maternal antibody, and if left untreated leads to 100% mortality (Kelly et al., 2013). DiGeorge syndrome, a genetic disorder associated with thymic hypoplasia or aplasia, results in selective absence of T cells (Stoller & Epstein, 2005; Yagi et al., 2003). Without thymic transplantation, patients born with DiGeorge syndrome usually die within the first two years of life (Hudson et al., 2007; Markert et al., 1998). Furthermore, extrinsic agents such as the human immunodeficiency virus 1 (HIV-1) which specifically target $CD4^+$ T helper cells, also underline the significance of T cells. HIV infection causes T cell deficiency, immune dysregulation and eventually leads to clinical acquired immune deficiency syndrome (AIDS; Boasso et al., 2008)

1.3. T cell subsets

T lymphocytes can be broadly classified into several subpopulations based on their effector functions and molecular phenotype. The majority of T cells express the heterodimeric $\alpha\beta$ TCR that recognise peptide fragments bound to MHC molecules at the cell surface. These 'conventional' $\alpha\beta$ T cells are further divided into two main classes: the $CD8^+$ cytotoxic T cells and the $CD4^+$ T helper cells. The $CD8^+$ cytotoxic T cells are responsible for the recognition and direct destruction of virally-infected or malignant cells. This is mediated by two possible pathways: engagement of death receptors such as the $TNF-\alpha R$ or $FasR$, or the release of cytolytic molecules - granzymes and perforin (Chattopadhyay et al., 2009; Lieberman, 2003; Trapani & Smyth, 2002). The $CD4^+$ T helper (Th) cells play a crucial role in

orchestrating the immune response – often involved in the activation of B cells, macrophages and the CD8⁺ cytotoxic T cells. CD4⁺ T helper subsets include Th type 1 (Th1), Th2, Th17, T follicular helper (Tfh) and T regulatory (Tregs) cells. Th1 cells secrete Th1 cytokines including IL-2, IFN- γ and TNF- β in order to activate cell-mediated antiviral and antibacterial immunity via macrophages and cytotoxic T cells (Kaiko et al., 2007). The Th2 subset coordinates humoral against large extracellular pathogens by secreting Th2 cytokines (IL-4, IL-5, IL-9 and IL-13) and are responsible for inducing antibody secretion and class-switching to IgE in B cells (Ueno, Banchereau & Vinuesa, 2015; Wynn, 2015). IL-17-producing Th17 cells mediate host defense mechanisms especially against extracellular bacterial infections, and are involved in the pathogenesis of many autoimmune diseases (Ouyang, Kolls & Zheng, 2008). Tfh cells, characterised by the expression of the chemokine receptor CXCR5 for migration to germinal centres in secondary lymphoid organs, aid in the differentiation of B cells into plasma cells and memory cells (Crotty, 2011; Ansel et al., 1999). Tregs play a key part in actively suppressing antigen-specific responses that can cause tissue damage through several mechanisms including the secretion of IL-4, IL-10 and TGF- β (Sakaguchi et al., 2008).

The ‘unconventional’ T cell population comprise of T cells that express $\alpha\beta$ TCRs with very limited diversity that do not engage with peptide-MHC (pMHC) ligands. This includes mucosal-associated invariant T (MAIT), invariant natural killer T (iNKT) cells, and germline-encoded mycolyl-reactive (GEM) T cells involved in anti-bacterial immunity. MAIT cells recognise pterins (microbial riboflavin derivatives) in the context of MR1, a non-polymorphic MHC-I-related protein (Kurioka et al., 2015; Kjer-Nielsen et al., 2012). The iNKT and GEM T cells bind to glycolipids presented by CD1d and CD1b, respectively, which are also non-polymorphic and ‘MHC-I-like’ molecules (Kronenberg & Zajonc, 2013; Treiner & Lantz, 2006). A minority of T lymphocytes express the somatically rearranged $\gamma\delta$ TCR, and are also grouped as ‘unconventional’ since they appear to recognise non-peptide antigens. Most $\gamma\delta$ T cells are found in epithelial tissues, and mediate protective immunity against extracellular and intracellular pathogens as well as tumour surveillance with innate-like kinetics (Vantourout & Hayday, 2013; Bonneville, O'Brien & Born, 2010).

1.4. T cell development

1.4.1. Thymocyte development

Despite the functional and phenotypical differences between the T cell subsets, all T lymphocytes derive from common lymphoid progenitors (CLP) and share early differentiation processes in the thymus (Attaf et al., 2015). The thymus facilitates an inductive microenvironment essential for these

progenitors to undergo TCR gene rearrangement, selection and proliferation into functionally mature T cells (Ciofani & Zúñiga-Pflücker, 2007). The thymic microenvironment is comprised of a network of stromal cells which provide structural support and appropriate signals to direct lymphoid development (Petrie & Zúñiga-Pflücker, 2007). Upon entering the thymus, the thymic progenitors establish an irreversible commitment to the T cell lineage and expression of clonally distributed and heterogeneous TCRs (Gerondakis et al., 2014). Additionally, this signals the loss in developmental potential towards myeloid, B cell, natural killer (NK) and dendritic cell (DC) lineages (Lu et al., 2005; Kawamoto et al., 1999).

Thymocyte development progresses through a series of checkpoints in discrete areas of the thymus, and are typically identified by the cell surface expression of CD4 and CD8 co-receptors (Figure 1.1; Gameiro, Nagib & Verinaud, 2010). The earliest thymocytes express neither co-receptor, hence denoted as CD4⁻CD8⁻ double negative (DN), then differentiate into CD4⁺CD8⁺ double positive (DP), and eventually maturing into single-positive (SP) CD4⁺ or CD8⁺ T cells (Anderson & Jenkinson, 2001). During the early phase of differentiation, the DN cells can be further subdivided into four main developmental stages (DN1 through DN4), based on the surface expression of CD44 (an adhesion molecule) and CD25 (the α chain of the IL-2 receptor; Ceredig & Rolink, 2002; Godfrey et al., 1993). At the DN1 stage (CD44⁺CD25⁻), the TCR genes largely remain in their germline configuration. Moreover, the DN1 stage represents a crucial checkpoint in T cell lineage commitment (Koch & Radtke, 2011). In particular, the evolutionarily conserved Notch signalling pathway has been shown to abrogate multiple cell fate potentials including myeloid, DC and B cell potential within the DN1 population (Feyerabend et al., 2009; Bell & Bhandoola, 2008). Differentiation proceeds to the DN2 stage (CD44⁺CD25⁺), where the cells upregulate recombination-activating genes (RAG-1 and RAG-2) and initiate simultaneous rearrangement of the *TCR β* , *TCR γ* and *TCR δ* gene loci (Livák et al., 1999; Capone, Hockett & Zlotnik, 1998).

Gene rearrangement at these loci predominantly continue into the DN3 stage (CD44⁻CD25⁺), where commitment to either $\alpha\beta$ or $\gamma\delta$ T cell fate is specified (Pereira, Boucontet & Cumano, 2012; Ciofani et al., 2006; Burtrum et al., 1996). Successful recombination of *TCR γ* and *TCR δ* , resulting in expression of the $\gamma\delta$ TCR and induction of Id3 (Inhibitor of DNA-binding 3) promote Notch-independent $\gamma\delta$ T cell specification (Zarin et al., 2014; Lauritsen et al., 2009; Ciofani et al., 2006; Wolfer et al., 2002). Conversely, development into $\alpha\beta$ T cells requires signalling through a functional pre-TCR complex, comprising of an in-frame rearranged TCR β chain, CD3 signalling molecules and an invariant pre-T α (pT α) chain (von Boehmer, 2005). The expression of the nascent TCR β chain marks an important checkpoint in T cell differentiation known as β -selection. Indeed, cells that fail to generate a functionally rearranged TCR β chain remain in the DN3 stage and die by apoptosis (Michie & Zúñiga-

Pflücker, 2002). Signals derived from the pre-TCR complex, along with active signalling from CXCR4 (the receptor for the chemokine CXCL12) and the Notch1 receptor, trigger a maturation program within the developing thymocytes (Maillard et al., 2006; Ciofani & Zúñiga-Pflücker, 2005; Ciofani et al., 2004). This includes cell survival, inhibition of further TCR β chain gene rearrangement by allelic exclusion, induction of rapid cell proliferation and transition into the DN4 (CD44⁺CD25⁻) and DP stages via upregulation of the CD4 and CD8 co-receptors (Yamasaki et al., 2006; Voll et al., 2000).

DP thymocytes constitute the largest proportion of all thymocytes at an estimated 80% due to the proliferative burst induced through pre-TCR signalling (Wong et al., 2012). At the DP stage, *RAG* genes are re-expressed and gene recombination at the *TCR α* loci is initiated. The expression of a functional TCR α chain replaces the pT α , resulting in low levels of $\alpha\beta$ TCR assembled with CD3 proteins (Germain, Stefanova & Dorfelan, 2002). These developing DP thymocytes then audition for thymic positive and negative selection once the $\alpha\beta$ TCR is expressed, eventually developing into naïve SP T cells (Kyewski & Klein, 2006). More than 90% of these precursors are subject to cell death as a result of failing thymic selection (Klein et al., 2014; Germain, 2002).

1.4.2. Thymic selection – central tolerance

The thymic microenvironment consists of functionally distinct niches that drive the processes of positive and negative selection. The positive selection of thymocytes occurs predominantly in the outer cortex of the thymus, and involves interactions with a single APC type, namely the cortical thymic epithelial cells (cTECs). The medullary region of the thymus represent the site of negative selection, where thymocytes engage with medullary thymic epithelial cells (mTECs) and thymic DCs. Accordingly, the specificity and binding strength of the pre-selection $\alpha\beta$ TCR repertoire for self-pMHC ligands displayed by these APCs determine the fate of the developing thymocytes (Klein et al., 2014; Petrie & Zúñiga-Pflücker, 2007).

Positive selection permits survival of those cells whose receptors engage effectively with self-pMHC ligands, thus ensuring MHC-restriction. During this checkpoint, most thymocytes express $\alpha\beta$ TCRs that cannot participate in such interactions and fail to receive a survival signal, which leads to death by neglect (Germain, 2002). Additionally, positive selection defines the lineage-specific differentiation into either SP CD8⁺ or CD4⁺ T cells depending on the binding efficiency with either MHC Class I or Class II molecules displayed by thymic APCs, respectively (Taniuchi, 2009). Upon migrating to the medulla, SP thymocytes undergo negative selection in which cells with high affinity for self-pMHC ligands are clonally deleted via apoptosis, thus removing autoreactive T cells that may cause damage to host

tissue (von Boehmer & Melchers, 2010). Here, medullary APCs employ a unique epigenetic mechanism which promotes low-level promiscuous expression of non-thymic and tissue-restricted self-antigens (Metzger & Anderson, 2011; Derbinski et al., 2001). The mTEC-produced self-antigens may be presented to thymocytes directly by mTECs or cross-presented by neighbouring DCs (Hubert et al., 2011). The ectopic expression of self-antigens in mTECs is regulated by the transcription factor autoimmune regulator (AIRE; Eldershaw, Sansom & Narendran, 2010). In the absence of AIRE, impaired clonal deletion of self-reactive thymocytes results in the onset of multi-organ and organ-specific autoimmune diseases such as autoimmune polyendocrinopathy-candidiasis-ectodermal dystrophy (APECED), type 1 diabetes (T1D) and thyroiditis (Mathis & Benoist, 2009). Overall, the thymic selection processes and checkpoints ensure that only immunological competent and self-tolerant T cells are released into the periphery.

1.4.3. CD4-CD8 T cell lineage commitment

Competent adaptive immunity requires CD4⁺ T helper cells that interact with MHC Class II ligands and CD8⁺ cytotoxic T cells that recognise MHC Class I ligands. The commitment to either CD4⁺ or CD8⁺ T cells lineage is simultaneously established during positive selection where developing thymocytes are educated for appropriate MHC restriction (Singer, Adoro & Park, 2008). Two main classical models have been proposed to elucidate the CD4-CD8 T cell lineage choice: 'stochastic' or 'instructive', depending on whether the termination of co-receptor transcription is random or instructed (Kappes, He & He, 2005). The stochastic selection model dictates that co-receptor gene downregulation occurs randomly and independent of TCR specificity during positive selection. A subsequent TCR-dependent mechanism then rescues and only permits SP thymocytes with matching TCR/MHC and co-receptors to differentiate into mature T cells (Singer, Adoro & Park, 2008).

The instructive model postulates that TCR signals direct DP thymocytes to specifically downmodulate the expression of the mismatching co-receptor. In the strength-of-signal instructive model, DP thymocytes are directed based on the relative differences in the signal strengths stimulated by TCR and co-receptor co-engagement during positive selection. TCR and CD4 co-engagement with MHC Class II generates stronger signals, whereas TCR and CD8 co-engagement with Class I molecule induces weaker signals (Itano et al., 1996). The updated duration-of-signal instructive model suggests that TCR signal duration, in addition to signal strength, determine the T cell lineage outcome. In this model, TCR signals of long duration induce CD8 downregulation and differentiation into CD4⁺ T cells, whereas TCR signals of short duration terminate CD4 expression thereby generates CD8⁺ T cells (Yasutomo et al., 2000).

Recently, molecular mechanisms operating in thymocytes have been described to further understand lineage specification. In particular, the mutually exclusive expression of transcription factors ThPOK and Runx3 are thought to determine the CD4-CD8 lineage fate. During thymic selection, ThPOK induces thymocytes that have received MHC-II signalling to enter the CD4⁺ lineage whereas Runx3 promotes cells that have received MHC-I signals to become CD8⁺ T cells (He et al., 2005; Sun et al., 2005; Sato et al., 2005; Taniuchi et al., 2002). Definitive lineage fate commitment requires that individual thymocytes express either ThPOK or Runx3 but not both. Accordingly, ThPOK upregulates SOCS (suppressor of cytokine signalling) cytosolic proteins that suppress Runx3 expression in order to adopt the CD4⁺ lineage fate (Luckey et al., 2014). Reciprocally, intrathymic cytokines signal thymocytes to express Runx proteins that bind to a silencer element in the *Thpok* locus to repress ThPOK expression (Park et al., 2010; He et al., 2008; Setoguchi et al., 2008).

1.4.4. Development of Tregs – peripheral tolerance

The central tolerance mechanism operating in the thymus functions to eliminate the development of self-reactive T cells. Although the negative selection process is thought to be efficient, some T cells expressing autoreactive TCRs are released into the periphery, in part because not all self-antigens are expressed in the thymus. Thus, peripheral tolerance mechanisms exist to balance the shortcomings of central tolerance and prevent many autoimmune diseases (Xing & Hogquist, 2012). Immunosuppressive CD4⁺CD25⁺ Tregs, characterised by the distinctive expression of the forkhead box P3 (FoxP3) transcription factor, are essential for maintaining peripheral tolerance (Benoist & Mathis, 2012). These cells suppress unwanted immune responses through the production of anti-inflammatory cytokines, direct cell-to-cell contact and modulating the activation state and function of APCs (Shevach, 2009). Accordingly, deficiencies in the *Foxp3* gene have been shown to cause lymphoproliferation and multi-organ autoimmunity in *scurfy* mice and human IPEX (immunodysregulation, polyendocrinopathy, enteropathy, X-linked) syndrome patients (Ziegler, 2006).

Two pathways of differentiation have been described for Tregs: in the thymus from immature DP precursors, as an alternative to the conventional CD4⁺ T cell lineage, and induction of FoxP3 in peripheral, conventional CD4⁺ T cells. Thymus-derived Tregs are generally termed as natural Tregs (nTregs), while the latter are labelled as peripheral Tregs (pTregs; Benoist & Mathis, 2012). In the thymus, antigen presentation on mTECs and thymic DCs induces FoxP3 expression and elicit differentiation into nTregs (Hanabuchi et al., 2010; Proietto et al., 2008; Aschenbrenner et al., 2007). The strength and duration of TCR engagement with these cells determine whether developing

thymocytes undergo clonal deletion or FoxP3 induction. Stronger binding is proposed to trigger deletion whereas weaker TCR signals lead to nTreg differentiation (Xing & Hogquist, 2012). In addition, CD28 co-stimulation signals of developing thymocytes can also induce Treg differentiation, and IL-2 signalling is required for Treg survival (Lio et al., 2010; Lio & Hsieh, 2008; Burchill et al., 2008; Vang et al., 2008; Tai et al., 2005). In the periphery, the cytokine TGF- β stimulates the conversion of mature T cells into the pTreg lineage (Kretschmer et al., 2005). However, its role in thymic differentiation into nTregs is much less understood. Liu and colleagues (2008) have shown that the combined loss of TGF- β and IL-2 signalling abrogates the development of nTregs in the thymus. TGF- β signalling may also be involved in preventing negative selection of nTregs that experience strong TCR signals from self-antigens (Ouyang et al., 2010).

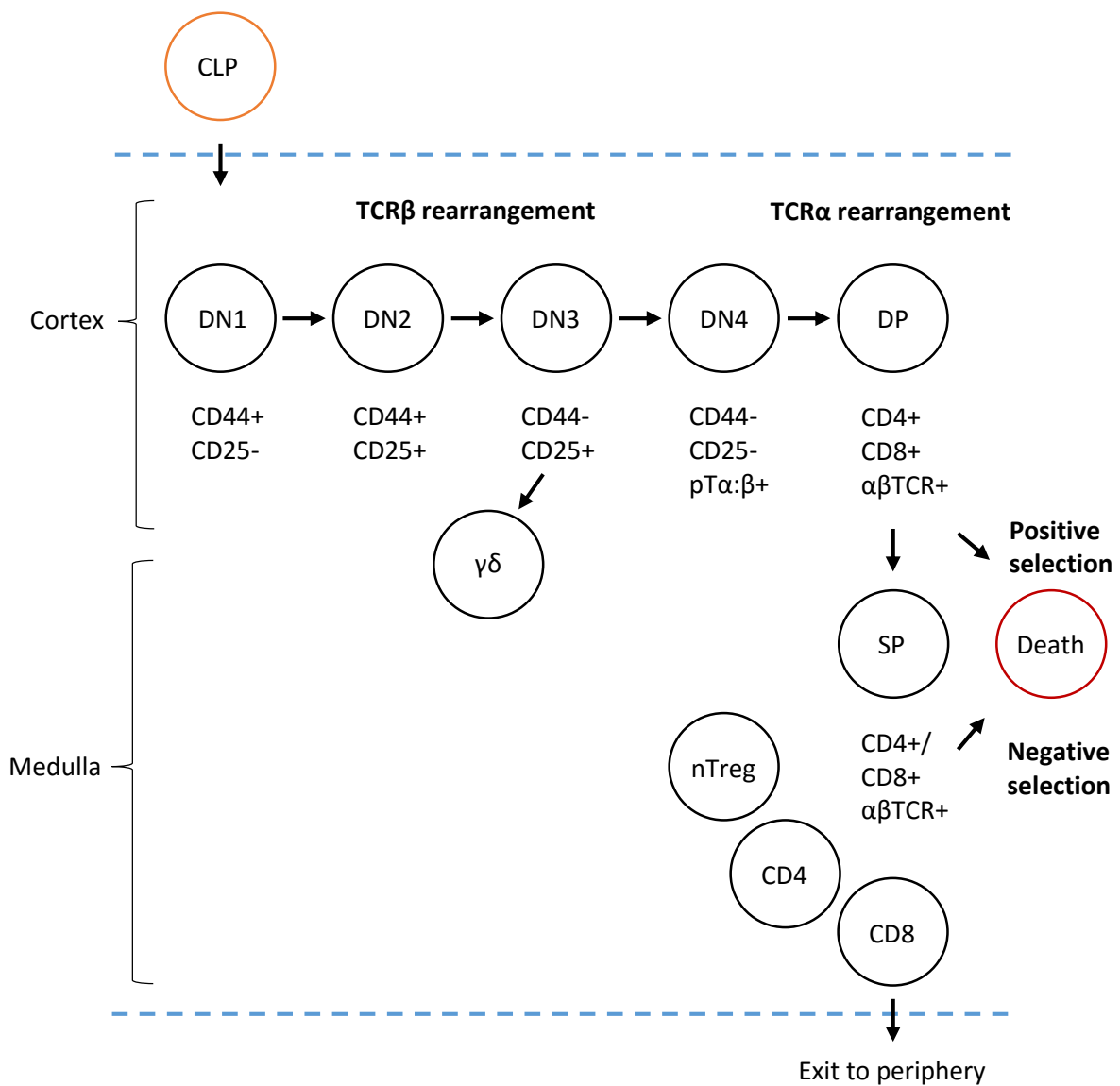


Figure 1.1. Schematic diagram of T cell development in the thymus. Haematopoietic stem cells (HSCs) originate from the bone marrow (BM) and give rise to common lymphoid progenitors (CLP), which either remain in the BM to produce B cells, or migrate to the thymus to develop T cells. In the thymus,

CLPs enter as double-negative (DN) thymocytes, and are further subdivided based on the expression of CD44 and CD25. T cell commitment is acquired at the DN2 stage where gene recombination of the TCR genes is initiated. At the DN3 stage, the TCR β chain is expressed and pairs with the pT α invariant chain to form the pre-TCR, and where the cell undergoes β -selection. Successful pre-TCR complex expression and β -selection give rise to DN4 cells, which later differentiate into double-positive (DP) cells. DP cells express both co-receptors and undergo positive selection on self-pMHC to further give rise to single-positive (SP) CD4⁺/CD8⁺ cells. SP cells are subject to negative selection, which removes TCRs which bind with high affinity, before exit into the periphery as naïve T cells.

1.5. Generation of the TCR repertoire

1.5.1. Architecture of the TCR

Depending on the T cell lineage, the TCR is a heterodimeric glycoprotein consisting of either disulphide-linked α and β or γ and δ polypeptide chains. Each chain of the TCR constitutes two extracellular Ig-like domains – a variable (V) and a constant (C) domain, followed by a hydrophobic transmembrane (TM) region with a short cytoplasmic tail (Rudolph, Stanfield & Wilson, 2006; Davis & Bjorkman, 1988). Each domain is composed of a pair of β -sheets that are packed face-to-face by hydrophobic interactions and disulphide bonds (Figure 1.2). The V domains are constructed from 9 antiparallel β strands (five inner and four outer strands) which are labelled A, B, C, C', C'', D, E, F, and G. In comparison, there are seven β strands that form the C domains (four inner and three outer strands) labelled A-G (Allison et al., 2001; Al-Lazikani, Lesk & Chothia, 2000; Novotný et al., 1986).

The V domain of each TCR chain contains three variable loops called the complementarity determining regions (CDRs), which protrude at the membrane-distal ends and collectively form the antigen-binding site. The germline-encoded CDR1 and CDR2 loops interact mainly with the MHC molecule and constitute the peptides linking the B-C and C'-C'' strands respectively. Additionally, the CDR1 and CDR2 loops are proposed to assume a set of unique conformations named canonical structures that are determined by the length of the loops and the presence of key residues at particular sites (Al-Lazikani, Lesk & Chothia, 2000; Garcia, Teyton & Wilson, 1999; Arden, 1998). The hypervariable CDR3 loop combines the ends of the F and G β -sheet strands and engages primarily with the MHC-bound peptide fragment (Allison et al., 2001; Al-Lazikani, Lesk & Chothia, 2000). Altogether, the sequence and structure of the CDRs determine the TCR binding specificity and affinity (Dunbar et al., 2014).

Directly adjacent to the amino (N)-terminal V domain and connected by a hinge region is the carboxyl-terminal C domain (Ely et al., 2005). The C domain functions as a scaffold for the V domain and an anchor in the cell membrane via the TM region. Despite not directly participating in antigen recognition, the amino acid composition of the C and TM domains play significant roles in the TCR

structure and function. Within the C domain, the conserved cysteine residue mediates the dimerisation of the TCR α and TCR β chains via disulphide bridges (Garcia et al., 1996a). Notably, this disulphide bond is not necessary for TCR membrane expression or signal transduction (Arnaud et al., 1997). Moreover, key residues within the TCR α and TCR β C domains have been described to drive proper assembly with the CD3 signalling subunits as well as antigen responsiveness (Kuhns, Davis & Garcia, 2006; Werlen, Hausmann & Palmer, 2000; Bäckström et al., 1998; Arnaud et al., 1997; Bäckström et al., 1996). Mutagenesis directed at the FG loop in the TCR β C domain has suggested its role in regulating $\alpha\beta$ T cell development through thymic selection processes (Touma et al., 2006; Sasada et al., 2002). In the TCR α TM region, two evolutionarily conserved positively-charged amino acids - an arginine and a lysine, have been shown to contribute to its thermodynamic instability and the rapid degradation of unassembled TCR α chains (Haga-Friedman, Horovitz-Fried & Cohen, 2012; Soetandyo et al., 2010; Bonifacino, Cosson & Klausner, 1990). The same basic residues were also essential for the interactions between the TCR and CD3 components (Wucherpfennig et al., 2010; Call & Wucherpfennig, 2005). Similarly, the TCR β chain TM domain contains two evolutionarily conserved tyrosine residues that have been proposed to be crucial for TCR signal transduction and complex assembly (Kunjibettu et al., 2001). The presence of another residue, Lysine 271, in the TM region may have a critical role in the association and stabilisation of the signalling complex (Alcover et al., 1990).

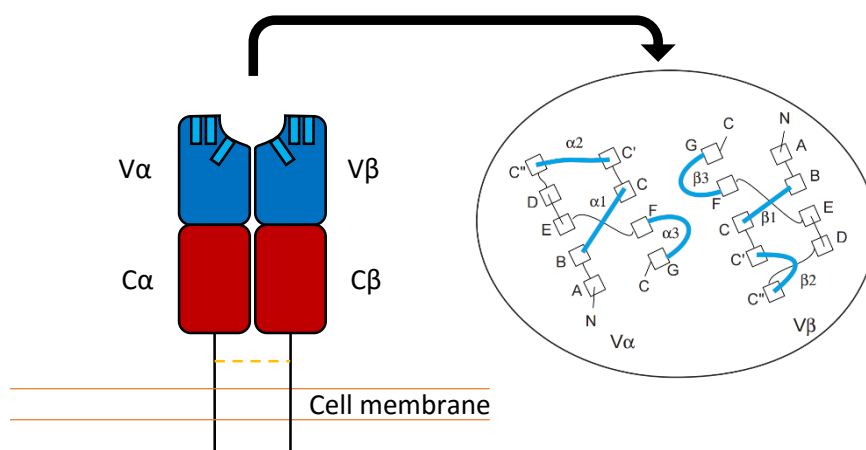


Figure 1.2. Schematic representation of $\alpha\beta$ TCR structure. The TCR comprises of a heterodimer of disulphide-linked α and β chains. Each chain is composed of a Variable (V; blue), with three CDRs (light blue), and a Constant (C; red) domain, followed by a transmembrane region and a short cytoplasmic tail. The diagram on the right represents the TCR antigen-binding site. The squares represent the top of the β strands that form the variable domains and are labelled accordingly. The blue lines represent the CDR loops; the black lines represent other non-CDR links between β strands. Diagram is adapted from Al-Lazikani et al., (2000).

1.5.2. Organisation of the $\alpha\beta$ TCR gene loci and potential diversity

A hallmark of the adaptive immunity is the intrinsic ability to generate a diverse TCR repertoire in order to respond to a plethora of potentially harmful antigens. Accordingly, TCR diversity is achieved through three main processes during thymocyte development: (a) somatic gene recombination, which facilitates the production of an extensive array of clonally variable receptors from a limited set of genes, (b) imprecise joining of the coding ends during gene recombination, and (c) combinatorial diversity, the pairing of different V domains within TCR α and TCR β chains (Turner et al., 2006; Al-Lazikani, Lesk & Chothia, 2000). The TCR α chain is constructed from the recombination of numerous variable (V) and joining (J) gene segments, juxtaposed to a constant (C) segment. Gene recombination at the TCR β locus is similar, with an additional diversity (D) segment inserted in between the V and J gene segments, and one of two C-segments utilised for a complete TCR β chain.

In the human genome, the TCR α locus is located on chromosome 14 and comprises a total of 96 functional V, J and C gene segments. The human TCR β locus found on chromosome 7 contains 64 functional V, D, J and C segments. The mouse loci for TCR α on chromosome 14 and TCR β on chromosome 6 are composed of a total of 123 and 37 functional gene segments respectively (Bosc & Lefranc, 2003). Both TCR gene loci are detailed in Table 1.1 below.

Table 1.1. Number of functional TCR gene segments encoded in the human and mouse genome. Data is based on IMGT website database.

Species	TCR Chain	V-segments	D-segments	J-segments	C-segments	Total
Human	TCR α	45	-	50	1	96
	TCR β	47	2	13	2	64
Mouse	TCR α	84	-	38	1	123
	TCR β	22	2	11	2	37

The focal point of TCR diversity is manifested within the 6 highly flexible CDRs in both TCR chains (Godfrey, Rossjohn & McCluskey, 2008). The CDR1 and CDR2 loops are encoded in the germline by the TCR α and TCR β V gene segments. By contrast, the CDR3 is hypervariable as a result of a combination of different V, (D) and J gene segments and random nucleotide addition and deletion at the junction between these segments (Attaf et al., 2015). V(D)J recombination determines both the length and the identity of the amino acid residues present within the CDR3 loops (Stadinski et al., 2014). As a result, much of the unique amino acid sequences found in the TCR are present within the CDR3 loop. The CDR3 residues have also shown to contribute to a large portion of the TCR binding site including MHC contacts, resulting in minimal involvement of the CDR1 and CDR2 loops (Bulek et al., 2012; Gras et al.,

2012; Borg et al., 2005). Thus the CDR3 loop may have a significant role in defining both the T cell peptide and MHC specificity (Stadinski et al., 2014).

During T cell development in the thymus, a theoretically large TCR repertoire of up to $\sim 10^{15}$ unique TCRs can be generated in the mouse (Davis & Bjorkman, 1988). Deep sequencing analysis has revealed that the actual number may more likely be around 10^{11} different TCRs (Robins et al., 2010). The theoretical number of possible TCRs in humans is projected to be much larger since humans possess a higher number of TCR β variable genes compared to mice (Sewell, 2012; Lefranc et al., 2009). From the pre-selection repertoire, TCRs that bind to self-pMHC with appropriate affinities are positively selected, while TCRs that bind too strongly are clonally deleted during negative selection (Goldrath & Bevan, 1999; Stockinger, 1999). Hence, the number of unique TCR β CDR3 sequences expressed in the peripheral blood lymphocytes of a healthy adult is estimated to be around $\sim 3 \times 10^6$ (Warren et al., 2011; Robins et al., 2010). The consequence of thymic selection is the absence of strong binding interactions which facilitate the prevention of autoimmunity. However, efficient tumour recognition is also prevented since most tumours are self-derived (Gattinoni et al., 2006; Boon, Coulie & Van Den Eynde, 1997; Kawakami et al., 1994).

1.5.3. V(D)J Recombination

V(D)J recombination is the central process which assembles functional TCR chains and generates antigen receptor diversity during T cell development. In both B and T cells, V(D)J recombination is initiated by the RAG recombinase, a lymphoid-specific endonucleolytic complex encoded by the *RAG1* and *RAG2* genes. RAG recognises and cleaves genomic DNA at highly conserved recombination signal sequences (RSS) flanking the 3' end of the V, the 5' end of the J and both ends of the D-segments. The RSS is composed of two conserved sequences, a palindromic heptamer residing adjacent to the encoding gene segment, and an A/T-rich nonamer. The heptamer and nonamer are separated by a non-conserved linker of either 12 or 23 base pairs (Schatz & Ji, 2011). The V-segments exclusively contain a 3'-7/23/9 RSS and J-segments a 5'-9/12/7 RSS. The D-segments contain both 5'-9/12/7 and 3'-7/23/9 RSSs on either ends (Figure 1.4A, B).

The recombination machinery is governed by the 12/23 rule, which means only RSSs with dissimilar sized linkers can recombine efficiently. Generally, an RSS with a 12-nucleotide linker may only fuse with an RSS with a 23-nucleotide linker and vice versa (Swanson, 2004). This mechanism prevents non-productive rearrangement of V or J genes within their own clusters and ensures the obligatory inclusion of the D β segment between the V β and J β segments in the correct orientation (Olaru, Petrie

& Livák, 2005; Sleckman et al., 2000). Moreover, the assembly of the TCR β V domain occurs via an ordered two-step process, in which D β and J β gene rearrangement precedes the recombination of V β to the D β -J β fusion segment (Figure 1.3; Schatz & Ji, 2011; Ferrier et al., 1990; Born et al., 1985).

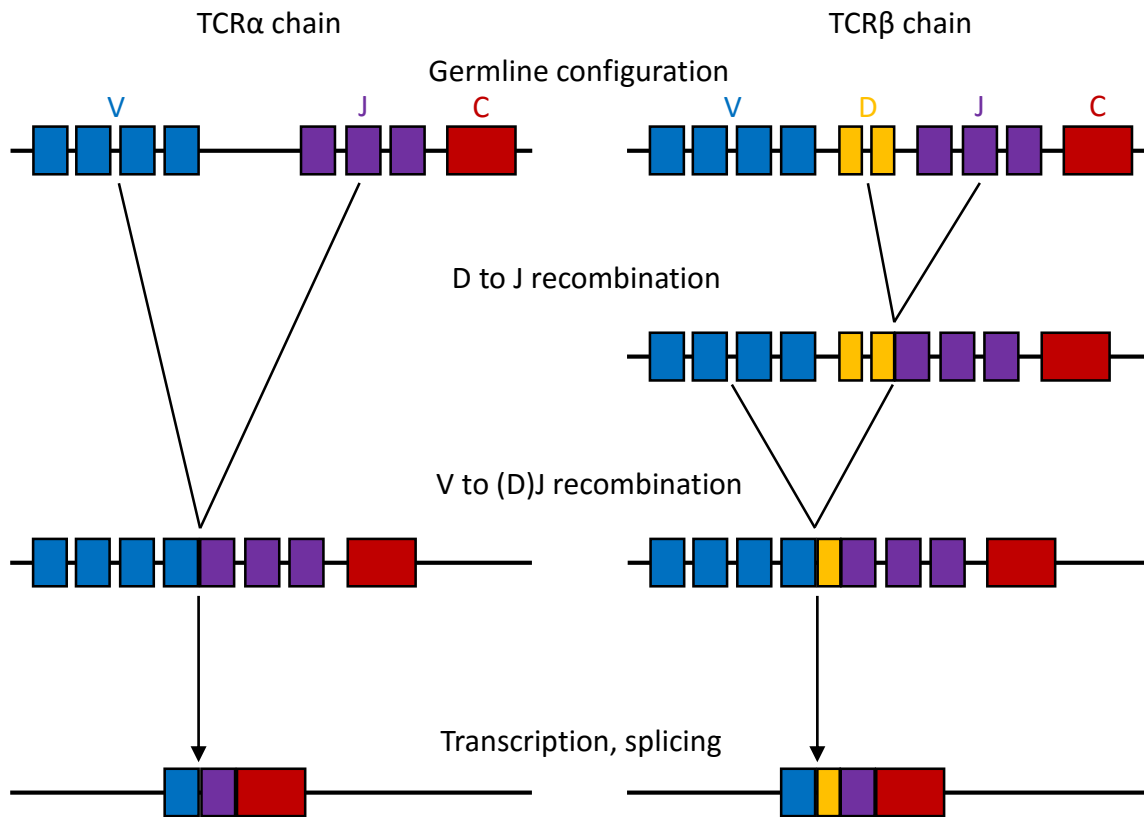


Figure 1.3. Generation of combinatorial diversity by V(D)J recombination. The TCR α and β chains are assembled from separate variable (V), diversity (D), junctional (J) and constant (C) gene segments. During thymocyte development, gene recombination machinery associates these gene segments together to form rearranged TCR α and β chain transcripts. Adapted from Schatz and Ji, (2011).

RAG1 is the principal DNA-binding component and contains most of the residues that catalyse the DNA cleavage process. RAG2 enhances the engagement of RAG1 with the heptamer of the RSS, and is a crucial cofactor for DNA cleavage (Swanson, 2004; Fugmann & Schatz, 2001). RSS recognition is proposed to occur via a capture model where the RAG complex binds to one RSS to form the signal complex, and subsequently captures a second different-sized RSS that lacks bound proteins. This forms the synaptic or paired complex (Mundy et al., 2002; Jones & Gellert, 2002). Cleavage of the DNA occurs in a two-step process: RAG first introduces a single strand nick between the heptamer and the gene segment. The free 3' hydroxyl group that is produced then attacks the phosphodiester bond of the

other strand to complete a DNA double strand break. The DNA break is sealed covalently at the end of the gene segment, resulting in the formation of a hairpin loop. Hairpin formation only occurs in the paired complex and is thought to take place simultaneously at the two RSSs. The single-stranded DNA nicking is less tightly regulated and can occur in the signal or paired complex (Swanson, 2004; Jones & Gellert, 2002).

After hairpin formation, the coding ends and the blunt 5' phosphorylated signal ends remain associated with the RAG complex, constituting a transitory structure called the 'post-cleavage complex' (Hiom & Gellert, 1998; Agrawal & Schatz, 1997). The RAG complex also recruits high mobility group (HMG) proteins of the HMG-box family (HMGB1 and HMGB2) for the binding of two RSS signal ends together. The HMG proteins interact with the nonamer-binding domain of RAG1 in the absence of DNA and enhance its intrinsic DNA-bending activity (Štros, 2010; Aidinis et al., 1999). The DNA coding ends are re-joined following RAG-mediated recruitment of a group of ubiquitous DNA repair enzymes, most of which facilitate the classical non-homologous end joining (NHEJ) repair pathway (Cui & Meek, 2007; Lee et al., 2004). The NHEJ components include Ku70, Ku80, DNA-dependent protein kinase catalytic subunit (DNA-PKcs), XRCC4, XLF and DNA ligase IV (Wyman & Kanaar, 2006). The Ku70 and Ku80 proteins form a heterodimer that specifically binds DNA ends via a preformed ring that can encircle DNA (Downs & Jackson, 2004; Walker, Corpina & Goldberg, 2001). The Ku70/80 dimer functions to recruit DNA repair kinase DNA-PKcs, which subsequently induces inward translocation of the Ku molecule by about one helical turn, allowing accessibility of other proteins (Rivera-Calzada et al., 2006; Yoo & Dynan, 1999). The final step of re-joining the DNA ends is mediated by ATP-dependent DNA ligase IV, which associates with a dimer of XRCC4 (Modesti et al., 2003; Lee et al., 2000). XRCC4 can interact with DNA and functions to stabilise the ligase and stimulate its adenylation and ligase activity (Bryans, Valenzano & Stamato, 1999; Modesti, Hesse & Gellert, 1999; Grawunder et al., 1998). XLF, a XRCC4-like factor also called Cernunnos, is recruited by Ku and promotes the ligation activity of DNA ligase IV towards non-compatible DNA ends (Mahaney, Meek & Lees-Miller, 2009; Yano et al., 2007; Ahnesorg, Smith & Jackson, 2006).

The initiation of V(D)J recombination is regulated at three distinct levels. Firstly, the RAG proteins are expressed at high levels only during specific stages of lymphocyte development: at the DN2-DN4 stages for TCR β gene recombination, and DP stage for TCR α . In particular, RAG activity is restricted to the G1 phase of the cell cycle since RAG2 is phosphorylated and degraded as cells enter S-phase (Desiderio, Lin & Li, 1996). This ensures that the reaction does not occur at other cell types or outside the T cell developmental stages, which may otherwise be detrimental to the cell stability. Second, the initiation of gene recombination by RAG is modulated by the accessibility of the RSSs within the chromatin (Yancopoulos & Alt, 1985). Lastly, V(D)J recombination efficiency is regulated by the spatial

location and conformation of the TCR loci in the nucleus, with chromosome looping and condensation proposed to facilitate recombination between widely spaced gene segments. *Cis*-acting transcriptional regulatory components such as promoters and enhancers mediate the alterations in DNA methylation, chromatin structure and nuclear positioning that affect ability of RAG to engage with the appropriate regions of the TCR gene loci (Schatz & Ji, 2011; Cobb et al., 2006; Dudley et al., 2005).

1.5.3. Junctional diversity

Junctional diversity is a key event during V(D)J recombination which amplifies the possible number of unique TCRs in the pre-selection repertoire. This phenomenon is initiated by the opening of the hairpin loop at the DNA coding ends, which facilitates the addition and deletion of random nucleotides at the recombination junctions. The hairpins of the coding ends are opened by the endonuclease activity of the Artemis:DNA-PKcs complex (Chang, Watanabe & Lieber, 2015; Lu, Schwarz & Lieber, 2007). Artemis alone has an inherent 5'-3' exonuclease activity on single-stranded DNA (Li et al., 2014). Upon association with DNA-PKcs, a serine/threonine protein kinase, Artemis is phosphorylated, thereby activating its 5'-3' endonuclease activity (Gu et al., 2010; Goodarzi et al., 2006; Ma et al., 2002). The Artemis:DNA-PKcs complex generally resects 5' and 3' DNA overhangs, to create DNA end structures that can be ligated by the DNA ligase IV/XRCC4 complex (Gu et al., 2006; Ma et al., 2002).

However, when processing DNA hairpins, it preferentially generates an asymmetric opening from nicking a few nucleotides away from the terminus, resulting in one DNA strand that is longer than the other (Ma, Schwarz & Lieber, 2005; Ma et al., 2002). The shorter strand is extended by the addition of nucleotides complementary to the longer strand, resulting in the insertion of palindromic (P) nucleotides at the coding junctions by DNA repair enzymes (Dudley et al., 2005). Template-independent polymerases, such as Terminal deoxynucleotidyl transferase (TdT) and DNA polymerase μ modify these junctions by promoting the addition of non-templated (N) nucleotides to the 3' single-stranded coding ends (Helmink & Sleckman, 2012; Motea & Berdis, 2010). In addition, TdT may also exhibit 3'-5' exonuclease activity that could further contribute to joint diversification by nucleotide removal (Motea & Berdis, 2010). Lastly, the DNA ligase IV/XRCC4 complex joins the processed ends together to generate a continuous double-stranded DNA (Figure 1.4C).

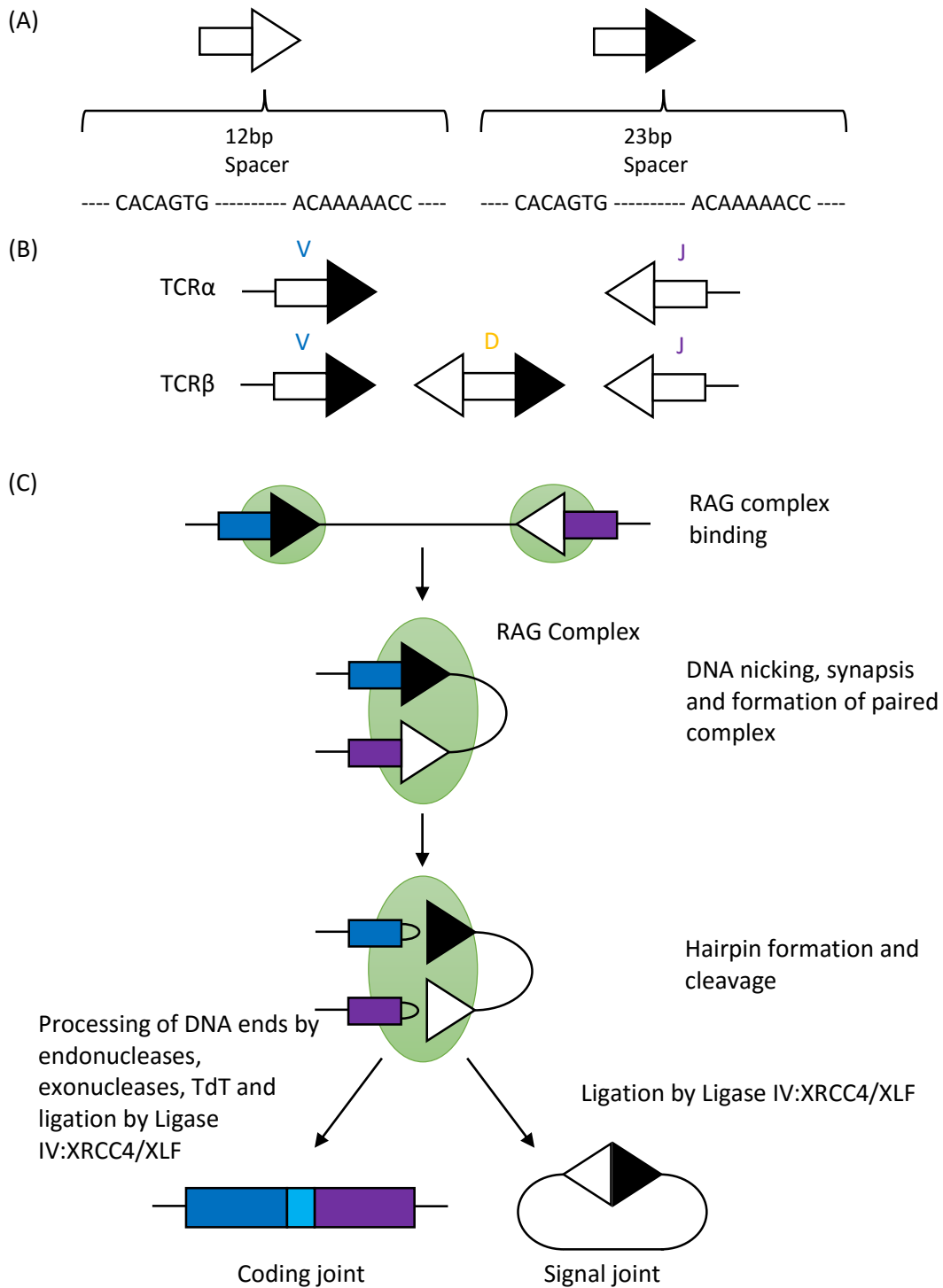


Figure 1.4. The mechanism of V(D)J recombination. (A) Recombination Signal Sequences (RSS). The RSS is composed of a heptamer adjacent to the encoding gene segment and a nonamer, separated by a non-conserved linker of either 12 or 23 base pairs. (B) Distribution of RSS flanking the gene segments. 23RSS flank the 3' end of V-segment and 12RSS in the 5' end of J-segment whereas 12RSS and 23RSS flank the 5' and 3' ends of the D-segment in TCRβ loci. (C) Schematic diagram of V(D)J recombination. 12RSS and 23RSS are brought together via a RAG complex where DNA nicks are introduced to form a hairpin loop at the end of the coding gene segments. These hairpin loops are then broken using endonucleases, and repaired and ligated by Ligase IV:XRCC4/XLF complexes. TdT and DNA Pol μ

contribute to junctional diversity by adding and/or removing nucleotides. Adapted from Nishana and Raghavan, (2012).

1.6. Conventional $\alpha\beta$ TCR ligands

1.6.1. Structure of the Major Histocompatibility Complex

The central interaction in cell-mediated adaptive immunity is between the $\alpha\beta$ TCR and the peptide fragment loaded onto specialised molecules called the major histocompatibility complex (MHC). In humans, the antigen-presenting MHC molecules are referred to as the human leukocyte antigen (HLA) whereas the mouse MHC are commonly termed as histocompatibility-2 (H2; Kulski et al., 2002). The classical MHC molecules are subdivided into MHC Class I (MHC-I) and MHC Class II (MHC-II), both of which are highly polymorphic. The classical MHC-I gene encode three classes in humans (HLA-A, HLA-B and HLA-C) and mice (H2-K, H2-D and H2-L). The MHC-II genes comprise three classes in humans (HLA-DR, HLA-DQ and HLA-DP) and two classes in mice (H2-A and H2-E). These gene loci are located on chromosome 6 and 17 in the human and mice genomes respectively (Miles et al., 2015; Miles, Douek & Price, 2011; Robinson et al., 2011).

Classical MHC-I molecules are heterodimeric glycoproteins composed of a membrane-spanning heavy α polypeptide chain that associates non-covalently with a single β 2-microglobulin subunit (β 2-m). The heavy α chain is composed of three domains: α 1 to α 3 (Figure 1.5A). The membrane-distal α 1 and α 2 domains are polymorphic, and form the peptide-binding groove composed of a β -sheet topped by two semi-parallel α -helices. Symmetry is achieved such that each domain contributes an α -helix and four strands of a β -sheet. The β 2-m forms the non-polymorphic membrane-proximal component of the protein along with the α 3 domain, which anchors the MHC-I molecule to the membrane via a hydrophobic TM stalk with a cytoplasmic tail (Adams & Luoma, 2013). In contrast to MHC-I, MHC-II molecules are assembled from the non-covalent association of relatively equivalent α and β chains consisting of two domains each (α 1, α 2; β 1, β 2; Figure 1.5B). The peptide-binding groove is constructed from the membrane-distal α 1 and β 1 domains, which fold into a seven-stranded β -sheet, flanked by two long α -helices. Both chains are also connected to the plasma membrane through TM stalks via the α 2 and β 2 domains (Rudolph, Stanfield & Wilson, 2006).

The majority of polymorphism in MHC molecules is concentrated in the residues within and around the peptide-binding groove, therefore maximising the possible number of peptides that the MHC can present. The peptides are bound to MHC via a series of chemically-distinct pockets within the peptide-binding groove, designated as A-F pockets in MHC-I and P1-P9 pockets in MHC-II (Rossjohn et al., 2015;

Adams & Luoma, 2013). The interaction between peptide and MHC is principally governed by primary anchor residues that are generally conserved at the N- and C-termini (Madura et al., 2015). The regions of the peptide that are exposed can directly contact the TCR, whereas the buried residues can indirectly alter TCR binding (Theodossis et al., 2010).

1.6.2. Antigen processing and presentation by MHC Class I

MHC Class I molecules are expressed at the cell surface of all nucleated cells and present short peptide fragments derived from endogenous proteins. The interaction of the $\alpha\beta$ TCR with pMHC-I ligands represents a valuable mechanism for T cells to inspect the intracellular proteome of the target cells and is pivotal in eliciting CD8⁺ T cell-mediated immunity. As such, this display system facilitates the eradication of cells that exhibit malignant cellular activity or express non-self, pathogen-derived proteins.

Peptides presented by MHC-I are primarily generated from the proteasome-mediated degradation of proteins in the cytoplasm. Standard proteasomes are expressed constitutively in nearly all cells. In response to IFN- γ stimulation under inflammatory conditions, the proteasome subunit composition changes from standard to “immunosubunits”. This subsequently assembles a specialised form of proteasome with altered peptide cleavage activity, called the immunoproteasome (McCarthy & Weinberg, 2015; Aki et al., 1994). After proteasome-mediated degradation, aminopeptidases in the cytosol or endoplasmic reticulum (ER) can further trim peptides into appropriate lengths necessary for MHC-I binding (Brouwenstijn, Serwold & Shastri, 2001; Stoltze et al., 2000; Craiu et al., 1997). The products of proteolysis are then translocated into the ER by an ER-based heterodimeric protein called the transporter associated with antigen processing (TAP). In the ER, nascent MHC-I molecules associate with ER chaperone proteins such as calreticulin, tapasin and ERp57 to form the peptide-loading complex (PLC). The PLC facilitates the loading of stabilising peptides into the peptide-binding groove, before expression on the cell surface (Hansen & Bouvier, 2009). Conversely, peptides and MHC-I molecules that fail to associate are returned to the cytosol for degradation (Neefjes et al., 2011).

MHC-I molecules possess a peptide-binding cleft, formed between the MHC-I $\alpha 1$ and $\alpha 2$ domain, with a closed configuration that is designed to support a single peptide fragment (Figure 1.5C). Consequently, antigen presentation by MHC-I is generally restricted to peptides of eight to 14 amino acids in length (Rossjohn et al., 2015). Due to this structural constraint, longer peptides (>10 amino acids) may adopt a bulging conformation, resulting in the exposure of peptide side chains that interact

directly with the TCR (Burrows, Rossjohn & McCluskey, 2006; Miles et al., 2005). Crystal structures of pMHC-I complexes have demonstrated that these bulged peptides, similar to peptides of normal length, are held at both termini and maintain highly conserved and energetically important contacts with the anchor residues within the MHC-I (Stewart-Jones et al., 2003; Speir et al., 2001; Guo et al., 1992). The central part of the bound peptide can either protrude with marked rigidity or display considerable flexibility (Tynan et al., 2005b; Tynan et al., 2005a; Probst-Kepper et al., 2004). A recent study has suggested that MHC-I-restricted T cells display an explicit preference for a single MHC-I-bound peptide of a defined length and that effective CD8⁺ T cell immunity can only be achieved by length-matched antigen-specific T cell clonotypes (Ekeruche-Makinde et al., 2012). Notably, the authors have proposed that every TCR is characterised by a unique “peptide-recognition signature” that is governed by: a preference for peptide length, the number of peptides that can be recognised at the preferred length, and the amino acid sequence of the peptides (Wooldridge, 2013).

1.6.3. Antigen processing and presentation by MHC Class II

In contrast to MHC-I, Class II MHC molecules predominantly present peptides derived from exogenous proteins and are mainly expressed on TECs and professional APCs, such as B cells, DCs and macrophages. Non-APCs, including mesenchymal stromal cells, fibroblasts, endothelial and epithelial cells can also express MHC-II molecules upon IFN- γ stimulation. The recognition of pMHC-II complexes typically leads to the activation of CD4⁺ Th cells which coordinate antigen-specific humoral and cell-mediated immune responses (Neefjes et al., 2011; Reith, LeibundGut-Landmann & Waldburger, 2005). The MHC-II α 1- β 1 peptide-binding groove display an open-ended conformation which allows the binding of N- and C-terminally extended peptides of up to 30 amino acids in length (Figure 1.5D). The peptide backbone in MHC-II adopt a poly-proline type II conformation and reside deeper in the groove (Rudolph, Stanfield & Wilson, 2006; Stern et al., 1994). MHC-II-restricted peptides generally exhibit the central binding motif of nine ‘core’ residues that form an extensive hydrogen bond network with the binding groove. Additionally, peptide side chains also engage with allelic-specific pockets within the peptide-binding cleft. The differences between these allelic-specific pockets usually establish the binding motif that can be accommodated by different MHC-II alleles (Bhati et al., 2014; Stern et al., 1994; Brown et al., 1993).

Proteins, whether self or non-self, are internalised via phagocytosis or clathrin-dependent endocytosis and undergo degradation in the endosomal-lysosomal antigen-processing compartments (Roche & Furuta, 2015). These compartments are enriched in proteases/cathepsins and disulphide reductases, and maintain sufficiently low pH for optimal proteolytic activity (Blum, Wearsch & Cresswell, 2013;

Trombetta & Mellman, 2005; Neefjes, 1999). In these compartments, both internalised antigen proteolysis and pMHC-II complex formation takes place. The transmembrane MHC-II α and β chains are assembled in the ER and associate with a non-polymorphic chaperone protein, the invariant chain (Ii). The Ii chain functions to stabilise the newly synthesised MHC-II molecule, and direct the Ii-MHC-II complex to an endosomal-lysosomal compartment (Cresswell, 1996). MHC-II cannot bind to antigenic peptides until Ii is proteolytically degraded and dissociates from the Ii-MHC-II complex. Hence, Ii is gradually digested, leaving a residual class II-associated invariant chain peptide (CLIP) which remains bound to the peptide-binding groove of MHC-II. The enzyme HLA-DM (H2-DM in mice), regulated by HLA-DO (H2-DO), facilitates the removal of CLIP so that antigenic peptides can be loaded onto nascent MHC-II molecules (Denzin, 2013). The pMHC-II complex is only trafficked to the plasma membrane once CLIP is substituted and the MHC-II is stabilised with an endosomal peptide (Münz, 2012; Trombetta & Mellman, 2005).

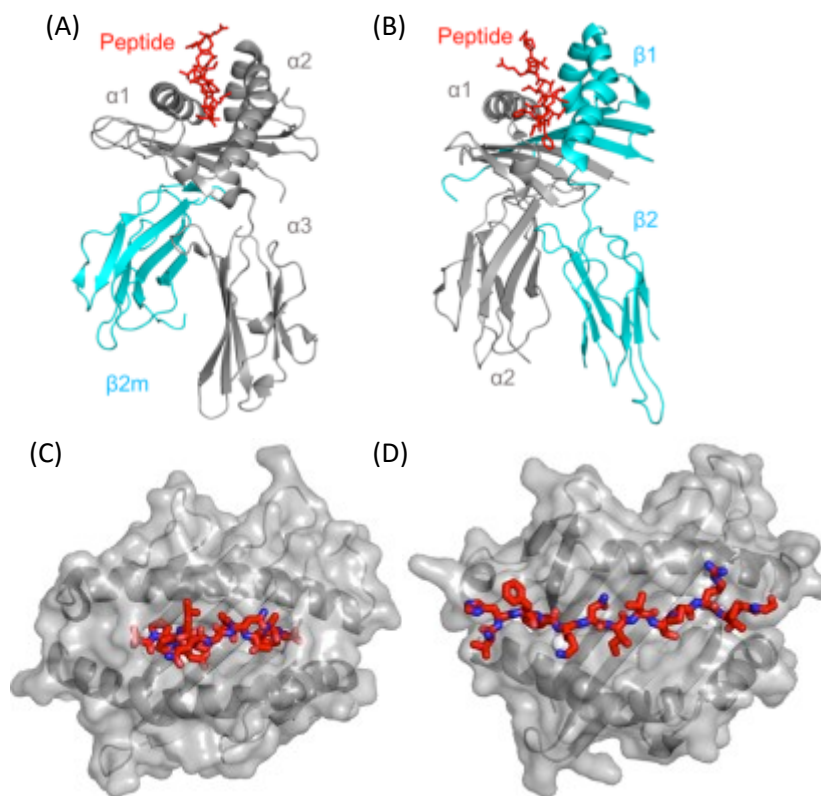


Figure 1.5. Crystal structure of peptide bound to MHC Class I and Class II. The two classes of MHC adopt similar overall structures despite different compositions. (A) MHC-I consists of a variable heavy chain (*grey*) folded with the invariant β 2-m molecule (*cyan*). (B) MHC-II is composed of an α -chain (*grey*) and β -chain (*cyan*). (C) The binding cleft in MHC-I has a closed configuration thereby limiting the size of the peptide (*red*) to 8-14 amino acids in length. (D) The MHC-II peptide-binding groove is open-

ended and enables longer peptides to form an elongated conformation with the peptide N- and C-termini extending outside the groove. Adapted from Attaf et al., (2015).

1.7. TCR-pMHC interactions

1.7.1. TCR signalling complex

TCR signalling is essential during multiple stages in the T cell lifecycle: for lineage commitment and thymic selection during development, the survival of naive T cells following emigration from the thymus, and for the differentiation of these cells into effector populations during an immune response (Call & Wucherpfennig, 2005). The signalling event relies on the participation of multiple membrane-spanning molecules surrounding the TCR microenvironment. In the $\alpha\beta$ T cell, the TCR signalling complex is comprised of the non-covalent association between the clonotypic $\alpha\beta$ TCR heterodimer for antigen recognition and the invariant CD3 subunits for signal transduction (Rossjohn et al., 2015).

The TCR α and β chains possess short cytoplasmic tails without signalling motifs, hence signal transmission is mediated via immunoreceptor tyrosine-based activation motifs (ITAMs) in the cytoplasmic domains of the TCR-associated CD3 subunits (Call & Wucherpfennig, 2005; Arnaud et al., 1997). The signal-transducing CD3 component is assembled from three distinct disulphide-linked dimers: CD3 $\gamma\epsilon$, CD3 $\delta\epsilon$ and CD3 $\zeta\zeta$ (Kuhns & Badgandi, 2012; Wucherpfennig et al., 2010). Upon TCR-pMHC engagement, the cytoplasmic ITAM motifs in the CD3 dimers are phosphorylated by the Src-family kinase Lck, constituting the earliest detectable biochemical consequence of TCR ligation (Wucherpfennig et al., 2010; Weiss & Littman, 1994). Each ITAM has two tyrosines and two aliphatic residues separated by six to twelve amino acids (Yxx[L/I]_{X(6-12)}Yxx[L/I]). Phosphorylation of both tyrosines by Lck facilitates docking for Src homology 2 domain (SH2)-containing proteins such as ZAP-70, which mediates further downstream signalling for T cell activation (Machida & Mayer, 2005; Hatada et al., 1995). Similar to the TCR, CD3 $\gamma\epsilon$ and CD3 $\delta\epsilon$ heterodimers are formed through disulphide interactions between two β strands in their extracellular Ig domains (Sun et al., 2004; Kjer-Nielsen et al., 2004; Arnett, Harrison & Wiley, 2004; Sun et al., 2001). In contrast, the CD3 $\zeta\zeta$ homodimer, which exhibit a very small ectodomain of nine amino acids, are linked predominantly via contacts within the TM domain (Call & Wucherpfennig, 2005; Call et al., 2002).

In humans and mice, the $\alpha\beta$ TCR-CD3 signalling complex exists in a 1:1:1:1 stoichiometry for the $\alpha\beta$ TCR:CD3 $\gamma\epsilon$:CD3 $\delta\epsilon$:CD3 $\zeta\zeta$ dimers, although higher-order stoichiometry have also been described (Schamel et al., 2005). The composition of the pre-TCR and $\gamma\delta$ TCR signalling complexes differ from $\alpha\beta$ TCR. Mice deficient in CD3 γ , CD3 ϵ or CD3 ζ subunits show a near-complete arrest at the DN stage

during thymocyte development, the point where pre-TCR signalling is required for further progression (Dave, 2009). However, in CD3 δ -deficient mice, thymocyte development proceeded to the DP stage, suggesting the pre-TCR was functionally intact, and the $\gamma\delta$ T cells were unperturbed (Dave et al., 1997). Collectively, these studies suggest CD3 γ , CD3 ϵ and CD3 ζ are necessary for all developmental stage and T cell lineages, whereas the CD3 δ subunit may be dispensable for pre-TCR and $\gamma\delta$ T cell function in mice. Indeed, murine $\gamma\delta$ T cells have been shown to lack CD3 $\delta\epsilon$, yielding a stoichiometry where there are only two CD3 $\gamma\epsilon$ and one CD3 $\zeta\zeta$ for every $\gamma\delta$ TCR (Hayes & Love, 2006). In contrast, the human $\gamma\delta$ TCR incorporates CD3 $\delta\epsilon$ (Siegers et al., 2007).

The TCR and CD3 domains are connected via the basic and acidic residues in their respective TM regions and their ectodomain interactions are thought to contribute to TCR-CD3 specificity (Call & Wucherpfennig, 2005; Call & Wucherpfennig, 2004; Cosson et al., 1991). Three basic residues are located in the TM region of the TCR heterodimer: two in TCR α and one in TCR β . Conversely, each CD3 subunit contains a single aspartic or glutamic acid in their TM domains, creating a pair of acidic residues in each dimeric molecule. The TCR α chain associates with CD3 $\delta\epsilon$ and TCR β with CD3 $\gamma\epsilon$ through lysine residues positioned near the centre of their TM domains. Additionally, TCR α associates with the aspartic acid pair of the CD3 $\zeta\zeta$ homodimer through an arginine residue in the N-terminal third of the TM domain (Call, Pyrdol & Wucherpfennig, 2004; Call et al., 2002). The identity and relative positions of the three basic TM residues are fully conserved among the pre-TCR, $\alpha\beta$ TCR and $\gamma\delta$ TCR, implying a similar assembly mechanism for all TCR forms (Wucherpfennig et al., 2010; Call et al., 2002).

1.7.2. Co-receptors

In addition to cognate TCRs, the MHC molecules are recognised by their respective co-receptors CD4 and CD8. CD4 and CD8 are Type I integral membrane glycoproteins expressed by MHC-II-restricted Th and MHC-I-restricted cytotoxic T cells, respectively, but lack the peptide specificity of the TCR (Germain, 2002).

CD4 consists of four extracellular Ig-like domains (D1 to D4), a TM region and a short cytoplasmic tail (Moldovan et al., 2002). The backbone of the Ig domains are assembled from seven β strands which form two β sheets (Wouters, Lau & Hogg, 2004; Brady et al., 1993). CD4 exists in three different forms on the cell surface, defined by the state of the D2 cysteine residues: an oxidised monomer, a reduced monomer and a covalent dimer linked through the D2 cysteines. The D1 and D4 disulphides are conventional cross-sheet Ig disulphides, while the D2 is unusual in that it forms a 'cross-strand' disulphide bond which links adjacent strands within the same β sheet (Wouters, Lau & Hogg, 2004).

The D2 cross-strand is cleaved on the cell surface by thioredoxin, which is a thiol-disulphide oxidoreductase secreted by CD4⁺ T cells (Matthias et al., 2002; Tagaya et al., 1989). Cleavage of the D2 bond leads to the formation of disulphide-linked homodimers of CD4 connected via the D2 cysteines (Maekawa et al., 2006; Lynch et al., 2003). The disulphide-linked dimer is the preferred immune co-receptor for binding to APCs, whereas HIV enters susceptible cells through the monomeric reduced CD4 form (Azimi et al., 2010; Maekawa et al., 2006).

Two isoforms of CD8 have been identified: disulphide-linked CD8 $\alpha\beta$ heterodimers or a CD8 $\alpha\alpha$ homodimers, which differ in their expression and function (Gangadharan & Cheroutre, 2004). The CD8 $\alpha\beta$ isoform serves as the true $\alpha\beta$ TCR co-receptor to enhance the functional avidity and is constitutively expressed on MHC-I-restricted T cells. In comparison, the CD8 $\alpha\alpha$ homodimer identifies populations of T cells distinct from conventional MHC-restricted CD4⁺ or CD8 $\alpha\beta$ ⁺ T cells, and are expressed predominantly in intraepithelial lymphocytes (Cheroutre, 2004). Despite insignificant sequence homology between the CD8 α and CD8 β subunits, crystal structure analysis of the CD8 homodimer and heterodimer ectodomains demonstrated striking resemblance in size, shape and surface electrostatic potential of CDRs of their paired Ig variable region-like domains (Chang et al., 2005; Devine & Kavathas, 1999). BIAcore binding data have indicated that soluble forms of both CD8 $\alpha\beta$ and CD8 $\alpha\alpha$ have similar affinity for classical MHC-I (Kern et al., 1999; Garcia et al., 1996b). However, when expressed as cell surface molecules, the coordinated binding of CD8 $\alpha\beta$ with TCR-engaged MHC-I is much stronger than membrane-bound CD8 $\alpha\alpha$ (Bosselut et al., 2000; Witte, Spoerl & Chang, 1999). Collectively, these observations imply that the CD8 β ectodomain and/or TM and cytoplasmic regions significantly contribute to enhance CD8-MHC interactions (Cheroutre & Lambolez, 2008). Furthermore, CD8 $\alpha\alpha$ has been described as a co-repressor that negatively regulates T cell activation (Cheroutre & Lambolez, 2008; Denning et al., 2007; Gangadharan et al., 2006).

The MHC binding sites for the CD4 and CD8 co-receptors differ from the peptide-binding domains that are recognised by the TCR, permitting both TCR and co-receptor to simultaneously bind to a single MHC molecule (Rudolph & Wilson, 2002; Gao et al., 1997). Structural analyses of CD8 $\alpha\alpha$ -MHC co-crystals have shown remarkable asymmetrical interaction where one CD8 α chain (CD8 α 1) contributes most MHC contact, binding primarily to the α 3 domain of the MHC-I molecules, with smaller interactions with β 2-m and α 2 domains, and the other CD8 α 2 subunit provides some contact with the α 3 domain only (Rudolph, Stanfield & Wilson, 2006; Kern et al., 1999; Gao et al., 1997). The specific binding site of the CD8 β subunit is not clear, but is proposed to be analogous to the asymmetric interaction of CD8 $\alpha\alpha$ homodimers, occupying either the CD8 α 1 or CD8 α 2 position (Cheroutre & Lambolez, 2008). While both domains of CD8 dimers cooperate to bind to MHC-I, only the N-terminal variable-like D1 domain of CD4 contacts the concavity between the non-polymorphic MHC-II α 2 and

β 2 domains, with the second tandem CD4 domain being distal to the interface (Rudolph, Stanfield & Wilson, 2006).

The binding of co-receptors to MHC molecules is thought to augment T cell antigen sensitivity (triggering threshold) and response to ligands primarily through the recruitment of essential kinases to the intracellular portion of the TCR-CD3 signalling complex (Artyomov et al., 2010; Li et al., 2004; Purbhoo et al., 2001). The critical role of Lck kinase association with the cytoplasmic tails of co-receptors in triggering T cell activation has been elucidated. Indeed, co-receptor-bound Lck mediates phosphorylation of ITAM motifs in the cytoplasmic tails of CD3 which is an essential initiation step for T cell signalling (Nika et al., 2010; Veillette et al., 1988). Additionally, the CD8 co-receptor facilitates enhancement of the TCR-pMHC-I association rate (Laugel et al., 2007; van den Berg et al., 2007; Gakamsky et al., 2005; Pecht & Gakamsky, 2005), and the stabilisation of TCR-pMHC-I interactions (Wooldridge et al., 2005; Luescher et al., 1995). In contrast, CD4 does not stabilise interactions of TCR with pMHC-II complexes (Huppa et al., 2010; Hamad et al., 1998).

In addition to TCR and co-receptor engagement with pMHC, the classical two-signal hypothesis posits that a secondary stimulus is necessary for T cell activation. Two receptors have been described to regulate this specific signal: the co-stimulatory CD28 and the co-inhibitory CTLA4 (cytotoxic T lymphocyte antigen 4) proteins. CD28 is constitutively expressed on Th and cytotoxic T cells, and provides an essential co-stimulatory signal for cell growth and survival following binding with B7-1 (CD80) and B7-2 (CD86) on APCs (Rudd, Taylor & Schneider, 2009). Conversely, CTLA4 is induced upon T cell activation and functions to inhibit immune responses by engaging in competitive binding with CD28 (Yao et al., 2011). When CTLA4 is upregulated, expression of CD28 is reduced by endocytosis (Rudd, Taylor & Schneider, 2009). Together, the modulation of CD28 and CTLA4 expression on T cells provide a regulatory mechanism which promotes T cell responses against non-self and tumour antigens and suppresses excessive and autoreactive responses (Chen & Flies, 2013).

1.7.3. TCR-pMHC binding geometry

Structural studies of TCRs in their free and MHC-bound states have demonstrated that the TCR-pMHC interaction abides to certain 'rules of engagement' (Attaf et al., 2015). Most human and mouse complexes exhibit a typical binding mode, which maximises the contact between the $\alpha\beta$ TCR and the MHC-bound peptide (Rudolph, Stanfield & Wilson, 2006; Garcia et al., 1996a; Garboczi et al., 1996). Generally, the hypervariable CDR3 loops bind to the peptide and the germline-encoded CDR1 and CDR2 primarily engage with the MHC molecule (Rossjohn et al., 2015). However, the CDR1 α and

CDR1 β loops frequently contribute to peptide recognition by binding over the N-terminal and C-terminal peptide regions respectively. Further, the CDR3 loops can also contribute to MHC binding and stabilise the TCR-pMHC complex (Wucherpfennig et al., 2010; Borg et al., 2005; Wu et al., 2002). Upon MHC ligation, the CDR3 loops undergo conformational change, which may indicate involvement in TCR cross-reactivity (Rudolph, Stanfield & Wilson, 2006; Lee et al., 2004). Studies have also shown that the germline loops can make variable contributions to TCR-pMHC engagement. In some cases, CDR1 and CDR2 are responsible for most of the total interaction energetics, whereas in others, the CDR3 loops are energetically dominant (Godfrey, Rossjohn & McCluskey, 2008).

Crystal structures of TCR-pMHC complexes have also revealed that TCRs engage with pMHC ligands in an approximately diagonal or orthogonal docking geometry whereby the TCR crosses the long axis of the MHC peptide-binding groove at a semi-conserved angle (ranging 22°-87°; Rudolph, Stanfield & Wilson, 2006). In this binding orientation, the TCR β chain resides over the α 1 helix of the MHC and the TCR α chain is positioned over the other MHC helix (α 2 in MHC-I, corresponding to β 1 of MHC-II; Rossjohn et al., 2015; Adams et al., 2011; Rudolph, Stanfield & Wilson, 2006). Several theories have been proposed to explain the invariant orientation. Particularly, the presence of key amino acids in the germline CDRs or the absence of blocking amino acids on MHC has been suggested to contribute to this stable polarity (Feng et al., 2007; Mazza & Malissen, 2007). Some amino acids in the CDR1 and CDR2 loops have shown a preference to bind to an MHC α -helix region that forms a cup. Their location on the MHC surface may also be responsible for the docking angle. The vital regions of the TCR on the MHC surface are commonly in the same position engaging peptide amino acids 4 to 6 in MHC-I and peptide amino acid 5 in MHC-II (Marrack et al., 2008). Extrinsic factors such as co-receptor steric influences or CDR3-mediated peptide selection during thymic selection can also be important determinants of the TCR-pMHC binding mode (Collins & Riddle, 2008; Huseby et al., 2005; Buslepp et al., 2003). Further, the N-terminus of the peptide can be involved in the interface with the TCR (Madura et al., 2015). Consequently, the TCR-pMHC docking geometry is considered to influence the other components of the TCR-signalling complex, such as the CD4 and CD8 co-receptors, and may likely affect efficiency of T cell signalling (Rudolph, Stanfield & Wilson, 2006).

1.7.4. TCR cross-reactivity

The clonal selection theory proposed that individual T lymphocytes are specific for a single pMHC antigen (Sewell, 2012). However, although a large repertoire of TCRs is generated as a result of combinatorial and junctional diversity, the theoretical number of possible antigen receptors is dwarfed by the vast array of potential antigens that can be encountered (Mason, 1998). Unlike the

BCR, the protein sequence of the TCR remains fixed after thymocyte development, and the TCR is not thought to undergo affinity maturation. The native T cell repertoire is expected to be able to respond to a majority of foreign antigens despite having never encountering them before and being unable to adapt to them at a protein sequence level (Sewell, 2012). Hence, each TCR is evoked to be inherently highly cross-reactive. Indeed, comprehensive analysis of TCR cross-reactivity demonstrated that a single TCR can recognise more than one million different peptides of a defined length presented in the context of a single MHC-I molecule (Wooldridge et al., 2012). TCRs are further able to recognise with high frequency distinct peptides presented by non-self MHC, known as alloreactivity (Felix & Allen, 2007). Additionally, a single TCR has shown to bind to both pMHC-I and pMHC-II ligands (Stadinski et al., 2011; Yin et al., 2011; Rist et al., 2009). This remarkable binding plasticity is achieved through a number of different molecular mechanisms, where the TCR can adopt either a rigid and focused mechanism or change the conformation of the flexible CDR loops (Bulek et al., 2012; Yin & Mariuzza, 2009; Garcia, Teyton & Wilson, 1999).

The intrinsic ability of TCRs to exhibit cross-reactivity has a number of important implications, both positive and negative. Firstly, it facilitates effective immune cover by a limited number of TCRs against a virtually unlimited number of foreign peptides that can bind to self-MHC molecules. Second, far fewer T cells are needed to inspect a cell presenting a foreign or malignant peptide to trigger an immune response, ensuring a more rapid response rate. The idea of extensive TCR cross-reactivity also implies that each peptide can be recognised by several TCRs, and that T cell responses are polyclonal. Pathogens are less likely to escape immune recognition through altering their antigens, as mutations that escape one TCR may still be recognised by another. A further advantage of TCR cross-reactivity is heterologous immunity, where an individual T cell can target several infections through different peptides (Welsh & Selin, 2002). However, TCR cross-reactivity and heterologous reactivity can also result in severe immunopathology (Welsh et al., 2010). The heterologous immune modulation of the CD4⁺ and CD8⁺ T cell compartments may contribute to incomplete protection leading to increased pathogen load and disease progression (Sharma & Thomas, 2013). Notably, several studies have also reported the induction of autoimmunity by molecular mimicry, in which exogenous microbial peptides with sequence identity to self-peptides induce activation of self-reactive T cells (Wucherpfennig & Sethi, 2011). Further, the allorecognition of self-peptides on non-self (allogeneic) MHC poses a significant challenge to organ transplantation. This mechanism is likely to be responsible for the clinical rejection of MHC-mismatched organs following the transplantation procedure (Ely et al., 2008). As a result, transplant candidates and recipients are at increased risk of complications and required to take immunosuppressive drugs, which is associated with adverse side effects (Attaf et al., 2015; Noris et al., 2007).

1.8. MHC restriction

MHC restriction is an essential feature of $\alpha\beta$ T cells which dictates that TCRs only recognise antigens as peptide fragments bound to MHC molecules on the surface of APCs. The mechanism by which MHC restriction is imposed on the TCR repertoire remains debatable. Two principal hypotheses have been proposed to account for the focus of $\alpha\beta$ TCRs on MHC: the germline and selection models.

According to the germline model, MHC restriction is intrinsic to the TCR structure because TCR and MHC have co-evolved to conserve the germline-encoded TCR sequences with the ability to bind MHC, and have discarded those that lack MHC reactivity (Garcia et al., 2012; Yin, Wang & Mariuzza, 2012; Scott-Browne et al., 2011; Adams et al., 2011; Marrack et al., 2008; Feng et al., 2007). Specific amino acids in the germline-encoded CDR1 and CDR2 loops of the TCR α and β chains are conserved during evolution because they impose MHC reactivity on TCRs through specific contacts with the MHC α -helices that form the peptide-binding groove. As mentioned above, structural studies have provided evidence for recurrent interactions between MHC and the CDR1 and CDR2 loops (Garcia et al., 2012; Marrack et al., 2008; Rudolph, Stanfield & Wilson, 2006). Mutation of key amino acids within the CDR2 loops to alanine reduced interaction with MHC molecules and resulted in impaired development of the TCR repertoire (Scott-Browne et al., 2009). Conversely, mutations to the CDR3 sequences preserved MHC recognition, further supporting the notion that the conserved germline CDR loops play a predominant role in engaging with MHC (Rubtsova et al., 2009).

An alternative to the germline theory, the selection model posits that MHC restriction is not intrinsic to TCR structure but is imposed by CD4 or CD8 co-receptor engagement (Garcia et al., 2012; Yin, Wang & Mariuzza, 2012; Holland et al., 2012; Van Laethem, Tikhonova & Singer, 2012; Adams et al., 2011; Van Laethem et al., 2007). In this view, thymic selection is responsible for enriching the peripheral T cell repertoire with MHC-specific TCRs and purging the MHC-independent TCRs. During thymocyte development, the preselection DN thymocytes express $\alpha\beta$ TCRs that can recognise a diversity of ligands, both MHC and non-MHC, similar to antibodies. However, only TCRs with specificity for MHC and co-receptor signalling can mediate positive selection (Rangarajan & Mariuzza, 2014; Tikhonova et al., 2012). The critical role of the co-receptors is to recruit the Src tyrosine kinase Lck to the TCR-CD3 signalling complex following co-receptor binding to MHC. The targeted delivery of Lck occurs via its association with the cytoplasmic tail of CD4 or CD8. Only when MHC ligands are engaged will Lck be positioned and concentrated to initiate signalling through the phosphorylation of CD3 ITAMs. Thymocytes that express $\alpha\beta$ TCRs and co-receptors that do not recognise MHC cannot transduce intracellular signals via Lck and are not positively selected (Van Laethem, Tikhonova & Singer, 2012).

The study of mice deficient in MHC-I, MHC-II and co-receptors, designated as 'quad-deficient mice', demonstrated that selection of MHC-specific TCRs was strictly governed by the CD4 or CD8 co-receptors. The deletion of both co-receptors in MHC-deficient mice did not impair T cell signalling and allowed the selection of T cells with MHC-independent specificities. MHC-independent signalling was presumably triggered by intracellular, co-receptor-free Lck. These observations imply a dominant role for co-receptors in imprinting MHC bias in addition to promoting cell signalling (Van Laethem et al., 2007). Complementary work from our group indeed suggested that the TCR structure is not hardwired to engage with MHC ligands. TCRs lacking germline-encoded CDR1 and CDR2 loops via extensive *in vivo* diversification were still capable of engaging with MHC and directing thymic positive selection (Holland et al., 2012; Attaf et al., unpublished).

1.9. Therapeutic use of the $\alpha\beta$ TCR

Harnessing the potential of T cell immunity to direct immunotherapy represents a promising and effective approach for combating tumour antigens. Adoptive T cell therapy, which involves the isolation and *ex vivo* expansion of tumour-specific T cells before transfer into immunodepleted patients, has shown to mediate cancer regression in patients with malignant melanoma (Morgan et al., 2006). However, the generation of tumour-specific T cells via this strategy is often disadvantaged in part due thymic selection and TCR cross-reactivity. Thymic selection subjects the T cell repertoire to positive selection for TCRs with intermediate affinity while those exhibiting a much higher affinity are clonally deleted during negative selection (Goldrath & Bevan, 1999; Stockinger, 1999). Although this mechanism operates to prevent autoimmunity, the effective tumour recognition is limited as most tumour antigens are derived from normal self-peptides and over-expressed on tumour tissues (Gattinoni et al., 2006; Boon, Coulie & Van Den Eynde, 1997; Kawakami et al., 1994). Additionally, intrinsic T cell cross-reactivity which provides immune cover implies that an individual TCR-pMHC interaction is highly likely to be suboptimal (Sewell, 2012). Altogether, these factors complicate the isolation of effective high-affinity TCRs that mediate more effective tumour rejection for therapeutic purposes (Malecek et al., 2013; Cole et al., 2007).

Thus, recent advances have focused on improving the binding of any given TCR to its cognate antigen by engineering high-affinity TCRs *in vitro* using yeast, phage or mammalian T cell display systems as well as computational design (Malecek et al., 2013; Linette et al., 2013; Smethurst, 2013; Hawse et al., 2012; Chervin et al., 2009; Zhao et al., 2007; Weber et al., 2005; Kieke et al., 1999). The transfer of TCR genes incorporating these augmentations can provide patients with autologous T cells that are genetically enhanced with high-affinity TCRs for tumour immunotherapy (Tan et al., 2015). High-

affinity TCRs as soluble molecules to induce cancer regression further opens up the therapeutic benefits of TCRs (Li et al., 2005; Boulter et al., 2003; Holler et al., 2000). Soluble TCRs can be fused to other molecules, such as a CD3-specific Fab fragment to suppress tumour growth *in vivo* (Liddy et al., 2012). These bispecific T cell-engaging TCRs recruit polyclonal T cells via the CD3-specific Fab component but do not induce T cell activation by themselves. Once these molecules interact with a target cell surface, they become potent activators of tumour-specific T cell responses.

Even though such strategies show great potential, the development of such enhanced TCRs *in vitro* dictates that modified T cells carry a risk of being autoreactive. The absence of *in vivo* thymic selection prior to adoptive cell transfer allows the existence of self-reactive T cells which may cause host tissue damage. Indeed, a recent trial of a TCR specific for the protein melanoma-associated antigen (MAGE) underlined this serious problem. Following transfusion of T cells with an enhanced MAGE-specific TCR, two cancer patients had developed rapid and fatal heart disease. Subsequent studies revealed that the modified TCR was also capable of cross-reaction with MHC-I-bound peptide derived from the heart protein titin (Linette et al., 2013; Cameron et al., 2013).

1.10. Aims of the project

Adoptive cell therapy using TCR gene transfer is a promising strategy for targeting leukaemia and solid tumours (Heemskerk, 2010; Rosenberg et al., 2008), especially as the TCR can be modified for improved performance. The current techniques used involve engineering high-affinity TCRs *in vitro* using computational design, or yeast, phage or mammalian T cell display systems. However, the limitations of *in vitro* generation of high-affinity TCRs include the risk of creating autoreactive TCRs that may be deleterious to the host tissue. This study is a proof-of-principle study to functionally enhance TCR binding by employing a novel *in vivo* mutagenesis approach. This technique involves inserting a gene recombination cassette into the peptide-binding CDR3 region of established TCRs (Holland et al., 2012). The recombination cassette is composed of two distinct RSSs separated by a spacer. In this *in vivo* system, we induce the somatic V(D)J recombination machinery to cleave out this cassette, subsequently introducing junctional diversity via addition, deletion or substitution of random nucleotides in the targeted CDR loop. This generates a pre-selection repertoire that undergoes positive and negative selection before entering the periphery in a mature naïve state.

To test out novel diversifying technique, we utilise two existing TCR templates that recognise the epitopes of the male-specific HY minor histocompatibility antigen: the Marilyn and the MataHari TCRs, which are expressed natively in CD4⁺ and CD8⁺ T cells respectively (Perez-Diez et al., 2007; Valujskikh

et al., 2002). As the CDR3 region is responsible for engaging with the MHC-bound peptide fragment and naturally subject to hypervariability, we diversify each TCR by designing the recombination cassette into the centre of their respective CDR3 β loops. *In vivo* recombination is permitted through applying the diversifying TCR in retrogenic mice (Holst et al., 2006). The retrogenic methodology provides key advantages for the study, which includes facilitating rapid generation and analysis of TCR transgenic mice. This system also allows the generation of TCR variants that have auditioned for thymic selection which eliminates self-reactive cells, and produces MHC-restricted T cells that compete to be functionally 'immunodominant' instead of focusing solely on increased affinity.

In the thesis, we aim to address:

1. Design of the novel *in vivo* mutagenesis approach,
2. The feasibility of this technique through the generation of TCR variants and immunologically competent T cells,
3. The extent of the modifications introduced through the diversifying approach by sequence comparison between the TCR template and variants,
4. Whether TCRs lacking germline-encoded CDRs can still mediate TCR-pMHC interactions and result in MHC restriction.

Chapter 2

Chapter 2: Overview of the *in vivo* optimisation approach and design of the diversifying $\alpha\beta$ TCR constructs

2.1. Introduction

Most $\alpha\beta$ T cells recognise peptide-MHC molecules on APCs through an interaction mediated by the cell surface expressed TCR and co-receptor. The TCR is a heterodimer of an α and a β chain, with each chain comprised of a constant and variable domain. The constant domains anchor the TCR to the cell membrane and associate with the invariant CD3 signalling complex, whereas the variable domains confer the antigen-binding site (Rudolph, Stanfield & Wilson, 2006). Within each variable domain are three regions where sequence variability is concentrated, termed the hypervariable or complementarity-determining regions (CDR). CDR1 and CDR2 are encoded within the V gene segment and interact primarily with the MHC molecule, whereas the CDR3 binds mainly with the peptide antigen and is formed through the process of V(D)J recombination (Turner et al., 2006; Al-Lazikani, Lesk & Chothia, 2000).

V(D)J recombination is an essential mechanism for the development of T and B cells allowing formation of vast antigen receptor repertoires and the establishment of a functional adaptive immune system (Bassing, Swat & Alt, 2002). V(D)J recombination generates the variable domains of antigen receptors from assembly of one gene segment each from arrays of V, D and J gene segments during lymphocyte development (Chun et al., 1991). Gene rearrangement is directed by recombination signal sequences (RSS) that flank all V, D and J segments. RSS consist of relatively conserved heptamer and nonamer sequences that are separated by a spacer of either 12 or 23bp. Efficient recombination occurs between a pair of gene elements with RSS that have different spacer lengths, referred to as the 12/23 rule (Jung & Alt, 2004; Fugmann et al., 2000).

The recombination process is initiated by a pair of lymphoid-specific recombinase proteins RAG1 and RAG2, encoded by the recombinase-activating genes *RAG1* and *RAG2*, respectively. The RAG proteins, with the help of HMG proteins, associate a pair of dissimilar RSSs into a synaptic complex and generate double-stranded breaks between the RSSs and coding segments. Ubiquitously expressed components of the NHEJ pathway repair these DNA breaks, forming precise signal end joints and imprecise coding end joints (Bassing, Swat & Alt, 2002). Nucleotide deletion and TdT-mediated, non-templated nucleotide insertion leads to extensive diversification at the resulting coding joint in the CDR3. Productive rearrangement is vital because only in-frame VDJ junctions can allow the translation of a complete TCR chain structure. Combinatorial association of V, D and J segments, pairing of the TCR α

with TCR β chains, along with imprecise joining of the coding ends, produce the vast diversity of the T cell repertoire.

As such, the amino acid content in the CDR loops are major determinants of TCR binding specificity and affinity. Indeed, there have been many studies highlighting enhanced TCR binding through the substitution of the amino acid residues within the CDR loops. This includes the use of *in vitro* yeast (Weber et al., 2005; Holler et al., 2000) or phage (Li et al., 2005) display systems, as well as mammalian cell display (Chervin et al., 2008; Kessels et al., 2000). Understandably, the purpose of generating higher affinity TCR was to overcome the problems associated with malignant cells. T cells that develop in the thymus are selected on self-pMHC and their affinity for self must be sufficiently low in order to prevent autoimmunity upon release into the periphery (Gallegos & Bevan, 2006; Kappler, Roehm & Marrack, 1987). However, many self-antigens are expressed on tumour tissues, and the most effective T cells against these antigens would have been deleted during thymic selection (Chervin et al., 2008; Dudley & Rosenberg, 2003; Ho et al., 2003). The underlying problem of generating higher affinity TCRs is the inevitable introduction of T cells that may respond to healthy tissues and result in autoimmunity. Furthermore, *in vitro* generation of modified TCRs may lead to cross-reactivity to self-pMHC.

In this study, we have developed a novel approach that focuses on isolating functionally optimised TCRs rather than affinity enhancement. In order to circumvent autoimmunity, the optimisation technique involves extensive *in vivo* diversification of a target CDR of an established TCR that is subsequently subject to positive and negative thymic selection. TCR variants were generated using a site-directed mutagenesis system based on redirecting the V(D)J recombination machinery. A retrogenic approach was employed to facilitate the *in vivo* processes necessary for TCR diversification and screening. By challenging the retrogenic TCR repertoire with their cognate antigen, we reasoned that 'optimal' TCRs would direct enhanced immunological T cell function allowing their isolation based on clonal 'immunodominance'. This chapter describes the design of the mutagenesis system and outlines the procedures in the generation of retrogenic mice to optimise two types of male-specific TCRs.

2.2. Design of the recombination cassette

In order to mediate diversification using the thymocyte V(D)J recombination machinery within the selected TCR CDR, we must provide the RSS for the recombinase enzymes to identify and initiate the process. Our technique involves the use of the novel 'recombination cassette' that is appropriately inserted into the targeted CDR of the TCR. Indeed, this mutagenesis system is adapted from the

concept used by Correia-Neves et al. (2001) that introduced focused diversity to the V-J junction of the TCR α chain. In their study, the authors utilised artificial rearrangement substrates between a single V α region and two J α elements to create a TCR α minilocus transgene. Similar to our system, their rearrangement substrate contains two natural RSSs from V α 2.3 and J α 26 segments linked by a 547bp sequence (Koop et al., 1992; Okazaki & Sakano, 1988).

The recombination cassette used in this study utilises the same elements used previously by our group (Holland et al., 2012). In the present study to limit vector size we modified the recombination cassette to use a shorter RSS linker of 400bp instead of 500bp. The recombination cassette is comprised of the murine V β 8.2 RSS upstream of the murine D β 1 RSS interlinked by 400bp consisting of genomic sequence flanking the RSS (Figure 2.1). The V β 8.2 and D β 1 RSS contain a conserved palindromic heptamer and A/T-rich nonamer connected by 23 and 12 non-conserved nucleotides respectively. This combination of RSSs adheres to the '12/23 rule', where only RSSs with dissimilar nucleotide spacer lengths permit efficient recombination between gene segments (Bassing, Swat & Alt, 2002). Additionally, the murine V β 8.2 and D β 1 RSSs have displayed efficient recombination with each other (Wilson, Maréchal & MacDonald, 2001).

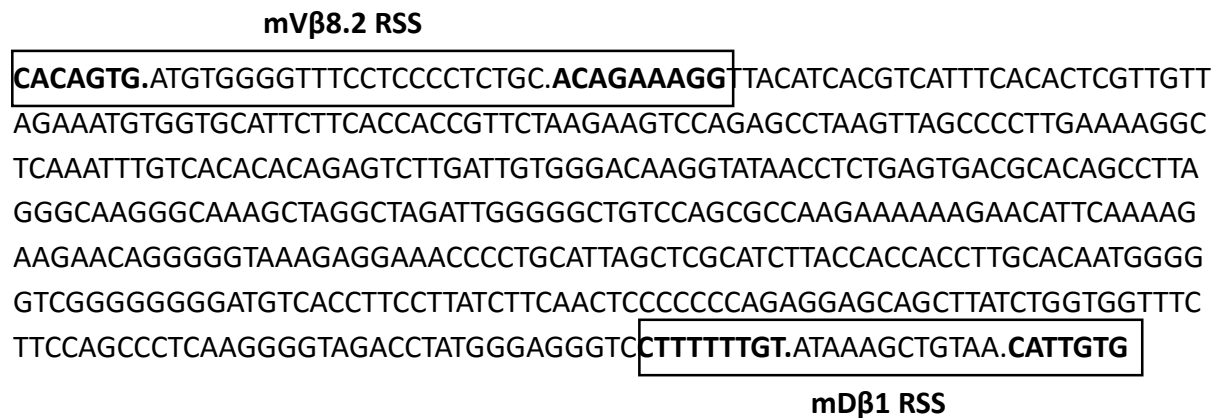


Figure 2.1. Design of the novel recombination cassette to diversify TCR. The nucleotide sequences of the murine V β 8.2 (7/23/9) and D β 1 (9/12/7) RSS used in the recombination cassette are defined (in boxes), connected by an inter-RSS genomic linker.

2.3. Design of multicistronic retroviral vectors for expression of CDR3 β diversifying $\alpha\beta$ TCRs

This study investigated the diversification of two male-specific (histocompatibility Y chromosome, HY) H2^b-restricted TCRs, Marilyn and MataHari from which TCR transgenic strains have been produced (Grandjean et al., 2003; Valujskikh et al., 2002). CD4⁺ T cells from the Marilyn transgenic strain express

a HY-specific TCR that recognises the NAGFNSNKANSSRSS peptide from the *Dby* gene, presented by MHC Class II H2-A^b. The CD8⁺ T cells from MataHari mice are specific for the HY peptide WMHHNMDLI derived from the *Uty* gene complexed with MHC Class I H2-D^b. Both *Dby* and *Uty* are expressed by most mammalian male nucleated cells.

This *in vivo* diversification approach has been shown to be effective in generating variants of wild-type (WT) germline CDR1 and CDR2 loops (Holland et al., 2012) and can potentially be used to mutate any target protein during lymphocyte development. The CDR3 loops of the TCR α and β chains represent the site of peptide recognition and contact, and have been highlighted to contain key residues that determine peptide specificity (Kessels et al., 2000; Davis & Bjorkman, 1988; Engel & Hedrick, 1988). Structural analysis of the diagonal binding between the TCR and pMHC molecule revealed the TCR α CDR3 loops to interact primarily with the N-terminus of the MHC-bound peptide, whereas the CDR3 of the TCR β bind with the C-terminus (Rudolph, Stanfield & Wilson, 2006). While the CDR3 α is formed as a result of recombination of two gene segments (V and J), the structure of the CDR3 β incorporates an additional D segment between the V and J genes. With additional junctional diversity, the CDR3 β region is the most diverse region of the TCR (Davis & Bjorkman, 1988). Thus CDR3 β is highly unique and can be used as a marker of T cell clones (Wlodarski et al., 2005; Plasilova, Risitano & Maciejewski, 2003). Furthermore, the CDR3 β region has been shown to be more critical in determining TCR affinity (Malecek et al., 2013). Hence, we have chosen to mutate the CDR3 β loop by inserting the recombination cassette into the centre of each WT TCR CDR3 β in order to diversify their binding affinity to identify functionally optimal receptors (Figure 2.2). Because of this, the constructs are termed 'CDR3 β diversifying' throughout this study.

Two systems for designating TCR genes have been widely used: the WHO-IUIS Nomenclature Subcommittee on TCR Designation (Radauer et al., 2014) and the International ImMunoGeneTics database (IMGT; Lefranc, 2005). In this study, we have used the IMGT system to identify the CDR loops of each TCR template (summarised in Table 2.1). The CDR3 loop of each TCR chain is defined as the amino acid sequence between the second conserved cysteine in third framework region (FR3) and the conserved phenylalanine (F-G-X-G) in FR4 of the variable domain.

Table 2.1. CDR1-3 amino acid sequences in each chain of Marilyn and MataHari transgenic TCRs. The CDR1-3 sequences were defined based on the guidelines of the IMGT website (Lefranc, 2005). The amino acids in CDR3 are underlined, in between residues of the third and fourth framework region (FR).

		CDR1	CDR2	CDR3
Marilyn transgenic	TCR α	DSASQY	IFSNGE	<u>CAVGNNNNAPRF</u> GAG
	TCR β	FNHDT	SITEND	<u>CASSIPGSNERLFF</u> GHG
MataHari transgenic	TCR α	DTASSY	IRSNVDR	CAAAMSNY <u>NFG</u> S
	TCR β	NSHNY	SYGAGN	<u>CASSDLVEVFF</u> GK

In this study, we introduced both TCR α and TCR β chains into the retrogenic mice (Figure 2.2A). To ensure simultaneous expression of both chains using a single plasmid, we employed the 2A peptide (P2A) sequence to mediate ‘self-cleavage’ between the two chains (Kim et al., 2011; Ryan, FAU & Thomas, 1991). The P2A system works through a ribosomal skip mechanism, whereby the 2A consensus motif appears to impair normal peptide bond formation between the glycine in the 2A peptide and the proline in the 2B peptide immediately adjacent to the 2A peptide. This cleavage does not affect translation of the 2B peptide and gene downstream thus ensuring stoichiometric expression of proteins flanking the P2A. The relatively smaller-sized P2A system overcomes the limitations of using internal ribosomal entry site (IRES) to express multicistronic vectors which exhibit inconsistent expression levels between genes positioned before and after the IRES (Szymczak & Vignali, 2005; de Felipe, 2004). The -GSG- sequence is attached upstream of the P2A sequence for added polypeptide flexibility and improves cleavage efficiency of the P2A (Holst et al., 2006; Szymczak et al., 2004).

The TCR (CDR3 β diversifying) constructs were cloned into the murine stem cell virus-based 6056bp pMigR1 retroviral vector (Pear et al., 1998). This vector contains a multiple cloning site (MCS), for insertion of the construct, and an IRES-EGFP (enhanced green fluorescent protein) marker cassette (Refer to *Chapter 7.2.2*). The transgene EGFP allows rapid and easy determination of transfection and transduction efficiencies using flow cytometry analysis. The percentage of cells that express EGFP will correlate to the number of cells that have viral integration and thus carry the diversifying construct. The 5’ and 3’ long terminal repeats (LTR) directs random genome integration upon transduction. Additionally, the 5’ LTR contains the viral enhancer/promoter that initiates transcription upstream of the MCS (Choi et al., 2001). The Marilyn and MataHari $\alpha\beta$ TCR (CDR3 β diversifying) constructs were synthesised *de novo*, and tagged with *Bgl*III and *Eco*RI restriction sites on the amino- and carboxyl-ends, respectively, to facilitate sub-cloning into the pMigR1 vector.

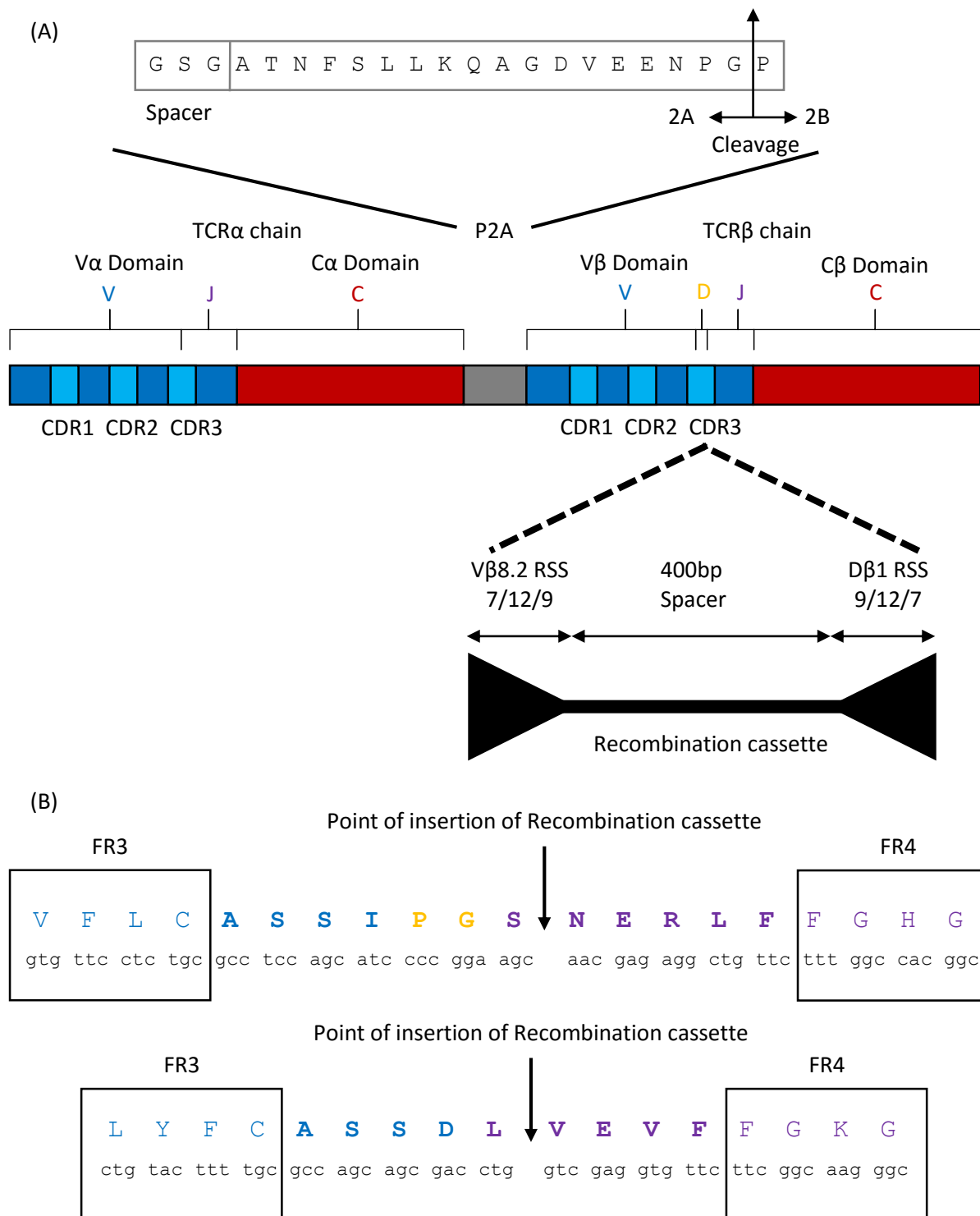


Figure 2.2. Schematic overview of the novel TCR diversifying technique. (A) The complete TCR α and TCR β chains are connected by the P2A sequence. The linker and P2A amino acid sequences are shown, with the 'cleavage' point between the 2A and 2B peptides indicated by the arrow. The recombination cassette (V β 8.2RSS-400bp spacer-D β 1RSS) is inserted into the centre of the TCR CDR3 β region. (B) The point of insertion of the recombination cassette into the CDR3 region (in *bold*) of Marilyn (*above*), and MataHari (*below*) transgenic TCR sequences. CDR3 is defined as the sequence between the second conserved cysteine residue in FR3 and the conserved phenylalanine residue in FR4.

2.4. Overview of retrogenic approach

The retrogenic mice approach was developed as a faster and flexible alternative to the use of conventional germline transgenesis for the study of T cell development (Holst et al., 2006). This system uses a single vector encoding both TCR α and TCR β chains to generate mice that express clonotypic T cells via retroviral-mediated stem cell gene transfer into HSCs. We have implemented the use of the retrogenic mice in this study for two main reasons. Firstly, this is a relatively quick method of generating transgenic mice expressing the desired TCR. Second, the retrogenic approach facilitates the *in vivo* environment necessary to diversify, express and screen the T cell repertoires produced by the TCR (CDR3 β diversifying) constructs. The thymic microenvironment of the retrogenic mice provides the essential spatial and temporal elements required for the V(D)J recombination-based mutagenesis technique. Diversification of the TCR is dependent upon RAG proteins that are expressed only during lymphocyte development (DN2-3 and DP stages) in the thymus (Casillas et al., 1995). The resultant TCR variants would then undergo thymic selection before release as mature T cells into the periphery. This includes positive selection of T cells that are able to bind to self-MHC, ensuring MHC restriction, thymocyte survival and commitment into either the CD4 or CD8 lineage. Negative selection deletes T cells that bind too weakly or too strongly to self-MHC and self-peptides thereby largely purging the peripheral T cell repertoire of autoreactive T cells and preventing autoimmunity (Klein et al., 2014).

The retrogenic approach used in this study is summarised in Figure 2.3 and detailed in *Chapter 7.7*. The multicistronic vector containing the P2A-linked TCR α and TCR β (CDR3 β diversifying) constructs were first introduced into the Phoenix™ ecotropic retroviral producer cell line (Holst et al., 2006). The virions generated from the transfected cell line were then used to transduce HSCs from pre-treated donor TCR- $\beta/\delta^{-/-}$ deficient mice via spin infection (Bettini et al., 2013). The donor mice were injected with 5'-Fluorouracil (5'-FU) to enrich the stem cell population (Wang et al., 2006). The transduced HSCs were cultured with the relevant cytokines before adoptive transfer into irradiated TCR- $\beta/\delta^{-/-}$ deficient female recipient mice. Transfection and transduction efficiencies were assessed based on the expression of the EGFP marker gene via flow cytometry. At least 2×10^5 EGFP⁺ HSCs were transferred into each recipient mouse, and left for 8-11 weeks to allow reconstitution of the T cell repertoire. The ratio of donor to recipient mice used was typically 3:1, to maximise the number of transduced cells carrying the TCR (CDR3 β diversifying) construct.

The use of TCR- $\beta/\delta^{-/-}$ deficient recipient mice ensures that the T cell repertoire will derive entirely from the transduced HSCs as only the transgene can express competent TCR β . Only transduced HSCs carrying the TCR constructs can enter the thymus and undergo *in vivo* T cell development, subsequently expressing in-frame TCR β (after recombination cassette removal). The retrogenic TCR β

chain will pair with either exogenous or endogenous TCR α . Using female recipients that do not express HY antigens allowed passage past thymic selection as male retrogenic mice would have otherwise removed Marilyn and MataHari T cells.

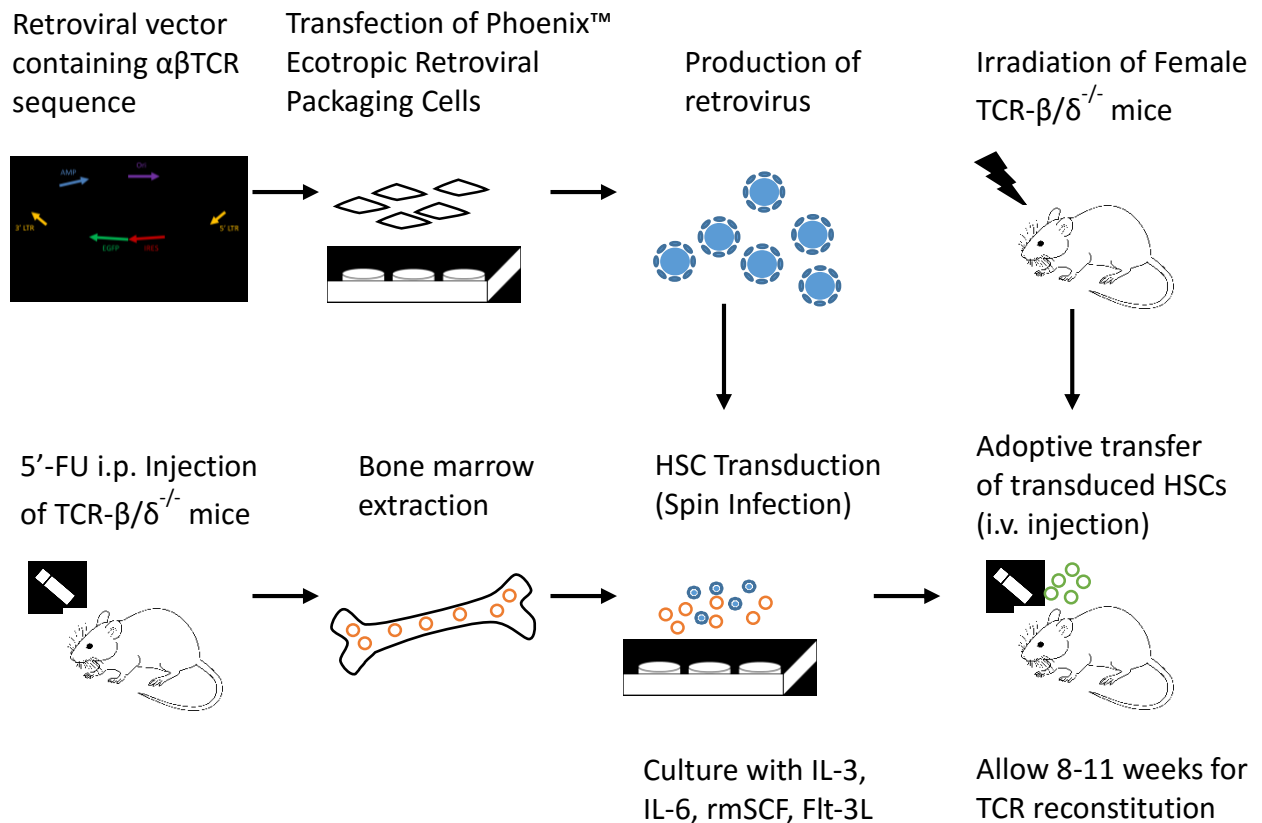


Figure 2.3. Schematic overview of the generation of retrogenic mice incorporating TCR diversification. The retroviral vector containing the TCR diversifying constructs is firstly used to transfect plated PhoenixTM ecotropic retroviral packaging cells, with the aid of the Lipofectamine[®] transfection reagent and helper plasmid pCLE. The viral supernatant is harvested after 48 hours and transfection efficiency is analysed by EGFP expression of the transfected cells. 72 hours before bone marrow extraction, the TCR- $\beta/\delta^{-/-}$ deficient donor mice are injected intraperitoneally (i.p.) with 5'-FU. The bone marrow cells are then cultured with the appropriate cytokines for 48 hours before transduction by the viral supernatant via spin infection. The transduced cells are cultured for a further 72 hours before injection intravenously (i.v.) into irradiated female TCR- $\beta/\delta^{-/-}$ deficient recipient mice. Transduction efficiency is measured by the EGFP expression of the transduced cells. The retrogenic mice generated are left to reconstitute the diversifying TCR for at least 8 to 11 weeks.

2.5. Results

2.5.1. Preparation of the retroviral vector containing the $\alpha\beta$ TCR (CDR3 β diversifying) constructs

The Marilyn and MataHari $\alpha\beta$ TCR (CDR3 β diversifying) constructs were each synthesised *de novo* and introduced separately into the pUC57 plasmid with the *Bgl*III and *Eco*RI restriction sites at the amino- and carboxyl- ends respectively. Both restriction sites were chosen to facilitate sub-cloning into the MCS of the pMigR1 retroviral vector. The constructs (excluding the recombination cassette) were synthesised with codons optimised for translation in mice.

The pMigR1 and pUC57 plasmids containing the CDR3 β diversifying constructs were subjected to double digestion using *Bgl*III and *Eco*RI enzymes, isolated using gel electrophoresis and purified. These open-ended inserts (Marilyn or MataHari $\alpha\beta$ TCR (CDR3 β diversifying) constructs) and 'empty' vector were then ligated together using T4 DNA ligase. Ligation was confirmed by running the products on a gel, undigested and digested using the same combination of *Bgl*III and *Eco*RI enzymes (Figure 2.4). Insertion of the constructs into the retroviral vector was further validated by sequencing, which showed 100% identity (not shown; refer to Appendices 1 and 2), verifying the correct orientation and sequences in the retroviral vector.

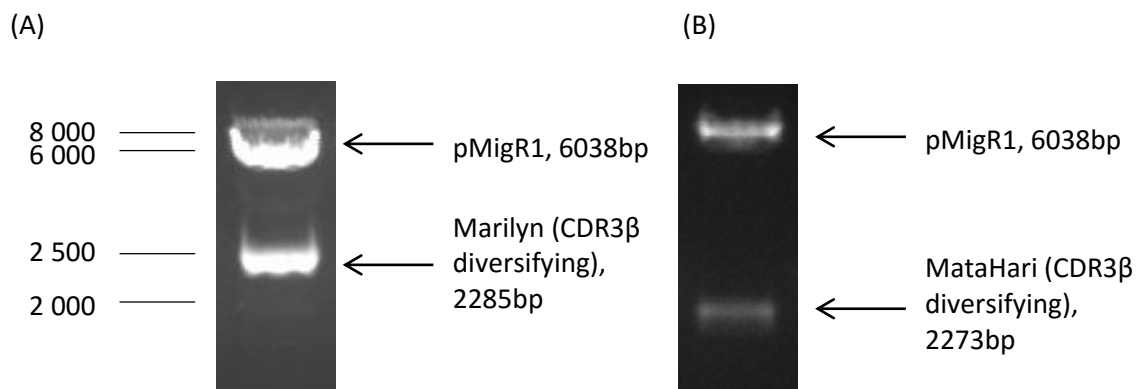


Figure 2.4. Ligation and sub-cloning of Marilyn and MataHari $\alpha\beta$ TCR (CDR3 β diversifying) constructs into the pMigR1 retroviral vector. The CDR3 β diversifying constructs were isolated from the pUC57 plasmid by double digestion using *Bgl*III and *Eco*RI enzymes, before insertion into the pMigR1 retroviral vector digested with the same combination of restriction enzymes. The ligated products were confirmed to contain the Marilyn (2285bp; A) and MataHari (2273bp; B) $\alpha\beta$ TCR (CDR3 β diversifying) constructs in the pMigR1 vector (6038bp).

2.5.2. Transfection of the Phoenix™ packaging cell line

The Marilyn and MataHari $\alpha\beta$ TCR (CDR3 β diversifying) constructs in the pMigR1 vector were introduced separately into the Phoenix™ ecotropic packaging cell line with the help of the Lipofectamine® 2000 transfection reagent and pCLE helper plasmid. The EGFP reporter gene in the pMigR1 vector allowed identification of transfected Phoenix™ cells, and assessment of transfection efficiencies by flow cytometry (Figure 2.5A). The transfection efficiency of different retroviral vectors were: 'empty' pMigR1 – $61.7 \pm 8.3\%$, pMigR1-(Marilyn CDR3 β diversifying) – $52.4 \pm 12.1\%$ and pMigR1-(MataHari CDR3 β diversifying) – $52.8 \pm 8.5\%$ (Mean \pm SD, n=10; Figure 2.5A, B). The transfection efficiencies between empty pMigR1 and either pMigR1-(Marilyn CDR3 β diversifying) or pMigR1-(MataHari CDR3 β diversifying) were shown to be statistically similar ($p > 0.5$; Figure 2.5B).

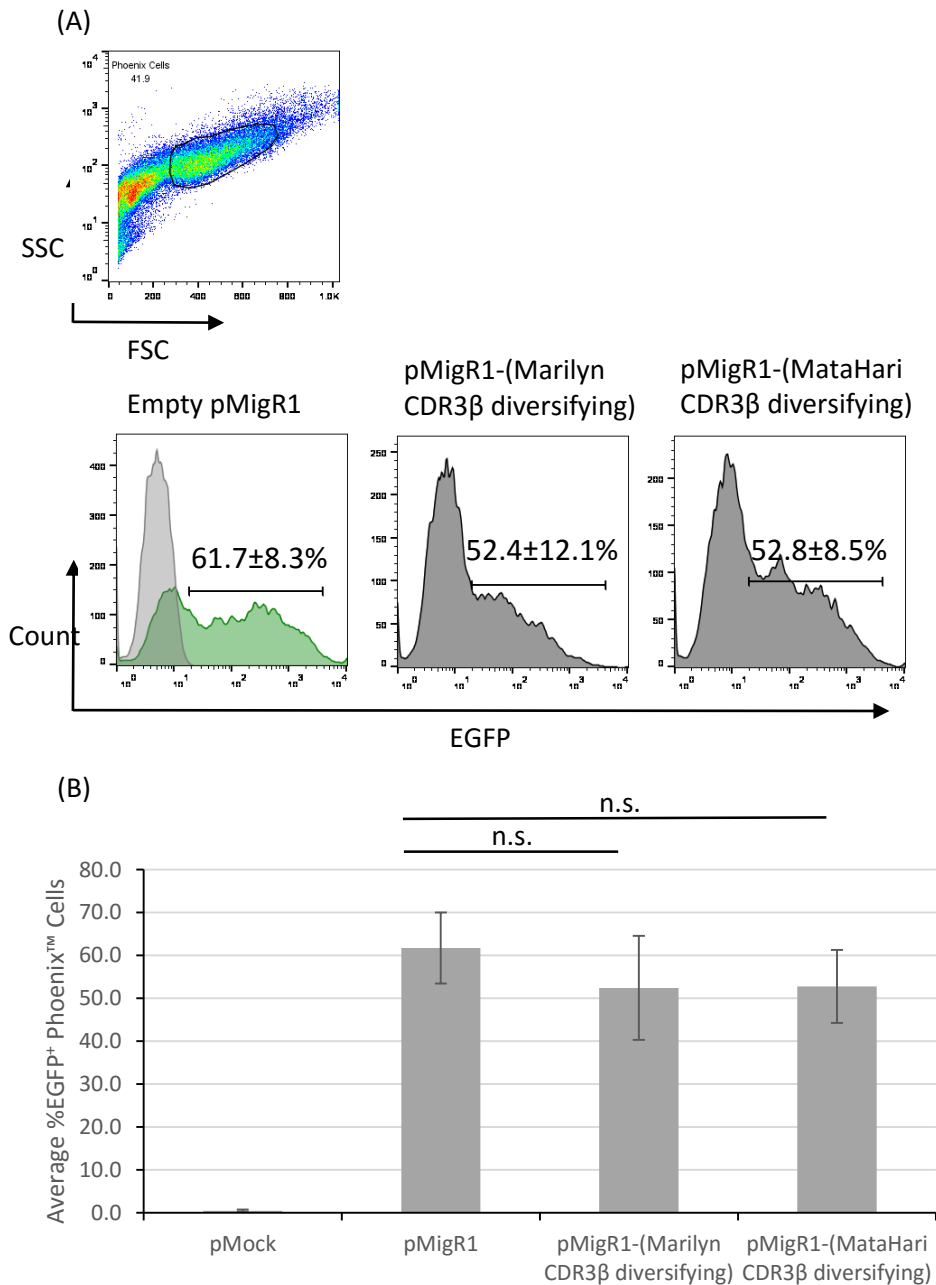


Figure 2.5. Flow cytometric analysis of EGFP reporter expression and summary of transfection efficiencies. The pMigR1 retroviral vector, either empty or containing the $\alpha\beta$ TCR (CDR3 β diversifying) constructs, was introduced into the PhoenixTM packaging cell line. After 48 hours of culture, the cells were harvested and analysed for EGFP expression, which represents cells that integrated the viral DNA and TCR constructs. (A) Example of FSC and SSC gating of PhoenixTM cells. Below are overlay histogram plots of PhoenixTM cells transfected with the pMock (no plasmid negative control; *light grey*) and empty pMigR1 vector (*green*), and PhoenixTM cells transfected with the pMigR1-(Marilyn CDR3 β diversifying) and pMigR1-(MataHari CDR3 β diversifying) vectors. Average transfection efficiencies \pm standard deviation (SD) are shown. (B) Transfection efficiencies of different retroviral vectors, as determined by average percentage of EGFP⁺ PhoenixTM cells (n=10 for each plasmid). Each bar represents the mean of ten different experiments and error bars the SD of the mean.

2.5.3. Transduction of HSC and generation of retrogenic mice

The pMigR1 retroviral vector contains the 5' LTR that promotes the expression of the TCR constructs cloned into the MCS, followed by IRES-mediated expression of the EGFP marker gene. The viral supernatant obtained from the transfected Phoenix™ cells were used for transduction of HSC-enriched cultures from at least eight-week-old TCR- $\beta/\delta^{-/-}$ deficient donor mice. The transduction efficiencies and the number of EGFP⁺ HSCs i.e. cells carrying the TCR constructs, were analysed via flow cytometry and summarised in Figure 2.6. During each retrogenic experiment set-up, we ensured at least 2×10^5 EGFP⁺ cells were adoptively transferred into each TCR- $\beta/\delta^{-/-}$ deficient female mouse. We generated retrogenic mice expressing the male-specific H2^b-restricted TCRs in two strains: MHC haplotype-mismatched FVB (H2^a) and MHC-matched C57BL/6 (H2^b) mice.

The transduction efficiencies for the Marilyn TCR (CDR3 β diversifying) were generally more than 40% during the generation of retrogenic mice of either FVB/N or C57BL/6 strain (Figure 2.6A, B). Conversely, the MataHari TCR (CDR3 β diversifying) displayed notably variable transduction efficiencies, ranging from 8.2% up to 40.4%. This observation, coupled with inconsistent HSC culture cell yield, resulted in variable numbers of EGFP⁺ transduced HSCs injected into each mouse between different experiment set-ups (Figure 2.6C).

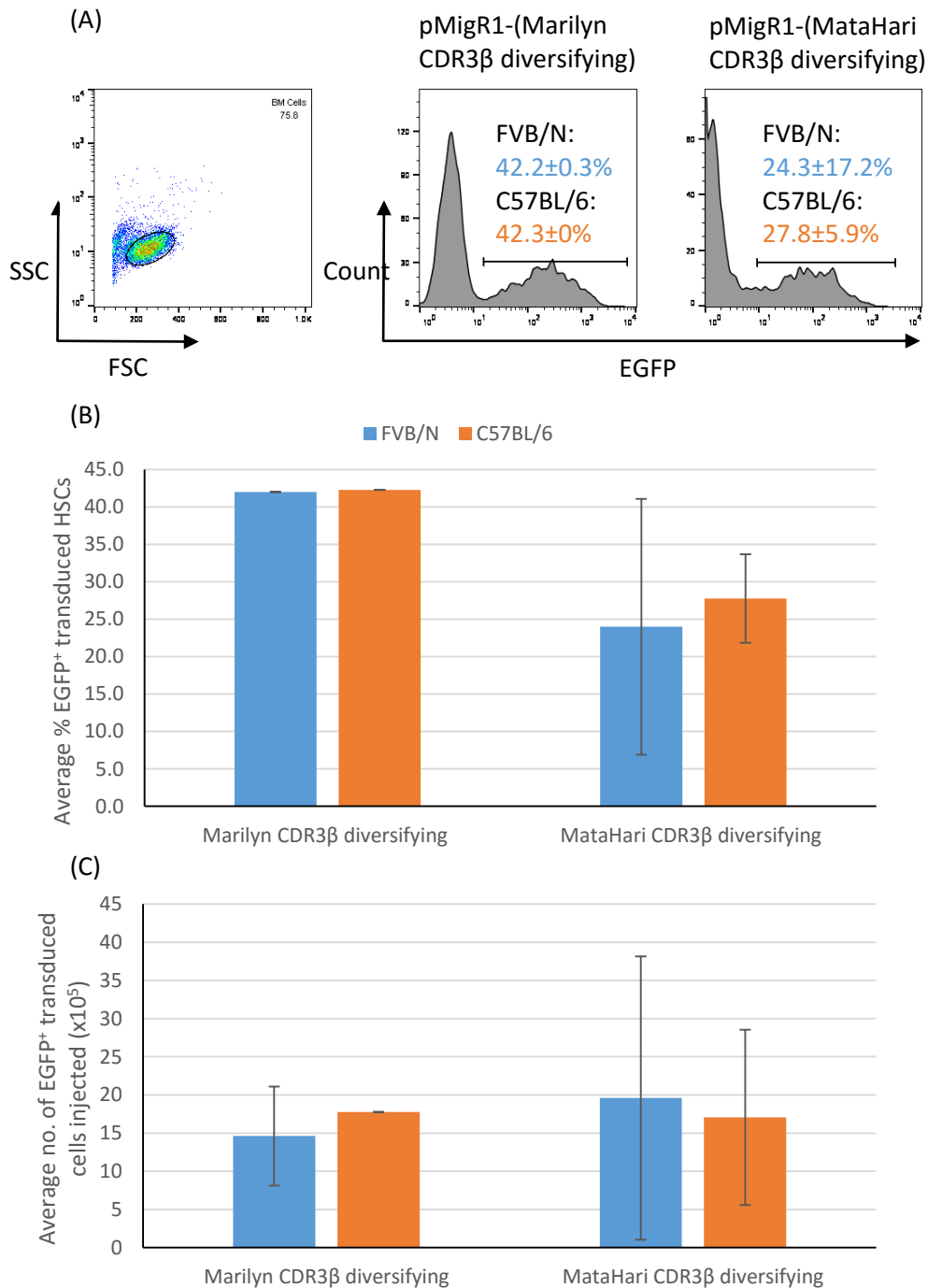


Figure 2.6. Summary of transduction efficiencies and the number of EGFP⁺ HSCs adoptively transferred into each retrogenic mice. (A) Example of FSC and SSC gating of the transduced BM culture is shown, followed by the histogram plots identifying the transduced EGFP⁺ HSCs. The range of transduction efficiencies in the generation of Marilyn and MataHari TCR (CDR3 β diversifying) retrogenic mice in either FVB/N (*blue*) or C57BL/6 strain (*orange*) is also displayed. (B) Transduction efficiency, is measured by the percentage of EGFP⁺ HSCs. (C) The number of EGFP⁺ HSCs, carrying the diversifying TCR constructs, injected into each mice. Each bar is the mean of different experiments and error bars the SD of the mean. The blue bars represent FVB (H2^q) recipients, while the orange bars denote C57BL/6 (H2^b) recipients. For Marilyn TCR (CDR3 β diversifying): FVB, n=8, C57BL/6, n= 4; MataHari TCR (CDR3 β diversifying): FVB, n=8, C57BL/6, n=11.

2.6. Discussion

2.6.1. Summary

A new strategy was developed to optimise TCR binding in the interest of enhancing functional T cell responses. This approach utilises a novel V(D)J recombination-based mutagenesis technique to create a library of TCR variants that undergoes normal *in vivo* T cell development. This is in contrast to the majority of approaches that employ *in vitro* yeast, phage or mammalian cell display systems to produce and isolate high affinity variants of template anti-tumour TCRs (Holler et al., 2000; Weber et al., 2005; Li et al., 2005; Kessels et al., 2000; Chervin et al., 2008).

We have tested this concept on two main T cell subsets: cytotoxic CD8⁺ T cells, obtained from MataHari transgenic mice (Valujskikh et al., 2002), and CD4⁺ T helper cells from Marilyn mice (Grandjean et al., 2003). Marilyn and MataHari T cells have both been characterised and compared with respect to anti-tumour responses *in vitro* and *in vivo*. Interestingly, even though cytotoxic MataHari T cells were able to eliminate tumours *in vitro*, the Marilyn T helper cells proved to be more effective *in vivo* (Perez-Diez et al., 2007). These observations offer an ideal setting to test our novel TCR optimisation strategy and provides an opportunity to investigate from two different aspects: Can we improve the *in vivo* anti-tumour activity of MataHari cytotoxic T cells? To what extent can we improve the TCR binding and functionality of Marilyn T cells that are already proven to be efficient anti-tumour effector cells?

Another contributing factor in selecting the Marilyn and MataHari TCRs for our novel approach is that retrogenic mice expressing these male Ag-specific TCRs have been shown to be generated successfully. Holst et al. (2006) were able to retrovirally introduce both exogenous TCR α and TCR β chains into T cell-deficient female mice, producing functional T cells that are comparable to their transgenic counterparts. Additionally, the phenotype of lymphocytes developed from $\alpha\beta$ TCR that lacks a mutagenesis-inducing recombination cassette provides valuable positive control for our study.

2.6.2. Advantages and limitations of retrogenic technology

The retrogenic aspect of our novel mutagenesis approach provides several key benefits. Firstly, retrogenic mice can be produced considerably faster than the traditional transgenic system, which may take up to 6 months to generate the required strain. Ideally, the design, production and functional analysis of retrogenic mice expressing mutated TCR can be achieved within 3-4 months. Secondly, this system permits the option to test and optimise many different TCRs specific for a particular antigen, which would be logistically challenging and costly using conventional transgenic approach. Retrogenic mice also limit the potential bias as a result of founder effects, as each mouse is individually generated

and fundamentally a founder. Further, the inter-mouse variation should be minimal as the multiple retroviral insertions give a similar range of expression as reported by EGFP (Figure 2.6B). The main advantage is that this approach facilitates *in vivo* gene recombination and thymic selection processes, which are crucial for creating functional TCR variants. Our novel strategy essentially mimics *in vivo* T cell development, tolerising the T cell repertoire through negative selection, thus circumventing the possibility of autoimmunity; in contrast, *in vitro* techniques that concentrate on isolating higher affinity TCRs may also confer autoreactivity through TCR cross-reaction.

However, the use of retrogenic technology comes with its own limitations. Retrogenic mice cannot be bred, requiring new mice to be generated for further experiments. Additionally, with a donor to recipient mice ratio of 3:1, each experiment set-up demands a substantial number of mice. For example, generating a group of 4 retrogenic mice involves extracting HSCs from 12 donor mice. Retrogenic mice can lose weight and may have to be culled necessitating repeat experiments and causing delays. From a technical standpoint, the variations between transfection efficiencies may lead to variable transduction rates of HSCs and thus the number of EGFP⁺ cells transferred into each retrogenic mouse. Moreover, BM extraction and culture proved to be a somewhat inconsistent procedure, affecting the number of HSCs available for transduction and adoptive transfer. These discrepancies can elicit differences in the TCR reconstitution period, and the number of cells that can be isolated for flow cytometric analysis and cell sorting (Scott-Browne et al., 2009). The number of T cells in retrogenic mice has already been reported to be generally less than in transgenic mice (Holst et al., 2006).

2.6.3. Conclusions

In this chapter, we have described the design of the recombination cassette that redirects mutagenesis using V(D)J recombination machinery. This approach is designed to diversify and optimise TCR binding to the cognate pMHC ligand, subsequently enhancing immunological functionality. TCR variants will be produced by modifying the CDR3 β , the most diverse region in the TCR that defines T cell clonotype and peptide specificity. The recombination cassette was placed in the centre of the CDR3 β to induce a fair chance of variability around the point of insertion. The pMigR1 vectors containing the Marilyn and MataHari TCR (CDR3 β diversifying) constructs showed comparable transfection efficiencies compared to 'empty' pMigR1 vectors. This suggests insertion of the diversifying TCR constructs into the MCS of the vector did not significantly affect its performance and quality. The transduction efficiencies of the HSCs proved to be markedly variable between each experiment set-up. However, every female retrogenic mouse generated was assuredly injected with

at least 2×10^5 EGFP⁺ cells to ensure sufficient thymocyte progenitors were available for T cell development. The reconstitution of the diversified TCR will be discussed in the Chapters 3 and 4.

Chapter 3

Chapter 3: Characterisation of H2^a retrogenic mice expressing diversifying H2^b-restricted TCR

3.1. Introduction

The previous chapter outlined the novel mutagenesis approach designed to optimise the binding of the TCR with its cognate antigen and enhance immunological function. Our system essentially redirects gene rearrangement to the target region using V(D)J recombination machinery to create variants of the TCR. In this study, we have inserted the mutagenesis-inducing recombination cassette into the centre of the CDR3 β region of two male antigen-specific receptors: the V β 6⁺ TCR of CD4⁺ Marilyn Th cells, and the V β 8.3⁺ TCR of CD8⁺ cytotoxic MataHari T lymphocytes. This strategy will induce recombination at the centre of the CDR3 loop apex, and introduce sequence diversity before and after the point of insertion (Figure 2.2).

The fate of the TCR (CDR3 β diversifying) constructs, introduced via retroviral vectors into TCR- $\beta/\delta^{-/-}$ deficient HSCs as a heterodimer of WT TCR α and diversifying TCR β separated by P2A, is summarised in Figure 3.1. During transduction of the HSCs, the LTRs flanking the $\alpha\beta$ TCR constructs facilitate random integration into the genomic DNA. After adoptive transfer into the TCR- $\beta/\delta^{-/-}$ deficient female recipient mice, the transduced HSCs enter the thymus where they enter the *in vivo* T cell developmental program. During the DN2-3 and DP stages, the RAG proteins are expressed to initiate the gene recombination process, which results in the random DNA sequence diversification with the help of NHEJ and TdT enzymes. This creates a permanent TCR β 'footprint' specific for each T lymphocyte which can signal progression past the β -selection checkpoint with the pT α (Trop et al., 2000). Only lymphocytes that integrate, express the TCR construct and produce an in-frame CDR3 β region can express a functional $\alpha\beta$ TCR. The vast peripheral T cell repertoire will comprise of the exogenous diversified TCR β chains paired with either its exogenous WT TCR α partner and/or an endogenous TCR α chain. Thymic positive and negative selection ensures the T lymphocytes are MHC-restricted and any autoreactive T cells are clonally deleted, respectively.

During the earlier part of the project, we experienced a shortage of available TCR- $\beta/\delta^{-/-}$ deficient C57BL/6 (H2^b) mice. As we awaited the breeding and acquisition of the relevant H2^b TCR- $\beta/\delta^{-/-}$ deficient mice, we decided to test our TCR optimisation approach in TCR- $\beta/\delta^{-/-}$ deficient FVB/N (H2^a) female recipient mice which were available at that time. In this chapter, we investigated the viability of the newly designed recombination cassette and whether a T cell repertoire can develop and

reconstitute the peripheral lymphoid tissues. Additionally, we assessed the phenotypic expression and consequences of MHC haplotype-mismatched FVB/N ($H2^a$) mice expressing $H2^b$ -restricted TCRs.

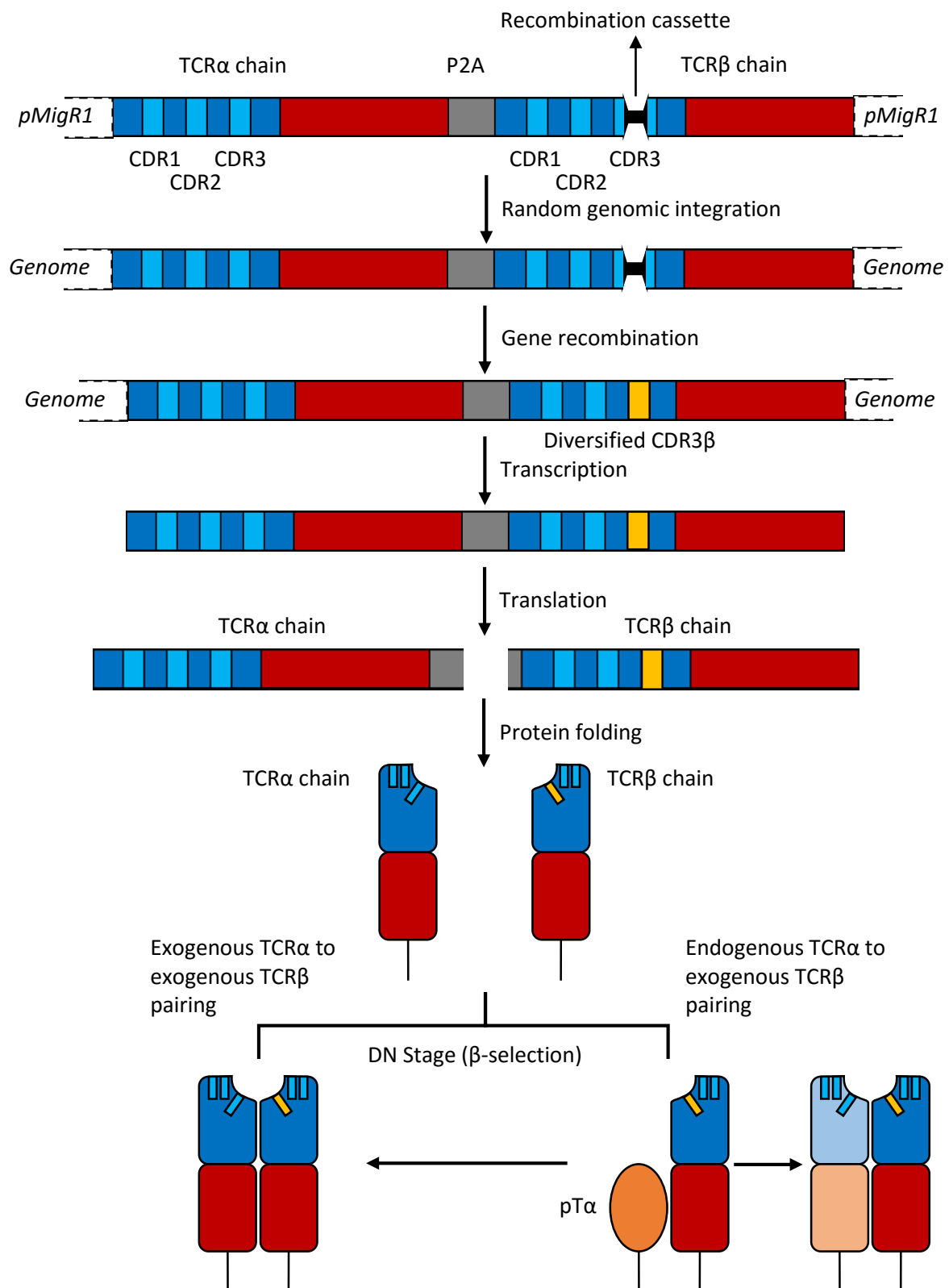


Figure 3.1. The fate of the TCR constructs from the retroviral vector to the creation of the T cell repertoire. The TCR construct heterodimer containing the WT TCR α and diversifying TCR β (containing

the recombination cassette), linked by P2A sequence is initially cloned into the retroviral vector pMigR1. Retroviral-mediated transduction of HSCs results in integration of the $\alpha\beta$ TCR construct randomly into the genomic DNA. The adoptively transferred HSCs enter the retrogenic mouse thymus, where V(D)J recombination-based mutagenesis during the DN2-3 stages removes the recombination cassette and generates TCR β variants via modification of the CDR3 β . Translation of the $\alpha\beta$ TCR construct mRNA containing the P2A sequence induces the ribosomal skip mechanism, resulting in two separate polypeptide chains – the WT TCR α and diversified TCR β chains. The diversified TCR β chain can pair with either the exogenous WT partner TCR α and/or endogenous TCR α chains produced by the competent TCR α locus of TCR- $\beta/\delta^{-/-}$ deficient thymocytes. The TCR complex directs positive and negative selection events in the thymus before release into the periphery.

3.2. Results

3.2.1. Detection of EGFP and TCR β expression in FVB/N retrogenic mice peripheral blood

Altogether, a total of 8 retrogenic FVB/N mice (2 cohorts of 4 mice) were generated for each of the two $\alpha\beta$ TCR (CDR3 β diversifying) constructs. Due to the varying nature of the transduction efficiencies and number of transduced HSCs injected into each TCR- $\beta/\delta^{-/-}$ recipient mice between different cohorts, the TCR reconstitution period and total number of T cells generated were not envisaged to be uniform. As such, analysis of cell-surface marker expressions and progression were calculated according to each independent retrogenic mice set-up. The groups of retrogenic mice generated are summarised below (Table 3.1).

Table 3.1. The cohorts of FVB/N retrogenic mice generated from adoptive transfer of HSCs containing Marilyn and MataHari $\alpha\beta$ TCR (CDR3 β diversifying) constructs.

Construct	Group	Transduction efficiency	No. of EGFP ⁺ HSCs injected into each mice	No. of retrogenic mice generated
Marilyn (CDR3 β diversifying)	1	42.4%	8.5×10^5	4
	2	41.9%	2.0×10^6	4
MataHari (CDR3 β diversifying)	1	8.2%	2.2×10^5	4
	2	40.4%	3.7×10^6	4

After adoptive transfer of transduced HSCs containing the $\alpha\beta$ TCR (CDR3 β diversifying) constructs, the TCR- $\beta/\delta^{-/-}$ deficient female recipient mice were allowed at least 8 weeks to develop the diversified T cell repertoires. After 9 weeks, blood of the retrogenic mice (Groups 1 for both Marilyn and MataHari $\alpha\beta$ TCR (CDR3 β diversifying)) were sampled from the tail vein, red blood cells lysed and stained using fluorochrome-conjugated antibodies (Ab) for TCR β (C domain) and the CD4 and CD8 co-receptors.

Flow cytometric analysis revealed sizeable levels of EGFP⁺ and EGFP⁺TCRβ⁺ expression in the lymphocyte populations of both Marilyn and MataHari αβTCR (CDR3β diversifying) retrogenic mice (Figure 3.2).

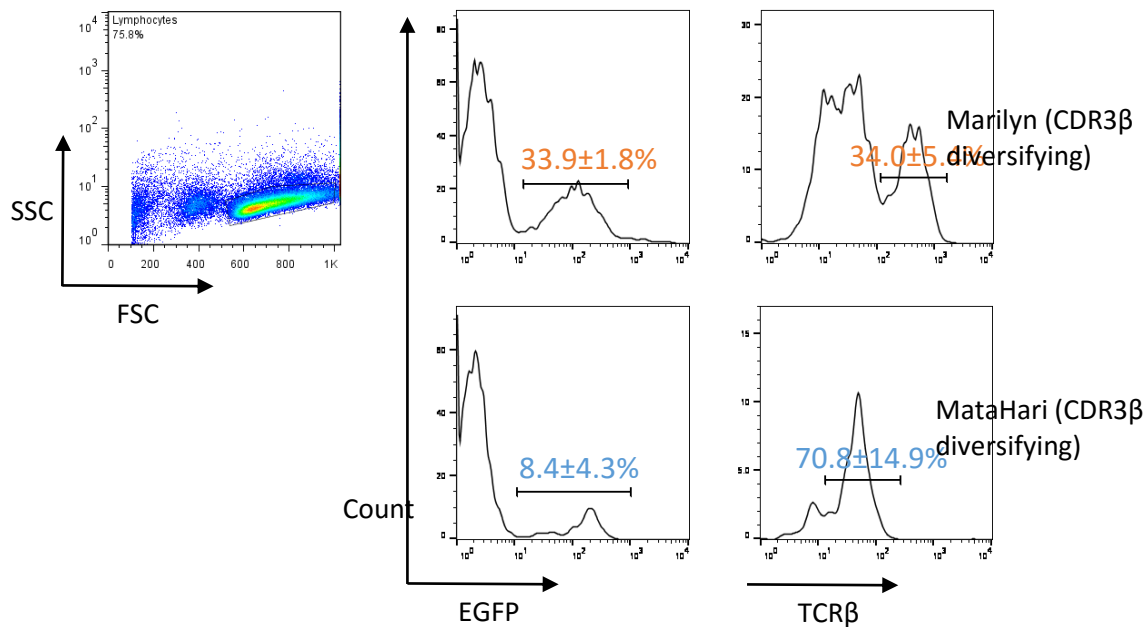


Figure 3.2. Flow cytometric analysis of peripheral blood from FVB/N retrogenic mice transduced with Marilyn and MataHari αβTCR (CDR3β diversifying) constructs. The representative gating of the lymphocyte population for all mice is shown, followed by analysis of EGFP⁺ and EGFP⁺TCRβ⁺ expression, 9 weeks after transduced HSC adoptive transfer, represented as averages ± SD. Marilyn TCR (CDR3β diversifying) data are from retrogenic mice (n=4, *above*) injected with 8.5×10^5 EGFP⁺ HSCs each (42.4% transduction efficiency). MataHari TCR (CDR3β diversifying) data was observed in retrogenic mice (n=4, *below*) adoptively transferred with 2.2×10^5 EGFP⁺ HSCs each (8.2% transduction efficiency).

Two more time points (12 and 16 weeks post-HSC transfer) showed steady progression of EGFP⁺ and EGFP⁺TCRβ⁺ levels in the lymphocyte population (Figure 3.3A). As T cell development in the TCR-β/δ^{-/-} deficient mice relies on the expression of a functional exogenous TCRβ chain, this data suggests that the recombination cassette successfully induced in-frame gene rearrangement in both Marilyn and MataHari αβTCR (CDR3β diversifying) constructs. The resultant diversified TCRβ paired with either endogenous and/or exogenous TCRα chains and underwent *in vivo* T cell development and thymic selection before maturing into the peripheral blood. Analysis of the EGFP⁺TCRβ⁺ lymphocytes also showed that both CD4⁺ and CD8⁺ T cell were generated, with a clear skewing to the CD4 lineage, for both TCR constructs (Figure 3.3B). This bias towards the MHC Class II in the generation of retrogenic mice has already been observed previously (Holland et al., 2012; Holst et al., 2006). Perhaps surprising

is the observation that the retrogenic mice expressing the diversified MataHari TCR showed dominance in the CD4⁺ T cell compartment even though MataHari transgenic T cells are natively CD8-positive and MHC Class I-restricted (Valujskikh et al., 2002). Similarly, T cells in from Marilyn transgenic mice are typically CD4-positive, but the Marilyn TCR (CDR3 β diversifying) retrogenic mice showed a small population of MHC Class I-restricted CD8⁺ T lymphocytes (Grandjean et al., 2003). This suggests that the MHC haplotype may play a key role in governing the lineage choice for a given TCR.

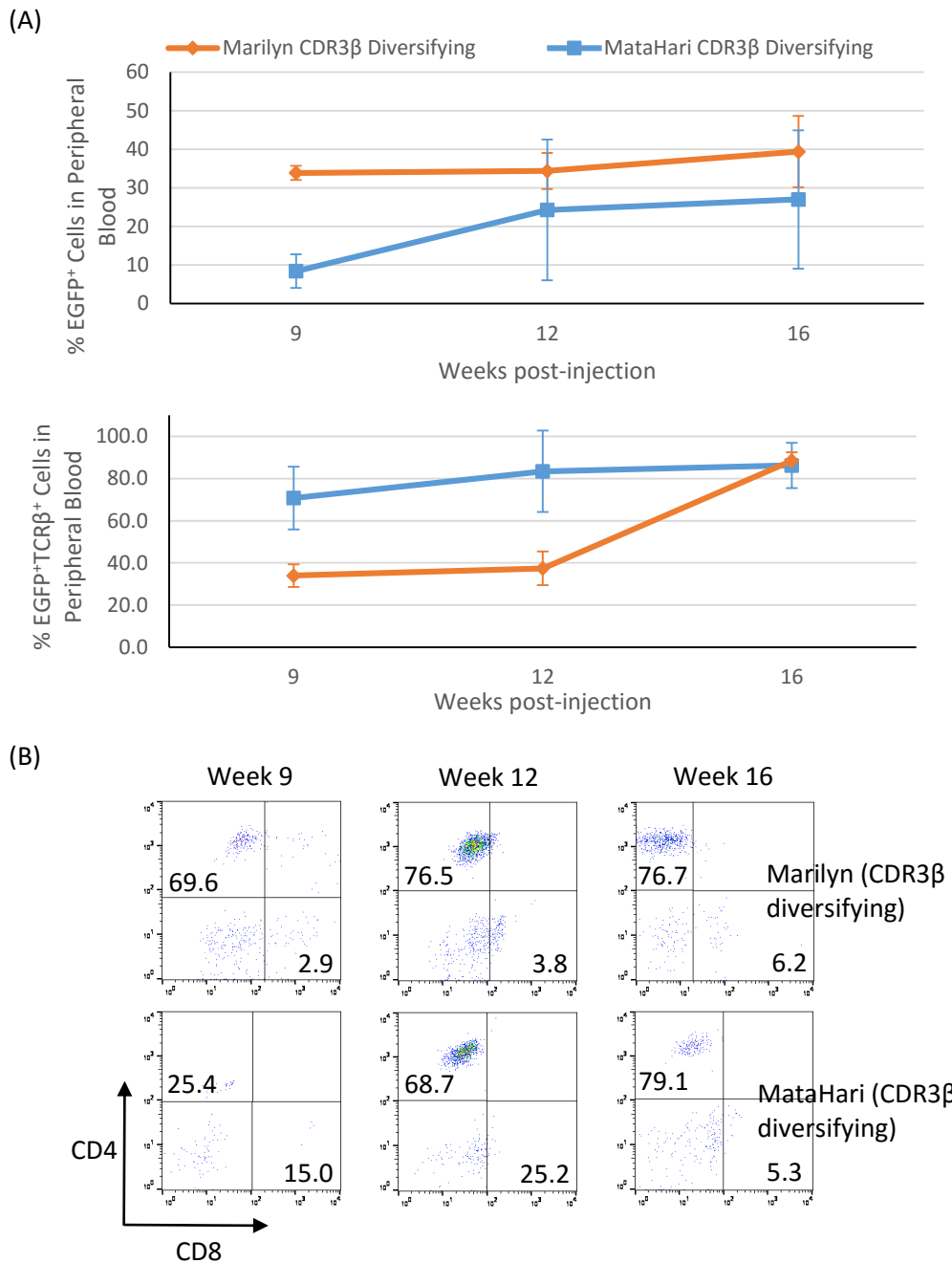




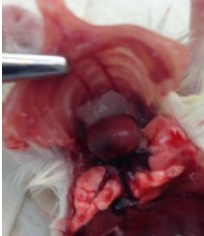

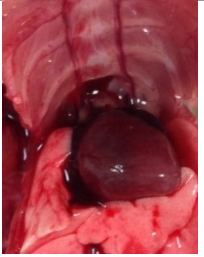

Figure 3.3. Progression of EGFP⁺TCR β ⁺ cells in the peripheral blood of FVB/N retrogenic mice. (A) Flow cytometric analysis of EGFP⁺ and EGFP⁺TCR β ⁺ expression levels sampled at 9, 12 and 16 weeks after transduced HSC transfer. Each point represents mean expression \pm SD. (B) Analysis of CD4 and

CD8 co-receptor expression in EGFP⁺ and EGFP⁺TCRβ⁺ lymphocytes at the same time points showing strong skewing to the CD4 lineage in both Marilyn (*above*) and MataHari (*below*) αβTCR (CDR3β diversifying) retrogenic mice. Representative figures showing mean co-receptor expression percentage for all mice at the specific time points are shown.

3.2.2. Analysis of the FVB/N retrogenic mice primary lymphoid organs

We have shown that the T cell compartment can indeed be restored in the TCR-β/δ^{-/-} deficient retrogenic mice, with a higher frequency of CD4⁺ compared to CD8⁺ T cells in the bloodstream. The peripheral T cell repertoire is dependent upon the migration of the adoptively transferred HSCs to the non-productive thymus of the TCR-β/δ^{-/-} deficient mice, which provides a specialised microenvironment for V(D)J recombination and T cell ontogeny. Characterisation of the thymocyte populations can reveal whether retrogenic mice follow a typical T cell development and elucidate the apparent peripheral bias to the CD4⁺ T cell lineage. Thus, we harvested thymi from Marilyn (n=7) and MataHari (n=5) TCR (CDR3β diversifying) retrogenic mice for analysis. Interestingly, the size of the retrogenic mice thymi displayed variable sizes that can be classified into three groups: small, normal and enlarged (possible thymoma), summarised in Figure 3.4A. Of the 7 Marilyn TCR (CDR3β diversifying) retrogenic mice analysed, there was one occurrence of a small thymus, two showed a normal-sized thymus while the remaining four exhibited possible thymomas that partly occupied the thoracic cavity. Only one of the five MataHari TCR (CDR3β diversifying) retrogenic mice displayed an enlarged and fibrous thymus, while the rest maintained the small thymus size of TCR-β/δ^{-/-} deficient mice. Total thymic cellularity was also measured, showing the apparent thymomas generally contained at least 1 x 10⁸ cells (Figure 3.4B), significantly higher compared to non-thymoma (small and normal) thymi (p=0.0025; p>0.05).

(A)

Mice Strain	Thymus type	Frequency	
TCR- $\beta/\delta^{-/-}$ deficient FVB/N	Small	100%	
Marilyn (CDR3 β diversifying) retrogenic	Small	14% (1/7)	
	Normal	29% (2/7)	
	Thymoma	57% (4/7)	
MataHari (CDR3 β diversifying) retrogenic	Small	80% (4/5)	
	Thymoma	20% (1/5)	

(B)

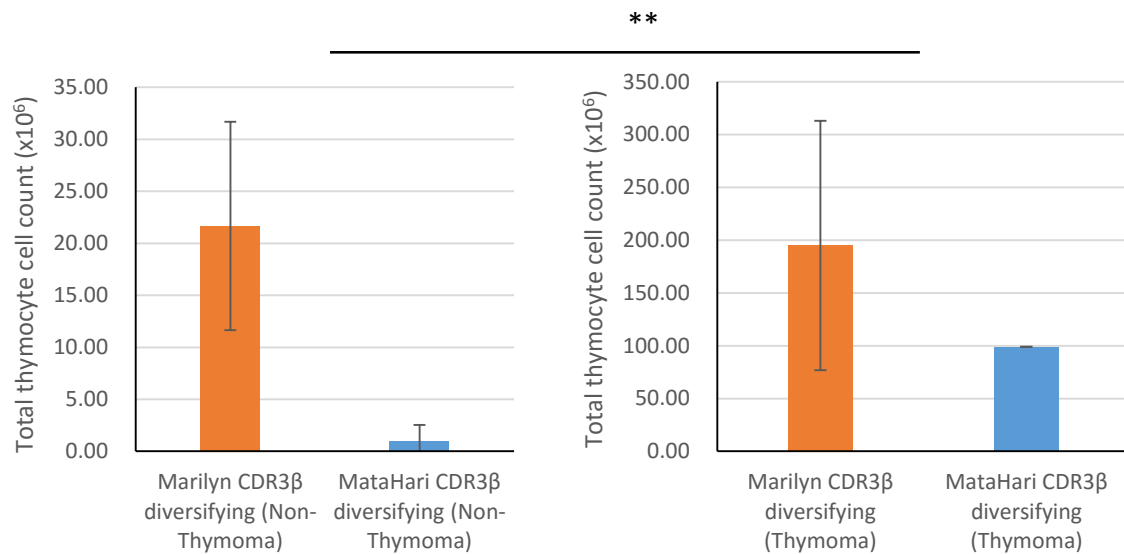


Figure 3.4. Thymic size and cellularity in Marilyn and MataHari TCR (CDR3 β diversifying) FVB/N retrogenic mice. Thymi were harvested after TCR reconstitution period (>8 weeks) from Marilyn (n=7) and MataHari (n=5) TCR (CDR3 β diversifying) retrogenic mice, with a small thymus of TCR- β / δ ^{-/-} deficient FVB/N mouse shown for comparison. (A) Thymi sizes of the retrogenic mice are pictured, and frequency of thymus type summarised. (B) Total thymic cellularity was determined from the same mice, classified based on the occurrence of non-thymoma (small and normal) and thymoma. Cell count showed significantly increased number of thymic cells in thymoma compared to non-thymoma ($p=0.0025$; $p>0.05$). Data shows mean \pm SD for all mice.

Thymocytes were subsequently analysed for expression of EGFP, TCR β , CD4 and CD8, via flow cytometry. Marilyn TCR (CDR3 β diversifying) retrogenic thymocytes displayed almost negligible expression of EGFP and TCR β in both thymoma and non-thymoma (Figure 3.5B, C, *left*). In contrast, non-thymoma MataHari TCR (CDR3 β diversifying) retrogenic thymocytes expressed pronounced levels of EGFP⁺ (25.4%) and EGFP⁺TCR β ⁺ (49.8%), more characteristic of normal thymic T cell development (Figure 3.5B, C, *right*). However, the single thymoma observed in the MataHari TCR (CDR3 β diversifying) retrogenic mice showed negligible expression of both EGFP and TCR β . From these observations, it is possible the thymoma may have indicated or resulted in a loss EGFP and TCR β expression in thymocytes.

The co-receptor expression profile describes T cell development in the thymus through the distribution of the DN, DP, SPCD4 and SPCD8 subsets. Marilyn TCR (CDR3 β diversifying) retrogenic mice demonstrated an accumulation at the DP stage, followed by a higher frequency of SPCD4 relative to SPCD8 thymocytes (Figure 3.5D, *left*). This supports the principle of Marilyn TCR expression in CD4⁺ T cells and the presence of higher CD4⁺ lymphocyte population observed in the circulation (Figure

3.3B). Interestingly, similar Marilyn TCR (CDR3 β diversifying) retrogenic thymocyte co-receptor profiles were seen in both thymoma and non-thymoma examples.

MataHari TCR (CDR3 β diversifying) retrogenic mice exhibited a higher frequency of the DN cells, the earliest precursor in T cell ontogeny, compared to DP cells, suggesting a partial block at the DN to DP stage in both thymoma and non-thymoma (Figure 3.5D, *right*). This phenotype is a trait of TCR- $\beta/\delta^{-/-}$ deficient mice, as the inability to express the *TCR β* gene causes a near complete block in the DN to DP transition (Mombaerts et al., 1992). The presence of SPCD4 thymocytes in the MataHari TCR (CDR3 β diversifying) retrogenic thymi indeed underpin the expression of CD4⁺ T cells in the periphery (Figure 3.3C). Again, it is interesting to observe the presence of SPCD4 as MataHari transgenic T cells typically express CD8 co-receptors (Valujskikh et al., 2002). Further, in the MataHari TCR (CDR3 β diversifying) retrogenic thymoma, there is a clear accumulation of SPCD4 thymocytes (96.5%), which indicates that there is a greater efficiency with MHC Class II selection. Conversely, the non-thymoma retrogenic mice demonstrated higher levels of SPCD8 (35.0%) compared to SPCD4 (13.6%) thymocytes, suggesting that selection favours MHC Class I more than Class II. In both cases, it appears CD4⁺ T cells appear to survive or proliferate more efficiently than CD8⁺ T lymphocytes, based on their higher frequency in the bloodstream (Figure 3.3C). Collectively, these findings suggest that the MHC haplotype may have contributed to thymus enlargement and/or unusual thymocyte development (co-receptor expression profiles) in the FVB/N retrogenic mice.

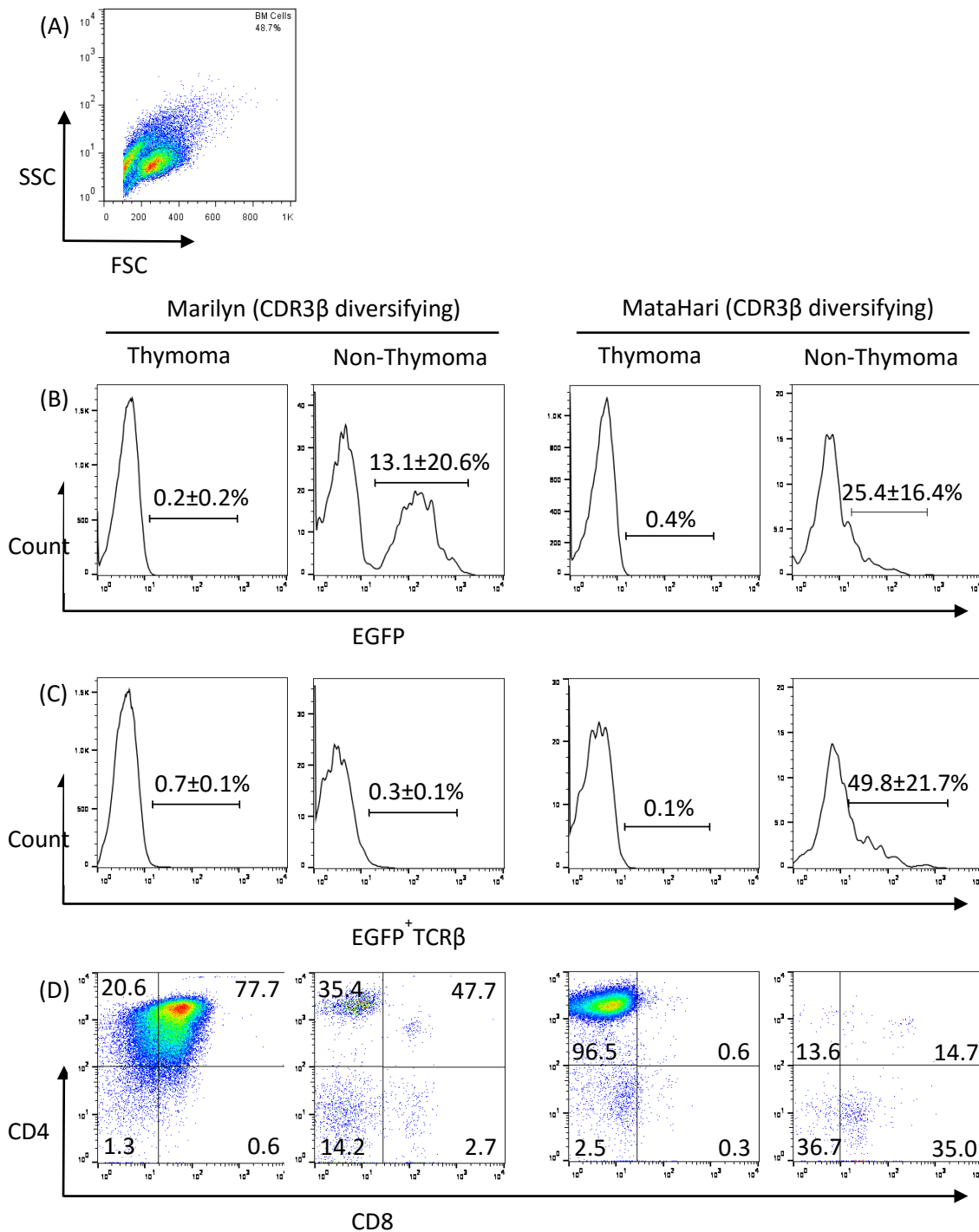


Figure 3.5. Flow cytometric analysis of thymocytes from Marilyn and MataHari TCR (CDR3 β diversifying) FVB/N retrogenic mice. Thymi were harvested after TCR reconstitution period (>8 weeks) from Marilyn (n=7) and MataHari (n=5) TCR (CDR3 β diversifying) retrogenic mice, and analysed for EGFP, TCR β , CD4 and CD8 expression to study T cell development. (A) The gating of the thymocyte population is shown, followed by analysis of (B) EGFP and (C) TCR β expressions based on the occurrence of thymoma and non-thymoma (small- and normal-sized thymi). (D) The DN, DP, SPCD4 and SPCD8 sub-population distribution is gated on the whole thymocyte population. Representative examples are shown. Percentages indicated on plots represent mean \pm SD for all mice (for (D) only means are shown), calculated to the first decimal place.

3.2.3. Analysis of FVB/N retrogenic mice secondary lymphoid tissue

After analysis of T cell development in the primary lymphoid organ, we examined the spleen to further characterise the peripheral T cell phenotype and confirm the observations seen in the circulation. Splens from Marilyn (n=7) and MataHari (n=5) TCR (CDR3 β diversifying) retrogenic mice were isolated and pictured (Figure 3.6A), showing similar sizes to that of a non-retrogenic TCR- $\beta/\delta^{-/-}$ deficient FVB/N mouse. Total splenic cellularity was measured and means of each cell count were calculated, displaying similar counts between the two types of retrogenic mouse ($p>0.05$; Figure 3.6B).

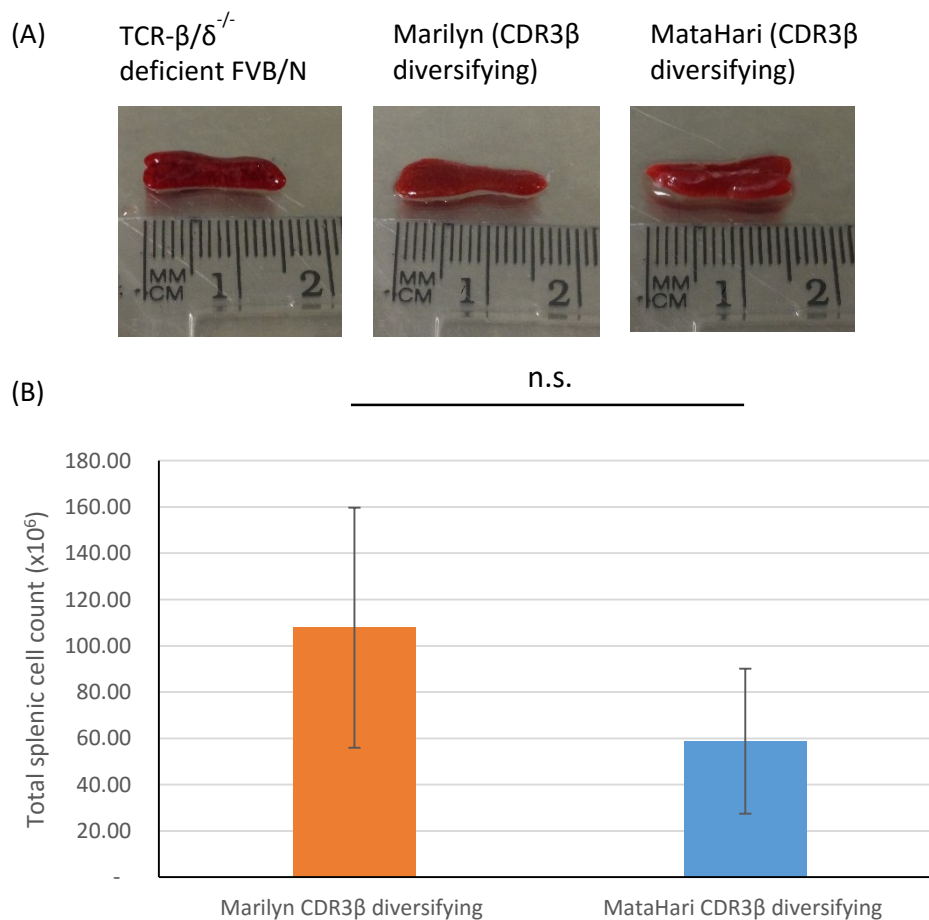


Figure 3.6. Splenic size and cellularity in Marilyn and MataHari TCR (CDR3 β diversifying) FVB/N retrogenic mice. Splens were harvested after TCR reconstitution period (>8 weeks) from Marilyn (n=7) and MataHari (n=5) TCR (CDR3 β diversifying) retrogenic mice. (A) Representative splens of the Marilyn and MataHari TCR (CDR3 β diversifying) retrogenic mice are shown, along with a non-retrogenic TCR- $\beta/\delta^{-/-}$ deficient FVB/N mouse spleen. (B) Total splenic cellularity was determined from the same animals. Average splenic cell counts of the two sets of retrogenic mice are shown with error bars and appear to be statistically similar ($p=0.0908$; $p>0.05$).

Splenocyte suspensions from the Marilyn (n=7) and MataHari (n=5) TCR (CDR3 β diversifying) retrogenic mice were prepared as described in *Chapter 7.8* and stained with the appropriate fluorochrome-conjugated Ab before analysis via flow cytometry. As expected, both Marilyn and MataHari TCR (CDR3 β diversifying) retrogenic splenocytes demonstrated pronounced levels of EGFP⁺TCR β ⁺ T cells (Figure 3.7). Additionally, analysis of co-receptor expressions in both retrogenic mice spleens confirmed the skew to the CD4⁺ T cell compartment as observed in the peripheral blood (Figure 3.3C).

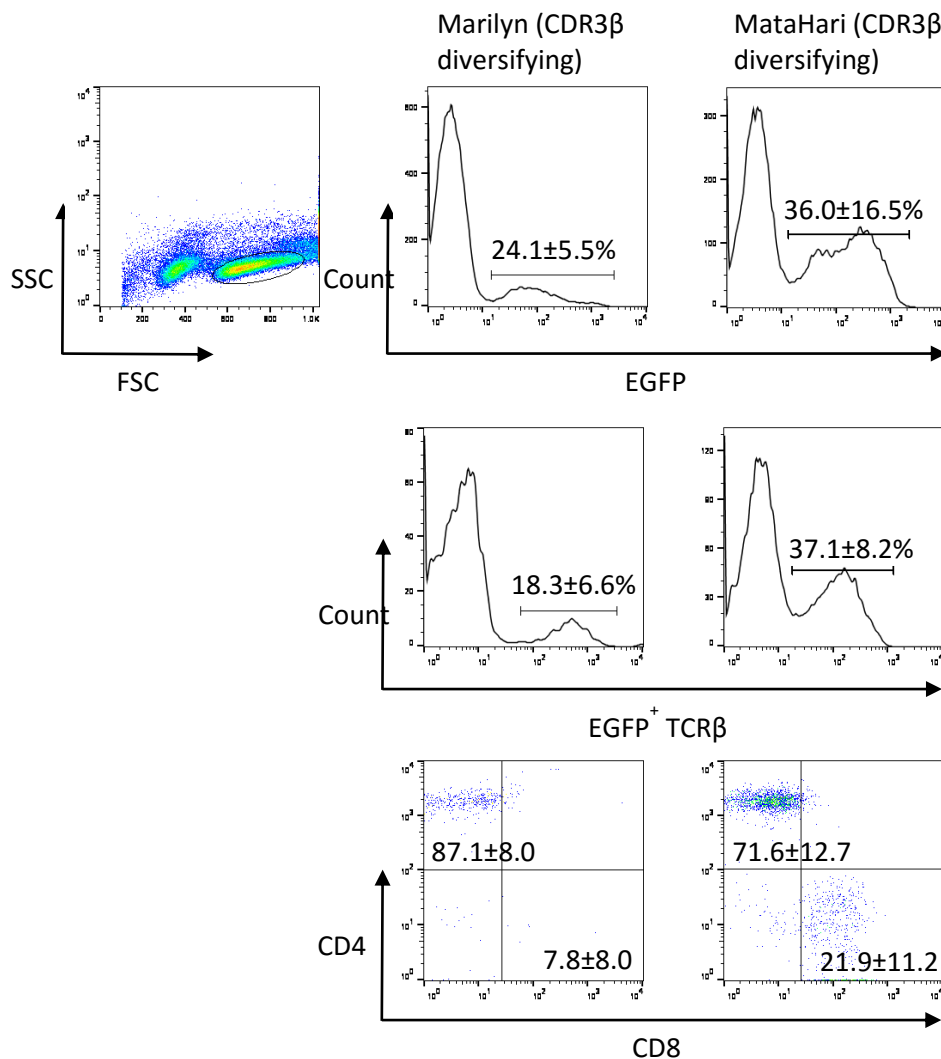


Figure 3.7. Flow cytometric analysis of Marilyn and MataHari TCR (CDR3 β diversifying) FVB/N retrogenic mice splenocytes. Spleens were harvested after the TCR reconstitution period (>8 weeks) from Marilyn (n=7) and MataHari (n=5) TCR (CDR3 β diversifying) retrogenic mice, and analysed for EGFP, TCR β , CD4 and CD8 expression to characterise the peripheral T cell compartment. Gating of the lymphocytes from the parental cell population is shown, followed by analysis of EGFP⁺ and EGFP⁺TCR β ⁺ expressions. The splenic CD4⁺ and CD8⁺ T cell distributions are also shown demonstrating a skewing to the CD4 compartment. Percentages of defined cell populations are shown as mean \pm SD.

Splenocytes from the retrogenic mice were also stained with fluorochrome-conjugated Ab for the specific V β chain; anti-V β 6 for Marilyn TCR (CDR3 β diversifying) and anti-V β 8.3 for MataHari TCR (CDR3 β diversifying) to detect the presence of their respective TCR β V domains. As the RSS sequences were directed to the TCR β chain CDR3 loop, mutations were not expected to interfere with the V β specific epitope. It was therefore anticipated that the TCR β constant and variable domain-specific Ab would detect the same populations and thus show matching percentages of staining. Indeed, a recent study by Dr Istvan Bartok, a colleague in the group, identified the germline CDR2 loop as critical for the anti-V β 6 Ab epitope (Istvan Bartok, unpublished data). The recombination cassette and gene recombination events are not expected to affect the CDR2 β region. Four of the seven Marilyn TCR (CDR3 β diversifying) retrogenic mice gave the expected result with similar levels of EGFP⁺TCR β ⁺ and EGFP⁺V β 6⁺ expression (~19.4%; Figure 3.8A; Table 3.2). Surprisingly, the remaining three retrogenic mice displayed negligible binding (1.3%) with the anti-V β 6 Ab in proportion to the 24.1% EGFP⁺TCR β ⁺ expression (Figure 3.8B; Table 3.2). Nevertheless, the complete dominance of this V β 6⁻ T cell population suggests it may even have a survival advantage linked to a novel TCR structure. Analysis of all five MataHari TCR (CDR3 β diversifying) splenocytes revealed more than 50% of the EGFP⁺ T lymphocytes were positively stained with the anti-V β 8.3 Ab (Figure 3.8C; Table 3.2). This observation indicates that the recombination event may alter the CDR3 β region to the extent that the structure of the TCR β V domain no longer exhibits the anti-V β 8.3 Ab epitope.

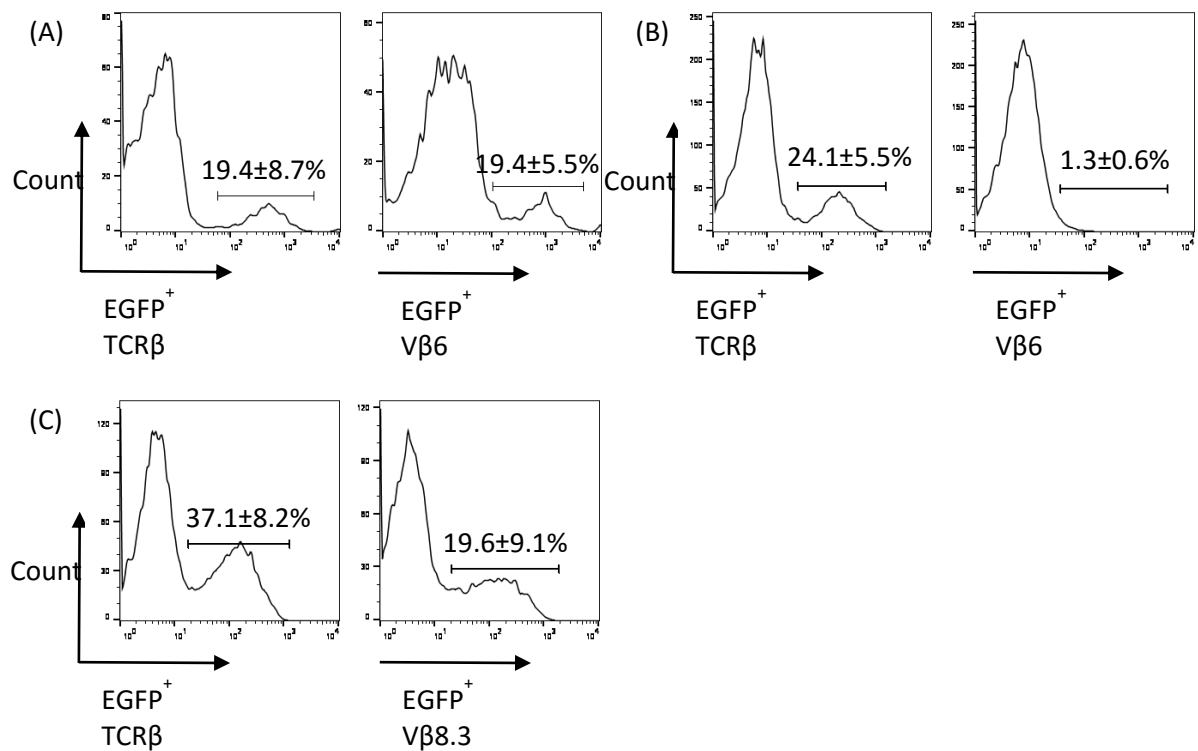


Figure 3.8. Retention and loss in binding with specific anti-Vβ6/8.3 Ab epitope. Splenocytes from the Marilyn (n=7) and MataHari (n=5) TCR (CDR3β diversifying) retrogenic mice were stained against anti-TCRβ, -Vβ6 and -Vβ8.3 Ab, and analysed using flow cytometry. (A) Example of four of seven Marilyn TCR (CDR3β diversifying) retrogenic mice which expressed similar levels of EGFP⁺TCRβ⁺ and EGFP⁺Vβ6⁺. (B) Example of the three retrogenic mice whose EGFP⁺TCRβ⁺ splenocytes appeared to exhibit profound total loss of the anti-Vβ6 Ab epitope. (C) Example of a MataHari TCR (CDR3β diversifying) retrogenic mouse splenocyte population displaying reduced positive binding to the anti-Vβ8.3 Ab relative to anti-TCRβ. Data represents mean ± SD for all mice in each respective classification.

Table 3.2. Retention and loss in binding with specific anti-Vβ6/8.3 Ab epitope. Summary of relative binding of the variable domain specific (Vβ6/8.3) and constant domain (TCRβ) Ab. Marilyn (CDR3β diversifying) EGFP⁺TCRβ⁺ retrogenic splenocytes are variably bound by anti-Vβ6 Ab. Reduced staining of EGFP⁺TCRβ⁺ retrogenic splenocytes with anti-Vβ8.3 Ab. Data represents mean ± SD.

Construct	Anti-Vβ6/8.3 Ab Binding	Frequency	%EGFP ⁺ TCRβ ⁺	%EGFP ⁺ Vβ6/8.3 ⁺	Ratio of Vβ6/8.3 to TCRβ (%)
Marilyn (CDR3β diversifying)	Complete	57% (4/7)	19.4 ± 8.7	19.4 ± 5.5	~100
	Negligible	43% (3/7)	24.1 ± 5.5	1.3 ± 0.6	0.1 ± 0
MataHari (CDR3β diversifying)	Reduced	100% (5/5)	37.1 ± 8.2	19.6 ± 9.1	53.7 ± 23.5

3.3. Discussion

3.3.1. Summary

The FVB/N $TCR\beta/\delta^{-/-}$ deficient mice used in the generation of retrogenic mice possess targeted mutations at the $TCR\beta$ and $TCR\delta$ gene loci hence are unable to express $\alpha\beta$ TCR or $\gamma\delta$ TCR (Mombaerts et al., 1992). The detection of peripheral T cell pools in the retrogenic mice indicates that exogenous $TCR\beta$ chains are generated and pair with endogenous and/or exogenous $TCR\alpha$ chains, resulting in functional $\alpha\beta$ TCRs. The T cells must have developed from the adoptively transferred HSCs (carrying the diversifying TCR constructs) that entered the thymic microenvironment and committed to the $\alpha\beta$ T cell lineage. In both types of retrogenic mice, we anticipate simultaneous expression of exogenous $TCR\alpha$ and $TCR\beta$ chains at the DN stage, with the expression of the latter chain dependent upon the lymphocyte-specific V(D)J recombinase enzymes. The expression of the $TCR\beta$ chain requires successful removal of the recombination cassette and productive, in-frame gene rearrangement resulting in DNA sequence diversification. At the end of the DN4 stage, the diversified $TCR\beta$ pairs with either the surrogate pT α chain to form the pre-TCR, or with the exogenous $TCR\alpha$ with higher affinity, which could disrupt pre-TCR formation and function (Borowski et al., 2003; Trop et al., 2000). Despite the possibility that premature establishment of the exogenous $\alpha\beta$ TCR could interfere with pre-TCR and conventional $\alpha\beta$ T cell development, the resultant T lymphocytes that exit the thymus into general circulation are still subject to thymic education and exhibit functional, MHC-restricted TCRs. Although unusual, $\alpha\beta$ TCR and other complexes such as $\gamma\delta$ TCR are proposed to be able to substitute the pre-TCR and signal the DN to DP transition in the absence of ligand engagement if they were expressed at the DN stage (Erman et al., 2002). As such, formation of the pre-TCR that normally directs development to the DP stage can be accompanied by prematurely expressed $\alpha\beta$ TCR comprised of exogenous $TCR\alpha$ with the diversified $TCR\beta$ chain.

In this chapter, we reported three significant findings in $H2^q$ retrogenic mice expressing $H2^b$ -restricted TCRs. Firstly, the occurrence of the abnormally enlarged thymi in some retrogenic mice for both Marilyn and MataHari (CDR3 β diversifying) TCRs. We have noted that the unusual co-receptor expression profiles, which describe the DN, DP and SP thymocyte distributions may be indicative of the thymoma event. It is possible that there is poorer selection efficiency as a result of expressing $H2^b$ -restricted TCRs in FVB/N ($H2^q$) mice which may limit ligand engagement, signalling and thymocyte progression to the SP compartments. However, as described in allogeneic graft rejection studies, TCRs are inherently cross-reactive and commonly allo-MHC reactive, allowing TCR engagement with different MHC haplotypes despite selection on autologous pMHC molecules (Zerrahn, Held & Raulet, 1997). Accordingly, any variant TCRs that respond to self-peptide and $H2^q$ MHC molecules in the

acceptable affinity range will not be negatively selected and can be positively selected and allowed to exit the thymus (D'Orsogna et al., 2011; Marrack & Kappler, 1988). Additionally, the use of H2^q retrogenic mice may facilitate development of H2^b-restricted HY-specific TCRs due to the absence of HY self-antigens. Hence, we do not expect clonal deletion nor blockage in the DP stage which can cause an accumulation of thymocytes.

Secondly, a skewing to the CD4⁺ T cell lineage suggests positive selection during transition from DP to SP thymocytes in retrogenic mice appears to be more efficient with MHC Class II. It is possible the Marilyn TCR has an intrinsic preference for MHC class II and may exhibit biased selection to the CD4 lineage on other H2 haplotypes (Grandjean et al., 2003). Conversely to Marilyn, MataHari TCR (CDR3 β diversifying) T cells did not follow their H2^b-directed CD8 lineage preference, demonstrating more than three-fold production of CD4⁺ compared to CD8⁺ T cells even though the MataHari TCR is characteristically expressed in CD8⁺ cytotoxic T cells (Valujskikh et al., 2002). Equally, the higher CD4⁺ T cell levels may have been caused by a higher death rate of CD8⁺ T cells, as they are more reliant on TCR-dependent survival signals (Sinclair et al., 2013; Seddon & Zamoyska, 2002). It is not clear whether the WT TCR/MHC haplotype mismatch, recombination cassette-inducing CDR3 β mutagenesis or the multi-cistronic retrogenic system expressing a premature $\alpha\beta$ TCR may have contributed to the CD4 lineage bias. Holst et al. (2006) previously showed that MataHari female RAG1^{-/-} retrogenic mice produced a competent CD4⁺ T cell compartment, albeit smaller than CD8⁺ T cells.

Lastly, in a proportion of retrogenic T cells, mutagenesis of the TCR appears to alter the structure of the TCR β V domain such that anti-V β 6 or anti-V β 8.3 Ab can no longer identify the diversified Marilyn and MataHari TCRs, respectively. Anti-TCR V β Ab are not expected to be generally influenced by the CDR3 structure as they are raised against clonal TCRs but detect large proportions of WT repertoires containing diverse CDR3 regions. The diversification of the CDR3 β , which is predicted to modify length and amino acid composition, may however result in significant conformational changes to the V domain. For the Marilyn TCR variants, we know that the anti-V β 6 Ab epitope includes germline CDR2 (Bartok, unpublished) and may therefore have undergone an aberrant recombination event which affects CDR2. Mutation of the CDR3 β does not seem to compromise the expression, thymic development and selection of the heterodimeric $\alpha\beta$ TCR. Analysis of the resulting diversified TCR CDR3 β DNA and peptide sequences can provide valuable information regarding the TCR structure, and will be investigated in the next chapter.

3.3.2. Conclusions

This chapter demonstrates the successful restoration of the T cell compartment in the T cell-deficient H2^a mouse strain. The expression of a functional peripheral T cell repertoire indicates that the $\alpha\beta$ TCR (CDR3 β diversifying) transgenes must have undergone successful *in vivo* removal of the recombination cassette and in-frame joining events. This confirms the viability of the recombination cassette strategy and supports the application for diversification of H2^b-restricted TCRs in MHC/TCR haplotype-matched retrogenic mice. The bias to the CD4⁺ T cell subset and loss of specific V β domain epitope will be further explored in the next chapter.

Chapter 4

Chapter 4: Phenotypic and sequence analysis of the T cell repertoire in H2^b retrogenic mice

4.1. Introduction

TCR repertoire diversity is one of the hallmarks of the adaptive immune system, which allows effective responses against a broad array of pathogens whilst maintaining self-tolerance. Such diversity is generated by somatic rearrangement of V, (D), and J genes across the TCR α and β loci, combined with random junctional insertion, deletion and substitution of nucleotides.

As discussed in Chapter 2, we have designed a recombination cassette to induce somatic gene recombination in retrogenic mice to facilitate the *in vivo* generation of TCR variants that are subject to thymic positive and negative selection. Together, the selection processes ensure $\alpha\beta$ T cells released into the periphery are restricted to recognising self-MHC within the appropriate affinity range. The $\alpha\beta$ TCR (CDR3 β diversifying) constructs were synthesised to contain the recombination cassette inserted into the centre of the CDR3 β loop before cloning into the pMigR1 retroviral vector (Figure 2.2). The previous chapter highlighted that the newly designed recombination cassette, which utilises a shorter inter-RSS linker compared to that used by Holland et al. (2012), can facilitate reconstitution of the peripheral T cell compartment in a lymphopenic host for both $\alpha\beta$ TCR templates. These data indicate that our novel mutagenesis system is functional and can be applied successively onto MHC haplotype-matched (H2^b) recipient mice.

In this chapter, we aimed to diversify the Marilyn (CD4⁺V β 6⁺) and MataHari (CD8⁺V β 8.3⁺) TCRs in TCR- $\beta/\delta^{-/-}$ deficient C57BL/6 (H2^b) mice separately to investigate the sequence variation introduced into their CDR3 β regions, where the recombination cassette is positioned. Removal of the recombination cassette and subsequent gene recombination resulting in in-frame mutation should generate variants of the TCR CDR3 β , with higher variability expected closer to the point of RSS insertion. The target of our optimisation system, CDR3 β , is the primary site of peptide binding that makes the greatest contribution to TCR specificity and which is also subject to great variation (Freeman et al., 2009; Bercovici et al., 2000). We will explore modifications to the CDR3 β peptide composition, length and net charge as a result of our mutagenesis approach. Further, we will challenge the diversified T cell repertoire with their cognate antigens in order to isolate and describe the functionally optimal receptors.

4.2. Results

4.2.1. Detection of T cell repertoire in retrogenic mice peripheral blood

Overall, we generated a total of 4 and 11 C57BL/6 retrogenic mice expressing the Marilyn and MataHari $\alpha\beta$ TCR (CDR3 β diversifying) constructs, respectively. The summary of transduction efficiencies and number of EGFP⁺ HSCs adoptively transferred into each retrogenic mouse is shown below (Table 4.1). Notably, the HSCs were obtained from both male and female C57BL/6 donor mice similar to FVB/N retrogenic mice (Refer to *Chapter 3.2.1*). There were variable transduction efficiencies and numbers of transduced HSCs which each TCR- $\beta/\delta^{-/-}$ recipient mice received during each experiment set-up.

Table 4.1. The cohorts of C57BL/6 retrogenic mice generated from adoptive transfer of retrovirally-transduced HSCs containing Marilyn and MataHari $\alpha\beta$ TCR (CDR3 β diversifying) constructs.

Construct	Group	Transduction efficiency	No. of EGFP ⁺ HSCs injected into each mice	No. of retrogenic mice generated
Marilyn (CDR3 β diversifying)	1	42.3%	1.8×10^6	4
MataHari (CDR3 β diversifying)	1	11.7%	2.0×10^5	1
	2	26.2%	6.0×10^5	4
	3	31.5%	2.7×10^6	6

We next analysed the presence of the peripheral T cell repertoires of both classes of retrogenic mice. After allowing at least 8 weeks to reconstitute the T cell pool, the mice were sampled at three-week intervals, 8, 11 and 14 weeks post-injection. Blood from the retrogenic mice tail vein were collected, red blood cells lysed and subsequently stained for TCR β (C domain), CD4 and CD8 co-receptors using the appropriate fluorochrome-conjugated Ab. Flow cytometric analysis indicated steady increases in the frequencies of EGFP⁺TCR β ⁺ T cells in Marilyn (Group 1; n=4) and MataHari (Group 2; n=4) TCR (CDR3 β diversifying) retrogenic mice (Figure 4.1A). The same selection bias to MHC Class II restriction as observed in WT/MHC-mismatched FVB/N strains appeared in the C57BL/6 retrogenic mice. Both groups of retrogenic mice demonstrated a higher frequency of CD4⁺ compared to CD8⁺ T cells at all time points (Figure 4.1B). Again, it is perhaps surprising to observe a prevailing peripheral CD4⁺ T cell pool in the MataHari TCR (CDR3 β diversifying) retrogenic mice since MataHari transgenic T cells are typically CD8-positive and MHC Class I-restricted.

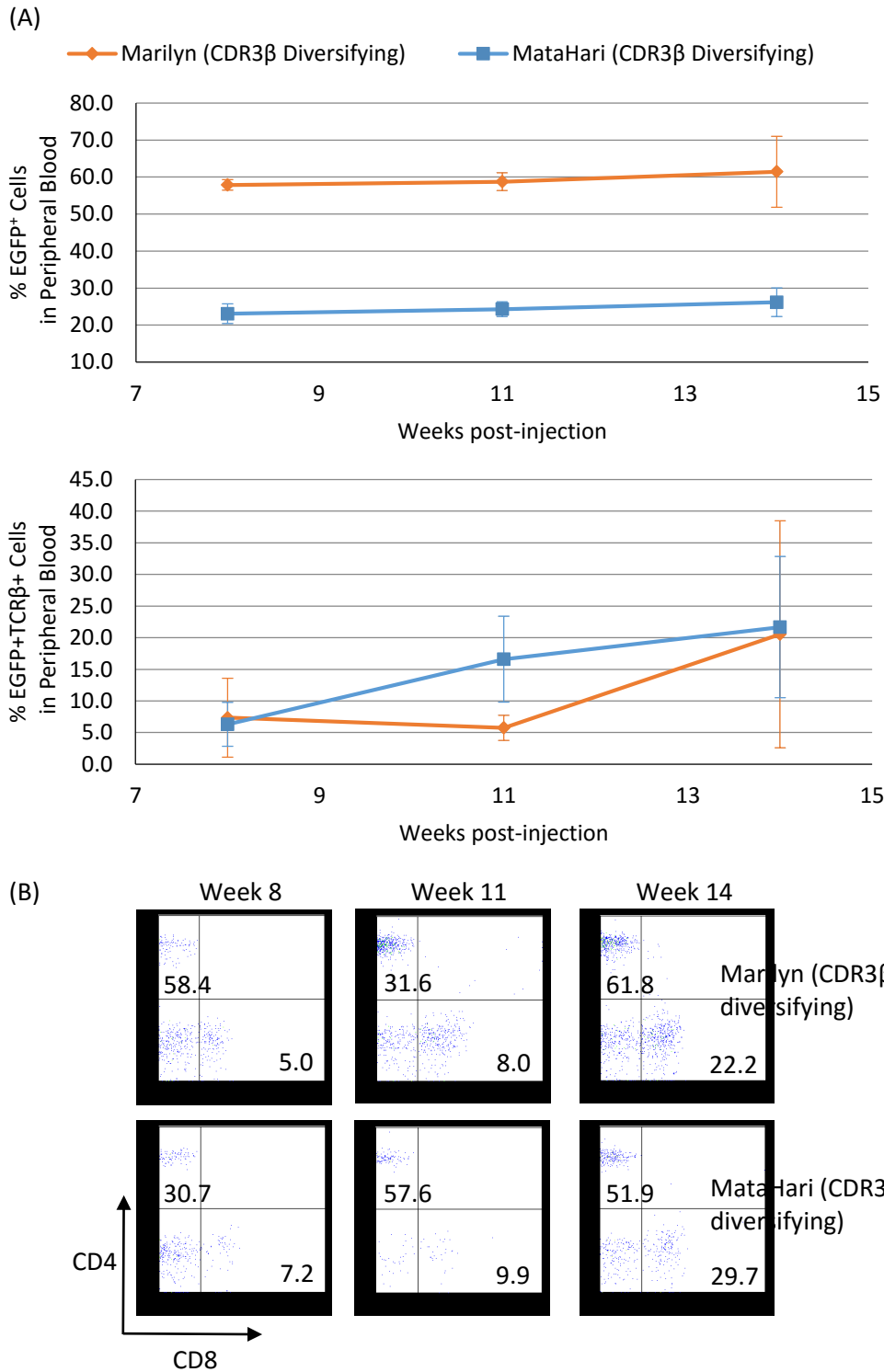


Figure 4.1. Flow cytometric analysis of peripheral blood from C57BL/6 retrogenic mice transduced with Marilyn and MataHari $\alpha\beta$ TCR (CDR3 β diversifying) constructs. Retrogenic mice were allowed 8 weeks to reconstitute the peripheral T cell pool after adoptive transfer of transduced HSCs. At 8, 11 and 14 weeks post-injection, blood was sampled for expression of EGFP and EGFP⁺TCR β , as well as CD4 and CD8 co-receptors. (A) Analysis of blood samples showed increasing numbers of EGFP⁺ and EGFP⁺TCR β ⁺ expressing cells in the lymphocyte population. Each point is shown as mean \pm SD. (B) Co-receptor expression profiles gated on EGFP⁺TCR β ⁺ cells during the analyses indicated more CD4⁺ than

CD8⁺ T cells in the periphery. Mean co-receptor expressions are shown on representative plots of Marilyn TCR (CDR3 β diversifying) retrogenic mice (Group 1; n=4) injected with 1.8×10^6 EGFP⁺ HSCs each (42.3% transduction efficiency), and MataHari TCR (CDR3 β diversifying) retrogenic mice (Group 2; n=4) adoptively transferred with 6.0×10^5 EGFP⁺ HSCs each (26.2% transduction efficiency).

4.2.2. Analysis of C57BL/6 retrogenic mice primary lymphoid organs

Following the detection of the peripheral T cells in the blood, we then sought to analyse the retrogenic mice thymocyte populations. Firstly, we aimed to determine the presence of T cell subsets that are not native to WT Marilyn (CD4⁺V β 6⁺) and MataHari (CD8⁺V β 8.3⁺) T cells, and the bias to the CD4 lineage. Secondly, we wanted to ascertain whether the C57BL/6 retrogenic mice developed the apparent thymomas observed in the FVB/N retrogenic mice (Refer to *Chapter 3.2.2*). Thymi from Marilyn (n=4) and MataHari (n=7) TCR (CDR3 β diversifying) retrogenic mice were isolated after the 8-week TCR reconstitution period. All Marilyn TCR (CDR3 β diversifying) retrogenic mice displayed a small thymus with an average of $12.4 (\pm 8.2) \times 10^6$ cells (Figure 4.2A, C). Conversely, the MataHari TCR (CDR3 β diversifying) retrogenic exhibited an average thymocyte count of $25.6 (\pm 31.0) \times 10^6$ cells (Figure 4.2C). The notably larger cell counts and SD were attributed to two retrogenic mice displaying normal-sized thymi (Figure 4.2A, *right*) which resembled that of WT C57BL/6 mice (Figure 4.2B). The majority of the MataHari TCR (CDR3 β diversifying) retrogenic exhibited the small thymus of the TCR- $\beta/\delta^{-/-}$ deficient mice (Figure 4.2A, *left*; B). Despite these differences, the average cellularity of the MataHari TCR (CDR3 β diversifying) retrogenic thymi appeared to be similar to that of the TCR- $\beta/\delta^{-/-}$ deficient mice ($p > 0.05$; non-significant difference) rather than of normal WT C57BL/6 mice ($p < 0.01$; Figure 4.2C).

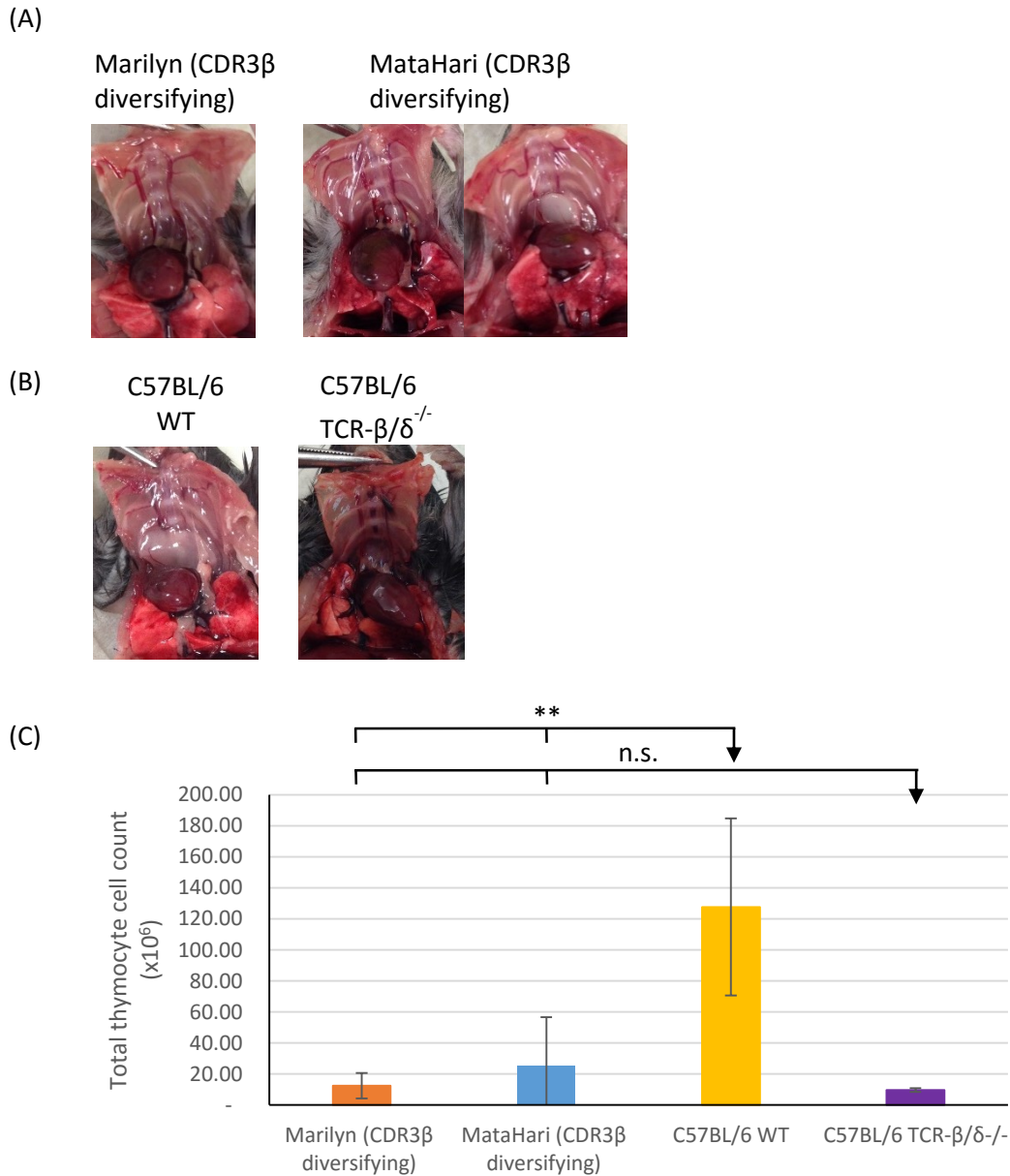


Figure 4.2. Thymic size and cellularity in Marilyn and MataHari TCR (CDR3 β diversifying) C57BL/6 retrogenic mice. Thymi from Marilyn (n=4) and MataHari (n=7) TCR (CDR3 β diversifying) retrogenic mice were harvested after the TCR reconstitution period (>8 weeks). (A) Thymi sizes of the retrogenic mice are pictured, with (B) the thymi of C57BL/6 WT and TCR- $\beta/\delta^{-/-}$ deficient mice shown for comparison. (C) Total thymocyte count is summarised for each type of retrogenic mice type, C57BL/6 WT (n=3) and TCR- $\beta/\delta^{-/-}$ deficient (n=2) mice. Data is represented as mean \pm SD for all mice.

We next analysed the thymocytes for cell surface expression of EGFP, TCR β , CD4 and CD8 via flow cytometry. As shown in Figure 4.3, both Marilyn and MataHari TCR (CDR3 β diversifying) thymocyte populations expressed sizeable levels of EGFP⁺ and EGFP⁺TCR β ⁺ (Figure 4.3A). Interestingly, the thymocyte populations showed a large accumulation of DN cells, with considerable detection of single-positive CD4⁺ and CD8⁺ lymphocytes (Figure 4.3). The near complete block from DN to DP stage is a phenotypic trait of TCR- β / δ ^{-/-} deficient mice (Mombaerts et al., 1992). The thymic SPCD4:SPCD8 ratio were found to be ~3:1 in from Marilyn and ~1:1 in MataHari TCR (CDR3 β diversifying) retrogenic mice. This suggests that, after adoptive transfer, the transduced HSCs migrated effectively to the thymic microenvironment, underwent commitment to the $\alpha\beta$ T cell lineage and differentiated into mature thymocytes which reconstituted the peripheral T cell repertoire. The bias to the CD4 lineage in Marilyn TCR (CDR3 β diversifying) thymocyte supports the higher CD4⁺ T cell frequency observed in the periphery (Figure 4.1B). A smaller proportion of CD8 thymocytes appeared, which may be responsible for the presence of the peripheral CD8⁺ T lymphocytes in the Marilyn TCR (CDR3 β diversifying) retrogenic mice. This may reflect intrinsic preference of the Marilyn TCR, despite CDR3 β diversification, for MHC Class II (Holst et al., 2006; Grandjean et al., 2003). Also noteworthy is the ~1:1 ratio of SPCD4 to SPCD8 amongst MataHari TCR (CDR3 β diversifying) thymocytes which seems to translate to a higher presence of circulating CD4⁺ T cells. This further supports the notion that the CD8⁺ T cells appear to survive or proliferate less efficiently compared to their CD4⁺ counterparts (Sinclair et al., 2013; Seddon & Zamoyska, 2002).

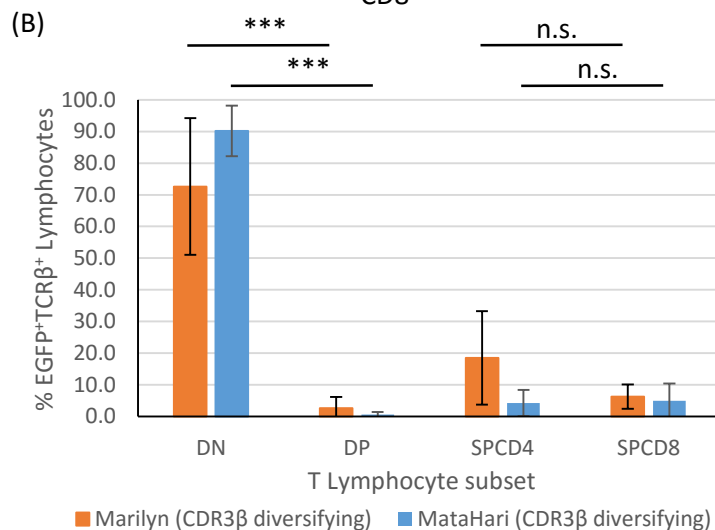
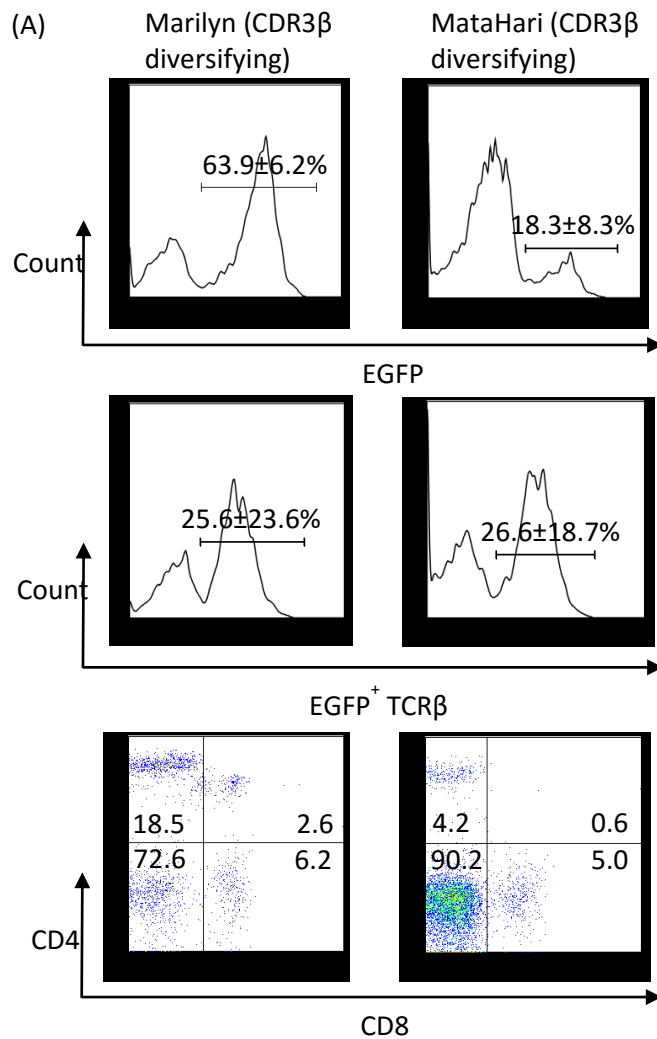


Figure 4.3. Flow cytometric analysis of Marilyn and MataHari TCR (CDR3 β diversifying) C57BL/6 retrogenic mice thymocytes. Thymi from Marilyn (n=4) and MataHari (n=7) TCR (CDR3 β diversifying) retrogenic mice were harvested after the TCR reconstitution period (>8 weeks), and analysed for EGFP, TCR β , CD4 and CD8 expression to study T cell ontogeny. (A) Gated on the lymphocyte population, the identification of the EGFP and EGFP⁺TCR β expression, and analysis of the T cell subsets based on co-receptor expression is shown. Data is represented as mean \pm SD, calculated to the first decimal place.

(B) Summary of lymphocyte population percentage based on co-receptor expression. DN: double-negative, DP: double-negative, SPCD4/CD8: single-positive CD4/CD8.

4.2.3. Analysis of C57BL/6 retrogenic mice secondary lymphoid tissue

Following the analysis of the primary lymphoid organs, we proceeded to analyse the spleen and lymph nodes (LN) to further characterise the peripheral T lymphocytes, and to study the diversification of the TCR CDR3 β region as a result of the mutagenesis approach. The spleens and LN of the retrogenic mice were harvested at the same time as the thymus after the TCR reconstitution period. Marilyn TCR (CDR3 β diversifying) retrogenic spleens demonstrated an average total cellularity of $86.6 (\pm 43.0) \times 10^6$ cells (n=4), whereas their MataHari counterparts displayed a similar mean count of $96.6 (\pm 71.5) \times 10^6$ cells (n=7; $p > 0.05$, Figure 4.4). The spleen cellularity of the retrogenic mice were shown to be statistically similar to that of WT and TCR- $\beta/\delta^{-/-}$ deficient mice ($p > 0.05$; Figure 4.4C).

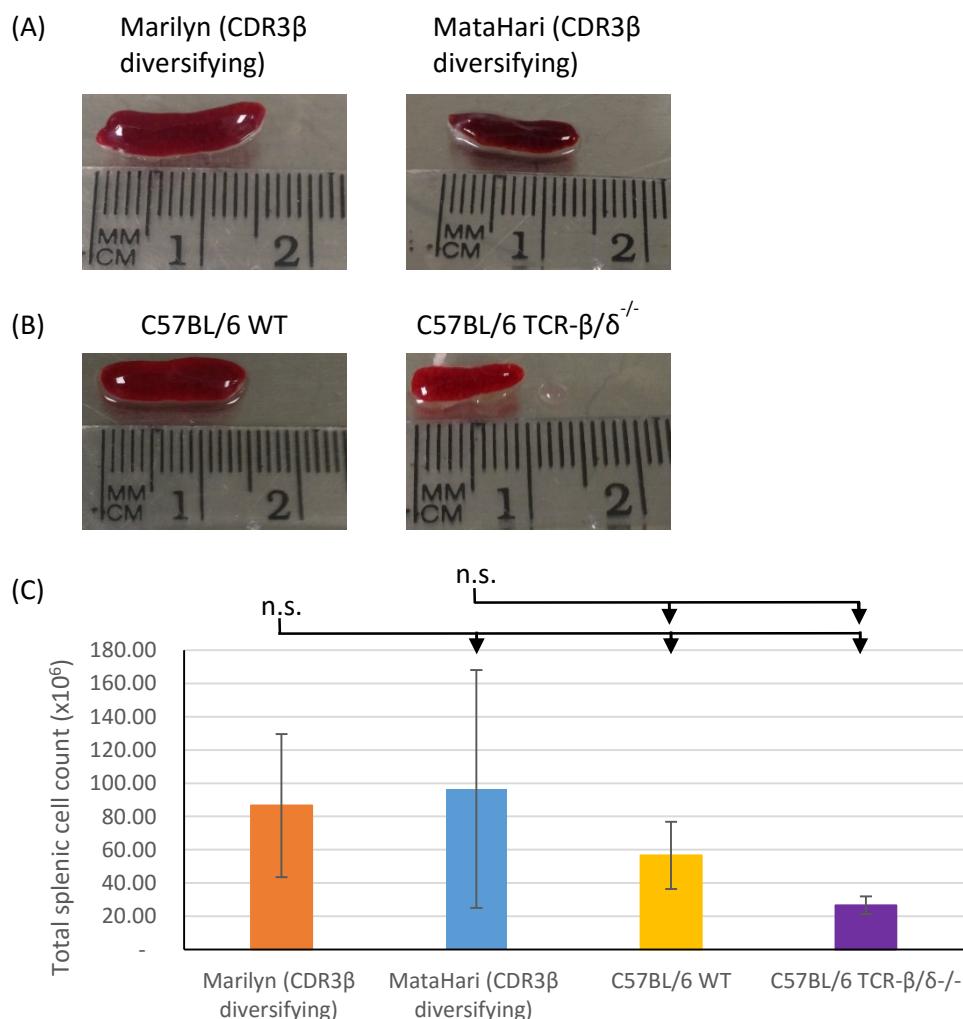


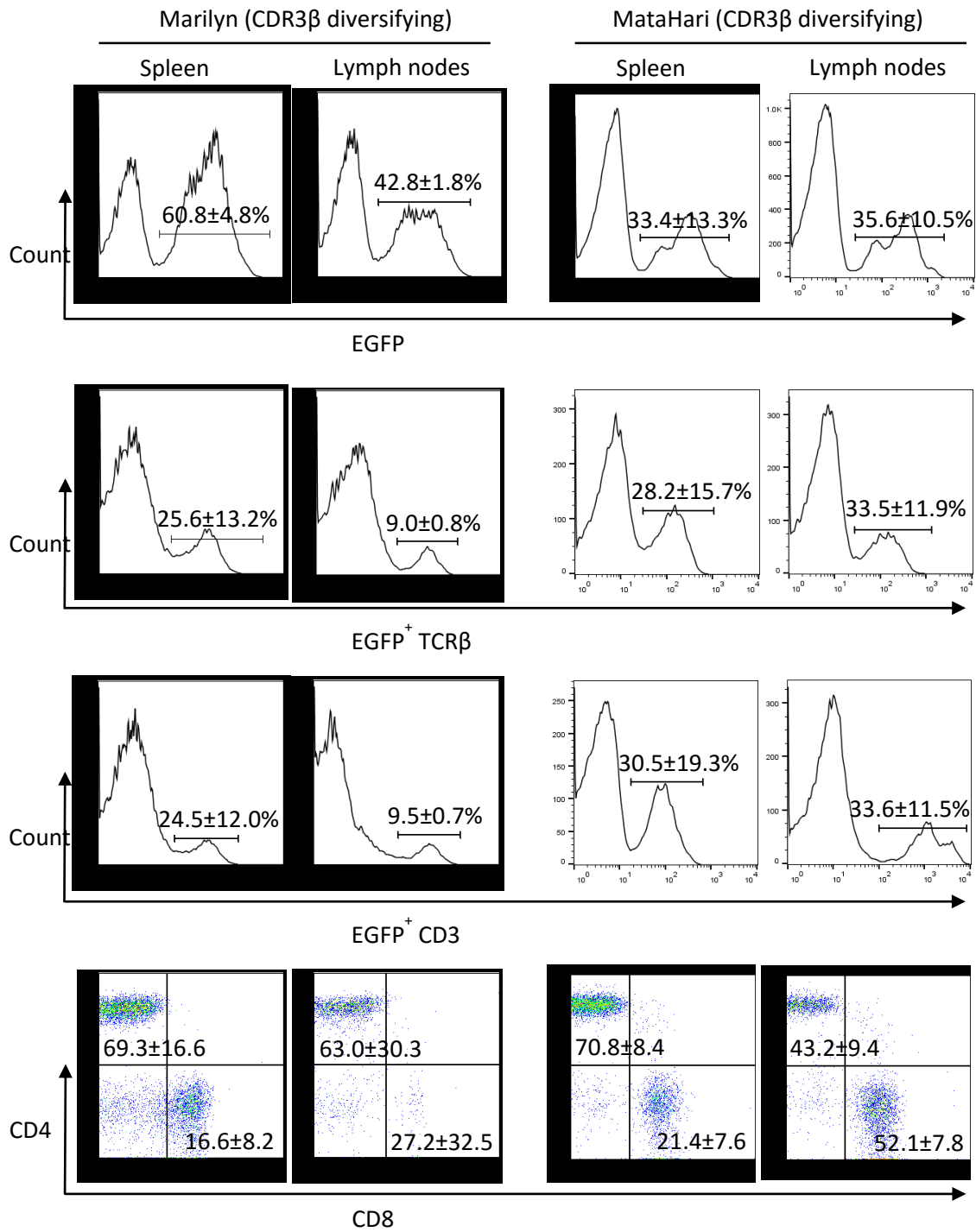
Figure 4.4. Splenic size and cellularity of Marilyn and MataHari TCR (CDR3 β diversifying) C57BL/6 retrogenic mice. (A) Spleens from the Marilyn (n=4) and MataHari (n=7) TCR (CDR3 β diversifying)

retrogenic mice, and (B) C57BL/6 WT (n=3) and TCR- $\beta/\delta^{-/-}$ deficient mice (n=2) were isolated and measured. (C) Total splenic cellularity was determined and calculated as mean \pm SD.

Spleen and LN cells from the retrogenic mice were subsequently stained for expression of the EGFP, TCR β , CD3, CD4 and CD8. As observed in the peripheral blood, the lymphocytes from the secondary lymphoid organs in both Marilyn and MataHari TCR (CDR3 β diversifying) retrogenic mice demonstrated sizeable levels of EGFP⁺TCR β ⁺ expression (Figure 4.5A). In both spleen and LN, CD3 expression in EGFP⁺ lymphocytes were analysed and shown to be very similar to TCR β expression levels confirming a complete and functional TCR signalling complex (Figure 4.5A, B). This suggests that the differentiation of the transduced HSCs into the T cell compartment, and further activation and functionality, is mediated by a functional signalling complex using the recombined retrogenic TCR β chain. As observed in the blood, both Marilyn and MataHari TCR (CDR3 β diversifying) retrogenic splenocytes showed skewing to the CD4⁺ T cell lineage with at least a ~3:1 CD4:CD8 ratio. The CD4⁺ lymphocyte population appeared to be statistically higher than the CD8⁺ cells in the spleen ($p < 0.001$), but similar in the lymph nodes ($p > 0.05$; Figure 4.5B).

Furthermore, we determined the mean fluorescence intensity (MFI) of TCR β expression in EGFP⁺ splenic lymphocytes in both retrogenic mice. MFI can be used to quantify the protein expression levels on each cell. TCR β MFI in Marilyn (223 ± 64) and MataHari (183 ± 42) TCR (CDR3 β diversifying) retrogenic mice were shown to be significantly reduced compared to that in WT C57BL/6 mice (731 ± 224 ; Figure 4.5C). This suggests that the retrogenic mice T cells may require lower expression of the TCR to achieve the equivalent homeostatic and activation signals required for thymic selection and release into the periphery observed in WT mice.

(A)



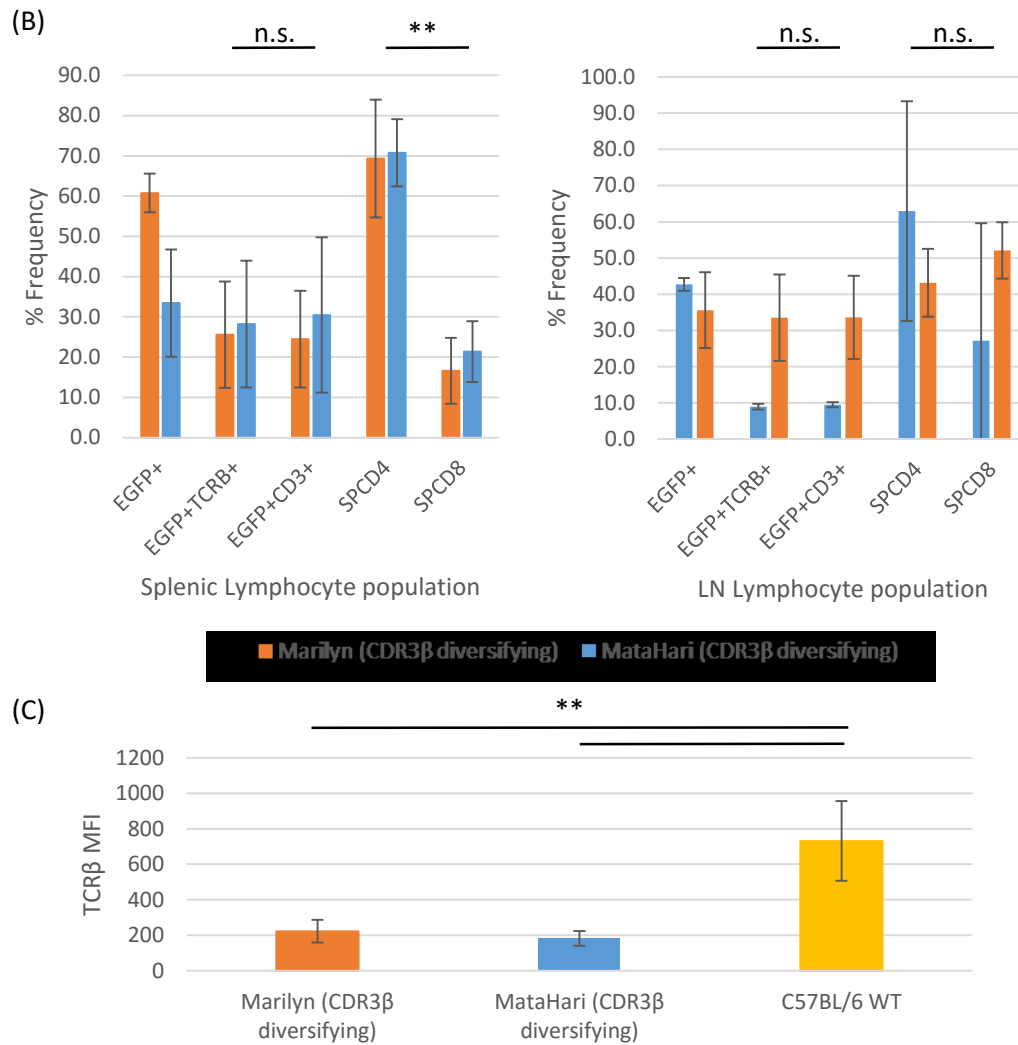


Figure 4.5. Flow cytometric analysis of retrogenic mice secondary lymphoid organs. (A) Spleens and LN were extracted from the Marilyn (spleen, n=4; LN, n=2) and MataHari (spleen, n=7; LN, n=4) TCR (CDR3 β diversifying) retrogenic mice and subsequently stained for expression of EGFP, TCR β , CD3, CD4 and CD8. (B) Graph summarising the expression of EGFP, TCR β , CD3, CD4 and CD8 in the splenic (*left*) and lymph node (*right*) lymphocyte populations. (C) TCR β MFI in splenic lymphocytes of retrogenic and WT mice (n=4) is illustrated. Data is presented as mean \pm SD for all mice.

We further characterised the T cell repertoire generated in the retrogenic mice based on the specific TCR β chain. The splenic lymphocytes were stained with Ab for their specific V β domains: anti-V β 6 for Marilyn TCR, and anti-V β 8.3 for MataHari TCR. Similar to our observations in the FVB/N retrogenic mice, 75% of the Marilyn TCR (CDR3 β diversifying) retrogenic mice splenic lymphocytes demonstrated very low binding (\sim 3.5%) with the anti-V β 6 Ab relative to \sim 31.0% positive staining for EGFP $^{+}$ TCR β^{+} expression (Figure 4.6B; Table 4.2). The remaining mouse displayed similar staining for anti-TCR β and anti-V β 6 Ab in the EGFP $^{+}$ lymphocyte population (9.9% to 9.2%; Figure 4.6A; Table 4.2). The almost complete dominance of this V β 6 $^{-}$ T cell population again suggests a survival advantage associated with

a structural alteration of the TCR promoting efficient selection during thymic T cell development and/or peripheral survival and homeostasis. Analysis of the MataHari TCR (CDR3 β diversifying) retrogenic mice splenic EGFP⁺ lymphocytes showed reduced positive staining (73.8%) with the anti-V β 8.3 (20.2%) compared to anti-TCR β Ab (28.2%; Figure 4.6C; Table 4.2). Altogether, the recombination event appears to mutate the CDR3 β region resulting in disruption of the specific V β epitopes. We have previously mentioned a possible link between the germline CDR2 β loop and the anti-V β 6 Ab epitope (Istvan Bartok, unpublished data). Sequence analysis of the CDR regions may explain whether this Ab epitope loss, reduced or complete depending on the $\alpha\beta$ TCR template, is a consequence of our mutagenesis approach.

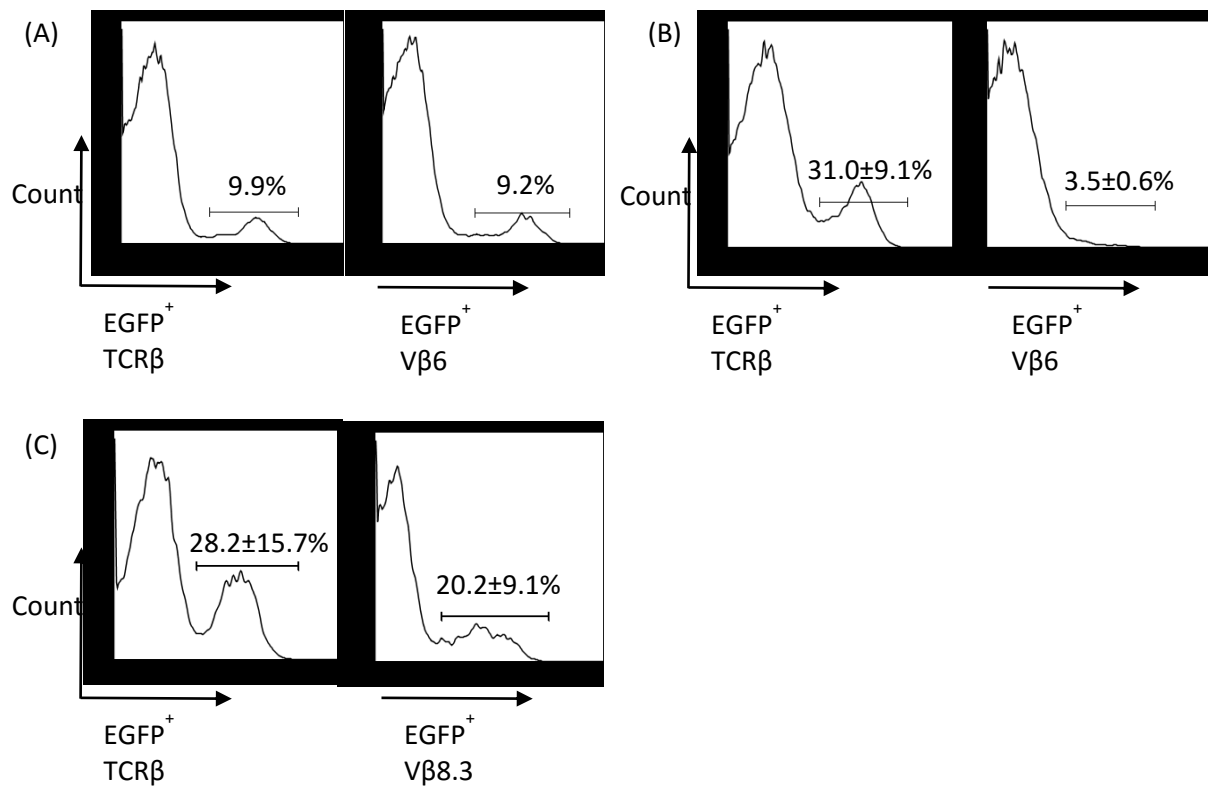


Figure 4.6. Retention and loss in binding with specific anti-V β 6/8.3 Ab epitope. Splenocytes from the Marilyn (n=4) and MataHari (n=7) TCR (CDR3 β diversifying) retrogenic mice were stained against anti-TCR β , -V β 6 and -V β 8.3 antibodies, and analysed using flow cytometry. (A) Only one Marilyn TCR (CDR3 β diversifying) retrogenic mice expressed similar levels of EGFP⁺TCR β ⁺ and EGFP⁺V β 6⁺. (B) The other three retrogenic mice EGFP⁺TCR β ⁺ splenocytes appeared to exhibit profound total loss in anti-V β 6 Ab epitope. (C) MataHari TCR (CDR3 β diversifying) retrogenic mice splenocytes displayed reduced positive binding to the anti-V β 8.3 Ab relative to anti-TCR β Ab. Data represents mean \pm SD.

Table 4. 2. Summary of retention and loss in binding with specific anti-Vβ6/8.3 Ab epitope compared to anti-TCRβ staining in retrogenic mice splenocytes.

Construct	Anti-Vβ6/8.3 Ab Binding	Frequency	%EGFP ⁺ TCRβ ⁺	%EGFP ⁺ Vβ6/8.3 ⁺	Ratio of Vβ6/8.3 to TCRβ (%)
Marilyn (CDR3β diversifying)	Complete	25% (1/4)	9.9	9.2	92.9
	Negligible	75% (3/4)	31.0 ± 9.1	3.5 ± 0.6	12.5 ± 6.1
MataHari (CDR3β diversifying)	Reduced	100% (7/7)	28.2 ± 15.7	20.2 ± 9.1	73.8 ± 10.1

In order to screen the specific pMHC binding capacity of the peripheral T lymphocytes *in vitro*, we stained splenocytes from the Marilyn TCR (CDR3β diversifying) retrogenic mice with fluorochrome-conjugated HY-IA^b multimer (TCMetrix). This multimer complex represents the cognate ligand of Marilyn TCR and comprises a fragment of the Dby protein (NAGFNSNRANSSRSS) bound to an H2-A^b MHC-II molecule. Gated on the EGFP⁺CD4⁺ T lymphocytes, the analysis revealed that only the sole Marilyn TCR (CDR3β diversifying) retrogenic mouse that retained the anti-Vβ6 Ab epitope was positively stained with the multimer, albeit at a low frequency (10.1%; Figure 4.7A, *right*). The other three retrogenic mice showed negligible staining with the CD4⁺ Marilyn-specific multimer (0.6 ± 0.1%; Figure 4.7A, *left*; Table 4.3).

Conversely, splenocytes from MataHari TCR (CDR3β diversifying) retrogenic mice were stained with CD8⁺ MataHari-specific multimers composed of *Uty* gene peptide (WMHHNMDLI) complexed with a H2-D^b MHC-I molecule (Immudex). Flow cytometric analysis of the EGFP⁺CD8⁺ T cells in MataHari TCR (CDR3β diversifying) retrogenic mice showed partial positive staining with the CD8⁺ MataHari-specific multimer pre-antigenic challenge (45.7 ± 27.2%; Figure 4.7B, *left*; Table 4.3). Additionally, we subjected some retrogenic mice (n=2) to antigenic challenge with male spleen cells expressing HY antigens in order to activate and expand antigen-specific lymphocytes. However, the data showed a three-fold reduction in multimer-positive CD8⁺ T cells after exposure to cognate ligands (Figure 4.7B, *right*; Table 4.3). This suggests that the immunisation induced proliferation of functionally enhanced T lymphocytes that exhibit a lower binding affinity to the cognate pMHC than the WT TCR. Finally, these data demonstrate that the mutagenesis approach may not only change the conformation of the TCRβ, but also affect the antigen-binding specificity and affinity of the TCR.

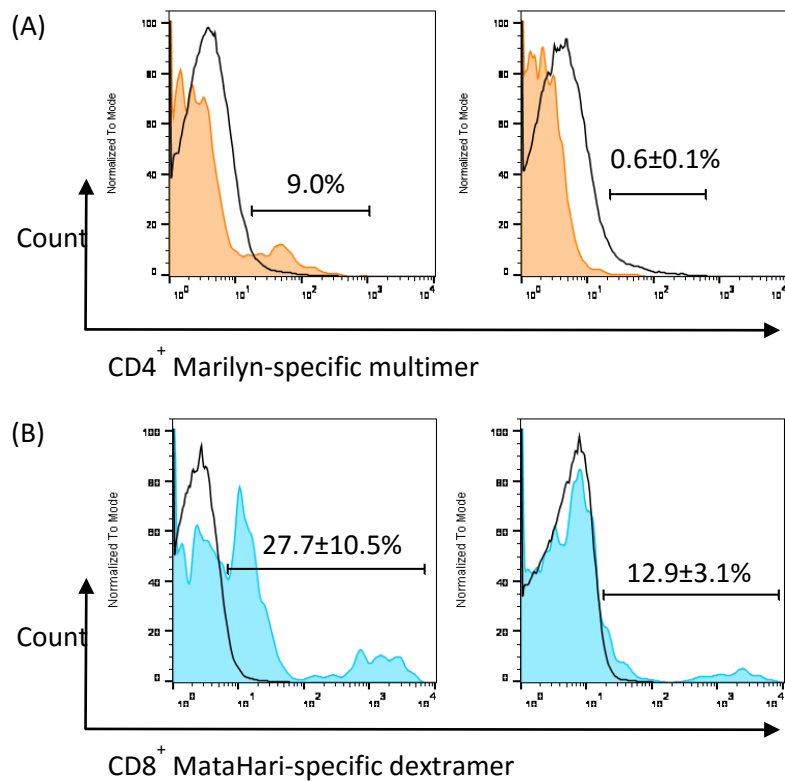


Figure 4.7. Identification of specific antigen-binding in diversified T cells. Splenocytes from the Marilyn (n=4) and MataHari (n=7) TCR (CDR3 β diversifying) retrogenic mice were stained against antigen-specific pMHC multimers and analysed using flow cytometry. (A) Gated on CD4⁺ lymphocytes (orange), analysis of multimer binding illustrated that only one retrogenic mice (left) showed positive staining, with negligible staining on the other three (right). (B) Comparison of CD8⁺ lymphocytes (blue) in MataHari TCR (CDR3 β diversifying) retrogenic mice before (n=5, left) and after (n=2, right) exposure to cognate ligands in the form of male splenocytes. Black line represents negative control (stained DN cells). Data represents mean \pm SD.

Table 4.3. Summary of specific antigen-binding in diversified T cells.

Construct	Anti-V β 6/8.3 Ab Binding	Frequency	%EGFP ⁺ TCR β ⁺ CD4/8 ⁺	%EGFP ⁺ Multimer ⁺ CD4/8 ⁺	Ratio of Multimer to TCR β (%)
Marilyn (CDR3 β diversifying)	Complete	25% (1/4)	89.2	9.0	10.1
	Negligible	75% (3/4)	93.3 \pm 1.7	0.6 \pm 0.1	0.6 \pm 0.1
MataHari (CDR3 β diversifying)	Reduced:	100% (7/7):	71.2 \pm 14.8:	23.5 \pm 11.3:	37.2 \pm 26.5:
	Pre-Ag challenge	71% (5/7)	67.9 \pm 16.7	27.7 \pm 10.5	45.7 \pm 27.2
	Post-Ag challenge	29% (2/7)	79.6 \pm 1.3	12.9 \pm 3.1	16.2 \pm 3.6

4.2.4. Generation of diversity in the TCR CDR3 β using novel *in vivo* recombination cassette

To investigate the V(D)J recombination events and resulting modifications to the TCR CDR3 β sequences, the retrogenic mice spleen cells were segregated into CD4⁺ and CD8⁺ lymphocytes using fluorescence-activated cell sorting (FACS). Furthermore, the different T cell subsets were separated based on Ab staining for their respective specific V β domains (Figure 4.8A, B). This would help describe the changes to CDR3 β sequence induced by the mutagenesis system, which may affect intrinsic preference of TCRs for different MHC classes and conformation of the TCR structure. Additionally, we were able to compare TCR sequences between naïve and memory peripheral T cells through antigenic challenge by injecting male spleen cells (expressing cognate HY antigens) into MataHari TCR (CDR3 β diversifying) retrogenic mice (Figure 4.8B). This enabled screening of potentially functionally enhanced T cells/TCRs that should be amplified relative to those with the WT CDR3 configuration.

While V(D)J recombination is proposed to be random (Venturi et al., 2006), some TCR sequences are generated at higher frequencies compared to others, leading to unequal distribution of T cell clonotypes. According to 'convergent recombination', multiple recombination events can produce the same nucleotide sequence, which subsequently converges to encode the same amino acid and TCR sequence (Quigley et al., 2010). Hence, for each sequencing analysis, the spleens of two retrogenic mice were pooled to reduce TCR clonotype bias due to 'convergent recombination' (Laydon, Bangham & Asquith, 2015). Although we expected to obtain four classes of cell populations (CD4⁺ V β 6/8.3^{+/-}, CD8⁺ V β 6/8.3^{+/-}) from each type of retrogenic mice, collection of CD8⁺ lymphocytes and naïve CD8⁺V β 8.3⁻ cells from Marilyn and MataHari TCR (CDR3 β diversifying) retrogenic mice, respectively, was inefficient (Figure 4.8A, B, labelled in red). Nonetheless, total RNA from the attainable sorted cells was extracted and cDNA synthesised. The cDNA libraries were subsequently analysed and amplified via PCR to confirm presence of the $\alpha\beta$ TCR construct (Figure 4.8C). PCR was performed using a pair of commercially synthesised primers specific for the TCR α V-region and the TCR β C-region, flanking both sides of the recombination cassette insertion point. This would facilitate analysis of CDR3 β diversification, including the germline CDR regions which should not be affected by the recombination cassette. PCR analysis confirmed the removal of the recombination cassette (467bp) and in-frame gene recombination in Marilyn and MataHari TCR (CDR3 β diversifying) retrogenic mice compared to the transgenes cloned into pMigR1 vector (Figure 4.8C). Surprisingly, the CD4⁺V β 6⁻ lymphocyte population from Marilyn TCR (CDR3 β diversifying) retrogenic mice demonstrated an enormous loss of about 800bp (Figure 4.8C), which was inconsistent with the expected V(D)J recombination event seen in the other populations.

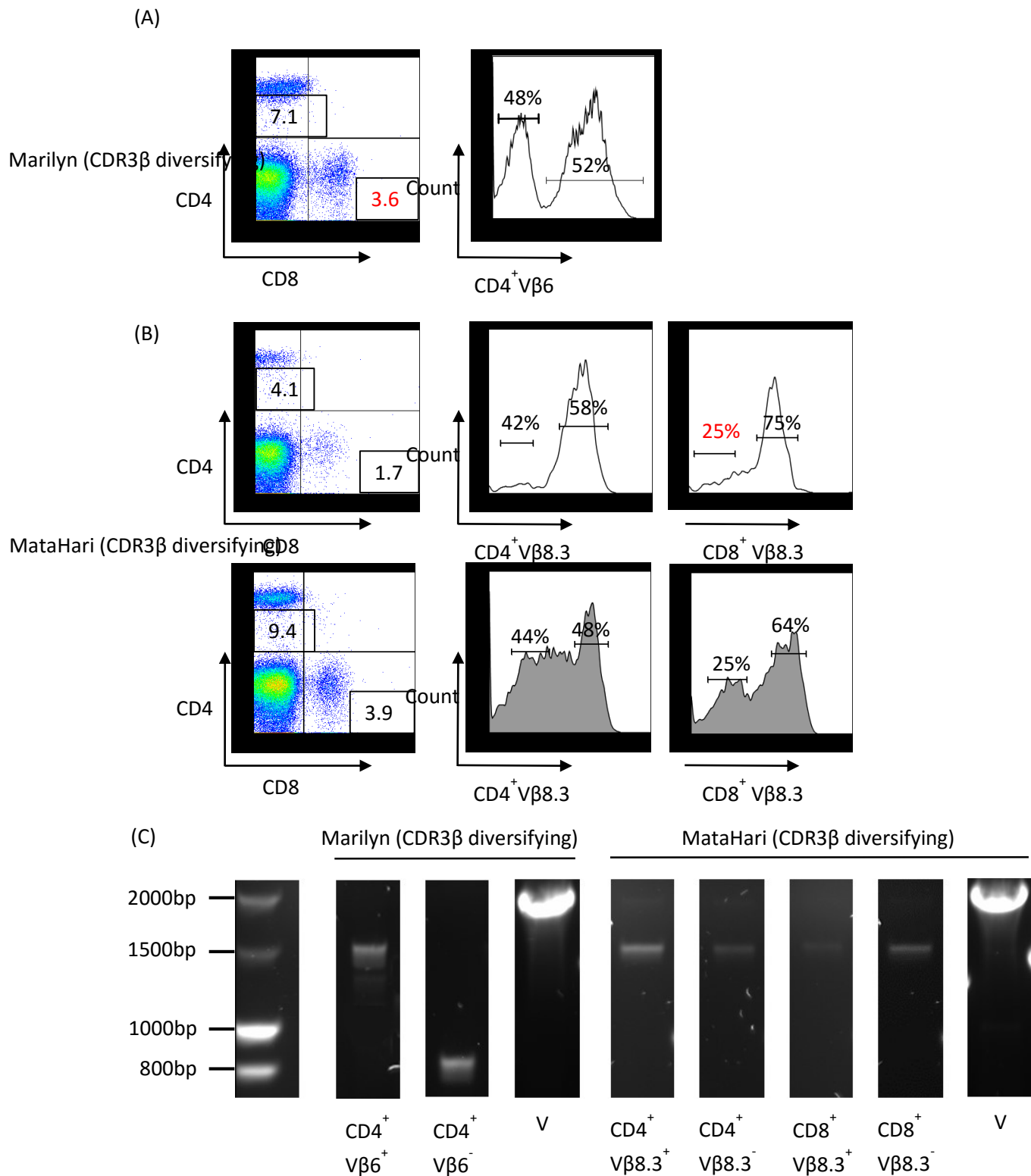


Figure 4.8. Cell sorting and PCR analysis of retrogenic mice splenocytes. Splenocytes from Marilyn (A) and MataHari (B; *top* - before, and *bottom* - after antigenic challenge) TCR (CDR3 β diversifying) retrogenic mice (n=2 each) were separated using FACS based on CD4⁺ and CD8⁺ expression, followed by specific anti-V β 6/8.3 Ab staining. Inadequate collection of cells are coloured in red. (C) PCR of sorted cells using primers upstream and downstream of recombination cassette insertion point. Analysis confirms removal of recombination cassette and in-frame gene recombination, compared to transgene in pMigR1 vector (V). CD8⁺ V β 8.3⁻ cells were collected only post-antigenic challenge.

The amplified PCR products were then cloned into a bacterial vector and used to transform competent *E. coli*. This facilitated sequence analysis of the diversified TCR repertoire at the single sequence level. Our TCR repertoire analysis of the retrogenic mice splenocytes focused on the CDR3 β segment as defined by LeFranc et al. (2005). As expected, both germline CDR1 and CDR2 sequences in the TCR β chain remained unchanged from the WT template in both retrogenic mice (not shown). Altogether, a total of 102 sequences were analysed from the Marilyn TCR (CDR3 β diversifying) retrogenic mice CD4⁺V β 6⁺ lymphocyte population, yielding 28 distinct events (Table 4.4). Interestingly, the WT CDR3 β sequence was not maintained after somatic gene recombination. This observation could be due to two possible reasons: mutation away from the WT CDR3 β sequence generating favourable binding with pMHC and *in vivo* selection during thymic T cell development, or that the transduced HSCs containing male BM-derived APCs may have deleted WT Marilyn T cells (Oh & Shin, 2015). Analysis of the CD4⁺V β 6⁻ lymphocyte TCR sequence showed an absolute loss of the TCR α C domain and TCR β V domain which resulted in the fusion of the V α and C β domains via the J α and J β segments (Figure 4.9). The TCR α CDR loops appeared to be conserved (not shown). This novel TCR chain will be explored in the next chapter.

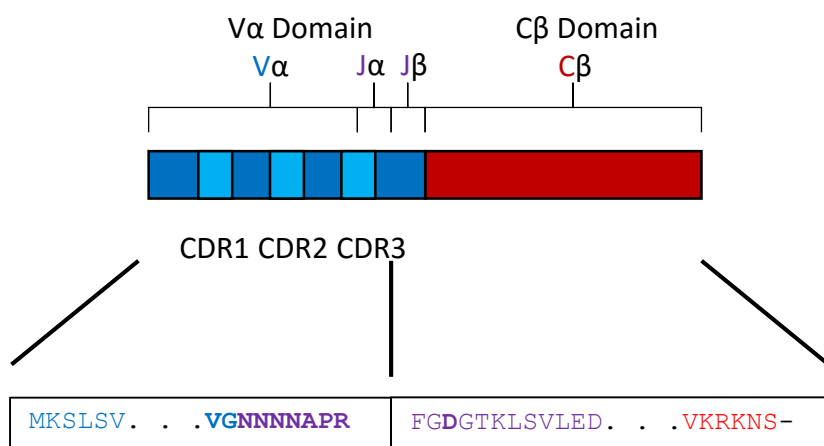


Figure 4.9. Schematic diagram of the diversified TCR repertoire from the naïve CD4⁺ V β 6⁻ lymphocyte population from Marilyn TCR (CDR3 β diversifying) retrogenic mice (n=2). Sequencing analysis of the CD4⁺ V β 6⁻ T cells revealed the complete loss of the C α and V β domains of the WT Marilyn TCR. This lymphocyte population appears to exhibit a novel TCR form comprising of the Marilyn V α (blue) and C β (red) joined by the J α and J β segments (purple).

Table 4.4. Sequence analysis of diversified TCR repertoire in naïve CD4⁺ Vβ6⁺ lymphocyte population from Marilyn TCR (CDR3β diversifying) retrogenic mice (n=2). Letters in **bold** indicate amino acid changes from WT template, **red** indicates positively-charged amino acids and **blue** designates negatively-charged amino acids at pH of blood (pH3.5-4.5).

MUTATION (TOTAL FREQUENCY)	CDR3β PEPTIDE SEQUENCE	LENGTH	CHARGE	FREQUENCY IN CD4 ⁺ Vβ6 ⁺
WT (0)				
	ASSIPGS N ERLF	12	0	0
DELETION (18)				
	ASS N ERLF	8	0	8
	ASSIP R ERLF	11	+1	4
	ASSI P LNERLF	11	0	2
	ASSIPG T ERLF	11	0	1
	ASSIG E ERLF	11	0	1
	ASSIPG N ERLF	11	0	1
	ASSIPG K ERLF	11	+1	1
SUBSTITUTION (46)				
	ASSIPGS D ERLF	12	-1	15
	ASSIPGS Y ERLF	12	0	9
	ASSIP F SNERLF	12	0	7
	ASSIPG K SERLF	12	+1	4
	ASSIPG I G E ERLF	12	0	3
	ASSIPG I D E ERLF	12	-1	2
	ASSIPG I S E ERLF	12	0	2
	ASSIPG R G E ERLF	12	+1	2
	ASSIPGS A ERLF	12	0	1
	ASS V PGS Y ERLF	12	0	1
ADDITION (38)				
	ASSIPGS G G E ERLF	13	0	7
	ASSIPG R P G ERLF	13	+1	7
	ASSIPGS A S E ERLF	13	0	6
	ASSIPGS A G E ERLF	13	0	4
	ASSIPGS A D E ERLF	13	-1	4
	ASSIPGS G A E ERLF	13	0	4
	ASSIPGS E S E ERLF	13	-1	2
	ASSIPGS V S E ERLF	13	0	1
	ASSIPGS F N E ERLF	13	0	1
	ASSIPG G D E ERLF	13	-1	1
	ASSIPAS D N E REF	13	-2	1

The naïve TCR repertoire in MataHari TCR (CDR3 β diversifying) retrogenic mice revealed 24 and 16 unique events from the analysis of 120 CD4⁺ and 61 CD8⁺ lymphocyte sequences, respectively (Tables 4.5 and 4.6). TCR variants in the CD4⁺ MHC Class II-specific cells proved to be exclusively different from the WT CDR3 β , whereas the majority of TCRs in the CD8⁺ cells were shown to retain the WT sequence. Most of the CD4⁺ lymphocytes (>80%) appear to carry a deletion in the CDR3 β loop. To determine whether the mutagenesis system, including deletions, affected the TCR β structure, we compared sequences within the CD4⁺ lymphocyte population based on staining against the anti-V β 8.3 Ab, a possible indicator of the overall TCR β V shape. Sequence comparison proved to be inconclusive since those that were positively and negatively stained showed overlapping CDR3 β sequences.

The high frequency of the WT MataHari CDR3 β in the CD8⁺ population is suggestive of a number of interesting insights. Firstly, the MataHari TCR may have a natural bias for MHC Class I during thymic selection, leading to a preference to retain the WT CDR3 β sequence and selection to the native MHC class. In contrast to the diversified Marilyn T cell repertoire, the development of WT MataHari T cells does not appear to be sensitive to the presence of male BM-derived APCs in the transduced donor HSCs. Instead, this suggests that efficient binding between the WT MataHari TCR and its cognate ligand may already exist.

Table 4.5. Sequence analysis of diversified TCR repertoire in naive CD4⁺ lymphocyte population from MataHari TCR (CDR3 β diversifying) retrogenic mice (n=2) without antigenic challenge. Letters in bold indicate amino acid changes from WT template, red indicates positively-charged amino acids and blue designates negatively-charged amino acids at pH of blood (pH3.5-4.5).

MUTATION (TOTAL FREQUENCY)	CDR3 β PEPTIDE SEQUENCE	LENGTH	CHARGE	FREQUENCY IN CD4 ⁺ V β 8.3 ⁺	FREQUENCY IN CD4 ⁺ V β 8.3 ⁻
WT (0)					
(0)	ASSDLVEVF	9	-2	0	0
DELETION (98)					
(27)	ASSD L LLF	8	-1	22	5
(19)	ASSD L R F	7	0	1	18
(14)	ASSG E VF	7	-1	9	5
(8)	ASSD L MF	7	-1	2	6
(7)	ASSD H VF	7	0	0	7
(4)	ASSD L LF	7	-1	0	4
(4)	ASSD L VF	7	-1	1	3
(3)	ASS E A E VF	8	-2	3	0
(3)	ASSD P E V F	8	-2	2	1
(2)	ASSD S E V F	8	-2	0	2
(2)	ASSD L R V F	8	0	0	2
(1)	ASSD L F V F	8	-1	1	0
(1)	ASSD L E V F	8	-2	1	0
(1)	ASSD L Q V F	8	-1	1	0
(1)	ASS V E V F	7	-1	1	0
(1)	ASSD R F	6	0	1	0
SUBSTITUTION (17)					
(8)	ASSD L F E VF	9	-2	8	0
(3)	ASSD P V E VF	9	-2	3	0
(3)	ASSD L R E VF	9	-1	0	3
(2)	ASS E D V E V F	9	-3	0	2
(1)	ASSD L Y E VF	9	-2	1	0
ADDITION (5)					
(3)	ASSD R L T E V F	10	-1	0	3
(1)	AS G D R L T E V F	10	-1	0	1
(1)	ASSD L Y V E V F	10	-2	1	0

Table 4.6. Sequence analysis of diversified TCR repertoire in naïve CD8⁺ lymphocyte population from MataHari TCR (CDR3 β diversifying) retrogenic mice (n=2) without antigenic challenge. Letters in **bold** indicate amino acid changes from WT template, **red** indicates positively-charged amino acids and **blue** designates negatively-charged amino acids at pH of blood (pH3.5-4.5).

MUTATION (TOTAL FREQUENCY)	CDR3 β PEPTIDE SEQUENCE	LENGTH	CHARGE	FREQUENCY IN CD8 ⁺ V β 8.3 ⁺
WT (26)				
	ASSDL L EVF	9	-2	26
DELETION (18)				
	ASSDL R VF	8	0	10
	ASSDL Q VF	8	-1	4
	ASSDL E VF	8	-2	2
	ASSD P RVF	8	0	1
	ASSDL P VF	8	-1	1
SUBSTITUTION (15)				
	ASSD P VEVF	9	-2	5
	ASSDL H EVF	9	-1	3
	ASS V HVEVF	9	0	2
	ASSDL D EVF	9	-3	1
	ASSDL R EVF	9	-1	1
	ASSDL A EVF	9	-2	1
	ASSDL H RVF	9	+1	1
	ASS E HVEVF	9	-1	1
ADDITION (2)				
	ASSDL H GRVF	10	+1	1
	ASSD F FLEVF	10	-2	1

We further analysed the diversified, including ‘optimised’, TCR repertoire in MataHari TCR (CDR3 β diversifying) retrogenic mice after intra-peritoneal injection with male spleen cells expressing HY antigens. Sequencing analysis of 128 CD4⁺ and 97 CD8⁺ lymphocytes yielded 9 unique events each (Tables 4.7 and 4.8). A few key observations can be noted during sequence analysis of the diversified and challenged TCR repertoire. Firstly, the diversified CDR3 β sequence ‘ASS**G**EVF’ appeared to be prevalent in both T cell subsets (regardless of anti-V β 8.3 Ab staining) demonstrating TCR ‘immunodominance’ after activation and stimulation/proliferation by the introduction of male-specific antigens. This also indicates that the diversified TCR does not seem to exhibit an intrinsic bias to a specific MHC class.

Surprisingly, the WT sequence, which was described to be retained in the majority of naïve CD8⁺ lymphocytes, was not identified. The reduction in MataHari-specific multimer binding suggests a

possible dilution of the WT TCR by the ‘immunodominant’ TCRs that appear to demonstrate lower binding affinities (Table 4.3). Indeed, clonal expansion of the ‘immunodominant’ T cells may dilute the WT cells resulting in the inability to detect the WT CDR3 β . Alternatively, it could be by chance that we were unable to recognise the WT sequence, although the likelihood of this seems improbable since we had sequenced about 100 sequences from each T cell subset.

Table 4.7. Sequence analysis of diversified TCR repertoire in CD4⁺ lymphocyte population from MataHari TCR (CDR3 β diversifying) retrogenic mice (n=2) after antigenic challenge. Letters in **bold** indicate amino acid changes from WT template, **red** indicates positively-charged amino acids and **blue** designates negatively-charged amino acids at pH of blood (pH3.5-4.5).

MUTATION (TOTAL FREQUENCY)	CDR3 β PEPTIDE SEQUENCE	LENGTH	CHARGE	FREQUENCY IN CD4 ⁺ V β 8.3 ⁺	FREQUENCY IN CD4 ⁺ V β 8.3 ⁻
WT (0)					
(0)	ASSDL L VEVF	9	-2	0	0
DELETION (125)					
(101)	ASSG E VF	7	-1	57	44
(16)	ASSD L EVF	8	-2	3	13
(2)	ASSD P EVF	8	-2	2	0
(2)	ASSD L QVF	8	-1	0	2
(1)	ASSD L A F	7	-1	1	0
(1)	ASSD G VF	7	-1	1	0
(1)	ASSG G EVF	7	-1	1	0
(1)	ASSD E VF	7	-2	0	1
SUBSTITUTION (3)					
(3)	ASSD P VEVF	9	-2	3	0

Table 4.8. Sequence analysis of diversified TCR repertoire in CD8⁺ lymphocyte population from MataHari TCR (CDR3 β diversifying) retrogenic mice (n=2) after antigenic challenge. Letters in **bold indicate amino acid changes from WT template, **red** indicates positively-charged amino acids and **blue** designates negatively-charged amino acids at pH of blood (pH3.5-4.5).**

MUTATION (TOTAL FREQUENCY)	CDR3 β PEPTIDE SEQUENCE	LENGTH	CHARGE	FREQUENCY IN CD8 ⁺ V β 8.3 ⁺	FREQUENCY IN CD8 ⁺ V β 8.3 ⁻
WT (0)					
(0)	ASS D LVEVF	9	-2	0	0
DELETION (97)					
(81)	ASSG E VF	7	-1	34	47
(8)	ASS D LVEVF	8	-2	1	7
(2)	ASSG Q VF	7	0	2	0
(1)	ASSG K VF	7	+1	1	0
(1)	AS R TCQVF	8	+1	0	1
(1)	ASSG E AF	7	-1	1	0
(1)	AS N GEVF	7	-1	1	0
(1)	ASSV E VF	7	-1	1	0
(1)	AS R G E VF	7	0	1	0

4.2.5. Analysis of TCR repertoire diversity and diversified CDR3 β length and net charge

The Shannon entropy index was used to measure the sequence diversity generated as a result of our mutagenesis approach (Wang et al., 1998; Stewart et al., 1997). Shannon entropy index incorporates both the number of sequences analysed and frequency of a particular sequence. This method had been previously used to describe TCR CDR3 α diversity in Tregs and the diversification of germline CDRs (Holland et al., 2012; Singh et al., 2010; Ferreira et al., 2009). The diversity index was normalised to account for the different number of sequences analysed for each sample. Normalised diversity index (D) was calculated as a ratio of the Shannon entropy index (H) expressed as a percentage of the maximum diversity (H') where every sequence analysed is presumed to be distinct. H, H' and D are calculated by:

$$H = - \sum_{i \text{ to } N} \left[\ln \left(\frac{\text{frequency of unique sequence } i}{\text{total number of sequences } N} \right) \right]$$

$$H' = -[N \times \ln\left(\frac{1}{N}\right)]$$

$$\text{Normalised diversity index (D)} = H/H'$$

The normalised diversity index (D) used to quantify overall diversification of the TCR CDR3 β at the peptide level facilitates direct comparison between the two $\alpha\beta$ TCR templates as well as differences among the T cell subsets, before and after exposure to cognate HY antigens (Figure 4.10). The D values calculated for the male-specific TCRs in their native T cells subset (CD4⁺ for Marilyn and CD8⁺ for MataHari) appeared to be similar (21.9% to 21.8%). Interestingly, diversity in the CD4⁺ lymphocytes in peripheral MataHari TCR (CDR3 β diversifying) repertoire was shown to be less than that in the CD8⁺ cells. This observation was continuous after antigenic challenge. Consistent with the reduction in total unique sequences and the accumulation of the diversified/'optimised' CDR3 β sequence 'ASSGEVF' after HY antigen exposure, both CD4⁺ and CD8⁺ lymphocytes in the MataHari TCR (CDR3 β diversifying) retrogenic mice showed a ~60% reduction in D values.

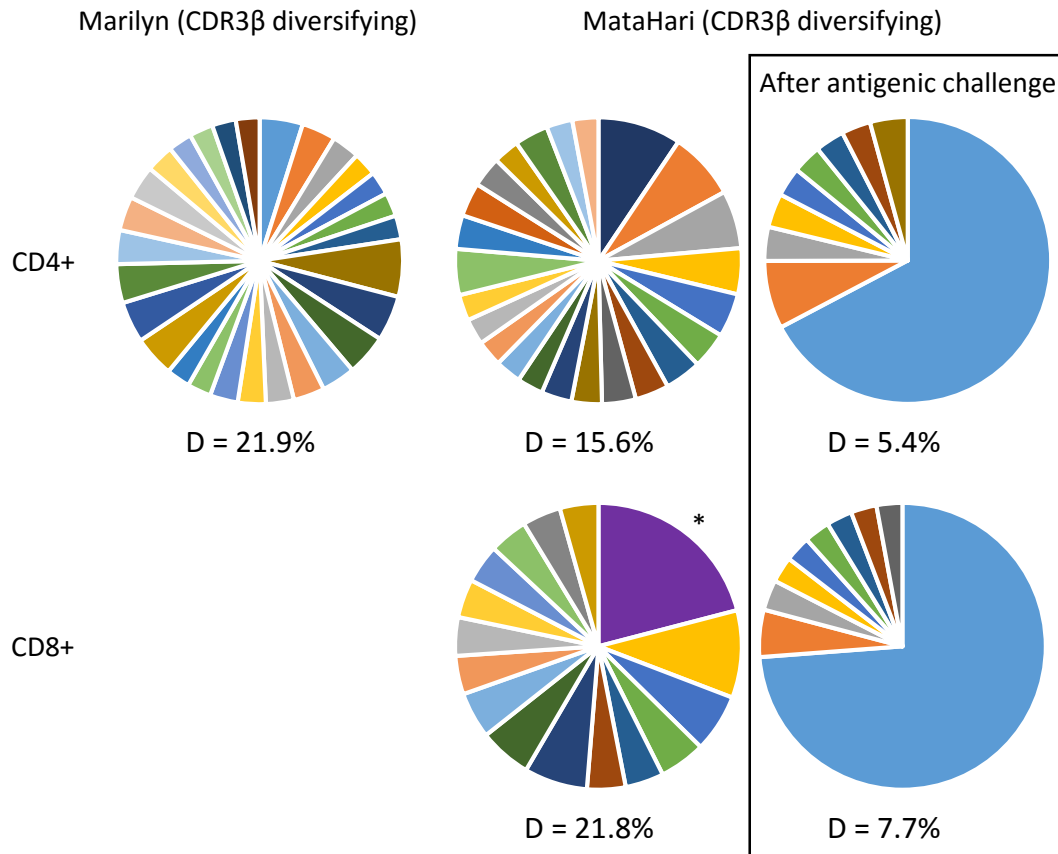


Figure 4.10. Overall peptide sequence diversity of peripheral TCR repertoire generated by the *in vivo* mutagenesis approach in Marilyn and MataHari TCR (CDR3 β diversifying) retrogenic mice. Normalised diversity index (D) was calculated by the Shannon entropy indices (H) as percentage of maximum diversity (H'). Each segment represents a unique CDR3 β peptide sequence. Size of each segment is proportional to the frequency of a distinct sequence. * denotes WT TCR.

To investigate the impact of the mutagenesis approach on the size of the peptide-binding loop, we then measured the length of the TCR CDR3 β amino acid residues. Analysis of the CDR3 β amino acid lengths in Marilyn TCR (CDR3 β diversifying) retrogenic mice showed a restricted variation in size. The CD4⁺V β 6⁺ Marilyn TCR (CDR3 β diversifying) sequences demonstrated a higher preference to either maintaining the WT loop size (12 a.a.) through substitution mutations or addition of one amino acid before any nucleotide deletions (Figure 4.11A). Likewise, native CD8⁺ lymphocytes from MataHari TCR (CDR3 β diversifying) retrogenic mice show a strong constraint in maintaining the WT CDR3 β loop size (9 a.a.), since the majority retained the WT sequence (Figure 4.11B, *left*). Over 80% of the MataHari TCR (CDR3 β diversifying) CD4⁺ lymphocytes exhibited a deletion of CDR3 β amino acids, implying binding preference to MHC Class II requires a smaller antigen-binding site (Figure 4.11B). Most importantly, after exposure to HY antigens, the resultant 'immunodominant' T cells indicate 'optimised' TCR/pMHC binding is driven by a shorter CDR3 β loop (7 a.a.; Figure 4.11B, *right*).

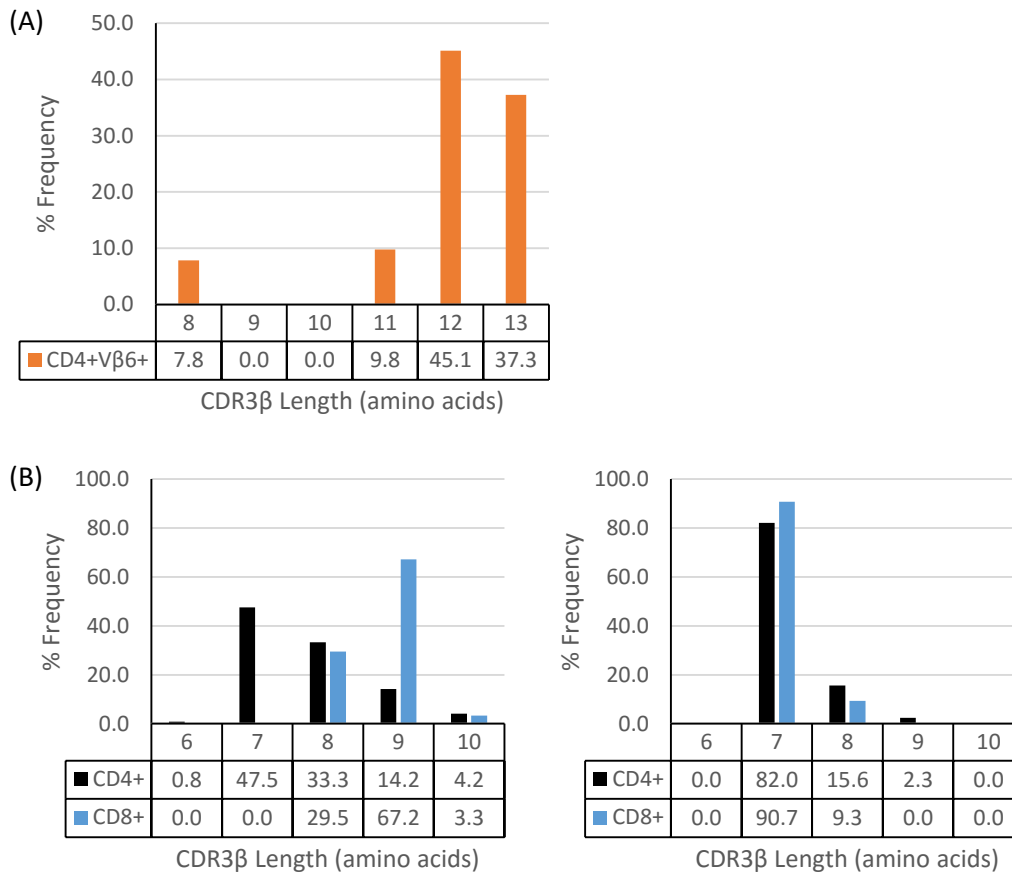
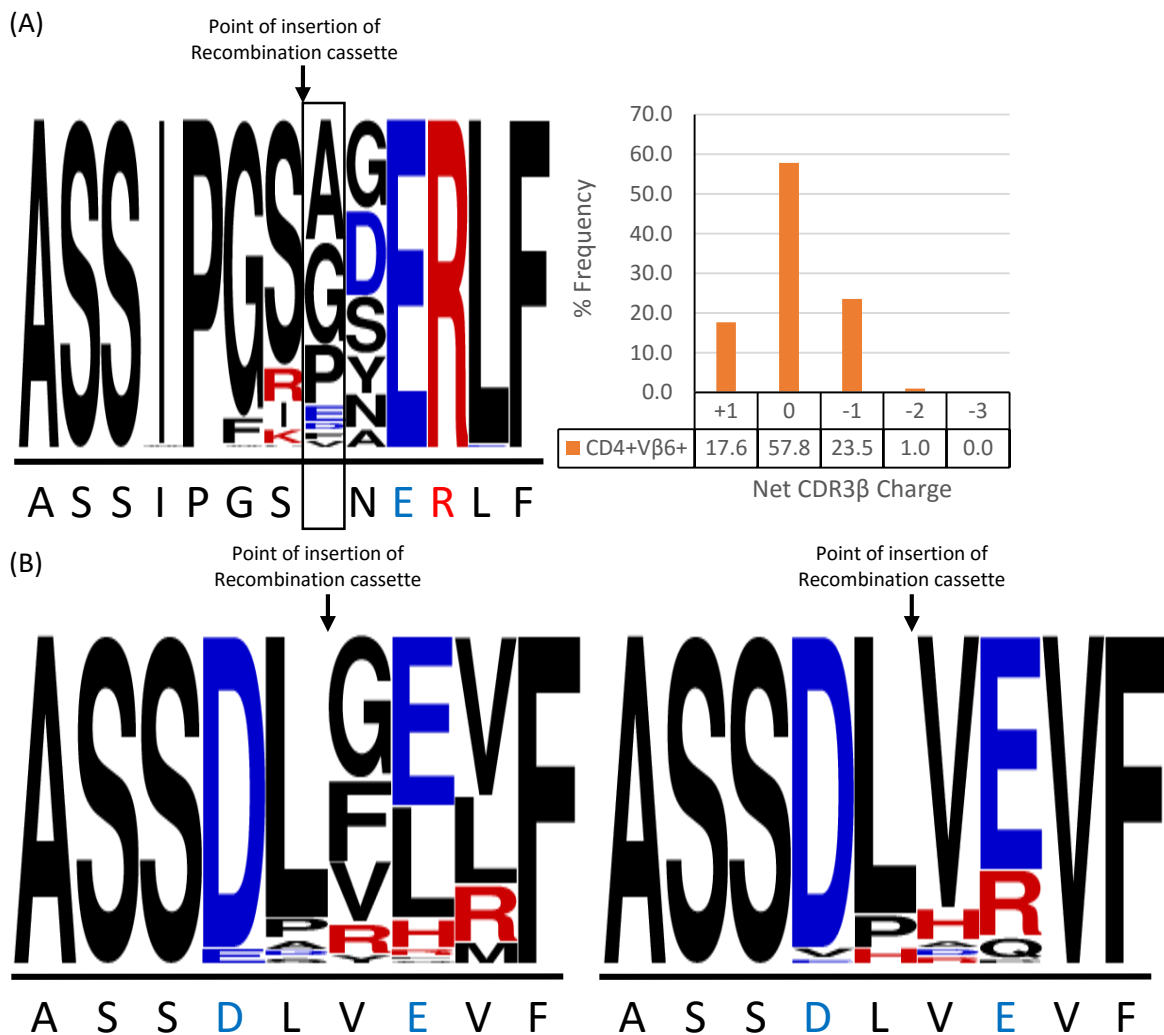


Figure 4.11. Analysis of the diversified CDR3β amino acid length distribution in the Marilyn and MataHari TCR (CDR3β diversifying) retrogenic mice. The CDR3β amino acid lengths from the sequences from Tables 4.4-4.8 are summarised in Marilyn (A) and MataHari (B) TCR (CDR3β diversifying) peripheral TCR repertoires. For MataHari TCR (CDR3β diversifying), we compare before (*left*) and after (*right*) exposure to HY antigens. Data is shown as frequency of length as a percentage of total sequences analysed, to one decimal place.

To further explore the TCR/pMHC binding interaction in the CDR3β loop, we examined the net charge of the peptide-binding site based on its amino acid composition (Figure 4.12). A summary of the most common mutations (substitution and addition; 12 and 13 a.a.) to the diversified CD4⁺Vβ6⁺ Marilyn TCR CDR3β is shown in Figure 4.12A (*left*), highlighting the resultant amino acid composition. Modifications to the loop were mostly concentrated to not more than three amino acid residues away from the insertion of the cassette. As such, the positively-charged glutamic acid (E) and negatively-charged arginine (R) remained conserved in all diversified CDR3β, hence the high frequency of 0 net charge (Figure 4.12, *right*). Additionally, most mutations appear to occur after the point of recombination cassette insertion.

Analysis of the most common lengths (8 and 9 a.a.) in the native CD8⁺ MataHari TCR repertoire revealed similar observations in that mutations were limited to not more than three amino acids from the recombination cassette insertion point (Figure 4.12B, *right*). Most CD8⁺ lymphocytes conserved the WT TCR, hence the high frequency of a negative CDR3 β net charge of (-2) (Figure 4.12C, *left*). Conversely, analysis of the most common amino acid lengths (7-9 a.a.) in the CD4⁺ MataHari TCR (CDR3 β diversifying) lymphocytes highlight that deletion mutations mainly remove the negatively-charged glutamic acid (E) residue which may affect the overall ‘interaction codons’ (Figure 4.12B, *left*). Therefore we observe a high frequency of net charge increasing to (-1) (Figure 4.12C, *left*). A smaller proportion of this population removed the negatively-charged aspartic acid (D) residue instead, forming the CDR3 β sequence ‘ASSGEVF’ with a net charge of (-1). The same CDR3 β is observed in almost all CD4⁺ and CD8⁺ MataHari TCR (CDR3 β diversifying) lymphocytes after antigenic ligand exposure (Figure 4.12C, *right*; Tables 4.7 and 4.8). Altogether, the data suggest that the ‘optimised’ engagement between MataHari TCR and pMHC seems to favour a shorter peptide-binding loop that introduces a glycine (G) residue, with an increased net charge of (-1).



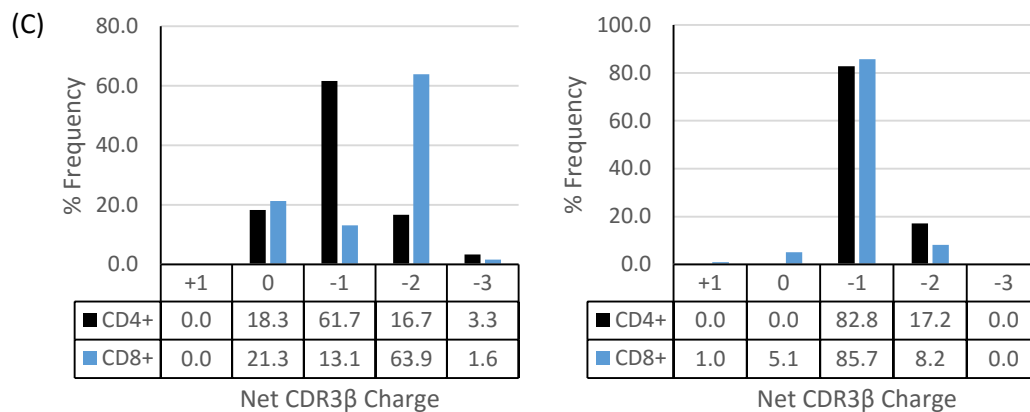


Figure 4.12. Analysis of the diversified TCR repertoire CDR3 β net charge and amino acid usage in the Marilyn and MataHari TCR (CDR3 β diversifying) retrogenic mice. The CDR3 β amino acid lengths from the sequences from Tables 4.4-4.8 are summarised. (A) The CDR3 β amino acid composition in CD4 $^+$ V β 6 $^+$ Marilyn TCR (CDR3 β diversifying) lymphocytes is shown (*left*), with the overall net charges (*right*). The black box indicates added residues not present in the WT. (B) The CDR3 β amino acid composition in CD4 $^+$ (*left*) and CD8 $^+$ (*right*) MataHari TCR (CDR3 β diversifying) lymphocytes are summarised. (C) Comparison of the overall net charge in CD8 $^+$ (*blue*) and CD4 $^+$ (*black*) MataHari TCR (CDR3 β diversifying) lymphocytes, before (*left*) and after (*right*) exposure to HY antigens. The height of each letter corresponds to its frequency. Colours of each letter represent: black - uncharged, red - positively-charged and blue - negatively-charged amino acids at pH of blood (pH3.5-4.5). Net charge data is shown as frequency as a percentage of total sequences analysed, to one decimal place.

4.3. Discussion

4.3.1. Summary

The data in this chapter demonstrates the successful application of the *in vivo* gene recombination-inducing mutagenesis approach in TCR/MHC haplotype-matched C57BL/6 retrogenic mice. Detection of a functional T cell repertoire indicates that the migration of the transduced HSCs into the thymic compartment led to effective removal of the recombination cassette and generation of an in-frame TCR β chain. Subsequent sequencing of distinct T cell populations also confirms the modification of the target CDR3 β that resulted in many variants of the template TCRs. Although the diversification was limited to a small range of amino acids around the point of gene recombination, we were able to define a sizeable number of novel post-selection CDR3 β sequences with similar levels of overall diversity in both retrogenic TCRs.

In addition, phenotypic comparisons between the FVB/N and C57BL/6 retrogenic mice and TCR sequence analysis enabled us to address some of the key observations discussed in the previous chapter. Firstly, in relation to the enlarged thymi discovered in some of the FVB/N retrogenic mice, all C57BL/6 retrogenic mice for both TCRs exhibited small or normal-sized thymi. It is likely that the TCR/MHC haplotype mismatch may have contributed to the formation of the enlarged thymus associated with an arrest at the DN to DP stage. The different genetic backgrounds of FVB/N and C57BL/6 could also underlie the susceptibility to thymoma in FVB/N.

Similar to the FVB/N strain, the T lymphocyte population in the C57BL/6 retrogenic mice also exhibited a skew to the CD4⁺ T cell lineage for both TCRs. Furthermore, we observed the presence of a small population of CD8⁺ T cells in the Marilyn TCR (CDR3 β diversifying) retrogenic mice. These observations are surprising since the WT Marilyn transgenic mice are typically selected on the CD4 lineage (Grandjean et al., 2003). Conversely, MataHari transgenic mice generally express only CD8⁺ cytotoxic T cells, but we instead observe not only presence, but also dominance of CD4⁺ T cells in the retrogenic mice (Valujskikh et al., 2002). As expected, the mutagenesis system did not affect the germline CDR1 and CDR2 sequences of both TCR α and β chains. Assuming efficient pairing between exogenous TCR α and β chains, we might expect the male-specificity to persist within a proportion of diversified TCR repertoires of the appropriate MHC class. Equally, mutation of CDR3 β in both constructs may lead to binding the alternative MHC class thus switching MHC restriction to the alternate class. The generation of unexpected T cell lineages was similarly observed in the generation of WT Marilyn and MataHari retrogenic mice which utilised the injection of transduced C57BL/6 bone marrow cells into female RAG-1^{-/-} recipient mice (Holst et al., 2006). Thus, it is possible that the presence of the endogenous

TCR α locus in the WT or TCR- $\beta/\delta^{-/-}$ deficient thymocytes allows formation of novel $\alpha\beta$ TCRs that results in the uncharacteristic T cell lineages.

We further propose that the higher frequency of CD4 $^{+}$ compared to CD8 $^{+}$ T cells in the MataHari TCR (CDR3 β diversifying) mice may be a consequence of the lower TCR surface expression associated with the multi-cistronic retrogenic approach. Upon analysing the TCR β MFI, we observed a significant reduction in TCR expression in the retrogenic T cells compared to their WT C57BL/6 counterparts. The multi-cistronic system is designed such that early TCR α expression in the DN4 stage allows formation of $\alpha\beta$ TCRs that are capable of ligand-independent signalling transition to the DP stage (Erman, Guinter & Singer, 2004; Erman et al., 2002). The retrogenic $\alpha\beta$ T cells are able to redirect normal thymocyte development and circumvent stringent thymic selection checkpoints with reduced TCR signalling complexes. Moreover, Sinclair and colleagues (2013) reported that the susceptibility of CD8 $^{+}$ thymocytes to apoptosis is the crucial determinant of CD4:CD8 ratio during T cell ontogeny by thymopoiesis. Native CD8 $^{+}$ T cells in the periphery also have a greater dependence on homeostatic TCR-dependent survival signals than CD4 $^{+}$ T cells (Seddon & Zamoyska, 2002). Hence, we consider the lower TCR expression may increase susceptibility of the CD8 $^{+}$ T cell to apoptosis resulting in the lower frequency of CD8 $^{+}$ in comparison to CD4 $^{+}$ T cells in the periphery.

Sequence analysis of distinct T cell populations separated based on staining with specific anti-V β antibodies was intended to elucidate whether the mutagenesis approach disrupted the overall TCR β structure. Interestingly, the diversification of each TCR produced different outcomes: For Marilyn TCR, diversification caused either full or null retention of the anti-V β 6 Ab epitope in T lymphocytes. In contrast, MataHari TCR diversification allowed partial staining of T cells with the anti-V β 8.3 Ab (~75%). We previously reported that the anti-V β 6 Ab epitopes include the germline CDR2 (Bartok, unpublished) which should not be affected by modifications to the CDR3 β structure. Indeed, the CD4 $^{+}$ V β 6 $^{-}$ T cell population from the Marilyn TCR (CDR3 β retrogenic) mice, which was shown to completely remove the V β domain, adheres to this principle. Otherwise, the CD4 $^{+}$ V β 6 $^{+}$ T lymphocytes appeared to conserve the TCR β structure and Ab epitope despite not retaining the WT CDR3 β sequence. In MataHari TCR (CDR3 β diversifying) retrogenic mice, we observed a loss of the anti-V β 8.3 Ab epitopes in a small proportion of the CD4 $^{+}$ and CD8 $^{+}$ T cells. To investigate whether the modifications to the CDR3 β resulted in this epitope loss, we compared the TCR sequences between positively and negatively stained cells. However, the overlapping CDR3 β sequences in both V β 8.3 $^{+}$ and V β 8.3 $^{-}$ cells, coupled with the unaltered germline CDRs, suggests that the mutagenesis may not necessarily affect the TCR β structure and Ab epitope. Instead, it may be the TCR α partner, which could be exogenous or endogenous, that may sterically hinder the Ab binding site.

Additionally, the diversification of CDR3 β and TCR α pairing may also result in reduced binding affinity and/or specificity as shown by the low specific pMHC multimer staining frequency; any high affinity TCRs would have been negatively selected during *in vivo* thymopoiesis. The current technology, lacking the available specific anti-V α antibodies, restricts the identification of TCR α usage in the diversified T cells. Altogether, this complicates fully understanding whether it is truly the mutagenesis approach or the TCR α that results in a T cell lineage and/or antigen-binding capacity which are more effective than the WT.

The analysis of the diversified CDR3 β sequences also allowed us to define significant findings regarding the mutagenesis. Firstly, the mutagenesis approach does not necessarily exhibit a preference to remove the WT template. We initially assumed a mutagenesis mechanism bias or the presence of male APCs that may delete WT male-specific TCRs contributing to the absence of WT sequences in the diversified Marilyn T cells (Oh & Shin, 2015). However, this is not the case for MataHari TCR since a high frequency of diversified sequences conserved the WT CDR3 β . Further, in both Marilyn and MataHari TCR diversification, we noticed a higher frequency of mutations occur after the recombination cassette insertion point and the majority introduce glycine residues. This bias may be attributed to the location of the CDR3 β region within the J-segment which was described to be guanine nucleotide rich (Moss & Bell, 1996). Alternatively, glycine may be introduced to confer flexibility to the CDR3 β in order to optimise the location of peptide contact points and pMHC docking upon removal of charged amino acids (Cole et al., 2014; Huang & Nau, 2003).

We also noted that the mutagenesis system generated a limited range of CDR3 β length distribution. For both TCRs, the diversified CDR3 β lengths appeared similar to within two amino acids of the WT CDR3 α and CDR3 β . Based on the limited length variation of processed peptides, the CDR3 antigen-binding sites of TCR α and β chains are under selective pressure to maintain a fairly narrow combined length distribution and efficient contact with pMHC ligands (Johnson & Wu, 1999). Previous work from our group have indeed shown that the long C6 TCR CDR3 β influences efficient pairing with its cognate TCR α chain whilst negating pairing with other endogenous TCR α chains (Bartok et al., 2010). Thus, we deduce that the CDR3 α partner may confer a selective pressure on the diversified CDR3 β in order to maintain a narrow combined CDR3 length distribution.

One of the biggest challenges encountered during the generation of the Marilyn TCR (CDR3 β diversifying) retrogenic mice was the unpredictable occurrence of the CD4⁺V β 6⁻ population. This cell population was revealed to express a novel TCR chain comprising of the Marilyn V α and C β domains fused at the J-segment. We propose that this novel TCR chain may be caused by the unexpected sequence identity in the J α - and J β -segments as a result of codon optimisation during $\alpha\beta$ TCR (CDR3 β

diversifying) synthesis. The lack of diversity in and around the point of gene recombination suggests that the recombination cassette may not be the causative factor, but rather the nucleotide sequence similarity caused a predominant ribosomal skip during transcription of the integrated exogenous TCR (Im et al., 2014). Hence, the random incidence of this phenomenon in either FVB/N or C57BL/6 mice impeded fully describing Marilyn TCR diversification and screening for optimised TCRs after exposure to cognate ligands as we have done for the MataHari TCR.

4.3.2. Conclusions

The present chapter highlights the successful utilisation of the novel mutagenesis concept. The recombination cassette was shown to redirect gene rearrangement and introduce variation to the targeted CDR3 β peptide-binding site. *In vivo* thymic selection ensured the generation of a functional self-tolerant and MHC-restricted T cell repertoire. Subsequent exposure to cognate ligands also allowed us to identify 'optimised' and 'immunodominant' TCRs. Although the development of $\alpha\beta$ T cells was generally unaffected, there were interesting observations with regards to uncharacteristic T cell lineages and consequences of the TCR modification. It should be born in mind that our analyses of the TCR repertoires is very limited (with $n=2$ in most cases) and will likely capture a small fraction of the total diversity. Furthermore, we have discovered a novel TCR chain which comprises of a V domain from the TCR α attached to the C domain of TCR β chain. In the next chapter, we will attempt to characterise the phenotype and functionality of this novel TCR.

Chapter 5

Chapter 5: Phenotypic characterisation and functional analysis of a novel chimeric TCR chain

5.1. Introduction

The primary focus of this study is the diversification of a template TCR using a recombination cassette that redirects somatic gene recombination in the target CDR. During analysis of the Marilyn TCR (CDR3 β diversifying) retrogenic mice, it was noted that a proportion (3 of 7 FVB/N and 3 of 4 C57BL/6 retrogenic mice) developed a dominant population of peripheral T cells which appeared to express the TCR β constant domain but not the Marilyn V β 6 domain as determined by flow cytometry (Figure 5.1A). PCR analysis of the transgene revealed deletion of a significant portion of the template TCR including the C α and V β domains (Figure 5.1B). Further sequence analysis confirmed the transgene comprised of only the V α and C β domains joined together by a fused J α -J β gene segment.

We hypothesised that an aberrant gene recombination event had resulted in the fusion of the TCR V α to the C β domain, forming a chimeric V α -C β chain which forms a heterodimer with endogenous TCR α chains (Figure 5.1C). Secondly, we hypothesised that this novel form of $\alpha\beta$ TCR would use a V α -V α dimeric antigen-binding surface which is able to engage functionally with self-MHC-I and -II and direct positive selection during thymocyte development. According to the germline hypothesis, the TCR requires both germline TCR α and TCR β CDRs to interact efficiently with cognate MHC ligands. As the chimeric V α -C β TCR chain lacks the germline TCR β CDRs, this hypothesis predicts it would be unable to support normal T cell engagement with APCs.

In this chapter, the nature of the recombination event that directed the removal of the TCR C α and V β domains was investigated. We also aimed to characterise the functionality of the V α -C β fusion TCR: Firstly by determining whether the V α -C β fusion TCR can be co-expressed on the surface of normal T cells expressing WT $\alpha\beta$ TCR *in vitro*. Second, we generated retrogenic mice expressing the novel V α -C β fusion TCR to investigate whether the chimeric chain can mediate *in vivo* thymic selection and T cell development.

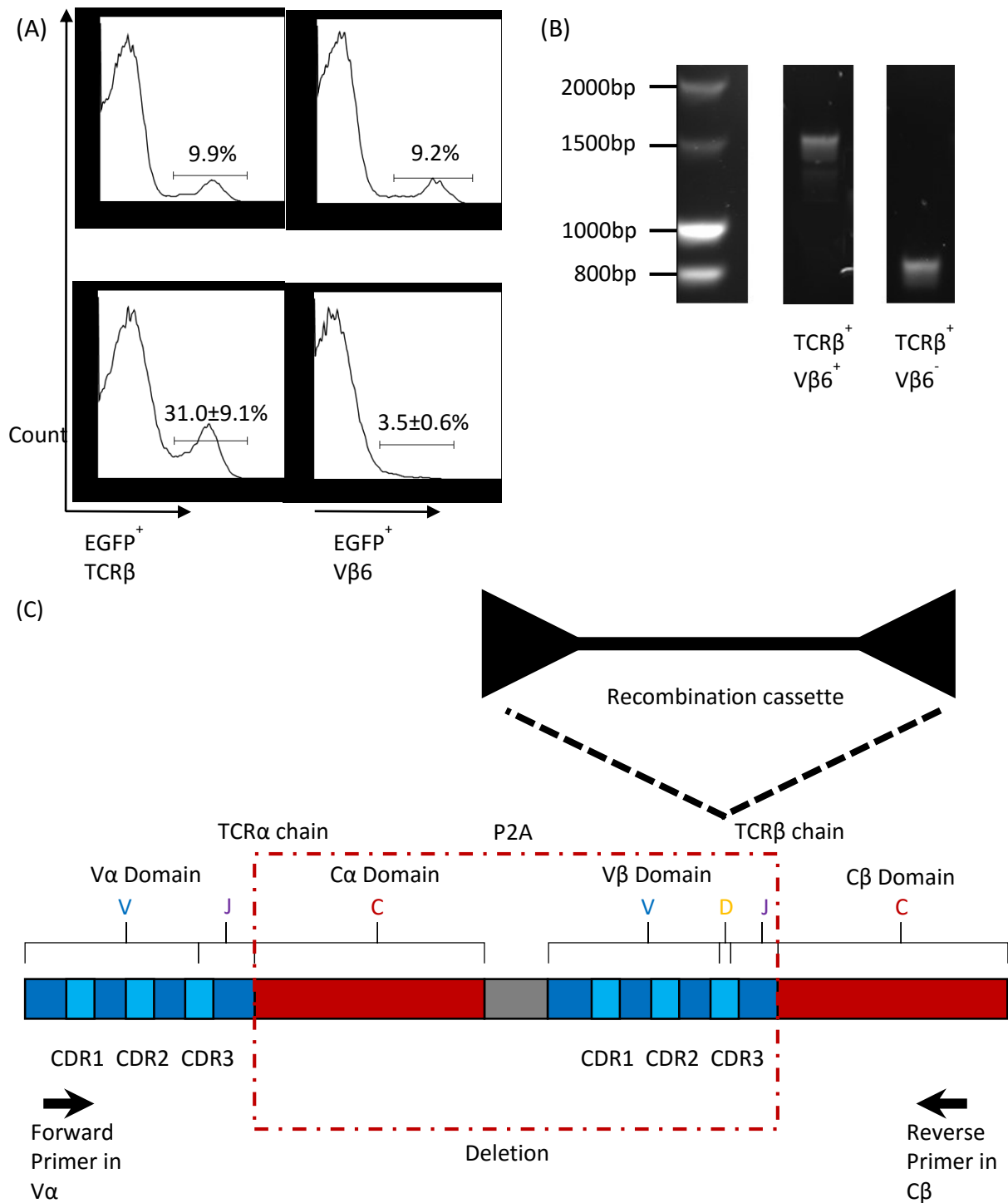


Figure 5.1. The loss of the Marilyn Vβ6 domain in Marilyn TCR (CDR3β diversifying) retrogenic mice. Analysis of the Marilyn TCR (CDR3β diversifying) C57BL/6 mice showed two classes of T lymphocyte populations: EGFP⁺TCRβ⁺Vβ6⁺ and EGFP⁺TCRβ⁺Vβ6⁻. (A) Retention (*top*) and loss (*bottom*) of the Vβ6 domain in the EGFP⁺ T lymphocytes. (B) PCR analysis using primers in the Vα and Cβ domains of the mRNA extracted from these two populations show the deletion of a large portion (~800bp) of the Marilyn αβTCR construct. (C) Schematic diagram of the Marilyn TCR (CDR3β diversifying) construct highlighting the deleted Cα and Vβ segments, and relative positions of the PCR primers used in (B).

5.2. Results

5.2.1. Preparation of sequencing and retroviral vectors containing the novel chimeric TCR

To amplify cDNA corresponding to the complete V α -C β fusion TCR construct, we performed PCR using *Taq* polymerase on the cDNA derived from the sorted CD4⁺V β 6⁻ Marilyn TCR (CDR3 β diversifying) lymphocytes (Refer to *Chapter 4.2.4*; Figure 4.8A). The PCR primers were designed to include the leader sequence upstream of the V α domain and termination codon of the C β domain to encode the entire open reading frame (ORF). The *Bgl*III and *Eco*RI restriction sites on opposite sides of the TCR construct were also incorporated to facilitate sub-cloning into the MCS of the pMigR1 vector. The PCR was shown via gel electrophoresis to synthesise the PCR product of the correct length (933bp; Figure 5.2A). To enable further amplification and stable sequencing of the V α -C β fusion TCR, we first sub-cloned the PCR product into the pCRTM2.1 vector. *Taq* polymerase has a non-template-dependent activity that adds a single deoxyadenosine (A) to the 3' ends of the PCR products. The pCRTM2.1 vector contains complementary 3' deoxythymidine (T) overhangs that enable efficient ligation with the PCR products. Further, the pCRTM2.1 vector includes primer sites flanking the ligation site to facilitate sequencing of the inserts. The ligation was confirmed by double digestion with *Bgl*III and *Eco*RI restriction enzymes, followed by gel electrophoresis analysis (Figure 5.2B). The open-ended inserts (V α -C β fusion TCR construct containing *Bgl*III and *Eco*RI restriction sites) were then isolated and purified before ligation into 'empty' pMigR1 vectors. Ligation was confirmed as before (Figure 5.2C). Insertion was further verified by sequencing, which showed 100% identity and correct orientation in the retroviral vector (not shown).

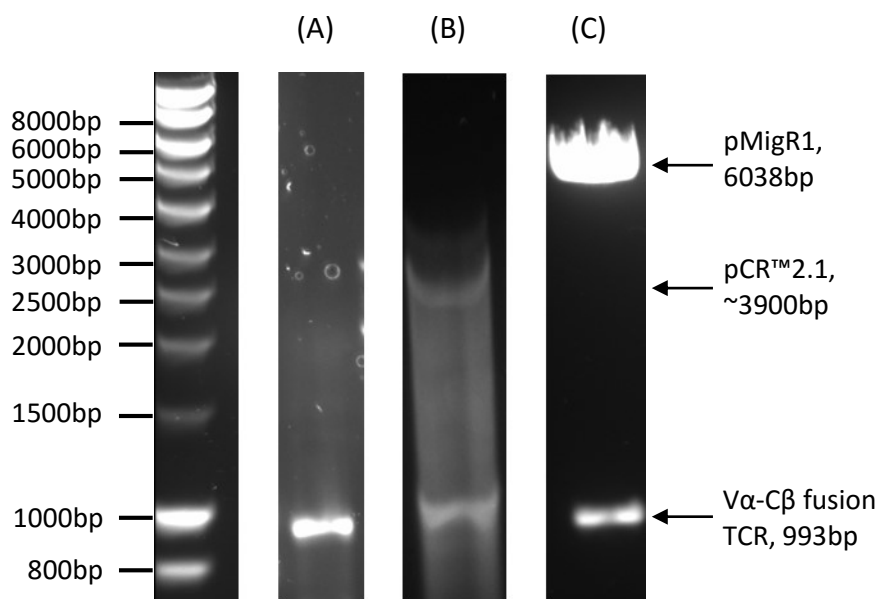


Figure 5.2. Amplification and sub-cloning of the complete V α -C β fusion TCR construct. (A) PCR was performed on the cDNA of the sorted CD4⁺V β 6⁻ Marilyn TCR (CDR3 β diversifying) lymphocytes using

primers that include *BglIII* and *EcoRI* restriction sites, and entire ORF. Gel electrophoresis analysis confirmed the presence of a PCR product of the correct size (933bp). The PCR product was then ligated into the pCR™2.1 and pMigR1 vectors. Sub-cloning of V α -C β fusion TCR into vectors pCR™2.1 (~3900bp; B) and pMigR1 (6038bp; C) was confirmed by double digestion using *BglIII* and *EcoRI* and gel electrophoresis.

5.2.2. Analysis of recombination event leading to deletion of C α and V β domains

To characterise the recombination event leading to the formation of the V α -C β fusion TCR, we compared the sequence of the complete V α -C β fusion TCR in the pCR™2.1 vector with the Marilyn TCR (CDR3 β diversifying) construct in the pMigR1 vector. Sequence analysis demonstrated that the J-segments of the Marilyn TCR α and β chains exhibited similar nucleotide and amino acid sequences (Figure 5.3). Further, we confirmed that the V α -C β TCR junction occurred within the J-segments of both TCR α and β chains (Figure 5.3B, *boxed*). The fusion V α -C β TCR contains an aspartic acid (D) amino acid residue at the junction rather than the alanine (A) or histidine (H) residues present in the TCR α and β J-segments of the original construct respectively. The aspartic acid codon (**g-ac**) appears to have been produced by a recombination event occurring within the alanine (**gcc**) and histidine (**cac**) codons. Indeed, there is a direct repeat of at least 18 nucleotides in the TCR α and β J-segments suggesting that the fusion may have been caused by a homologous recombination event. We propose that the codon optimisation applied during the *de novo* synthesis of the Marilyn TCR (CDR3 β diversifying) construct to increase translation, and which introduced differences from the original germline, may have contributed to this unexpected nucleotide sequence homology shared by the J-segments of the Marilyn TCR α and β chains. Notably, this aberrant recombination event appears to lack any diversity and may be unrelated to the presence of the recombination cassette. All three CDRs of the Marilyn TCR α chain also remain unaltered.

We hypothesise that the fusion, at the point where the V α and C β domains are joined, allows efficient folding of the V α and C β protein domains and their linkage through the chimeric J-segment. A molecular model, made by Istvan Bartok (unpublished), illustrates the proposed position the novel V α domain assumes in place of the WT V β of the Marilyn TCR β chain (Figure 5.4). The combined J α -J β segment does not appear to affect the protein folding of the V α and C β domains. Hence, the novel V α -C β TCR chain is able to maintain a conformation similar to that of the WT Marilyn TCR β chain.

(A) Marilyn TCR α chain:

MKSLSVSLVVLWLLLLNWNVNSQQNVQQSPESLIVPEGARTSLNCTFSDSASQYFWWYRQHS
GKAPKALMS**IFSNGEKEEGRFTIHLNKASLHFS**LHIRDSQPSDSALYLC**AVGN**NNN**APRF**
G**A**GTKLTVK**PNIQNPEPAVYQLK**DP**RSQDSTLCLFTDFDSQ**INVPK**TMESGTFITDKTVL**
DMKAMDSKSN**GAI**AWSN**QTSFTCQDIFKETNATYPSS**DVPCD**ATL**TEK**SFETDMN**LN**FQN**
LSVMGLR**ILL**LKVAGFN**LLM**TLRL**WSS**

Marilyn TCR β chain (“,” denotes insertion of recombination cassette):

MNKWVFCWVTLCLLT**VETHGDGGIITQTPKFLIGQEGQKLT**LKCQQN**FNHDT**MYWYRQD
SGKGLRLIYY**SITEND**LQK**DLSEGYDASREKSSFSLTVT**SAQKNEMAVFL**CASSIPGS**,
NERLFFGHGTKLSVLEDLRN**VTPPKVSLFEP**SKAEIANK**QKATLVCLARGFFPDHVELSW**
WVNGKEVHSGVSTDPQAYKESNYSYCLSSRLRVSATFWHNPRNH**FRCQVQFHGLSEEDKW**
PEGSPK**PVTQ**NI**SAEAWGR**ADCGITSASYHQVLSATILYEILLG**KATLYAVLVSGLVLM**
AMV**KRKNS**-

V α -C β fusion TCR:

MKSLSVSLVVLWLLLLNWNVNSQQNVQQSPESLIVPEGARTSLNCTFSDSASQYFWWYRQHS
GKAPKALMS**IFSNGEKEEGRFTIHLNKASLHFS**LHIRDSQPSDSALYLC**AVGN**NNN**APRF**
G**D**GTKLSVLEDLRN**VTPPKVSLFEP**SKAEIANK**QKATLVCLARGFFPDHVELSW**
WVNGKEVHSGVSTDPQAYKESNYSYCLSSRLRVSATFWHNPRNH**FRCQVQFHGLSEEDKW**
PEGSPK**PVTQ**NI**SAEAWGR**ADCGITSASYHQVLSATILYEILLG**KATLYAVLVSGLVLM**
AMV**KRKNS**-

(B) Marilyn TCR α chain:

R **F** **G** **A** **G** **T** **K** **L** **T** **V** **K**
agg ttc gga **gca** ggc acc aag ctg acc gtg aag

Marilyn TCR β chain:

F **F** **G** **H** **G** **T** **K** **L** **S** **V** **L**
ttt ttc ggc **cac** ggc acc aag ctg tcc gtg ctg

V α -C β fusion TCR:

R **F** **G** **D** **G** **T** **K** **L** **S** **V** **L**
agg ttc gga **gac** ggc acc aag ctg tcc gtg ctg

Key

Leader Sequence
V Region
D Region
J Region
C Domain
Connecting Region
Transmembrane Region
Cytoplasmic Region

Figure 5.3. Comparison of the nucleotide and amino acid sequences of the Marilyn TCR α and β chains with the V α -C β fusion TCR. (A) The complete amino acid sequences of the TCR α and β chains Marilyn TCR (CDR3 β diversifying) constructs are shown, and compared with that of the V α -C β fusion TCR. CDRs are shown in bold. (B) The sequence homology in the J-segments of the TCR α and β chains are proposed to have led to recombination of the V α and C β domains at point of fusion (*boxed*). Nucleotide and amino acid sequences maintained into the V α -C β fusion TCR are shown underlined.

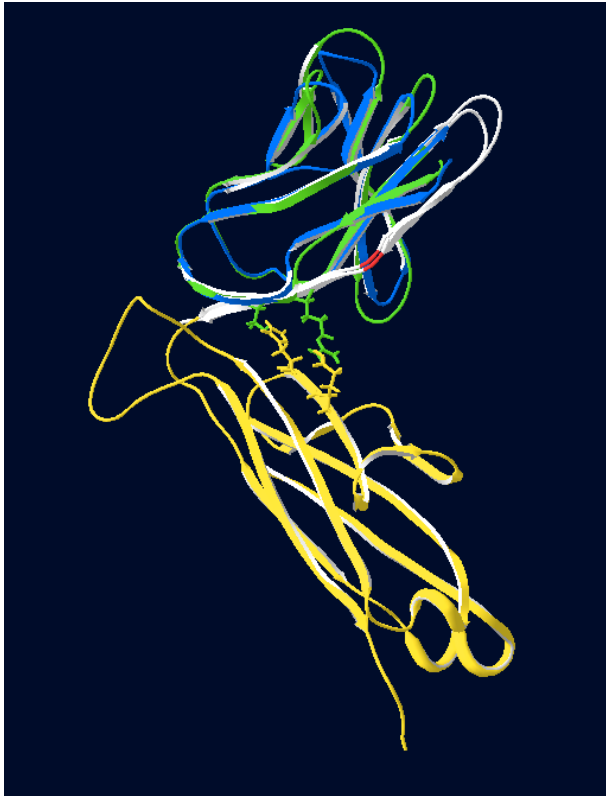


Figure 5.4. Molecular model of V α -C β fusion TCR. The three-dimensional structure of the V α -C β TCR chain is illustrated based on its primary structure. The TCR V α (*blue*) is shown superimposed onto the V β (*green*) domain, attached to the C β (*yellow*) of the Marilyn TCR β chain. The J-segment (*white*) connects the V α and C β domains, with the point of fusion shown in red. Provided by Istvan Bartok, unpublished.

5.2.3. Functional characterisation of V α -C β fusion TCR chain

5.2.3.1. Phoenix™ cell transfection and generation of C57BL/6 retrogenic mice

In order to deliver the V α -C β fusion TCR construct in the pMigR1 vectors into HSCs for the development of T cells in retrogenic mice, we used the Phoenix™ ecotropic packaging cell line to produce retroviral particles. As described in Chapter 2, we transfected the Phoenix™ cells with the help of the Lipofectamine® 2000 transfection reagent and pCLE helper plasmid. The expression of the EGFP gene in the pMigR1 vector facilitated the identification of transfected and transduced cells. The transfection efficiencies measured by flow cytometry were: ‘empty’ pMigR1 – $61.7 \pm 8.3\%$ and pMigR1-(V α -C β fusion TCR) – $70.6 \pm 0.9\%$ (Figure 5.5A). The transfection efficiencies between the empty pMigR1 and pMigR1-(V α -C β fusion TCR) were shown to be statistically similar ($p > 0.5$).

The retroviral particles in the supernatant were then used for the transduction of HSC-enriched cultures from at least eight-week-old TCR- $\beta/\delta^{-/-}$ deficient donor mice (C57BL/6; male and female). Two

sets of two retrogenic mice were generated. The average transduction efficiencies during each set-up was $8.5 \pm 7.8\%$ (Figure 5.5B). Although transduction efficiency rates were quite low, we ensured at least 2×10^5 GFP⁺ cells were injected into each C57BL/6 TCR- $\beta/\delta^{-/-}$ deficient female recipient mouse. This would be sufficient to determine whether the V α -C β fusion TCR chain can direct T cell development.

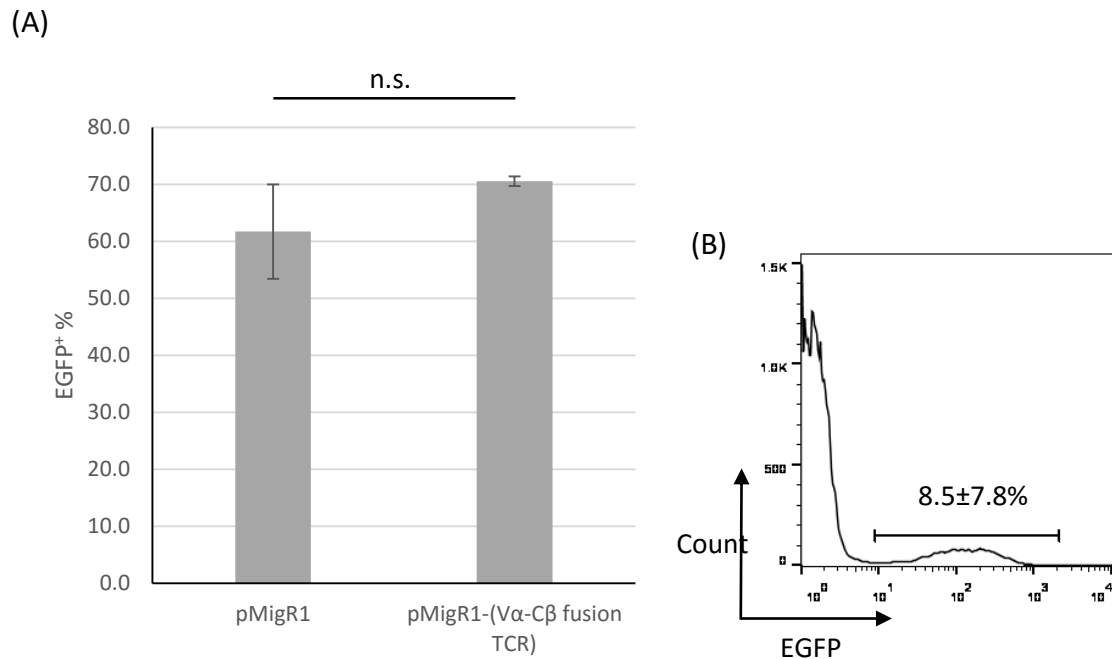


Figure 5.5. Flow cytometric analysis of EGFP reporter expression in transfected and transduced cells. (A) Transfection efficiencies of ‘empty’ pMigR1 (n=10) and pMigR1-(V α -C β fusion TCR) (n=3) determined by the average percentage of EGFP⁺ PhoenixTM cells. Each bar represents the mean \pm SD. (B) Transduction efficiency, measured by percentage of EGFP⁺ HSCs, during the generation of retrogenic mice (n=2). Data is presented as mean \pm SD.

5.2.3.2. Analysis of co-expression of novel TCR in normal $\alpha\beta$ T cells

The V α -C β fusion TCR was initially reported in a proportion of Marilyn TCR (CDR3 β diversifying) retrogenic mice which expressed V β 6⁺ T lymphocytes (Chapters 3 and 4). Conversely, we also observed Marilyn TCR (CDR3 β diversifying) retrogenic mice that exhibited positive V β 6 expression. We proposed that the V α -C β fusion chain pairs with endogenous TCR α chains instead of forming a V α -C β TCR homodimer. However, the proposed V α -C β /TCR α heterodimer may be relatively unstable since it lacks the V α -V β interface required for normal $\alpha\beta$ TCR pairing. Additionally, the V α -C β TCR may be disadvantaged from pairing with endogenous TCR α when competing with WT TCR β . To investigate

this hypothesis, we transduced the V α -C β TCR chain into peripheral T cells which already express a WT $\alpha\beta$ TCR repertoire.

The retroviral supernatant (Figure 5.5) was used to transfer the V α -C β TCR transgene into splenocytes collected from V β 11⁺ TCR transgenic mice. After culturing for 48 hours, the transduced T cells were stained with anti-TCR β (C domain) and anti-V β 11 Ab and analysed via flow cytometry. The anti-TCR β Ab would detect both the WT TCR β and V α -C β TCR chains. In contrast, the anti-V β 11 Ab staining would detect only the WT transgenic TCR. EGFP expression facilitates detection of transduced T cells and correlates to the expression of the V α -C β TCR chain since both proteins are translated from the same mRNA.

Flow cytometric analysis demonstrated a relatively low transduction efficiency, shown by the 14.0% EGFP expression in CD4⁺ and CD8⁺ T cells (Figure 5.6). In both CD4⁺ and CD8⁺ T lymphocytes, we observed an increase in cell surface TCR β expression levels with increasing EGFP expression (Figure 5.6B). This upward trend indicates the expression of the exogenous V α -C β fusion chain with the endogenous TCR α . Conversely, a downward trend of endogenous V β 11⁺ TCR was seen with increasing EGFP levels. To support this observation, we measured the MFI of TCR β and V β 11 expressions in the transduced T cells relative to EGFP expression levels (EGFP⁻, low and high EGFP). The TCR β MFI showed a progressive increment while the V β 11 MFI showed a gradual reduction with increasing EGFP (Table 5.1). This downward V β 11:EGFP trend is likely due to the exogenous V α -C β fusion chain successfully competing with endogenous TCR β chains for pairing with endogenous TCR α .

Thus it can be concluded that both types of TCRs can be co-expressed on the T cell surface. These data also demonstrate that the V α -C β fusion chain pairs efficiently with the endogenous TCR α chain and appears to form stable heterodimers despite exhibiting the uncharacteristic V α -C β interface. Since the up-modulation of the TCR is observed in the majority both CD4⁺ and CD8⁺ T lymphocytes, we may assume that pairing is possibly efficient across the majority of V α segments expressed by V β 11 transgenic T cells.

Table 5.1. Comparison of the MFI of TCR β and V β 11 expressions relative to EGFP expression in transduced CD8⁺ and CD4⁺ T cells.

EGFP expression level	CD8			CD4		
	Non EGFP	Low EGFP	High EGFP	Non EGFP	Low EGFP	High EGFP
MFI (TCR β)	474	990	1976	363	776	1577
MFI (V β 11)	143	146	89	157	160	103

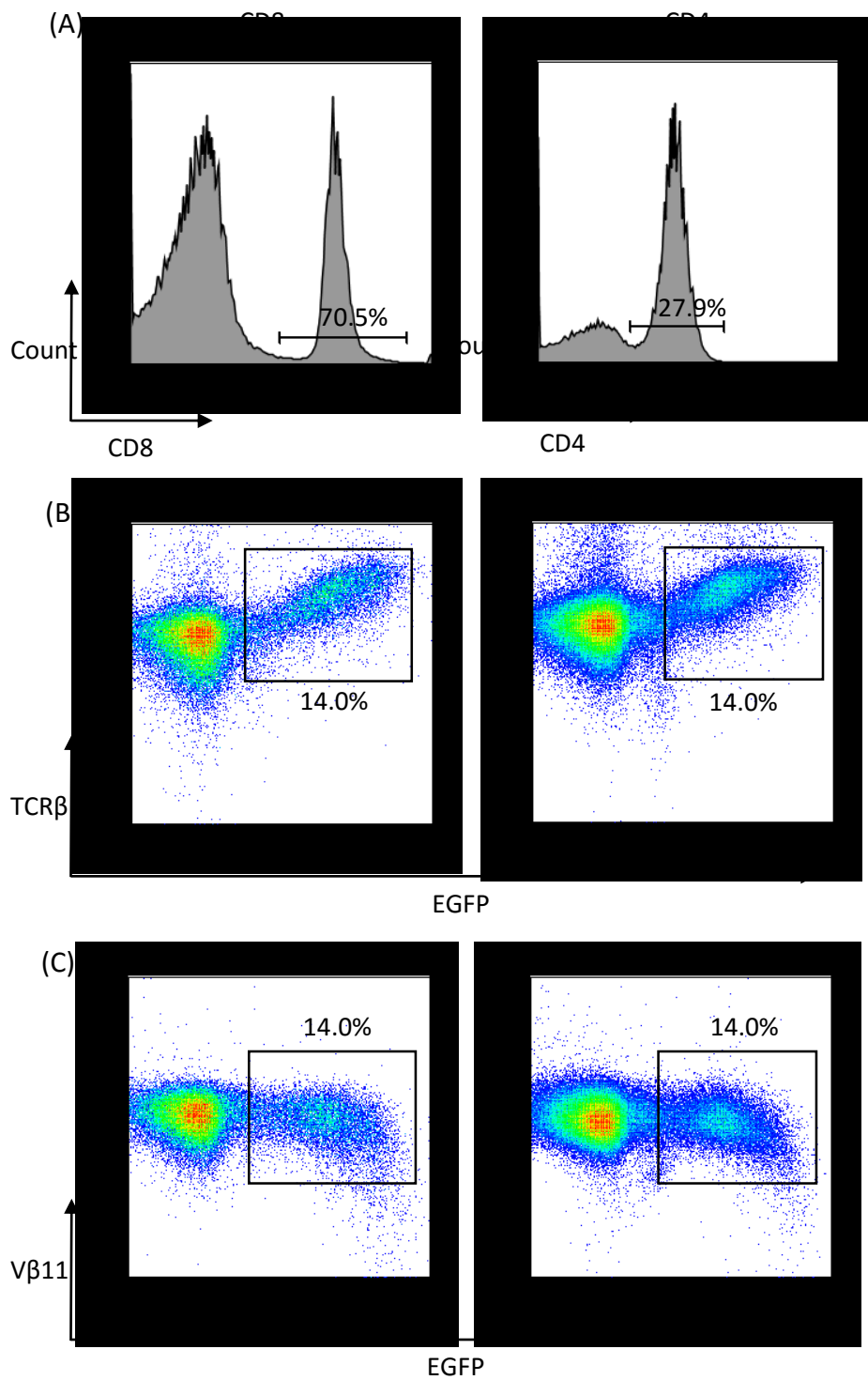


Figure 5.6. Flow cytometric analysis of transduced T cells. The retroviral supernatant containing the $V\alpha$ -C β TCR transgene was used to transduce T cells extracted from $V\beta 11^+$ transgenic mice. After culturing for 48 hours, the transduced cells were harvested and stained with anti-TCR β and anti- $V\beta 11$ Ab. (A) The transduced cells were analysed based on co-receptor expression. The CD8 $^+$ and CD4 $^+$ T cells were then analysed for expression the reporter EGFP gene against (B) anti-TCR β and (C) anti- $V\beta 11$ Ab staining.

5.2.4. Phenotypic analysis of the retrogenic mice expressing the V α -C β fusion TCR chain

5.2.4.1. Analysis of retrogenic mice primary lymphoid organs

The retrogenic mice were given at least 8 weeks to reconstitute the peripheral T cell repertoire. After this period, the mice were culled and analysed to characterise T cell development directed by the V α -C β fusion TCR chain. The retrogenic mice (n=3) displayed a small thymus with an average of $16.7 (\pm 12.7) \times 10^6$ cells (Figure 5.7A, B). The thymocyte cell count was statistically lower than that of WT C57BL/6 mice ($p > 0.05$).

Thymocytes were subsequently analysed for EGFP, TCR β , CD4 and CD8 expression via flow cytometry. The retrogenic thymocytes expressed pronounced levels of EGFP⁺ ($15.6 \pm 9.4\%$) and within this, EGFP⁺TCR β ⁺ represented $84.8 \pm 15.3\%$ (Figure 5.7C). The thymocyte co-receptor expression profile demonstrated a higher frequency of DN cells relative to DP cells, suggesting a partial block at the DN to DP stage – a trait of the TCR- $\beta/\delta^{-/-}$ deficient recipient mice (Mombaerts et al., 1992). There are also sizeable proportions of SPCD4 and SPCD8 cells at a ratio of 4:1, similar to that observed in WT C57BL/6 thymocytes (Figure 5.7C). Altogether, this data suggests that the transduced HSCs successfully migrated to the thymic microenvironment to undergo T cell development which results in a higher frequency of CD4⁺ compared to CD8⁺ T cells. The T cells can only develop from expressing the V α -C β fusion TCR chain, followed by pairing with endogenous TCR α chains to produce a functional TCR heterodimer. Additionally, the similar SPCD4:SPCD8 ratios imply that the T cells expressing the V α -C β fusion TCR chain may exhibit a development fate similar to that of WT thymocytes.

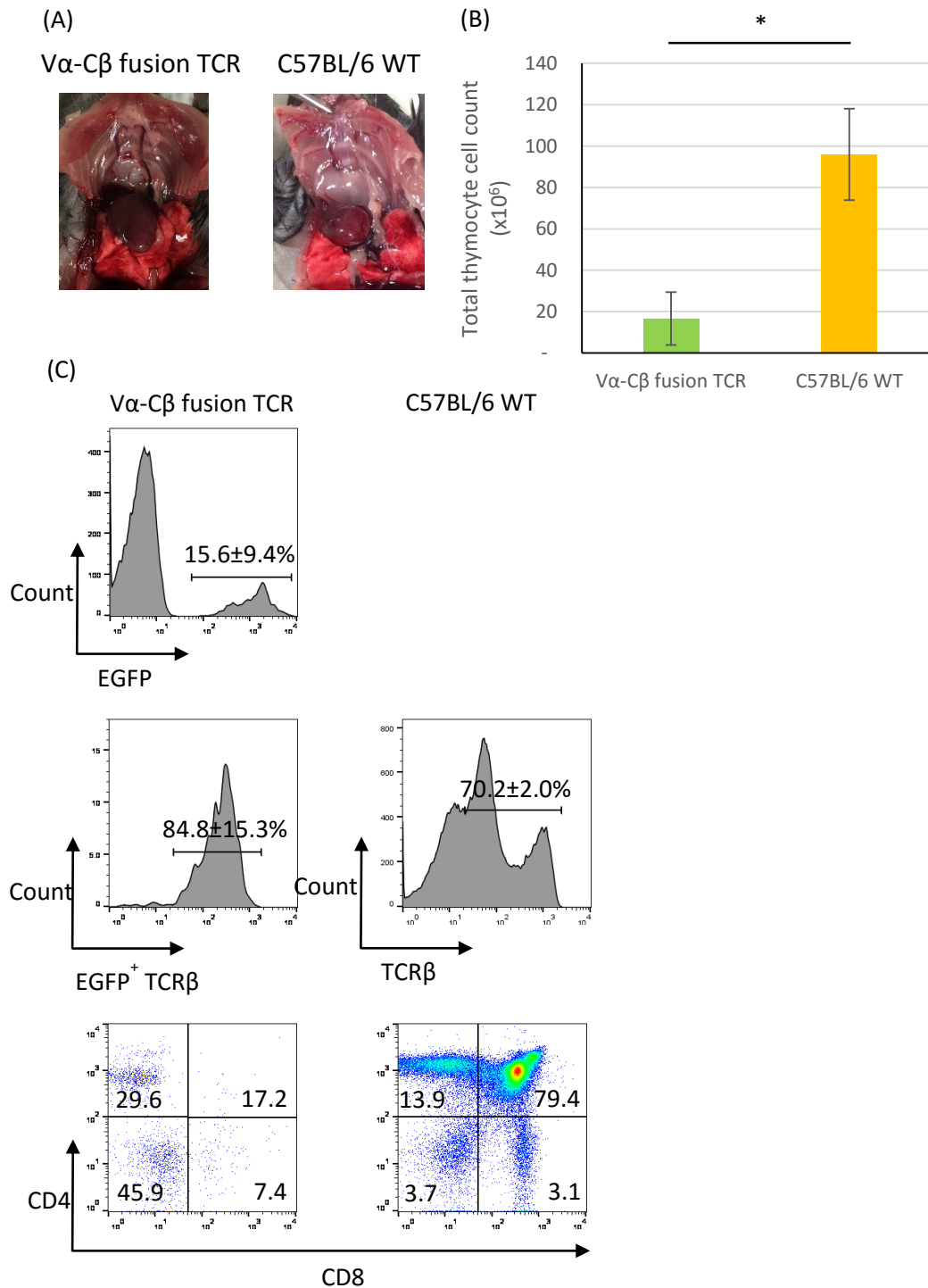


Figure 5.7. Analysis of thymus from C57BL/6 retrogenic mice expressing the V α -C β fusion TCR chain.

Thymi from the retrogenic mice (n=3) were harvested after the TCR reconstitution period (>8 weeks). (A) Representative example of the retrogenic thymus is shown, compared to that of a WT C57BL/6 thymus. (B) The average thymocyte cell count of the retrogenic mice is shown to be statistically lower than that of WT C57BL/6 mice (p>0.05). (C) The flow cytometric analysis of EGFP, TCR β , CD4 and CD8 expression in the thymocytes are shown. The DN, DP, SPCD4 and SPCD8 sub-population distribution is gated on the whole thymocyte population. Similar staining in WT mice are shown for comparison. Percentages indicated on representative plots denote mean \pm SD for all mice, calculated to the first decimal place.

5.2.4.2. Analysis of retrogenic mice secondary lymphoid tissue

Following the analysis of T cell development, we investigated the peripheral T cell phenotype by analysing the spleen and LN of the retrogenic mice. Splens from the retrogenic mice were isolated (Figure 5.8A), and shown to be of similar size to that of a WT mice. The total splenic cellularity was measured and the mean calculated ($43.0 \pm 15.9 \times 10^6$), showing a statistically similar count to WT ($p < 0.05$; Figure 5.8B).

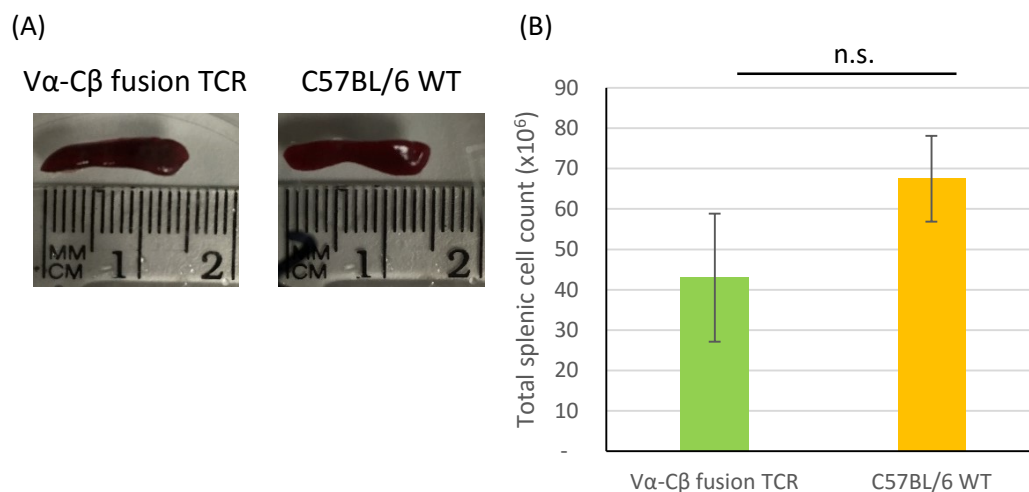


Figure 5.8. Splenic size and cellularity in retrogenic mice expressing the Vα-Cβ fusion TCR chain. Splens from the retrogenic mice (n=3) after the TCR reconstitution period and WT mice (n=2) were harvested. (A) Representative spleen of the retrogenic mice is shown, along with a WT mouse spleen. (B) Total splenic cellularity was determined and average splenic cell counts are shown with error bars. Cellularity appeared to be statistically similar ($p < 0.05$).

Splenocyte and LN suspensions from the retrogenic and WT mice were then prepared for Ab staining and flow cytometric analysis. Both secondary lymphoid organs displayed sizeable proportions of EGFP⁺ and a relatively high EGFP⁺TCRβ⁺ expression (Figure 5.9A, B). Staining with anti-CD3 Ab in the splenocyte revealed similar levels of EGFP⁺TCRβ⁺ and EGFP⁺CD3⁺, indicating the T cells express a functional TCR signalling complex (Figure 5.9B, C). The presence of peripheral T cells also confirms that the lymphocytes emigrate from the thymus after undergoing the sequential stages of thymic selection. It is likely that selection mechanisms ensuring self-tolerance and self-MHC restriction are operating as for conventional αβT cell development. Analysis of the co-receptor expression demonstrated a skew to the CD4⁺ T cell compartment in both spleen and LN (Figure 5.9D). Notably, the splenocytes maintained the 4:1 CD4:CD8 ratio observed in the thymus, whereas the LN showed a lower ratio of

about 2:1, similar to that of WT spleens. From these data we may infer that the novel form of TCR engages productively with both MHC-I and -II.

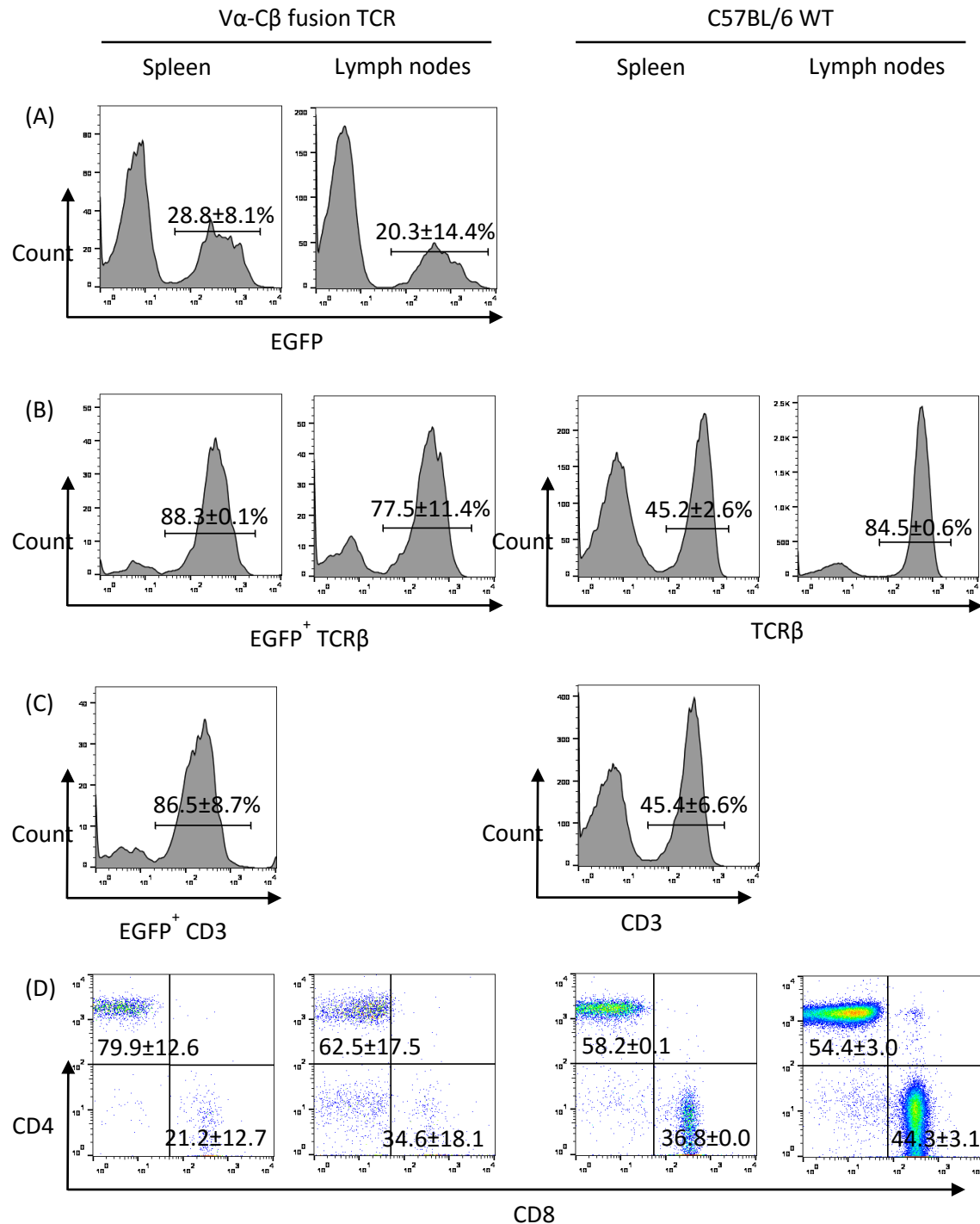


Figure 5.9. Flow cytometric analysis of retrogenic mice expressing the Vα-Cβ fusion TCR chain. The spleen and LN from the retrogenic mice (n=3) and WT mice (n=2) were harvested and analysed for (A) EGFP, (B) TCRβ, (C) CD3 and (D) CD4 and CD8 co-receptor expression to characterise the peripheral T cell compartment. Percentages of defined populations are shown as mean ± SD for all mice.

To investigate TCR α pairing with the V α -C β fusion TCR chain, we stained the splenocytes with a small panel of anti-V α Abs. There were variable levels of positive staining in EGFP⁺ retrogenic lymphocytes for all three anti-V α Ab tested (V α 2, V α 3.2 and V α 11; Figure 5.10A). The co-receptor expression profiles for each V α usage were also shown to be variable (Figure 5.10A, *bottom*). This data further confirms our previous observation (Refer to *Chapter 5.2.3.2*) that the V α -C β fusion TCR forms heterodimers with a wide range of endogenous TCR α chains rather than forming homodimers. To further characterise the peripheral T cell compartment, we stained the splenocytes for intracellular FoxP3 expression in order to identify the presence of CD4⁺ Treg cells. The retrogenic lymphocyte population showed positive staining for intracellular FoxP3 expression (7.5 \pm 11.6%), with the expected skew to the CD4 lineage (Figure 5.10B). Altogether, the lymphocytes expressing the V α -C β fusion TCR appear to exhibit a typical T cell phenotype closely resembling WT mice.

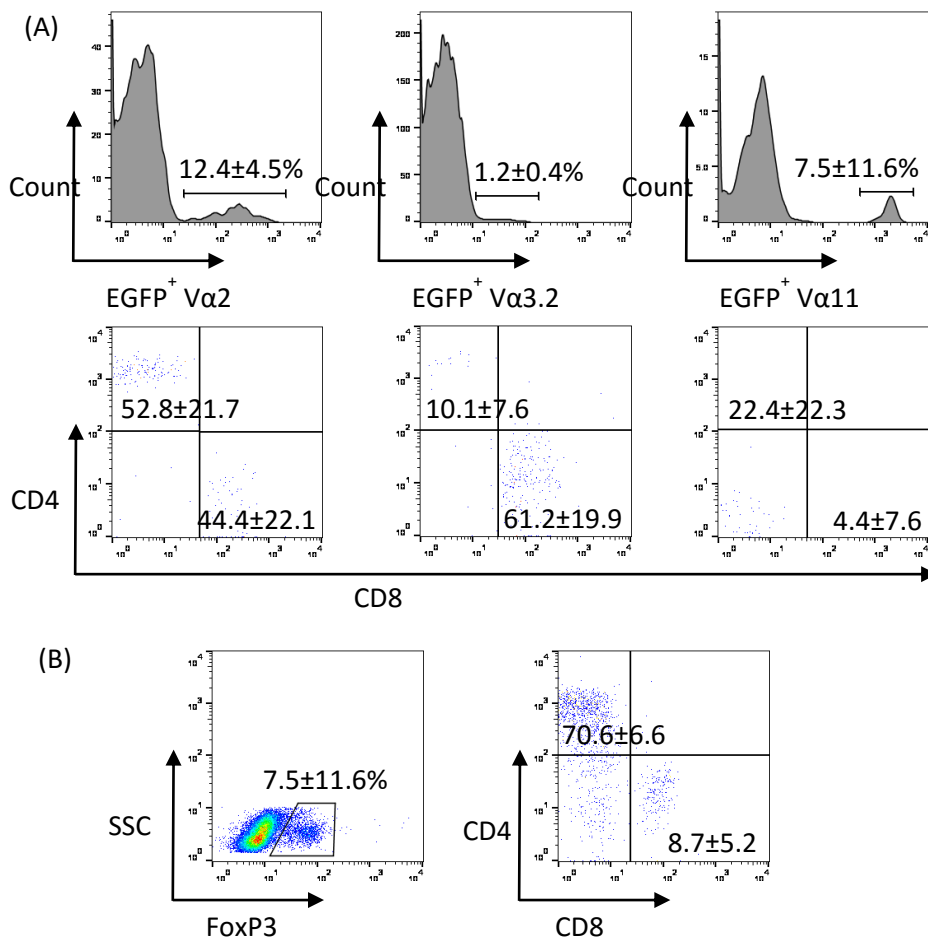


Figure 5.10. Flow cytometric analysis of V α usage and FoxP3 staining in the retrogenic peripheral T lymphocytes. (A) The splenocytes from the retrogenic mice (n=3) were stained against specific anti-V α Ab, along with their respective co-receptor expression profiles. (B) Flow cytometric analysis of intracellular Foxp3 staining in splenocytes after fixation/permeabilisation, with a CD4 lineage skew. Percentages of defined populations are shown as mean \pm SD for all mice.

5.3. Discussion

5.3.1. Summary

The functional $\alpha\beta$ T cell repertoire is specialised to recognise and respond to MHC-bound peptide ligands (Garcia, Teyton & Wilson, 1999; Davis & Bjorkman, 1988). There are two main mechanisms thought to underpin MHC restriction across $\alpha\beta$ T cell repertoires, namely the germline and selection models. According to the germline theory, the TCR is evolutionarily biased to engage only with MHC through the germline CDR1 and CDR2 loops. Functional and structural studies have suggested that some conserved amino acids within TCR α and β chains have co-evolved to interact with MHC Class I and II (Garcia et al., 2012; Scott-Browne et al., 2009; Marrack et al., 2008). In contrast, the alternative selection model proposes that MHC restriction is imposed by the CD4 and CD8 co-receptors that bind and co-localise Lck to the TCR signalling complex only during MHC engagement (Tikhonova et al., 2012; Van Laethem, Tikhonova & Singer, 2012; Van Laethem et al., 2007). The present chapter describes a TCR heterodimer expressing two sets of germline TCR α CDRs which provides support for the selection model.

In the previous chapter, the fortuitous expression of a Marilyn TCR (CDR3 β diversifying) T cell population that completely lacked the specific anti-V β 6 Ab epitope led to the discovery of a large deletion in the template TCR construct through PCR analysis. Indeed, sequencing of the fusion TCR chain confirmed the loss of the C α and V β domains in the primary structure of this construct. We proposed a recombination-deletion event between homologous sequences in the J α and J β segment directed a fusion between the V α and C β domains. Previous studies have described a high frequency of recombination-deletion events during retroviral reverse transcription (Im et al., 2014; Zhang & Sapp, 1999). Hence, it is possible that this aberrant recombination may have occurred during the transduction of HSCs by the retroviral particles. Nonetheless, this fusion, which occurred within the J-segment, left the C α and V β sequences unaltered. Such modifications within the C α and V β domains could have disrupted the folding and pairing of this fusion TCR chain. Sequence analysis showed that the recombination introduced an aspartic acid in place of the arginine and histidine residues within the J α and J β segments respectively. According to the IMGT database, aspartic acid is found at this position (FR4 region) in other J α segments, so we can presume this substitution to have minimal impact (Lefranc, 2005).

Further, we generated retrogenic mice in order to characterise whether the novel V α -C β fusion TCR chain can direct T cell development. The presence of peripheral T cells in the retrogenic mice indicate that the exogenous V α -C β TCR chain are expressed, pairing with endogenous TCR α chains, to form a novel TCR heterodimer. We have shown that despite displaying a distinct V α -C β interface that replaces

the natural V β -C β interface, the novel TCR chain is capable of efficiently pairing with TCR α chains. Similarly, even though the novel TCR heterodimer forms an abnormal V α -V α antigen-binding interface, the retrogenic T cells are able to undergo thymic selection and develop a functional repertoire that is educated in MHC restriction and self-tolerance. Even with the entire V β structure replaced by the V α domain, there may be only subtle differences in the positions of the CDRs and overall topology of the novel TCR chain. The binding between the side chains in the J-segment with those of C β remain conserved, consequently maintaining the molecular ball-and-socket joint that modulates flexibility between the V α and C β domains (Landolfi et al., 2001; Lesk & Chothia, 1988).

The development of both CD4⁺ and CD8⁺ T cell compartments also indicate that the V α -C β TCR relies on co-receptors for efficient TCR signalling, consistent with the selection model. Moreover, this shows that the V α -C β TCR can engage with both classes of MHC despite their V α -V α homodimer antigen-binding site. Additionally, we observe a typical frequency of regulatory T cells within the peripheral CD4⁺ lymphocyte population. Regulatory CD4⁺ T cells arising in the thymus (nTregs) require higher affinity engagement with MHC-II than conventional CD4⁺ T cells. Hence, we can deduce that the novel TCR featuring the V α -C β TCR chain, can efficiently engage with MHC in a co-receptor-dependent manner similar to that of conventional TCR repertoires.

5.3.2. Conclusions

Altogether, these data support the view that the WT $\alpha\beta$ TCR is not intrinsically specific for MHC, as the exchange of the germline CDR β with that of CDR α does not significantly impair MHC recognition, and aberrant CDR configurations can still engage with MHC forming unconventional interfaces. The V α -C β fusion TCR chain is shown to have limited impact regarding T cell development. Despite an unusual antigen-binding site, thymocytes are able to develop normally and generate functional T cells typical of a conventional repertoire. The novel V α -C β TCR chain provides a new platform to study the bias to MHC restriction that utilises a change in the entire V domain rather than just modifying the CDRs. Previous studies in our group have already shown the expendability of the CDRs in terms of facilitating MHC recognition and thymic T cell selection (Holland et al., 2012; Attaf et al., unpublished).

Chapter 6

Discussion

Chapter 6: Discussion

$\alpha\beta$ T cells orchestrate cell-mediated immunity against foreign pathogens and cellular malignancies via the interaction between the TCR and pMHC (Garcia, Teyton & Wilson, 1999; Davis & Bjorkman, 1988). CD8⁺ cytotoxic T lymphocytes recognise mainly intracellular proteins, processed by the proteasome into short peptides, and presented on all nucleated cells by MHC-I molecules. Cytotoxic T cell immunity provide an important mechanism to scrutinise the internal proteome of virally-infected or aberrant cells that would be otherwise hidden from the immune system. On the contrary, CD4⁺ Th cells recognise peptides derived from exogenous proteins in the context of MHC-II molecules on the surface of professional APCs. Conventional Th cells control adaptive immunity in an antigen-specific manner by activating other effector immune cells such as B cells, macrophages and the cytotoxic T cells.

The TCR-pMHC interaction is a significant event that initiates T cell signalling and governs T cell-mediated immune responses. Due to the rigors of thymic selection, natural tumour-reactive TCRs generally bind to cognate pMHC ligands with weak affinity, thus limiting their therapeutic potential (Bridgeman et al., 2012; Cole et al., 2007). Thymic selection is presumably designed to ensure host protection against foreign pathogens and to limit autoreactivity (Chervin et al., 2009; Dudley & Rosenberg, 2003; Ho et al., 2003). Additionally, in order to fully defend the host against all possible immunogenic epitopes, TCR cross-reactivity likely results in suboptimal engagement of the TCR with a proportion of pMHC ligands (Sewell, 2012; Wooldridge et al., 2012). Current efforts implemented to overcome this limitation focus on enhancing the TCR binding affinity by modifying key residues within the antigen-binding CDR loops. This is achieved using several *in vitro* techniques, leading to the development of novel immunotherapeutics including TCR-engineered T cells for adoptive therapy and soluble TCRs bound to anti-CD3 Ab fragments (Malecek et al., 2013; Linette et al., 2013; Smethurst, 2013; Chervin et al., 2009; Zhao et al., 2007; Weber et al., 2005; Li et al., 2005; Kieke et al., 1999). However, the lack of natural screening processes risk the possibility of off target reactivity. A recent clinical trial reported fatal cardiac toxicity in two patients following administration of T cells expressing high-affinity MAGE-A3-specific TCRs (Linette et al., 2013). The cross-reactive recognition, through molecular mimicry, of an unrelated peptide derived from the muscle protein Titin and presentation of this peptide on cardiac tissues *in vivo* was suggested to mediate the observed toxicity (Raman et al., 2015; Cameron et al., 2013).

The principal aim of this study was to develop a new strategy that optimises TCR binding and T cell functionality in contrast to emphasising only on affinity enhancement. This approach involves the insertion of a gene recombination cassette into the hypervariable CDR3 to diversify an established TCR

template and generate a library of TCR variants. The main difference between this novel technique and previous approaches is the diversification of TCRs *in vivo* using retrogenic mice, which facilitates the deletion of potentially autoreactive cells. We tested this approach using two male-specific TCRs, Marilyn and MataHari, and successfully identified at least 20 unique variants each, with modifications concentrated mostly around the insertion point. Despite variations in the CDR3 length, amino acid composition and shape, the retrogenic TCRs were capable of directing T cell development and creating a functionally competent T cell repertoire. In addition, an unexpected phenomenon that led to the formation of a chimeric TCR chain comprising a V α fused to a C β domain provided a new platform of understanding the mechanisms underlying MHC restriction.

6.1. Implications of this study

6.1.1. Viability of the *in vivo* mutagenesis approach

The generation of double-stranded DNA breaks can be both detrimental and beneficial to organisms. Those stimulated by exogenous DNA-damaging agents or endogenously-produced reactive oxygen species can result in disruption to the genome and lead to tumorigenesis or apoptosis (Hoeijmakers, 2001). Conversely, DNA breaks are beneficial when regulated properly in the context of specialised events such as V(D)J recombination, which necessitates genome rearrangement in order to produce functional antigen receptors (Wyman & Kanaar, 2006). In B cells, additional DNA strand breaks are induced to further diversify the Ig variable region genes by somatic hypermutation. This process essentially introduces point mutations and generates mutant clones that have a wide range of affinities for the immunising antigen (De Silva & Klein, 2015).

Analogous to somatic hypermutation in B cells, we designed a novel approach to diversify and ameliorate TCR binding affinity using V(D)J recombination machinery. The mutagenesis approach used in this study utilises essentially the same principle applied previously by our group: a recombination cassette comprised of two dissimilar-sized RSSs separated by a genomic linker (Holland et al., 2012). In this study, we shortened the size of the linker from 500bp to 400bp with the intention of optimising the efficiency of HSC transduction. Having used this approach for remodelling the germline CDR1 and CDR2 loops, we decided to test the effect of the recombination cassette in the peptide-binding CDR3 β loop. In Chapters 3 and 4, we demonstrated the successful restoration of the T cell repertoire in T cell-deficient mice through analyses of the peripheral blood and lymphoid organs. The sampling of peripheral blood at three week intervals after the T cell reconstitution period showed steady increases in the frequency of EGFP⁺TCR β ⁺ cells in the retrogenic mice. Moreover, in MataHari TCR (CDR3 β

diversifying) retrogenic mice, we injected male spleen cells to mimic a vaccination event to examine the functional capability of the retrogenic T cells. The results revealed a sharp increase and gross 'immunodominance' of a specific TCR (ASSG**E**VF) in the MataHari TCR (CDR3 β diversifying) T cells. Sequence analysis of the TCR repertoire indicated that the WT and inferior TCR variants were possibly outcompeted by the 'optimised' affinity competitors over time. Despite limited investigation into the T cell function, these observations underpin the ability of the retrogenic T cells to undergo homeostatic proliferation, survival and antigen-specific expansion.

Indeed, these observations broadly demonstrate the structural integrity of the TCR-CD3 signalling complex following modifications to the CDR3 β loop. Regardless of possible conformational changes to the TCR, as observed with the reduced anti-V β 8.3 relative to anti-TCR β Ab staining in MataHari TCR (CDR3 β diversifying) retrogenic mice, we can presume TCR-MHC and/or TCR-peptide interaction points may be modified. The mutations directed to the TCR CDR3 β loop are not expected to alter the germline CDR loop conformation as the framework regions of the V domain that provide a protein scaffold for these loops are maintained. Further, CDR3 β diversification is unlikely to affect pairing of the TCR β with a TCR α partner, exogenous or endogenous, since inter-chain interface is mostly concentrated at the constant domain of each chain (Richman et al., 2009). With regards to TCR association with the CD3 subunits, the very similar levels of CD3 and TCR β expression levels indicate that the retrogenic T cells exhibit a functional T cell signalling complex. Hence, we can presume the critical extracellular and TM contacts were also conserved. This includes the extracellular interface in which TCR C α D-E and C β C-C' loops interact with CD3 $\delta\epsilon$ and CD3 $\gamma\epsilon$, respectively, allowing the stabilisation of the TCR-CD3 organisation (Kuhns & Davis, 2007). Assembly at the TM level is mediated by interactions between the TCR α with CD3 $\delta\epsilon$ and CD3 $\zeta\zeta$, and TCR β with CD3 $\gamma\epsilon$ (Wucherpfennig et al., 2010; Call & Wucherpfennig, 2005; Call et al., 2002). Moreover, the physical association between the TCR C β F-G loop with CD3 $\gamma\epsilon$ is proposed to regulate $\alpha\beta$ T cell development through the control of negative selection in DP cells (Touma et al., 2006). CDR3 β mutagenesis also did not appear to affect the conformational change in the A-B loop within the TCR C α domain which is triggered upon pMHC ligation to initiate T cell signalling (Beddoe et al., 2009).

Interestingly, T cell development in retrogenic mice was not characteristic of a normal T cell setting. Most of the retrogenic mice displayed reduced thymic cellularity and accumulated DN cells, which is suggestive of impaired DN to DP transition. We mentioned earlier that the early expression of the exogenous TCR α chain, to which the diversified TCR β chain has a higher affinity compared to pT α chain, may have contributed to this observation (Trop et al., 2000). The presence of the exogenous TCR α outcompetes pT α for pairing with TCR β , thereby impairing normal formation and function of the pre-TCR and produces a block in proliferation and differentiation (Borowski et al., 2003; Lacorazza et

al., 2001). The analysis of the TCR β expression MFI (Figure 4.5) in the peripheral lymphocytes indicated a lower cell surface expression of the retrogenic TCR compared to WT, which reflects an $\alpha\beta$ TCR signalling apparatus that is capable of ligand-independent signalling with a lower activation threshold (Erman, Guinter & Singer, 2004). However, this may also result in a signalling complex that is less efficient for development into the DP stage. Alternatively, the limited reserve of HSCs that can give rise to $\alpha\beta$ T cells may have depleted at the time of culling, resulting in the return to the TCR- $\beta/\delta^{-/-}$ deficient mice phenotype (Mombaerts et al., 1992). Another possibility is that the retrogenic TCR β chain only has one attempt at gene rearrangement and may be less efficient than the two WT *TCR β* loci, thus fewer DN thymocytes can progress past β -selection. Most important, we conclude that the recombination cassette-based mutagenesis did not contribute to the atypical T cell development pattern.

6.1.2. Diversification profile using *in vivo* recombination cassette and its consequences

Sequence analysis performed in Chapter 4 provided valuable insight into the extent of *in vivo* diversification induced by the recombination cassette. The sizeable number of TCR variants generated for each TCR emphasise the requirement of diversity in the CDR3 loop in order to maximise peptide recognition (Freeman et al., 2009; Bercovici et al., 2000). According to the Shannon entropy index, the degree of diversity generated for both TCRs before stimulation by male HY antigens was found to be approximately similar (~15-20%). In MataHari TCR (CDR3 β diversifying) retrogenic mice, this diversity reduced in both T cell subsets mainly through bias to the 'ASSG**E**VF' CDR3 loop. This signifies 'immunodominance' of this TCR which may mediate more optimal binding and signalling in response to antigenic stimulation than the WT and other variants. From this limited information, we may infer that an 'optimised' affinity requires a shorter loop than the WT, whilst introducing a glycine and an increased net charge of (-1) to the peptide-binding region. The most commonly used flexible linkers have sequences comprising primarily of glycine and serine residues ('GS' linker); small or polar amino acids which provide good flexibility and solubility (Chen, Zaro & Shen, 2012). Glycine has low preference to form an α -helix, and its lack of a sidechain maximises rotational freedom of the polypeptide backbone so that adjacent domains are free to move relative to one another (Pace & Scholtz, 1998). Furthermore, comparative sequence analysis of the TCR chain showed that amino acid usage in the guanine-rich CDR3 β region is non-random with a preference for glycines (Moss & Bell, 1996). We can only speculate at this point that the 'immunodominant' mutation in the MataHari TCR confers an intrinsic glycine bias to the CDR3 β that either prevents steric hindrance or provides polypeptide flexibility to facilitate improved contact points with the MHC-bound peptide.

The analysis of the diversified Marilyn and MataHari TCR repertoires also revealed a restricted length distribution of the CDR3 β loops. Both TCR repertoires appeared to exhibit CDR3 β lengths to within two amino acids of the original WT CDR3 α and CDR3 β combined size. Relative to Ig heavy and light chains, and TCR γ and δ chains, the CDR3 loop size distributions of TCR α and β chains are narrow and closely matched, which suggests that pairing of CDR3 loops with similar size may be preferred to generate functional repertoire of $\alpha\beta$ TCR (Hughes et al., 2003; Rock et al., 1994; Pannetier et al., 1993). Structural studies of TCR-pMHC-I crystals have also shown that the restricted sizes of the CDR3 loops are influenced by the minor length variations of the processed peptide bound to the MHC-I cleft. The CDR3 loops of the TCR α and β chains are in close contact with each other such that the CDR3 α loop primarily binds to residues 4 and 5 of the peptide, whereas the CDR3 β binds to residues 5-8 (Johnson & Wu, 1999; Garcia et al., 1996a). Thus, we can assume that these loops have direct impact on each other, particularly with regards to size and shape, and are under selective pressure to maintain fairly narrow combined length distributions in order to facilitate efficient contact with the pMHC ligands. Previous work from our group have also described the influence of the partner CDR3 α loop in the C6 TCR. The unusually long C6 TCR CDR3 β was shown to pair efficiently only with its cognate TCR α chain whilst pairing poorly with other endogenous TCR α chains (Bartok et al., 2010). We propose that the novel recombination cassette approach has limited bearing on the CDR3 β loop size due to the structural constraints conferred by either the partner TCR α chain and/or the MHC-bound peptide.

One of the more surprising findings throughout the whole study was the apparent bias to MHC Class II and the CD4⁺ T cell lineage. This observation is particularly unexpected in the MataHari TCR (CDR3 β diversifying) retrogenic mice. MataHari transgenic mice typically express only CD8⁺ cytotoxic T cells, but the retrogenic mice exhibited not only a presence but a strong preference for CD4⁺ T cells (Holst et al., 2006; Valujskikh et al., 2002). As expected, analysis of the CDR1 and CDR2 loops showed that the recombination cassette did not affect the sequences outside the CDR3 β loop. Assuming efficient pairing between the exogenous TCR α and diversified TCR β chains, we might expect the diversified T cell repertoire to be selected predominantly with MHC Class I. Mutation of the CDR3 β should not diverge binding to the alternative MHC class since MHC contacts are primarily mediated by the CDR1 and CDR2 loops. However, even though some studies have reported inherent preference of TCR V genes for specific MHC class (Sim et al., 1996; DerSimonian, Band & Brenner, 1991; Jameson, Kaye & Gascoigne, 1990), all V-segments can give rise to MHC-I or MHC-II-restricted receptors (Stadinski et al., 2011; Jorgensen et al., 1992; Garman et al., 1986). Thus, it should not be perplexing that the diversified MataHari TCR is able to mediate selection on class II whilst maintaining the WT CDR1 and CDR2 loops. Likewise, this explains the presence of retrogenic CD8⁺ T cells expressing the diversified Marilyn TCR, which is characteristically restricted on MHC Class II in Marilyn transgenic mice

(Grandjean et al., 2003). Altogether, these observations challenge the notion that germline residues within the V-segments determine an intrinsic MHC class preference.

From the analysis of the thymi in Marilyn TCR (CDR3 β diversifying) retrogenic mice, we observed a higher frequency of SPCD4 relative to SPCD8 thymocytes suggesting a more efficient positive selection process with pMHC-II, which translates to more CD4⁺ than CD8⁺ T cells in the periphery. Conversely, although the SPCD4:SPCD8 ratio was found to be ~1:1 in the MataHari TCR (CDR3 β diversifying) retrogenic thymi, a higher frequency of peripheral CD4⁺ T cells was detected. Instead of a more efficient selection on pMHC-II, we propose a higher death rate of CD8⁺ T cells may be the causative factor for the predominance of CD4⁺ lymphocytes in MataHari TCR (CDR3 β diversifying) retrogenic mice. Asymmetric cell death between SPCD8 and SPCD4 thymocytes due to different signalling requirements was described to be the key determinant of a higher naïve CD4:CD8 ratio in the periphery (Sinclair et al., 2013). Naïve CD8⁺ T cells are more dependent on IL-15 survival signals than CD4⁺ T cells and die more rapidly in the absence of either IL-7 or TCR-dependent survival signals (Seddon & Zamoyska, 2002). It is possible the reduced TCR cell surface expression, shown by the lower TCR β MFI in retrogenic mice, may enhance this susceptibility to cell death. This MHC Class II skew was similarly observed in retrogenic T cells following mutation of the germline CDR loops using glycine-linkers and the recombination cassette approach which suggest that the bias was independent of the mutagenesis system (Holland et al., 2012). Since each TCR can be expressed in either CD4⁺ or CD8⁺ T cell subsets, the clear benefit is the extended ability to elicit both cytotoxic and Th immune responses within the same host upon engagement with the appropriate pMHC ligand. This is particularly useful for MataHari CD8⁺ T cells, which were reported to be less effective against tumours *in vivo* compared to Marilyn CD4⁺ T cells (Perez-Diez et al., 2007). The class switching was demonstrated to not diminish the T cell activation and function in MataHari TCR (CDR3 β diversifying) retrogenic mice, as evidenced by the 'immunodominance' of the 'optimised' TCR in both T cell subsets.

6.1.3. Limitations and improvements to the *in vivo* mutagenesis approach

At the end of Chapter 2, we discussed the advantages and limitations encountered during the generation of the retrogenic mice. In particular, the retrogenic mutagenesis approach is marked by the high consumption of mice which is directly related to the variable transduction and transfection rates. It is clear that this novel approach requires optimisation in order to be more economical and efficient. Since its inception, modifications to the original protocol have been applied to improve the overall experimental procedures (Holst et al., 2006). Recent improvements have been focused on maximising the efficiency of the HSC transduction and T cell reconstitution (Bettini et al., 2013). As

recommended by the original authors, the present study implemented spin transduction of HSC-enriched cultures with the viral supernatant which replaces the previous method of co-culturing with the viral producer cell line. This change was proposed to increase consistency of HSC transduction and reconstitution, as well as reduce the ratio of donor to recipients.

Comparison of the transfection efficiencies between the empty pMigR1 vector and those containing the TCR (CDR3 β diversifying) sequences revealed a slight drop in EGFP reporter expression (Figure 2.5). Although these differences were not significant, it appears that the insertion of the diversifying TCR constructs may directly reduce efficiency of the transduction, and downstream transfection rates. Hence, it is important to optimise the size of the recombination cassette to improve the efficiency of these processes. The present study has already established that shortening the genomic linker by 100bp from the original design (Holland et al., 2012) maintains a functional recombination cassette that is capable of diversifying the target CDR. It is therefore theoretically possible to further reduce the size of the genomic linker and decrease the overall recombination cassette. A new linker size must be short to facilitate a more efficient genomic integration, but long enough to allow bending of the DNA strand and juxtaposition of the RSS and coding ends in the RAG complex for gene rearrangement.

In terms of correcting the atypical thymic selection due to early TCR α expression, Baldwin and colleagues (2005) have designed a new model in which TCR α would be delayed until the DP stage as is the case in WT and transgenic mice. This technique utilises a Cre/lox-based conditional strategy to express the TCR α chain specifically at the DP stage and allow the exogenous TCR β chain to pair efficiently with the pT α to form a functional pre-TCR. The pre-TCR could then signal efficient passage past the β -selection checkpoint and progression to DP compartment, during which the TCR β will pair accordingly with the TCR α partner chains. Indeed, appropriate timing of TCR α expression should amend defects in the thymocyte development observed in the present retrogenic mice.

Other than improvements to the TCR (CDR3 β diversifying) construct design, to fully maximise the potential diversified TCR repertoire, further studies must ensure adoptive transfer of the appropriate BM cells. As the BM cells generally contain APCs/DCs in addition to HSCs, an improvement to the current study should either separate these cells from the donor HSCs or utilise only female donor BM cells. Thymic DC presentation of self-antigens play an important role in negative selection of CD4 $^+$ thymocytes (Oh & Shin, 2015). When MHC-II expression was specifically ablated in BM-derived APCs in mice, SPCD4 thymocytes accumulated in the thymus (Hinterberger et al., 2010; Liston et al., 2008; van Meerwijk et al., 1997). Also, when MHC-II I-E molecule was specifically expressed on DCs in transgenic mice, the I-E-reactive CD4 $^+$ T cells were negatively selected (Brocker, 1999). The presence of male BM-derived APCs presenting HY antigens in the transduced BM graft may have contributed to

the absence of the WT Marilyn sequence in the diversified TCR repertoire. The role of DCs in CD8⁺ T cell deletion is less clear; specific removal of MHC-I expression in BM-derived APCs slightly increased levels of SPCD8 thymocytes, but DC depletion had no effect on CD8⁺ T cell frequency (Ohnmacht et al., 2009; van Meerwijk et al., 1997). Importantly, DCs that may present the specific target antigen must be removed before adoptive transfer into the retrogenic host to prevent deletion of potentially 'optimised' TCRs.

6.1.4. Future perspectives

The present study describes the ability of the recombination cassette to induce *in vivo* modification to the target CDR3 β and generate a variant TCR library with an extensive range of affinities. It would therefore be interesting to further investigate the functional capacity of the diversified TCRs *in vivo*. Future work can aim to evaluate the potential anti-tumour activity of retrogenic T cells expressing the diversified/'optimised' TCRs. The H2^b murine MB49 bladder carcinoma represents a model tumour to assess the diversified Marilyn and MataHari TCRs (Summerhayes & Franks, 1979). MB49 cells express both MataHari-specific Uty peptide complexed with H2-D^b and Marilyn-specific Dby complexed with H2-A^b. Both antigens can be presented directly by target cells, or indirectly by host cells (Grandjean et al., 2003; Valujskikh et al., 2002; Braun et al., 2001). Like most tumour cells, MB49 does not express H2-A^b under normal circumstances *in vitro*, but can upregulate the Class II molecule *in vivo* or when cultured with IFN- γ (Perez-Diez et al., 2007). Currently, the CD4⁺ Th cells expressing Marilyn TCRs partnered with NK cells have been shown to serve as efficient anti-tumour effectors against MB49 *in vivo*. CD8⁺ T cells expressing MataHari TCR demonstrate potent anti-tumour activity *in vitro*, but does not translate equally effective *in vivo* without the addition of other aids. We can therefore further strengthen the use of our novel mutagenesis approach by examining whether an 'optimised' MataHari TCR can mediate an improved ability to clear MB49 *in vivo*.

The next stage of the study can also aim to diversify the partner CDR3 α loop or a combination of both CDR3 α and CDR3 β regions using the *in vivo* recombination cassette approach. The TCR CDR3 β mediates the majority of binding with the MHC-bound peptide relative to the CDR3 α loop (Rudolph, Stanfield & Wilson, 2006; Stewart-Jones et al., 2003; Garcia et al., 1996a). Comparing the functional improvements between diversifying either the CDR3 α or CDR3 β , or both, would help elucidate the best way of maximising the TCR immunotherapeutic potential. Further, we have also performed pilot experiments involving the generation of retrogenic mice which develop both Marilyn and MataHari TCR (CDR3 β diversifying) sequences simultaneously through co-injection of HSCs expressing Marilyn and MataHari diversifying TCR vectors. The aim of this study was to assess whether both diversifying

TCRs would outcompete each other or co-operate leading to enhanced immunity following the CDR3 β modifications. The preliminary results have shown similar levels of V β 6⁺ and V β 8.3⁺ T cells. However, due to the unpredictable nature of the Marilyn TCR diversification (i.e. homologous ribosomal skip mechanism generating the chimeric TCR chain), we could not continue and fully interpret the efficacy of this study. Notably, further studies regarding Marilyn TCR diversification should utilise a new sequence that avoids a stretch of nucleotide homology in the J-segments.

Expansion of the current study should also address the structural and molecular basis that govern the 'optimised' TCR binding affinity. Analysis of co-crystal structures of the TCRs bound to cognate pMHC would reveal differences in the recognition patterns between the WT TCR and the diversified TCR. We would be able to determine the optimal CDR3 β -peptide contact points that mediate an enhanced immune response (Cole et al., 2014; Huang & Nau, 2003). Moreover, in the context of pMHC-I recognition, it would be of interest to see what type of conformation the processed peptide adopts as a result of an 'optimised' CDR3 β loop; whether it forms a 'bulge' or gets flattened into the peptide-binding groove to allow the TCR to contact the MHC better (Cole et al., 2014; Tynan et al., 2005b; Tynan et al., 2005a). If MHC contacts are mediated exclusively by the germline CDR1 and CDR2 loops, it is unlikely that the TCR-pMHC docking orientation would vary significantly. Sequence analysis of the diversified TCR sequences have already shown that the germline loops remain intact. However, with the MHC class switching, we would expect a possible difference in the TCR docking modes.

6.1.5. A new understanding of the mechanism underpinning MHC restriction

In Chapters 3 and 4, we reported the occurrence of the V β 6⁻ T cells in 3 out of 7 FVB/N and 3 of 4 C57BL/6 mice produced during the diversification of the Marilyn TCR CDR3 β . We deduce that the codon optimisation applied during the *de novo* synthesis of the Marilyn TCR (CDR3 β diversifying) sequence may have contributed to these observations. The stretch of at least 18 identical nucleotides within the J-segments of the WT Marilyn TCR α and β chains is thought to facilitate a possible homologous recombination-deletion process which resulted in the formation of the chimeric TCR chain comprising of a V α connected to a C β domain (Im et al., 2014; Zhang & Sapp, 1999). Importantly, the skip mechanism and resultant hybrid TCR chain did not show any significant effects on the development and maintenance of a functional ' $\alpha\beta$ T cell' repertoire. Through PCR analysis of the V β 6⁻ retrogenic T cells, we found that the V α and C β domains remained intact, and the fusion was focused at an amino acid substitution for aspartic acid in resulting J α -J β segment. According to the IMG T database, this particular amino acid can be found in the same position within the FR4 region of other

J-segments (Lefranc, 2005). Hence, we believe this substitution to have minimal, if any, difference in the folding of the essential β -sheets that make up the connected $V\alpha$ and $C\beta$ structures.

Based on the dominance of this TCR chain when it occurs in the retrogenic mice (i.e. almost all T cells were $V\beta 6^-$), the TCR may have enhanced MHC recognition or signalling properties. This suggests a potential selection advantage of this TCR chain or that it is able to outcompete the other diversified Marilyn TCRs. The novel TCR configuration has major differences from the regular $\alpha\beta$ TCR configuration. First, the antigen-binding site is a $V\alpha$ - $V\alpha$ dimer without any $V\beta$ CDR structure. Second, the inter-domain interfaces are modified, whereby the natural $V\beta$ - $C\beta$ interface is replaced with a distinct $V\alpha$ - $C\beta$ interface. Similarly, the natural $V\alpha$ - $V\beta$ antigen-binding surface is replaced by a $V\alpha$ - $V\alpha$ interface. As shown by the three-dimensional model of the fusion TCR chain, there may subtle differences between the conformation and position assumed by the $V\alpha$ domain in place of the WT $V\beta$ domain (Figure 5.4). As the novel $V\alpha$ - $C\beta$ TCR chain is produced following a non-V(D)J recombination event, we do not know the stage(s) of T cell development when this event occurs. Indeed it could take place prior to the 'window' of V(D)J recombination within the DN thymocyte compartment and so remove the recombination cassette. It is likely the $V\alpha$ - $C\beta$ chain will associate with the pre-TCR through the conventional $C\beta$ -pT α interface (Pang et al., 2010). Retrogenic mice produced directly with the novel $V\alpha$ - $C\beta$ TCR chain developed peripheral T cell repertoires (Refer to *Chapter 5.2.4*). We can therefore presume a novel configuration of the pre-TCR comprised of the $V\alpha$ - $C\beta$ fusion/pT α chain is expressed and is able to substitute for the WT pre-TCR in progressing through the β -selection checkpoint. Following gene rearrangement of the endogenous $V\alpha$ - $J\alpha$ genes at the DP stage, the fusion TCR chain is able to pair efficiently with TCR α . The fusion chain retains an intact $C\beta$ domain, which provides a protein scaffold for the $V\alpha$ domain and CDR loops, and allows inter-chain disulphide interactions with the endogenous TCR $C\alpha$ domain (Richman et al., 2009). Despite alterations to the antigen-binding surface, the hybrid TCR-endogenous TCR α 'heterodimer' can recognise self-pMHC and direct progression past thymic positive and negative selection. Further, higher affinity engagement with pMHC-II on mTECs and thymic DCs can also induce FoxP3 expression and stimulate differentiation into nTregs (Hanabuchi et al., 2010; Proietto et al., 2008; Aschenbrenner et al., 2007). As a result, we identified a typical T cell repertoire in the peripheral lymphoid organs, with a higher frequency of $CD4^+$ than $CD8^+$ T cells, and a sizeable population of regulatory T cells. This data also indicates that the novel TCR dimer engages productively with pMHC-I and pMHC-II, which further challenges the notion that germline TCR V-segments and CDR loops have intrinsic preference to bind to specific MHC classes (Sim et al., 1996; DerSimonian, Band & Brenner, 1991; Jameson, Kaye & Gascoigne, 1990).

Importantly, the novel TCR dimer is capable of associating efficiently with the CD3 signalling apparatus, as indicated by the similar levels of CD3 and TCR β expression levels in the splenic T cells. Similar to the T cell signalling complex in Marilyn and MataHari diversified TCRs, it is reasonable to assume that the extracellular and TM structures within the C β domain are conserved to facilitate the crucial interactions with the CD3 subunits. In particular, the TCR C β F-G loop which mediates association with CD3 $\gamma\epsilon$ and regulates $\alpha\beta$ T cell development may be advantaged to explain the dominance of the V β 6⁻ T cell population (Wucherpfennig et al., 2010; Touma et al., 2006; Call & Wucherpfennig, 2005; Call et al., 2002).

With a new V α -V α antigen-binding interface, we may expect the novel TCR dimer to exhibit a different docking orientation and affinity compared to the WT Marilyn TCR. Generally, the TCR β interacts with the α 1 helix of the MHC and the C-terminus of the peptide, whereas the TCR α binds primarily to the α 2 or β 1 MHC helices and the peptide N-terminus (Rudolph, Stanfield & Wilson, 2006; Garboczi et al., 1996). Further structural studies would provide valuable insight into the new docking mode applied by the V α -V α interface, whether the hybrid TCR chain assumes the place of a conventional TCR β chain. It is possible that a lack of CDR β loops may necessitate the aid of compensatory mechanism for ligand engagement or that the novel TCR CDR must undergo numerous and possibly large conformational changes upon pMHC binding (Burrows et al., 2010; Armstrong, Piepenbrink & Baker, 2008). However, the challenge of producing TCR-pMHC co-crystals here is that the specific antigen of this hybrid TCR is not yet clear. Since it only retains the Marilyn V α 1.1 segment, and binds to a wide array of endogenous TCR α chains, logic dictates that the TCR would not be restricted to the Marilyn-specific Dby complexed with H2-A^b. Conversely, minimal conservation of key germline contacts has been shown to retain pMHC specificity in TCRs where the rest of the sequence remain unchanged (Scott-Browne et al., 2011). Functional studies must then be performed to investigate and identify the immunogenic ligands, including antigenic challenge with model antigens such as hen egg lysozyme (HEL) or ovalbumin (OVA; Kumar, Cristan & Paul, 2008). Preliminary proliferation assays (not shown) where retrogenic T cells expressing the chimeric TCR chain are cultured with syngeneic (C57BL/6) and allogeneic (FVB/N) spleen cells have demonstrated that the TCR retains pMHC specificity and can respond to foreign pMHC.

Overall, the study presented in Chapter 5 demonstrated the dispensability of the germline-encoded TCR CDR β as well as the entire V β domain in mediating MHC-directed events such as T cell selection, signalling, development of nTregs and homeostatic proliferation. Such observations are not in line with the model which proposes germline CDRs have co-evolved with MHC over time and play key roles in contacting MHC chains and impose MHC restriction on $\alpha\beta$ TCR recognition (Garcia et al., 2012; Marrack et al., 2008). The tremendous plasticity of the TCR despite substitution of a V β with a V α

domain without significantly affecting the ability to recognise MHC supports the idea that extrinsic factors enforce MHC restriction on the $\alpha\beta$ TCR during thymic selection (Tikhonova et al., 2012; Van Laethem, Tikhonova & Singer, 2012; Van Laethem et al., 2007). The TCR appears to employ an opportunistic antigen-binding interface, rather than being hardwired to engage MHC ligands (Holland et al., 2012; Attaf et al., unpublished).

6.2. Concluding remarks

Researchers designing immunotherapy have long focused on enhancing the TCR binding affinity. The work presented in this Thesis demonstrates a novel *in vivo* mutagenesis approach that aims to generate TCR variants with an array of binding affinities before screening for an 'optimised' TCR with enhanced immunological function. This technique involves insertion of a recombination cassette into the target CDR in order to induce diversification using *in vivo* V(D)J recombination machinery. $\alpha\beta$ T cells expressing these diversified TCRs are subject to positive and negative selection during thymocyte development which purges the pre-selection repertoire of autoreactive T cells, whilst ensuring that these cells are self-MHC restricted before entering the periphery. Collectively, our lab has tested the recombination cassette approach on all three CDR loops of the TCR β chain, and successfully generated a functional T cell repertoire. Despite changes to the amino acid composition, length and shape of the CDR loops, the diversified TCR maintains the ability to recognise pMHC ligands and direct T cell development, activation and cellular responses. These studies highlight the adaptable nature of the TCR structure and underpins the flexibility of the ligand recognition portion. In summary, the recombination cassette provides an effective and unbiased alternative to maximising the TCR immunotherapeutic potential.

Chapter 7

Materials and Methods

Chapter 7: Materials and Methods

7.1. TCR Nomenclature

Both Marilyn and MataHari $\alpha\beta$ TCRs recognise epitopes of the male-specific HY minor histocompatibility antigen. Marilyn TCR recognise the NAGFNSNKANSSRSS peptide from the *Dby* gene, presented by MHC Class II H2-A^b, whereas MataHari TCR are specific for the HY peptide WMHHNMDLI derived from the *Uty* gene complexed with MHC Class I H2-D^b. The nomenclature system used to label the V and J regions of these TCRs is based on the work by Arden et al. (1995) and proposed by the International Union of Immunological Societies (WHO-IUIS TCR; Radauer et al., 2014). The same system is adopted by the companies supplying the antibodies. According to this nomenclature, Marilyn TCR expresses V α 1.1-J α 35 and V β 6-J β 2.3 whereas MataHari TCR uses V α 15-J α 16 and V β 8.3-J β 1.1. The ImMunoGeneTics (IMGT) database (www.imgt.org/IMGTrepertoire) was used as reference during sequence analysis to identify the CDR loops and C domains of each TCR α and β chain. The CDR3 β region of the Marilyn and MataHari TCRs is defined by the amino acid sequence supported by two highly conserved framework branches: between the second conserved cysteine in FR3 and the conserved phenylalanine (F-G-X-G) in FR4 of the V domain (Lefranc, 2005).

7.2. Design of the $\alpha\beta$ TCR (CDR3 β diversifying) Sequences

7.2.1. Recombination cassette design and synthesis

The Marilyn and MataHari $\alpha\beta$ TCR sequences, including the 2A peptide sequence, were kindly provided by Dr. Kate Vignali (St. Jude, Memphis, USA). To generate diversity in the Marilyn and MataHari TCRs, a recombination cassette was inserted into the centre of the target CDR3 β regions. The recombination cassette used in the present study is composed of an RSS from murine V β 8.2 (heptamer-23bp-nonamer) at the 5' end and an RSS from murine D β 1 (nonamer-12bp-heptamer) at the 3' end, separated by a 400bp genomic linker (modified from (Holland et al., 2012)). The complete Marilyn and MataHari $\alpha\beta$ TCR (CDR3 β diversifying) constructs were synthesised *de novo* into a pUC57 vector containing the kanamycin resistance gene (GENEWIZ, USA). The *Bgl*III and *Eco*RI restriction sites were tagged at the 5' and 3' ends respectively to facilitate cloning into the pMigR1 vector.

7.2.2. Plasmid vector

The Marilyn and MataHari $\alpha\beta$ TCR (CDR3 β diversifying) constructs were sub-cloned into the 6056-bp retroviral vector, pMigR1. pMigR1 is a murine stem cell virus (MSCV)-based vector containing a multiple cloning site (MCS), and IRES-EGFP (internal ribosomal entry site-enhanced green fluorescent protein) marker cassette and ampicillin resistance gene (Figure 7.1). The plasmid vector was kindly provided by Dr. Istvan Bartok. The pCR™2.1 cloning vector was used for amplification and sequencing of PCR products (Thermo Scientific, UK). pCR™2.1 contains complementary 3' deoxythymidine (T) overhangs that enable efficient ligation with the PCR products and primer sites flanking the ligation site to facilitate sequencing of the inserts.

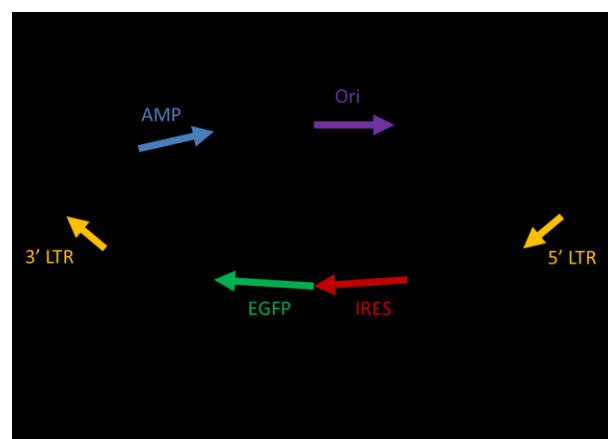


Figure 7.1. Plasmid vector pMigR1. The plasmid map illustrates the positions of the origin (Ori), the 5' and 3' long terminal repeats (LTR), internal ribosome entry site (IRES), and the enhanced green fluorescent protein (EGFP) and ampicillin resistance (AMP) genes. The multiple cloning sites (MCS) contain the *Bgl*II, *Xho*I, *Hpa*I and *Eco*RI restriction sites.

7.3. Mice

C57BL/6 and FVB/N TCR- $\beta/\delta^{-/-}$ deficient mice, male and female, were used as donors of BM cells to generate retrogenic mice. Only female TCR- $\beta/\delta^{-/-}$ deficient mice were used as lymphopenic recipients. TCR- $\beta/\delta^{-/-}$ deficient mice contain a deletion from the D β 1.3 segment to the C β 2 gene segment, and thus lack the ability to generate any TCR β chain due to the loss of both constant domains (Mombaerts et al., 1992). WT C57BL/6 (H2^b) and FVB/N (H2^q) mice were obtained from Harlan (Blackthorn, UK). Marilyn transgenic C57BL/6 mice were kind gifts from Prof. Marina Botto. These mice were used as controls during various parts of this study.

All mice were maintained under specific pathogen-free conditions at the Central Biological Services Unit in Hammersmith Hospital Campus, Imperial College London. All procedures involving mice were

carried out in accordance with Home Office guidelines as stated in the project licence and Animals (Scientific Procedures) Act 1986.

7.4. Cell counting

Cells were mixed 1:1 with trypan blue solution (Invitrogen, UK). The mixture was loaded into a haemocytometer (Neubauer 0.0025mm², Germany) and the number of cells in four grids was counted to obtain an average. The total number of cells in each sample was calculated by:

Total number of cells = Average number of cells counted x Dilution factor x 10⁴ x Volume of media

7.5. Media and Reagents

Table 7.1. List of reagents and buffers.

Medium	Use	Composition
Ampicillin	Antibiotics for growth of bacteria in LB media	Stock solution of 50mg/ml (500mg Ampicillin powder (Sigma) dissolved in 10ml ddH ₂ O; diluted 1:1000 in LB media
Blood buffer	Collection of blood	1x PBS, 100U/ml Heparin, 2mM EDTA (Ethylenediaminetetraacetic acid)
Collection buffer	Collection of cells after sorting	1x PBS, 10% FCS, filtered through 0.45µm filter
Complete RPMI medium (R10)	Maintenance of non-adherent mouse/tumour cell lines	RPMI (Roswell Park Memorial Institute) 1640 supplemented with 10% foetal calf serum (FCS; GIBCO, UK), 20mM HEPES (N-2-hydroxyethylpiperazine-N-2-ethane sulfonic acid), 100U/ml penicillin, 10µg/ml Streptomycin, 2mM L-glutamine and 2 x10 ⁻⁵ M β2-mercaptoethanol
Complete IMDM medium (D10)	Maintenance of adherent phoenix cell line	IMDM (Iscove's Modified Dulbecco's Medium) supplemented with 10% FCS and 2mM L-glutamine

FoxP3 Fixation/Permeabilisation working solution	Preparation of cells for intracellular staining	FoxP3 Fixation/Permeabilisation Concentrate (1 part), FoxP3 Fixation/Permeabilisation Diluent (3 parts); Purchased from eBioscience, UK
Freezing medium	Preservation of cells in liquid nitrogen	FCS containing 20% dimethylsulphoxide (DMSO). 1ml freezing medium + 1ml cell suspension
LB (Luria-Bertani) Broth/Agar	Medium for growth of bacteria	Supplied by MRC (unspecified)
Opti-MEM®	Cationic lipid transfection of plasmids into Phoenix cells	Purchased from GIBCO, UK
Permeabilisation buffer	Re-suspension of cells for intracellular staining	Dilution of the 10X Permeabilisation Buffer concentrate with distilled water
Phosphate buffered saline (PBS)	Re-suspension and washing of cells. Also for reagents for <i>in vivo</i> use	Reconstituted from tablets (Oxoid Ltd, Hampshire, UK); Supplied by MRC (unspecified)
RBC (Red blood cells) lysis buffer	Depletion of red blood cells before cell counting/FACS	Purchased from Qiagen, UK (unspecified)
Sort buffer	Re-suspension of cells before sorting	1x PBS (Ca/Mg ⁺⁺ free), 1mM EDTA, 25mM HEPES pH7.0, 1% FCS and 0.02% sodium azide
Tris-Acetate-EDTA (TAE) buffer	Agarose gel electrophoresis – gel and running buffer	Supplied by MRC (unspecified)

7.6. Molecular Biology

7.6.1. DNA digestion with restriction enzymes

The pMigR1 vector, and the Marilyn (2285bp) and MataHari (2273bp) $\alpha\beta$ TCR (CDR3 β diversifying) constructs in the pUC57 plasmid, were digested using the same set of *BglIII* and *EcoRI* restriction enzymes. For 5 μ g of DNA double digestion, a reaction mixture of 20 μ l containing 2 μ l 10X NEB buffer 3, 10 units of each enzyme and ddH₂O was incubated at 37°C for an hour (all from New England Biolabs, UK).

7.6.2. Agarose gel electrophoresis of DNA

Electrophoresis gels containing 1.2% (w/v) agarose (Sigma) dissolved in 1X TAE buffer were prepared for the separation of DNA fragments (300 - 7,000bp). For visualisation of DNA, the gels were stained

with SYBR® Safe at a 1:10,000 dilution (Life Technologies, UK). Samples were mixed with 5X loading buffer (1:5 dilution; Biorun, UK) before loading into gel. HyperLadder™ 1kb (Biorun, UK) was used as a molecular weight standard. The electrophoresis was performed in a 1X TAE running buffer at 90-120V. Gels were visualised under Safe Imager™ blue-light transilluminator (Invitrogen, UK) for gel extraction, or with G:BOX iChemi XR for documentation using the GeneSnap software (Syngene, UK).

The desired DNA bands from the agarose gels were excised carefully using a clean blade or scalpel. The QIAEX II Gel Extraction kit (Qiagen, UK) was used to purify DNA from the agarose gels as per manufacturer's instructions. The kit uses the principle of binding DNA to silica bead suspensions in the presence of chaotropic salts.

7.6.3. Determination of nucleic acid concentration

The concentrations of RNA and DNA were obtained using the NanoDrop 2000C Spectrophotometer (Thermo Scientific, UK). Nucleic acid purity was assessed by observing ratio of absorbance at wavelengths 260nm and 280nm. A 260/280 ratio of ~1.8 is generally accepted as 'pure' for DNA; a ratio of ~2.0 is generally accepted as "pure" for RNA. If the ratio is appreciably lower or higher in either case, it may indicate the presence of protein, phenol or other contaminants that absorb strongly at or near 280nm.

7.6.4. DNA ligation

Ligation reactions were performed using T4 DNA Ligase according to the manufacturer's protocol (New England BioLabs, UK). Digested inserts and vectors were mixed at a molar ratio of 3:1 for efficient ligation. Along with 1µl T4 DNA ligase and 2µl 10X ligation buffer, made up to 20 µl with ddH₂O, the vector and insert mixture was incubated overnight at 16°C. Ligation mixtures were heat inactivated at 65°C for 10 minutes before storage at -20°C.

7.6.5. Bacterial transformation

One Shot® TOP10 Chemically Competent *E.coli* (Life Technologies, UK) was used for bacterial transformation of pUC57 and pCR™2.1 vectors. Conversely, One Shot® Stbl3™ Chemically Competent *E.coli* (Life Technologies, UK) was used for pMigR1 vectors which contain multiple nucleotide repeats. Both transformation procedures were performed according to the kit instructions. To summarise,

chemically competent *E.coli* cells were first thawed on ice. 1 to 5µl of DNA was then gently mixed into each vial containing 50µl cells and incubated on ice for 30 minutes. The bacteria were heat shocked for 30-45 seconds at 42°C and immediately cooled on ice for 2 minutes. After addition of 250µl SOC media, bacteria were incubated at 37°C with shaking for 1 hour. Each transformation mixture was then spread on selective LB agar plates containing 50µg/ml ampicillin (Sigma, UK) and incubated overnight at 37°C. Plates were stored at 4°C.

7.6.6. Isolation of plasmid DNA

Following bacterial transformation, individual colonies from the selective LB agar plates were picked and grown overnight in selective LB broth containing 50µg/ml ampicillin (Sigma, UK) and incubated at 37°C overnight with shaking. For small scale extraction of plasmid DNA, colonies were grown in 2-3ml of selective LB media and isolated using either the QuickLyse Miniprep Kit or QIAprep® Spin Miniprep Kit (Qiagen, UK). For large scale extractions, 100ml of overnight culture were used and purified using EndoFree® Plasmid Maxi Kit (Qiagen, UK). Both isolation of plasmid DNA techniques were performed according to the manufacturer's protocol.

7.6.7. RNA extraction and cDNA synthesis

RNA was extracted from the sorted cells (*Section 7.8.5*) using the RNeasy Mini Kit (Qiagen, UK) according to the manufacturer's protocol. Briefly, 1×10^7 spleen cells were first lysed and homogenised using a 30-gauge needle and 1ml syringe (Becton Dickinson, UK) with lysis buffer, before precipitation with ethanol. The RNA from the sample was then collected and washed in a spin column, and later eluted in 50µl of RNase-free water. RNA concentration was measured using appropriate settings on the spectrophotometer.

Complementary DNA (cDNA) was synthesised from RNA using the iScript™ cDNA Synthesis Kit (Bio-Rad, UK) following the company's manual. cDNA was produced into a total volume of 20µl. Successful cDNA synthesis was confirmed by polymerase chain reaction (PCR; see next section) using specific primer pairs. cDNA was stored at -20°C.

7.6.8. Polymerase Chain Reaction

PCR was used to amplify cDNA using sequence-specific oligonucleotide primers for genotyping the retrogenic mice and determining the $\alpha\beta$ TCR (CDR3 β diversifying) sequences. Additionally, PCR was also performed to synthesise the Marilyn fusion sequence before cloning into the pCRTM2.1 vector. A standard PCR contained: 1 μ l of template DNA, 1 μ l of each forward and reverse primer at 10 μ M concentration, 5 μ l of 10X PCR buffer, 1.5 μ l of 50mM MgCl₂, 1 μ l of 10 μ M deoxyribonucleoside triphosphate (dNTP) mix, 0.5 μ l of BIOTAQTM DNA Polymerase, and made up to 50 μ l with ddH₂O. All reagents were from Bioline, UK. The PCR was performed using the 2720 Thermal Cycler (Applied Biosystems, Warrington, UK) under the following programme in Table 7.2. PCR samples were analysed by agarose gel electrophoresis (*Section 7.6.2*), and stored at -20°C.

Table 7.2. General PCR programme.

PCR Step	No. of cycles	Duration	Temperature
Initial denaturation	1 cycle	5 minutes	94°C
Denaturation	30-35 cycles	30 seconds	94°C
Annealing		30 seconds	62°C
Extension		30 seconds	72°C
Final extension	1 cycle	5 minutes	72°C
Cooling		Indefinite	4/20°C

7.6.9. Primer design and synthesis

The forward and reverse primers were designed based on guidelines from Life Technologies, UK. This included designing primers complementary to the target sequence that were 18-21 nucleotides long, with AT/GC content ratios at ~1:1 whilst avoiding single nucleotide repeats. In order to facilitate efficient PCR, forward and reverse primers for genotyping PCR were intentionally designed to facilitate matching annealing temperatures of 62°C. Sequencing primers were designed to have melting temperatures of 50°C to 55°C following guidelines from the MRC CSC Genomics Core Laboratory at Imperial College London, UK. Primers were stored at -20°C. The full list of PCR primers are listed in Table 7.3; the list of sequencing primer is shown in Table 7.4.

Table 7.3. List of PCR primers. *, ** and *** denote the same reverse primers for Marilyn and MataHari $\alpha\beta$ TCRs.

Target sequence	Primer name (F/R; Binding site)		Sequence (5'-3')	Annealing temperature (°C)
Marilyn $\alpha\beta$ TCR (CDR3 β diversifying)	F	1G 28C 676G 812C 939C	GGAGATCTACCACCATGAAGA CCGTGAGCCTGGTGGTGC GCGATGCCACCCTGACCG CAGCGGATCCGGCGCTAC CACGGCGACGGAGGCATC	62
	R	1926C* 2042C** 2135G*** 2266G	GTGGACACGCCGGAGTGC CTCCTCGGAGAGGCCGTG GCTGGCGGAGGTGATGCC CCGAATTCGCTCAGCTGTTT	
MataHari $\alpha\beta$ TCR (CDR3 β diversifying)	F	65G 676G 828G 941C	GGACTGGGAGTCCCACGG GCGACGTGCCCTGCGATG GGCAGCGGAGCCACCAAC CATGGAGGCCCGCCGTAC	62
	R	1914C* 2030C** 2123G***	GTGGACACGCCGGAGTGC CTCCTCGGAGAGGCCGTG GCTGGCGGAGGTGATGCC	

7.6.10. Preparation of DNA for sequencing

The TOPO® TA Cloning® Kit was used for cloning fresh PCR samples into the pCR™2.1-TOPO® vector according to the manufacturer's protocol. The cloning reaction was transformed into One Shot® TOP10 Chemically Competent *E.coli* (Life Technologies, UK) and 50-150 μ l of the transformation mix was plated onto selective LB agar plates containing 50 μ g/ml ampicillin before overnight incubation at 37°C. Randomly selected colonies were cultured and purified DNA were analysed for positive insertion of the desired PCR samples (Refer to Sections 7.6.6-7.6.8). This was done by digestion using *EcoRI* restriction enzyme and agarose gel electrophoresis (Section 7.6.2). 500-600ng of the positively identified DNA plasmids were mixed with 1 μ l of the appropriate sequencing primer (10 μ M concentration) and made up to 10 μ l with sterile ddH₂O prior to sequencing. The full list of sequencing primers are listed below (Table 7.4).

Table 7.4. List of sequencing primers used. * denotes the same reverse primers for Marilyn and MataHari $\alpha\beta$ TCRs.

Target sequence	Primer name (F/R; Binding site)		Sequence (5'-3')	Melting temperature (°C)
Marilyn $\alpha\beta$ TCR (CDR3 β diversifying)	F	287C 1819C	CTTCAGCCTGCACATC CAACAAGCAGAAGGCTAC	50 54
	R	1939C 1942C*	TAGTTGCTCTCCTTGTAG GAGTAGTTGCTCTCCTTG	54 52
MataHari $\alpha\beta$ TCR (CDR3 β diversifying)	F	927C	CTGTGCACCAAACACATG	54
	R	1930C*	GAGTAGTTGCTCTCCTTG	54
pCR™2.1-TOPO® Insert	F	M13 Forward Primer	GTAAAACGACGGCCAG	50
	R	M13 Reverse Primer	CAGGAAACAGCTATGAC	50

7.6.11. DNA Sequencing

Sequencing of the TCR DNA/PCR samples was performed by the MRC CSC Genomics Core Laboratory (Imperial College London, UK) using an Applied Biosystems 3730xl DNA Analyser (Applied Biosystems, Warrington, UK). Read-out and quality of sequences at nucleotide level were analysed using the Chromas Lite version 2.1.1 software (Technelysium Pty Ltd, Australia). The nucleotide sequences were translated into amino acid sequences using the ExPASy Translate tool (<http://web.expasy.org/tools/translate/>). Sequence alignments between two or more sequences were generated using the NCBI Basic Local Alignment Search Tool (BLAST; <http://blast.ncbi.nlm.nih.gov/Blast.cgi>).

7.7. Cell culture

7.7.1. Maintenance of Phoenix™ ecotropic retrovirus packaging cell line

The Phoenix™ ecotropic packaging cell line was kindly provided by Dr. Istvan Bartok. Frozen vials of cells were removed from liquid nitrogen and thawed rapidly at 37°C before washing with 50ml complete IMDM growth media (D10) and spinning at 1,500rpm for 5 minutes. The supernatant was removed and the cells were grown in a 75cm³ cell culture flask containing 15ml of fresh D10 media, in a 37°C incubator supplied with 5% CO₂. Phoenix™ cells were split at 1:4 or 1:5 at 70-80% confluence every 2-3 days to maintain growth and transfection efficiencies. Cells were split by rinsing with PBS, trypsinised for detachment from flask and quenched with D10 media prior to subculture in fresh media.

7.7.2. Lipofectamine®-based transfection of Phoenix™ cells

Prior to transfection, Phoenix™ cells were plated onto 6-well cell culture plates at 0.5×10^6 cells in 2ml fresh D10 media per well (37°C, 5% CO₂). After 24 hours, the cells in each well were transfected with 3µg of pMigR1 plasmid containing the desired TCR (CDR3β diversifying) constructs and 1µg of pCLE retroviral helper plasmid using the Lipofectamine® 3000 Reagent (Life Technologies, UK). Briefly, 10µl of Lipofectamine® 3000 Reagent was mixed with 250µl of Opti-MEM® media and incubated for 5 minutes at room temperature. This mixture was then added to the 250µl of the same media containing both plasmids and left to stand for 20 minutes at room temperature. The transfection mixture was finally added to each well and incubated overnight at 37°C with 5% CO₂.

The following day, the cells were washed and the media was replaced with 2ml fresh D10. 48 hours post-transfection, the viral supernatant (D10 media covering the transfected Phoenix™ cells) was collected from individual wells and used for stem cell transduction (*Section 7.7.3*). The transfected Phoenix™ cells were harvested to determine transfection efficiency based on GFP expression. In brief, the cells were removed from the plates using cell scrapers and washed twice with PBS and centrifuged at 1,500rpm for 5 minutes. Samples were re-suspended in 400µl of PBS and analysed immediately by flow cytometry (*Section 7.8*).

7.7.3. Transduction of murine haematopoietic stem cells (HSCs)

BM cells were obtained from mice that were about six to eight weeks old. 72 hours prior to harvesting, BM donor mice were administered intraperitoneally (i.p.) with 5'-Fluorouracil (5'-FU; InvivoGen, USA) using a sterile 27-gauge needle and 1ml syringe (Becton Dickinson, UK), at a concentration of 150mg/kg body weight. The femur and tibia were cut off the donor mice and surrounding skin and muscle tissues removed using scissors to obtain clean bones. Both ends of each bone were cut and a 10ml syringe containing ice-cold sterile PBS and 30-gauge needle were used to flush out the BM cells. The cells were then washed twice with ice-cold sterile PBS. Red blood cells were lysed for 10 minutes on ice using RBC lysis buffer (Qiagen, UK). Total cell number was determined after washing, and a single-cell suspension of 10^6 cells per ml in complete RPMI media (R10) supplemented with 20ng/ml recombinant mouse IL-3, 10ng/ml recombinant mouse IL-6, 50ng/ml recombinant mouse Stem Cell Factor (SCF) and 50ng/ml recombinant human Flt-3 Ligand (All from Life Technologies, UK). The cell suspension was distributed onto 12-well plates and incubated overnight at 37°C with 5% CO₂.

After 48 hours, the BM cells were harvested, and re-suspended at 2×10^6 cells per ml viral supernatant (*Section 7.7.2*) with 8µg/ml polybrene, and plated onto 12-well plates. Spin infection was induced by

centrifugation at 2,000rpm for 90 minutes. After centrifugation, half the viral supernatant in each well was replaced with fresh R10 media containing fresh cytokines at the same concentrations as stated before. Cells were then incubated overnight at 37°C with 5% CO₂. 48 hours later, the cells were harvested and washed twice with sterile PBS. 0.5 x 10⁶ cells were analysed by flow cytometry (*Section 7.8*) for GFP expression. The remaining cells were prepared for injection intravenously (i.v.) into female TCR-β/δ^{-/-} deficient mice that have been irradiated at 600rad. At least 0.2 x 10⁶ GFP⁺ HSCs in 200μl sterile PBS were injected into the lateral tail vein of each recipient mouse.

7.7.4. Blood collection

Mice were initially pre-warmed in a thermobox (Datesand Ltd, UK) at 37°C for 10 minutes to allow blood vessels to dilate and increase blood flow. Each mouse was then gently held in a restraining cone before its vein was pricked using a 25G needle. Blood droplets were aspirated immediately using 29G Insulin Syringe & Needle (Terumo, UK) and collected into an Eppendorf tube containing 200μl blood buffer.

7.8. Flow cytometry

7.8.1. Preparation of single-cell suspensions

Lymphoid organs from relevant mice were harvested by dissection. Cell suspensions from the isolated lymphoid organs were obtained by passing the organs through a 70μm nylon mesh strainer (Becton Dickinson, Oxford, UK) using the base of a 1ml syringe plunger. The cells were washed twice with PBS and spinning at 1,500rpm. Where necessary, blood, thymus and spleen cells were depleted of RBC using 1ml of RBC lysis buffer (Qiagen, UK) and incubated for 10 minutes at room temperature. Cells were counted after washing, as described in *Section 7.4*, to prepare a cell concentration of 10⁷ cells per ml re-suspended in PBS.

7.8.2. Cell surface staining

For each cell staining condition, 0.5μl of the necessary fluorochrome-conjugated antibody (1:200 dilution) was added to a suspension of 10⁶ cells in 100μl of PBS. The samples were incubated in the dark at room temperature for 20 minutes. This was followed by washing twice with 3ml of PBS and spinning at 1,500rpm for 5 minutes. The supernatant was discarded and the cells were re-suspended

in a final volume of 400µl of PBS. The samples were kept at 4°C before acquisition. Acquisition of flow cytometry data was performed on a FACSCalibur™ cytometer using the CellQuest™ software (BD Biosciences). At least 50,000 and 100,000 cells were collected for thymus and spleen analyses respectively. Cells from WT C57BL/6 mice were used as single-stained controls to set up compensation settings. Data analysis was performed using the FlowJo version 10 software (FlowJo, LLC, USA). The full list of antibodies is summarised below (Table 7.5). All antibodies were purchased either from BioLegend, UK or eBioscience, UK.

Table 7.5. List of monoclonal antibodies.

Antigen	Fluorochrome	Origin	Clone
FoxP3 (Intracellular)	PE	Rat	NRRF-30
TCRβ (C domain)	PE, APC	Armenian hamster	H57-597
Vβ6 TCR	PE	Rat	RR4-7
Vβ8.3 TCR	PE	Mouse	8C1
CD3ε	PE	Armenian hamster	145-2C11
CD4	PerCP, APC	Rat	RM4-5
CD5	PE	Rat	53-7.3
CD8α	PerCP	Rat	53-6.7
CD8β	PerCP	Rat	YTS156.7.7
CD69	PE	Armenian hamster	H1.2F3

7.8.3. MHC Dextramer™ staining

Cells from the MataHari TCR (CDR3β diversifying) retrogenic mice were stained with PE-conjugated CD8⁺ MataHari-specific Uty peptide (WMHHNMDLI) in the context of H2-D^b MHC Dextramer™ (Immudex, Denmark). Staining of cells was performed according to the manufacturer's protocol. In brief, 1-3 x 10⁶ cells were transferred into polystyrene tube and 2ml PBS containing 5% FCS at pH7.4 added before centrifugation at 300g for 5 minutes. The supernatant was removed and the cells were re-suspended in a total volume of 50µl of PBS (5% FCS, pH7.4). 10µl of the MHC Dextramer™ was added and to this suspension and incubated in the dark for 10 minutes. Additional antibodies (e.g. anti-CD4 and anti-CD8 Ab) were added afterwards and incubated in the dark at 2-8°C for 20 minutes. This was followed by washing twice with 2ml PBS (5% FCS, pH7.4) and spinning at 300g for 5 minutes. The supernatant was discarded and the cells were re-suspended in 400µl of PBS and stored at 2-8°C in the dark until analysis.

7.8.4. Multimer staining

Cells from the Marilyn TCR (CDR3 β diversifying) retrogenic mice were stained with PE-conjugated CD4⁺ Marilyn-specific Dby peptide fragment (NAGFNSNRANSSRSS) bound to an H2-A^b multimer (TCMetrix, Switzerland). Multimer staining was performed following the recommended staining of CD4⁺ T cells. Briefly, 10⁶ cells were re-suspended in 50 μ l of PBS containing 0.5% BSA, 5mM EDTA and 0.02% sodium azide. The cell suspension was incubated with 10 μ l of the multimer (50 μ g/ml concentration), along with other antibodies (anti-CD4, anti-CD8 Ab), at 37°C in the dark for 30-60 minutes. The cells were then washed twice with 2ml of PBS (0.5% BSA, 5mM EDTA and 0.02% sodium azide) before a final wash with 2ml PBS. The supernatant was removed before re-suspending the cells in 400 μ l of PBS. Cells were stored at 4°C in the dark before flow cytometry analysis.

7.8.5. Fluorescence-activated cell sorting (FACS)

For purification of specific splenic T cell subsets from retrogenic mice, single-cell suspensions were prepared as in *Section 7.8.1*. These cells were stained with a combination of anti-V β 6, anti-CD4 and anti-CD8 Ab for Marilyn TCR (CDR3 β diversifying) or anti-V β 8.3, anti-CD4 and anti-CD8 Ab for MataHari TCR (CDR3 β diversifying) as described in *Section 7.8.2*. The samples were re-suspended in sort buffer at a concentration of 20 million cells per ml and filtered through 35 μ M nylon mesh. The FACSArial™ flow cytometer at the MRC Clinical Sciences Centre Flow Cytometry Facility in Hammersmith Hospital was used for sorting cells. For Marilyn TCR (CDR3 β diversifying) samples, T cells were separated based on CD4⁺V β 6⁺ and CD4⁺V β 6⁻ gating. Conversely, MataHari TCR (CDR3 β diversifying) T cells were divided based on CD4⁺V β 8.3⁺, CD8⁺V β 8.3⁺ CD8⁺V β 8.3⁻ gating. Sorted cells were collected into collection buffer, centrifuged at 1,500rpm for 5 minutes and supernatant removed before RNA extraction (*Section 7.6.7*).

7.8.6. Intracellular FoxP3 staining

Cells from the retrogenic mice expressing the V α -C β fusion TCR chain were first stained with anti-CD4 and anti-CD8 Ab as described in *Section 7.8.2*. After the last wash, the supernatant was removed and sample vortexed before adding 1ml of FoxP3 Fixation/Permeabilisation working solution. The cell suspension was then incubated at 4°C for 60 minutes in the dark and washed twice with 2ml of 1X Permeabilisation buffer. Following re-suspension in 100 μ l 1X Permeabilisation buffer, the cells were labelled with PE-conjugated anti-FoxP3 (intracellular) Ab and incubated at room temperature for 30

minutes. The stained cells were washed twice with 2ml of 1X Permeabilisation buffer before re-suspension in 400µl of PBS. Cells were stored at 4°C in the dark before data acquisition. Splenocyte suspensions from WT C57BL/6 mice which have been treated with the FoxP3 Fixation/Permeabilisation working solution and either stained or unstained with the anti-FoxP3 Ab were used as the positive and negative controls respectively.

7.9. Statistical analysis

7.9.1. Shannon entropy analysis

The Shannon entropy index was used to measure the sequence diversity generated from the mutagenesis approach (Wang et al., 1998; Stewart et al., 1997). Refer to *Chapter 4.2.5* for calculation and explanation details.

7.9.2. Unpaired student's t-test

Variations between different groups were analysed by two-tailed, unpaired t-tests using GraphPad Prism 5 (<http://graphpad.com/quickcalcs/ttest1/>; GraphPad Software Inc, La Jolla, USA). All data is shown in relevant figures as mean ± standard deviation. P values are given for 95% confidence intervals where $p \geq 0.05$ is not significant (n.s.), $p < 0.05$ is significant (*), $p < 0.01$ (**) is very significant and $p < 0.001$ (***) is extremely significant.

Appendices

Appendices

Appendix 1

Marilyn TCR (CDR3 β diversifying) Construct

GGAGATCTACCACCATGAAAGAGCCTGTCCGTGAGCCTGGTGGTGCTGTGGCTCCTGCTGAACTGGGTGAACAGCCAGCA
GAACGTGCAGCAGTCCCCGAAAGCCTGATCGTCCCTGAGGGCGCTAGGACCTCCCTGAACTGCACATTTAGCGACAGC
GCTAGCCAGTACTTCTGGTGGTACAGACAGCATAGCGGCAAAGCCCCCTAAGGCCCTGATGAGCATCTTCAGCAATGGCG
AGAAAGAGGAGGGCAGGTTCCACCATCCACCTCAACAAAGCCTCCCTCCACTTCAGCCTGCACATCAGGGACAGCCAACC
CAGCGATAGCGCCCTGTATCTGTGCGCCGTCGGCAATAACAACAACGCTCCAGGTTCCGGAGCCGGCACCAGCTGACC
GTGAAGCCCAACATCCAGAACCCCGAACCCTGCTGTCTACCAACTGAAAGACCCAGGAGCCAGGATTCCACCCTCTGTC
TGTTACCGACTTCGACTCCAGATCAATGTCCCAAGACCATGGAGTCCGGAACCTTCATCACCGACAAGACCGTGCT
GGACATGAAGGCCATGGATTCCAAGTCCAACGGCGCCATCGCTTGGTCCAACCAGACCAGCTTCACCTGCCAGGACATC
TTCAAGGAAACCAACGCCACCTACCCCTCCAGCGACGTCCTTGGGATGCCACCCTGACCAGAAAGAGCTTCGAGACCG
ACATGAACCTCAACTTTCAGAACCTGTCCGTGATGGGACTCAGAATCCTCCTCAAAGTCGCCGGATTCAACCTCCT
CATGACCTGAGACTGTGGTCCAGC **GATCCGGCGCTACCAACTTTCCCTGCTGAAGCAGGCTGGCGACGTGGAAGAG**
AACCCCGGACCTATGAACAAGTGGGTGTCTGCTGGGTACCCTCTGCCTGCTCACAGTGAGACCACACAGGCGACG
GAGGCATCATCACCCAGACCCCAAGTTCCTGATCGGCCAGGAAGGACAGAAGCTCACACTGAAGTCCAGCAGAACTT
TAACCACGACACCATGTACTGGTACAGGCAGGACAGCGGAAAAGCCTGAGGCTGATCTACTACT**TCATCACCGAGAAC**
GATCTGCAGAAGGGCGATCTCAGCGAGGGCTATGACGCCCTCCAGAGAGAAGAAGAGCTCCTTCAGCCTCACAGTGACAT
CCGCCAGAAGAACGAGATGGCCGTGTTCCT**TGCGCCTCCAGCATCCCCGGAAGC**CACAGTGATGTGGGGTTTCCTCC
CCTCTGCACAGAAAGTTACATCACGTCAATTCACACTCGTTGTTAGAAATGTGGTGCATCTTCACCACCGTTCTAAG
AAGTCCAGAGCCTAAGTTAGCCCTTGAAAAGGCTCAAATTTGTACACACAGAGTCTTGATTGTGGGACAAGGTATAA
CCTCTGAGTGACGCACAGCCTTAGGGCAAGGGCAAAGCTAGGCTAGATTGGGGCTGTCCAGCGCCAAGAAAAAGAAC
ATTCAAAAGAAGAACAGGGGTAAGAGGAAACCCCTGCATTAGCTCGCATCTTACCACCCTTGCAATGGGGGTC
GGGGGGGATGTCACCTTCTTATCTTCAACTCCCCCAGAGGAGCAGCTTATCTGGTGGTTTCTCCAGCCCTCAAG
GGGTAGACCTATGGGAGGGTCTTTTTTGTATAAAGCTGTAACATTGT**AACGAGAGGCTGTTCTTTGGCCACGGCACC**
AAGCTGTCCGTGCTGGAAAGACCTGAGGAACGTGACCCCCCAAGGTGAGCCTCTTCGAGCCAGCAAGGCCGAGATCG
CCAACAAGCAGAAGGTTACCCTGGTCTGCCTGGCCAGGGGATTCTTCCCGACCACGTGGAGCTGAGCTGGTGGGTGAA
CGGCAAGGAGGTGCACTCCGGCGTGTCCACAGACCCTCAGGCCTACAAGGAGAGCAACTACTCTACTGCCTGAGCTCC
AGACTGAGGGTGAGCGCCACCTTCTGGCAATCCCAGGAACCACTCAGGTGCCAGGTGCAGTTCCACGGCCTCTCCG
AGGAGGACAAGTGGCCTGAGGGCAGCCTAAGCCTGTGACCCAGAACATCTCCGCCAAGCCTGGGGAAGGGCTGATTG
CGGCATCACCTCCGCCAGCTACCATCAGGGCGTGTCTCAGCGCTACCATCCTGTACGAGATCCTGCTGGGCAAGGCCACA
CTGTACGCCCTCTGGTACAGCGCCTCGTGTGATGGCCATGGTAAAAGGAAGAACAGCTGAGCGAATTCGG

Key

Start codon - ATG

Stop codon - TGA

–GSG– linker - **GATCCGGC**

P2A sequence - **GCTACCAACTTTCCCTGCTGAAGCAGGCTGGCGACGTGGAAGAGAACC**

TCR α CDRs are shown underlined; TCR β CDRs shown underlined and in bold

Recombination cassette is highlighted in grey box

Appendix 2

MataHari TCR (CDR3 β diversifying) Construct

GGAGATCTACCACCATGATGAAGACCTCCCTGCACACCGTCTTTCTCTTCTCTGGCTGTGGATGGACTGGGAGTCCCA
CGGCGAGAAGGTGCAACAGCACGAGAGCACCCCTGAGCGTGAGGGAAGGCGATAGCGCCGTGATCAATTGCACCTACACA
GACACCGCCTCCAGCTACTTTTCTTGGTACAAGCAGGAGGCTGGCAAGGGACTGCACTTTGTGATCGACATCAGAAGCA
ACGTGGACAGGAAGCAGAGCCAGAGGCTGATCGTCCCTGCTCGACAAGAAGGCCAAGAGGTTAGCCTGCACATTACCGC
CACCCAGCCTGAGGACTCCGCTATCTACTTCTGTGCCGCCGCCATGAGCAACTATAACGTGCTCTACTTCGGCTCCGGC
ACCAAACTGACCGTGGAGCCCAACATCCAAAACCCCGAACCCGCCGTGTACCAGCTCAAGGACCCAGGAGCCAAGATA
GCACACTGTGCCTCTTACCAGACTTCGACAGCCAGATCAACGTCCCCAAGACCATGGAATCCGGCACCTTATTACCGA
CAAGACCGTCTCGACATGAAGGCCATGGACAGCAAGTCCAACGGAGCTATTGCTTGGAGCAACCAGACCGACTTCACA
TGCCAGGATATCTTCAAAGAGACCAACGCCACCTATCCAGCAGCGACGTGCCCTGCGATGCCACACTGACCGAGAAAA
GCTTCGAGACCGACATGAACCTCAACTCCAGAACCTCAGCGTCATGGGCTGAGGATTCCTGCTGAAGGTGCTG
CTTCAAACCTGCTCATGACCTGAGACTCTGGAGCAGCEGCAGCGGAGCCACCAACTTTAGCCTGCTCAAGCAAGCCGGC
GACGTCGAGGAAAATCCTGGCCCTATGGGCTCCAGACTCTTTCTGGTCCGTGTCCTGCTGTGCACCAAACACATGGAGG
CCGCCGTACACAATCCCCAGGAACAAGGTGACCGTCACCGGGCAACGTGACCCCTCCTGCAGGCAGACCAACTC
CCATAACTATATGTACTGGTACAGGCAGGACACCGGCCACGGCCTGAGACTCATCCACTACAGCTACGGCGCTGGCAAC
CTCCAGATTGGCGACGTCCCCGACGGATACAAGGCCACCAGGACAACACAGGAAGACTTCTTTCTGCTGCTGGAGCTGG
CTAGCCCTAGCCAGACCAGCCTGTACTTTTGGCCAGCAGCGACCTGCACAGTGATGTGGGGTTTCTCCCTCTGCAC
AGAAAGTTACATCACGTCAATTCACACTCGTTGTTAGAAATGTGGTGCATTCTTACCACCGTTCTAAGAAGTCCAGA
GCCTAAGTTAGCCCCTTGAAAAGGCTCAAATTTGTACACACAGAGTCTTGATTGTGGGACAAGGTATAACCTCTGAGT
GACGCACAGCCTTAGGGCAAGGGCAAAGCTAGGCTAGATTGGGGCTGTCCAGCGCCAAGAAAAAGAACATTCAAAAG
AAGAACAGGGGGTAAAGAGGAAACCCCTGCATTAGCTCGCATCTTACCACCACCTTGCACAATGGGGTTCGGGGGGGA
TGTCACCTTCTTATCTTCAACTCCCCCAGAGGAGCAGCTTATCTGGTGGTTTCTTCCAGCCCTCAAGGGGTAGACC
TATGGGAGGGTCTTTTGTATAAAGCTGTAACATTTGTGGTCGAGGTGTTCTTCGGCAAGGGCACCAGGCTGACCGTG
GTGGAAGACCTGAGGAACGTGACCCCCCAAGGTGAGCCTCTTCGAGCCAGCAAGGCCGAGATCGCCAACAAGCAGA
AGGCTACCTGGTCTGCCTGGCCAGGGGATTCTTCCCCACCACGTGGAGCTGAGCTGGTGGTGAACGGCAAGGAGGT
GCACTCCGGCGTGTCCACAGACCCTCAGGCCTACAAGGAGAGCAACTACTCCTACTGCCTGAGCTCCAGACTGAGGGTG
AGCGCCACCTTCTGGCACAATCCCAGGAACCACTTCAGGTGCCAGGTGCAGTTCACGGCCTCTCCGAGGAGGACAAGT
GGCCTGAGGGCAGCCCTAAGCCTGTGACCCAGAACATCTCGCCGAAGCCTGGGGAAGGGCTGATTGCGGCATCACCTC
CGCCAGCTACCATCAGGGCGTGTCTCAGCGCTACCATCTGTACGAGATCCTGCTGGGCAAGGCCACACTGTACGCCGT
CTGGTACGGCCCTCGTGTGATGGCCATGGTGAATAAAGAAACAGCTGAGCGAATTCCG

Key

Start codon - ATG

Stop codon - TGA

–GSG- linker - GATCCGGC

P2A sequence - GCTACCAACTTTTCCCTGCTGAAGCAGGCTGGCGACGTGGAAGAGAACCCCGACCT

TCR α CDRs are shown underlined; TCR β CDRs shown underlined and in bold

Recombination cassette is highlighted in grey box

References

References

References

Adams, E. J. & Luoma, A. M. (2013) The Adaptable Major Histocompatibility Complex (MHC) Fold: Structure and Function of Nonclassical and MHC Class I-Like Molecules. *Annual Review of Immunology*. 31 (1), 529-561.

Adams, J., Narayanan, S., Liu, B., Birnbaum, M., Kruse, A., Bowerman, N., Chen, W., Levin, A., Connolly, J., Zhu, C., Kranz, D. & Garcia, K. . (2011) T Cell Receptor Signaling Is Limited by Docking Geometry to Peptide-Major Histocompatibility Complex. *Immunity*. 35 (5), 681-693.

Agrawal, A. & Schatz, D. G. (1997) RAG1 and RAG2 Form a Stable Postcleavage Synaptic Complex with DNA Containing Signal Ends in V(D)J Recombination. *Cell*. 89 (1), 43-53.

Ahnesorg, P., Smith, P. & Jackson, S. P. (2006) XLF Interacts with the XRCC4-DNA Ligase IV Complex to Promote DNA Nonhomologous End-Joining. *Cell*. 124 (2), 301-313.

Aidinis, V., Bonaldi, T., Beltrame, M., Santagata, S., Bianchi, M. E. & Spanopoulou, E. (1999) The RAG1 Homeodomain Recruits HMG1 and HMG2 To Facilitate Recombination Signal Sequence Binding and To Enhance the Intrinsic DNA-Bending Activity of RAG1-RAG2. *Molecular and Cellular Biology*. 19 (10), 6532-6542.

Aki, M., Shimbara, N., Takashina, M., Akiyama, K., Kagawa, S., Tamura, T., Tanahashi, N., Yoshimura, T., Tanaka, K. & Ichihara, A. (1994) Interferon-gamma; Induces Different Subunit Organizations and Functional Diversity of Proteasomes. *The Journal of Biochemistry*. 115 (2), 257-269.

Alcover, A., Mariuzza, R. A., Ermonval, M. & Acuto, O. (1990) Lysine 271 in the transmembrane domain of the T-cell antigen receptor beta chain is necessary for its assembly with the CD3 complex but not for alpha/beta dimerization. *Journal of Biological Chemistry*. 265 (7), 4131-4135.

Al-Lazikani, B., Lesk, A. M. & Chothia, C. (2000) Canonical structures for the hypervariable regions of T cell $\alpha\beta$ receptors1. *Journal of Molecular Biology*. 295 (4), 979-995.

Allison, T. J., Winter, C. C., Fournie, J., Bonneville, M. & Garboczi, D. N. (2001) Structure of a human gamma delta T-cell antigen receptor. *Nature*. 411 (6839), 820-824.

Anderson, G. & Jenkinson, E. J. (2001) Lymphostromal interactions in thymic development and function. *Nat Rev Immunol*. 1 (1), 31-40.

Ansel, K. M., McHeyzer-Williams, L. J., Ngo, V. N., McHeyzer-Williams, M. G. & Cyster, J. G. (1999) In Vivo-Activated Cd4 T Cells Upregulate Cxc Chemokine Receptor 5 and Reprogram Their Response to Lymphoid Chemokines. *The Journal of Experimental Medicine*. 190 (8), 1123-1134.

Arden, B. (1998) Conserved motifs in T-cell receptor CDR1 and CDR2: implications for ligand and CD8 co-receptor binding. *Current Opinion in Immunology*. 10 (1), 74-81.

Arden, B., Clark, S. P., Kabelitz, D. & Mak, T. W. (1995) Mouse T-cell receptor variable gene segment families. *Immunogenetics*. 42 (6), 501-530.

Armstrong, K., Piepenbrink, K. & Baker, B. (2008) Conformational changes and flexibility in T-cell receptor recognition of peptide-MHC complexes. *Biochemical Journal*. 415 (2), 183-196.

Arnaud, J., Hucheq, A., Vernhes, M. C., Caspar-Bauguil, S., Lenfant, F., Sancho, J., Terhorst, C. & Rubin, B. (1997) The interchain disulfide bond between TCR alpha beta heterodimers on human T cells is not required for TCR-CD3 membrane expression and signal transduction. *International Immunology*. 9 (4), 615-626.

Arnett, K. L., Harrison, S. C. & Wiley, D. C. (2004) Crystal structure of a human CD3-e/d dimer in complex with a UCHT1 single-chain antibody fragment. *Proceedings of the National Academy of Sciences of the United States of America*. 101 (46), 16268-16273.

Artyomov, M. N., Lis, M., Devadas, S., Davis, M. M. & Chakraborty, A. K. (2010) CD4 and CD8 binding to MHC molecules primarily acts to enhance Lck delivery. *Proceedings of the National Academy of Sciences*. 107 (39), 16916-16921.

Aschenbrenner, K., D'Cruz, L., M., Vollmann, E. H., Hinterberger, M., Emmerich, J., Swee, L. K., Rolink, A. & Klein, L. (2007) Selection of Foxp3+ regulatory T cells specific for self antigen expressed and presented by Aire+ medullary thymic epithelial cells. *Nature Immunology*. 8 (4), 351-358.

Attaf, M., Legut, M., Cole, D. K. & Sewell, A. K. (2015) The T cell antigen receptor: the Swiss army knife of the immune system. *Clinical & Experimental Immunology*. 181 (1), 1-18.

Azimi, I., Matthias, L. J., Center, R. J., Wong, J. W. H. & Hogg, P. J. (2010) Disulfide Bond That Constrains the HIV-1 gp120 V3 Domain Is Cleaved by Thioredoxin. *Journal of Biological Chemistry*. 285 (51), 40072-40080.

Azuma, M. (2006) Fundamental mechanisms of host immune responses to infection. *Journal of Periodontal Research*. 41 (5), 361-373.

Bäckström, B. T., Milia, E., Peter, A., Jaureguiberry, B., Baldari, C. T. & Palmer, E. (1996) A motif within the T cell receptor alpha chain constant region connecting peptide domain controls antigen responsiveness. *Immunity*. 5 (5), 437-447.

Bäckström, B. T., Müller, U., Hausmann, B. & Palmer, E. (1998) Positive selection through a motif in the alpha beta T cell receptor. *Science*. 281 (5378), 835-838.

Baldwin, T. A., Sandau, M. M., Jameson, S. C. & Hogquist, K. A. (2005) The timing of TCRalpha expression critically influences T cell development and selection. *The Journal of Experimental Medicine*. 202 (1), 111-121.

Bartok, I., Holland, S. J., Kessels, H. W., Silk, J. D., Alkhinji, M. & Dyson, J. (2010) T cell receptor CDR3 loops influence alpha beta pairing. *Molecular Immunology*. 47 (7-8), 1613-1618.

Bassing, C. H., Swat, W. & Alt, F. W. (2002) The Mechanism and Regulation of Chromosomal V(D)J Recombination. *Cell*. 109 (2, Supplement 1), S45-S55.

Beddoe, T., Chen, Z., Clements, C. S., Ely, L. K., Bushell, S. R., Vivian, J. P., Kjer-Nielsen, L., Pang, S. S., Dunstone, M. A., Liu, Y. C., Macdonald, W. A., Perugini, M. A., Wilce, M. C. J., Burrows, S. R., Purcell, A. W., Tiganis, T., Bottomley, S. P., McCluskey, J. & Rossjohn, J. (2009) Antigen Ligation Triggers a

Conformational Change within the Constant Domain of the $\alpha\beta$ T Cell Receptor. *Immunity*. 30 (6), 777-788.

Bell, J. J. & Bhandoola, A. (2008) The earliest thymic progenitors for T cells possess myeloid lineage potential. *Nature*. 452 (7188), 764-767.

Benoist, C. & Mathis, D. (2012) Treg Cells, Life History, and Diversity. *Cold Spring Harbor Perspectives in Biology*. 4 (9), a007021.

Bercovici, N., Duffour, M. T., Agrawal, S., Salcedo, M. & Abastado, J. P. (2000) New Methods for Assessing T-Cell Responses. *Clinical and Diagnostic Laboratory Immunology*. 7 (6), 859-864.

Bettini, M. L., Bettini, M., Nakayama, M., Guy, C. S. & Vignali, D. A. A. (2013) Generation of T cell receptor retrogenic mice: improved retroviral-mediated stem cell gene transfer. *Nat. Protocols*. 8 (10), 1837-1840.

Bhati, M., Cole, D. K., McCluskey, J., Sewell, A. K. & Rossjohn, J. (2014) The versatility of the $\alpha\beta$ T-cell antigen receptor. *Protein Science*. 23 (3), 260-272.

Blum, J. S., Wearsch, P. A. & Cresswell, P. (2013) Pathways of Antigen Processing. *Annual Review of Immunology*. 31 (1), 443-473.

Boasso, A., Hardy, A. W., Anderson, S. A., Dolan, M. J. & Shearer, G. M. (2008) HIV-Induced Type I Interferon and Tryptophan Catabolism Drive T Cell Dysfunction Despite Phenotypic Activation. *PLoS ONE*. 3 (8), e2961.

Bonifacino, J. S., Cosson, P. & Klausner, R. D. (1990) Colocalized transmembrane determinants for ER degradation and subunit assembly explain the intracellular fate of TCR chains. *Cell*. 63 (3), 503-513.

Bonneville, M., O'Brien, R. L. & Born, W. K. (2010) $\gamma\delta$ T cell effector functions: a blend of innate programming and acquired plasticity. *Nat Rev Immunol*. 10 (7), 467-478.

Boon, T., Coulie, P. G. & Van Den Eynde, B. (1997) Tumor antigens recognized by T cells. *Immunology Today*. 18 (6), 267-268.

Borg, N. A., Ely, L. K., Beddoe, T., Macdonald, W. A., Reid, H. H., Clements, C. S., Purcell, A. W., Kjer-Nielsen, L., Miles, J. J., Burrows, S. R., McCluskey, J. & Rossjohn, J. (2005) The CDR3 regions of an immunodominant T cell receptor dictate the 'energetic landscape' of peptide-MHC recognition. *Nature Immunology*. 6 (2), 171-180.

Born, W., Yague, J., Palmer, E., Kappler, J. & Marrack, P. (1985) Rearrangement of T-cell receptor beta-chain genes during T-cell development. *Proceedings of the National Academy of Sciences of the United States of America*. 82 (9), 2925-2929.

Borowski, C., Li, X., Aifantis, I., Gounari, F. & von Boehmer, H. (2003) Pre-TCRalpha and TCRalpha Are Not Interchangeable Partners of TCRbeta during T Lymphocyte Development. *The Journal of Experimental Medicine*. 199 (5), 607-615.

Bosc, N. & Lefranc, M. (2003) The mouse (*Mus musculus*) T cell receptor alpha (TRA) and delta (TRD) variable genes. *Developmental & Comparative Immunology*. 27 (6-7), 465-497.

- Bosselut, R., Kubo, S., Guinter, T., Kopacz, J. L., Altman, J. D., Feigenbaum, L. & Singer, A. (2000) Role of CD8 β domains in CD8 coreceptor function: Importance for MHC I binding, signaling, and positive selection of CD8⁺ T cells in the thymus. *Immunity*. 12 (4), 409-418.
- Boulter, J. M., Glick, M., Todorov, P. T., Baston, E., Sami, M., Rizkallah, P. & Jakobsen, B. K. (2003) Stable, soluble T-cell receptor molecules for crystallization and therapeutics. *Protein Engineering*. 16 (9), 707-711.
- Brady, R. L., Dodson, E. J., Dodson, G. G., Lange, G., Davis, S. J., Williams, A. F. & Barclay, A. N. (1993) Crystal structure of domains 3 and 4 of rat CD4: relation to the NH₂-terminal domains. *Science*. 260 (5110), 979-983.
- Braun, M. Y., Grandjean, I., Feunou, P., Duban, L., Kiss, R., Goldman, M. & Lantz, O. (2001) Acute Rejection in the Absence of Cognate Recognition of Allograft by T Cells. *The Journal of Immunology*. 166 (8), 4879-4883.
- Bridgeman, J. S., Sewell, A. K., Miles, J. J., Price, D. A. & Cole, D. K. (2012) Structural and biophysical determinants of ?? T-cell antigen recognition. *Immunology*. 135 (1), 9-18.
- Brocker, T. (1999) The role of dendritic cells in T cell selection and survival. *Journal of Leukocyte Biology*. 66 (2), 331-335.
- Brouwenstijn, N., Serwold, T. & Shastri, N. (2001) MHC Class I Molecules Can Direct Proteolytic Cleavage of Antigenic Precursors in the Endoplasmic Reticulum. *Immunity*. 15 (1), 95-104.
- Brown, J. H., Jardetzky, T. S., Gorga, J. C., Stern, L. J., Urban, R. G., Strominger, J. L. & Wiley, D. C. (1993) Three-dimensional structure of the human class II histocompatibility antigen HLA-DR1. *Nature*. 364 (6432), 33-39.
- Bryans, M., Valenzano, M. C. & Stamato, T. D. (1999) Absence of DNA ligase IV protein in XR-1 cells: evidence for stabilization by XRCC4. *Mutation Research/DNA Repair*. 433 (1), 53-58.
- Buckley, R. H. (2004) Molecular Defects in Human Severe Combined Immunodeficiency and Approaches to Immune Reconstitution. *Annual Review of Immunology*. 22 (1), 625-655.
- Bulek, A. M., Cole, D. K., Skowera, A., Dolton, G., Gras, S., Madura, F., Fuller, A., Miles, J. J., Gostick, E., Price, D. A., Drijfhout, J. W., Knight, R. R., Huang, G. C., Lissin, N., Molloy, P. E., Wooldridge, L., Jakobsen, B. K., Rossjohn, J., Peakman, M., Rizkallah, P. J. & Sewell, A. K. (2012) Structural basis for the killing of human beta cells by CD8 + T cells in type 1 diabetes. *Nature Immunology*. 13 (3), 283-289.
- Burchill, M. A., Yang, J., Vang, K. B., Moon, J. J., Chu, H. H., Lio, C. J., Vegoe, A. L., Hsieh, C., Jenkins, M. K. & Farrar, M. A. (2008) Linked T Cell Receptor and Cytokine Signaling Govern the Development of the Regulatory T Cell Repertoire. *Immunity*. 28 (1), 112-121.
- Burrows, S. R., Chen, Z., Archbold, J. K., Tynan, F. E., Beddoe, T., Kjer-Nielsen, L., Miles, J. J., Khanna, R., Moss, D. J., Liu, Y. C., Gras, S., Kostenko, L., Brennan, R. M., Clements, C. S., Brooks, A. G., Purcell, A. W., McCluskey, J. & Rossjohn, J. (2010) Hard wiring of T cell receptor specificity for the major histocompatibility complex is underpinned by TCR adaptability. *Proceedings of the National Academy of Sciences*. 107 (23), 10608-10613.

- Burrows, S. R., Rossjohn, J. & McCluskey, J. (2006) Have we cut ourselves too short in mapping CTL epitopes? *Trends in Immunology*. 27 (1), 11-16.
- Burtrum, D. B., Kim, S., Dudley, E. C., Hayday, A. C. & Petrie, H. T. (1996) TCR gene recombination and alpha beta-gamma delta lineage divergence: productive TCR-beta rearrangement is neither exclusive nor preclusive of gamma delta cell development. *The Journal of Immunology*. 157 (10), 4293-4296.
- Buslepp, J., Wang, H., Biddison, W. E., Appella, E. & Collins, E. J. (2003) A Correlation between TCR V α Docking on MHC and CD8 Dependence: Implications for T Cell Selection. *Immunity*. 19 (4), 595-606.
- Call, M. E., Pyrdol, J., Wiedmann, M. & Wucherpfennig, K. W. (2002) The Organizing Principle in the Formation of the T Cell Receptor-CD3 Complex. *Cell*. 111 (7), 967-979.
- Call, M. E., Pyrdol, J. & Wucherpfennig, K. W. (2004) Stoichiometry of the T-cell receptor CD3 complex and key intermediates assembled in the endoplasmic reticulum. *The EMBO Journal*. 23 (12), 2348-2357.
- Call, M. E. & Wucherpfennig, K. W. (2005) THE T CELL RECEPTOR: Critical Role of the Membrane Environment in Receptor Assembly and Function. *Annual Review of Immunology*. 23 (1), 101-125.
- Call, M. E. & Wucherpfennig, K. W. (2004) Molecular mechanisms for the assembly of the T cell receptor-CD3 complex. *Molecular Immunology*. 40 (18), 1295-1305.
- Cameron, B. J., Gerry, A. B., Dukes, J., Harper, J. V., Kannan, V., Bianchi, F. C., Grand, F., Brewer, J. E., Gupta, M., Plesa, G., Bossi, G., Vuidepot, A., Powlesland, A. S., Legg, A., Adams, K. J., Bennett, A. D., Pumphrey, N. J., Williams, D. D., Binder-Scholl, G., Kulikovskaya, I., Levine, B. L., Riley, J. L., Varela-Rohena, A., Stadtmauer, E. A., Rapoport, A. P., Linette, G. P., June, C. H., Hassan, N. J., Kalos, M. & Jakobsen, B. K. (2013) Identification of a Titin-Derived HLA-A1-Presented Peptide as a Cross-Reactive Target for Engineered MAGE A3-Directed T Cells. *Science Translational Medicine*. 5 (197), 197ra103-197ra103.
- Capone, M., Hockett, R. D. & Zlotnik, A. (1998) Kinetics of T cell receptor β , γ , and δ rearrangements during adult thymic development: T cell receptor rearrangements are present in CD44+CD25+ Pro-T thymocytes. *Proceedings of the National Academy of Sciences*. 95 (21), 12522-12527.
- Casillas, A. M., Thompson, A. D., Cheshier, S., Hernandez, S. & Aguilera, R. J. (1995) RAG-1 and RAG-2 gene expression and V(D)J recombinase activity are enhanced by protein phosphatase 1 and 2A inhibition in lymphocyte cell lines. *Molecular Immunology*. 32 (3), 167-175.
- Ceredig, R. & Rolink, T. (2002) A positive look at double-negative thymocytes. *Nat Rev Immunol*. 2 (11), 888-897.
- Chang, H. C., Tan, K., Ouyang, J., Parisini, E., Liu, J. H., Le, Y., Wang, X., Reinherz, E. L. & Wang, J. H. (2005) Structural and mutational analyses of a CD8a β heterodimer and comparison with the CD8aa homodimer. *Immunity*. 23 (6), 661-671.
- Chang, H. H. Y., Watanabe, G. & Lieber, M. R. (2015) Unifying the DNA End Processing Roles of the Artemis Nuclease: Ku-Dependent Artemis Resection at Blunt DNA Ends. *Journal of Biological Chemistry*.

- Chattopadhyay, P. K., Betts, M. R., Price, D. A., Gostick, E., Horton, H., Roederer, M. & De Rosa, S. C. (2009) The cytolytic enzymes granzyme A, granzyme B, and perforin: expression patterns, cell distribution, and their relationship to cell maturity and bright CD57 expression. *Journal of Leukocyte Biology*. 85 (1), 88-97.
- Chen, L. & Flies, D. B. (2013) Molecular mechanisms of T cell co-stimulation and co-inhibition. *Nat Rev Immunol*. 13 (4), 227-242.
- Chen, X., Zaro, J. & Shen, W. (2012) Fusion Protein Linkers: Property, Design and Functionality. *Advanced Drug Delivery Reviews*. 65 (10), 1357-1369.
- Cheroutre, H. (2004) *Starting at the beginning: New perspectives on the biology of mucosal T cells*. Annual Review of Immunology.
- Cheroutre, H. & Lambolez, F. (2008) Doubting the TCR Coreceptor Function of CD8 α . *Immunity*. 28 (2), 149-159.
- Chervin, A. S., Aggen, D. H., Raseman, J. M. & Kranz, D. M. (2008) Engineering higher affinity T cell receptors using a T cell display system. *Journal of Immunological Methods*. 339 (2), 175-184.
- Chervin, A. S., Stone, J. D., Holler, P. D., Bai, A., Chen, J., Eisen, H. N. & Kranz, D. M. (2009) The Impact of TCR-Binding Properties and Antigen Presentation Format on T Cell Responsiveness. *The Journal of Immunology*. 183 (2), 1166-1178.
- Choi, J. K., Hoang, N., Vilardi, A. M., Conrad, P., Emerson, S. G. & Gewirtz, A. M. (2001) Hybrid HIV/MSCV LTR Enhances Transgene Expression of Lentiviral Vectors in Human CD34+ Hematopoietic Cells. *Stem Cells*. 19 (3), 236-246.
- Chun, J. J. M., Schatz, D. G., Oettinger, M. A., Jaenisch, R. & Baltimore, D. (1991) The recombination activating gene-1 (RAG-1) transcript is present in the murine central nervous system. *Cell*. 64 (1), 189-200.
- Ciofani, M., Knowles, G. C., Wiest, D. L., von Boehmer, H. & Zúñiga-Pflücker, J. C. (2006) Stage-Specific and Differential Notch Dependency at the $\alpha\beta$ and $\gamma\delta$ T Lineage Bifurcation. *Immunity*. 25 (1), 105-116.
- Ciofani, M., Schmitt, T. M., Ciofani, A., Michie, A. M., Çuburu, N., Aublin, A., Maryanski, J. L. & Zúñiga-Pflücker, J. C. (2004) Obligatory Role for Cooperative Signaling by Pre-TCR and Notch during Thymocyte Differentiation. *The Journal of Immunology*. 172 (9), 5230-5239.
- Ciofani, M. & Zúñiga-Pflücker, J. (2005) Notch promotes survival of pre-T cells at the beta]-selection checkpoint by regulating cellular metabolism. *Nature Immunology*. 6 (9), 881-888.
- Ciofani, M. & Zúñiga-Pflücker, J. C. (2007) The Thymus as an Inductive Site for T Lymphopoiesis. *Annual Review of Cell and Developmental Biology*. 23 (1), 463-493.
- Cobb, R. M., Oestreich, K. J., Osipovich, O. A. & Oltz, E. M. (2006) Accessibility Control of V(D)J Recombination. *Advances in Immunology*. 9145-109.
- Cole, D. K., Miles, K. M., Madura, F., Holland, C. J., Schauenburg, A. J. A., Godkin, A. J., Bulek, A. M., Fuller, A., Akpovwa, H. J. E., Pymm, P. G., Liddy, N., Sami, M., Li, Y., Rizkallah, P. J., Jakobsen, B. K. &

- Sewell, A. K. (2014) T-cell Receptor (TCR)-Peptide Specificity Overrides Affinity-enhancing TCR-Major Histocompatibility Complex Interactions. *Journal of Biological Chemistry*. 289 (2), 628-638.
- Cole, D. K., Pumphrey, N. J., Boulter, J. M., Sami, M., Bell, J. I., Gostick, E., Price, D. A., Gao, G. F., Sewell, A. K. & Jakobsen, B. K. (2007) Human TCR-Binding Affinity is Governed by MHC Class Restriction. *The Journal of Immunology*. 178 (9), 5727-5734.
- Collins, E. J. & Riddle, D. S. (2008) TCR-MHC docking orientation: natural selection, or thymic selection? *Immunologic Research*. 41 (3), 267-294.
- Correia-Neves, M., Waltzinger, C., Mathis, D. & Benoist, C. (2001) The Shaping of the T Cell Repertoire. *Immunity*. 14 (1), 21-32.
- Cosson, P., Lankford, S. P., Bonifacino, J. S. & Klausner, R. D. (1991) Membrane protein association by potential intramembrane charge pairs. *Nature*. 351 (6325), 414-416.
- Craiu, A., Akopian, T., Goldberg, A. & Rock, K. L. (1997) Two distinct proteolytic processes in the generation of a major histocompatibility complex class I-presented peptide. *Proceedings of the National Academy of Sciences of the United States of America*. 94 (20), 10850-10855.
- Cresswell, P. (1996) Invariant Chain Structure and MHC Class II Function. *Cell*. 84 (4), 505-507.
- Crotty, S. (2011) Follicular Helper CD4 T Cells (TFH). *Annual Review of Immunology*. 29 (1), 621-663.
- Cui, X. & Meek, K. (2007) Linking double-stranded DNA breaks to the recombination activating gene complex directs repair to the nonhomologous end-joining pathway. *Proceedings of the National Academy of Sciences*. 104 (43), 17046-17051.
- Cunningham-Rundles, C. & Ponda, P. P. (2005) Molecular defects in T- and B-cell primary immunodeficiency diseases. *Nat Rev Immunol*. 5 (11), 880-892.
- Dave, V. P., Cao, Z., Browne, C., Alarcon, B., Fernandez-Miguel, G., Lafaille, J., de, I. H., Tonegawa, S. & Kappes, D. J. (1997) CD3 delta deficiency arrests development of the alpha beta but not the gamma delta T cell lineage. *The EMBO Journal*. 16 (6), 1360-1370.
- Dave, V. P. (2009) Hierarchical role of CD3 chains in thymocyte development. *Immunological Reviews*. 232 (1), 22-33.
- Davis, M. M. & Bjorkman, P. J. (1988) T-cell antigen receptor genes and T-cell recognition. *Nature*. 334 (6181), 395-402.
- de Felipe, P. (2004) Skipping the co-expression problem: the new 2A "CHYSEL" technology. *Genetic Vaccines and Therapy*. 213-13.
- De Silva, N. S. & Klein, U. (2015) Dynamics of B cells in germinal centres. *Nat Rev Immunol*. 15 (3), 137-148.
- Denning, T. L., Granger, S., Mucida, D., Graddy, R., Leclercq, G., Zhang, W., Honey, K., Rasmussen, J. P., Cheroutre, H., Rudensky, A. Y. & Kronenberg, M. (2007) Mouse TCR $\alpha\beta$ +CD8 $\alpha\alpha$ intraepithelial lymphocytes express genes that down-regulate their antigen reactivity and suppress immune responses. *Journal of Immunology*. 178 (7), 4230-4239.

- Denzin, L. K. (2013) Inhibition of HLA-DM Mediated MHC Class II Peptide Loading by HLA-DO Promotes Self Tolerance. *Frontiers in Immunology*. 4465.
- Derbinski, J., Schulte, A., Kyewski, B. & Klein, L. (2001) Promiscuous gene expression in medullary thymic epithelial cells mirrors the peripheral self. *Nature Immunology*. 2 (11), 1032-1039.
- DerSimonian, H., Band, H. & Brenner, M. B. (1991) Increased frequency of T cell receptor Va12.1 expression on CD8+ T cells: Evidence that Va participates in shaping the peripheral T cell repertoire. *Journal of Experimental Medicine*. 174 (3), 639-648.
- Desiderio, S., Lin, W. C. & Li, Z. (1996) *The cell cycle and V(D)J recombination*.
- Devine, L. & Kavathas, P. B. (1999) Molecular analysis of protein interactions mediating the function of the cell surface protein CD8. *Immunologic Research*. 19 (2-3), 201-210.
- D'Orsogna, L. J., Roelen, D. L., Doxiadis, I. I. N. & Claas, F. H. J. (2011) TCR cross-reactivity and allorecognition: new insights into the immunogenetics of allorecognition. *Immunogenetics*. 64 (2), 77-85.
- Downs, J. A. & Jackson, S. P. (2004) A means to a DNA end: the many roles of Ku. *Nature Reviews. Molecular Cell Biology*. 5 (5), 367-378.
- Dudley, D. D., Chaudhuri, J., Bassing, C. H. & Alt, F. W. (2005) Mechanism and Control of V(D)J Recombination versus Class Switch Recombination: Similarities and Differences. *Advances in Immunology*. 8643-112.
- Dudley, M. E. & Rosenberg, S. A. (2003) Adoptive-cell-transfer therapy for the treatment of patients with cancer. *Nat Rev Cancer*. 3 (9), 666-675.
- Dunbar, J., Knapp, B., Fuchs, A., Shi, J. & Deane, C. M. (2014) Examining Variable Domain Orientations in Antigen Receptors Gives Insight into TCR-Like Antibody Design. *PLoS Computational Biology*. 10 (9), e1003852.
- Ekeruche-Makinde, J., Miles, J. J., van den Berg, H. A., Skowera, A., Cole, D. K., Dolton, G., Schauenburg, A. J. A., Tan, M. P., Pentier, J. M., Llewellyn-Lacey, S., Miles, K. M., Bulek, A. M., Clement, M., Williams, T., Trimby, A., Bailey, M., Rizkallah, P., Rossjohn, J., Peakman, M., Price, D. A., Burrows, S. R., Sewell, A. K. & Wooldridge, L. (2012) Peptide length determines the outcome of TCR/peptide-MHCI engagement. *Blood*. 121 (7), 1112-1123.
- Eldershaw, S. A., Sansom, D. M. & Narendran, P. (2010) Expression and function of the autoimmune regulator (Aire) gene in non-thymic tissue. *Clinical and Experimental Immunology*. 163 (3), 296-308.
- Ely, L. K., Burrows, S. R., Purcell, A. W., Rossjohn, J. & McCluskey, J. (2008) T-cells behaving badly: structural insights into alloreactivity and autoimmunity. *Current Opinion in Immunology*. 20 (5), 575-580.
- Ely, L. K., Kjer-Nielsen, L., McCluskey, J. & Rossjohn, J. (2005) Structural Studies on the $\alpha\beta$ T-cell Receptor. *IUBMB Life*. 57 (8), 575-582.
- Engel, I. & Hedrick, S. M. (1988) Site-directed mutations in the VDJ junctional region of a T cell receptor β chain cause changes in antigenic peptide recognition. *Cell*. 54 (4), 473-484.

Erman, B., Feigenbaum, L., Coligan, J. E. & Singer, A. (2002) Early TCR[alpha] expression generates TCR[alpha][gamma] complexes that signal the DN-to-DP transition and impair development. *Nature Immunology*. 3 (6), 564-569.

Erman, B., Guintert, T. I. & Singer, A. (2004) Defined $\alpha\beta$ T Cell Receptors with Distinct Ligand Specificities Do Not Require Those Ligands to Signal Double Negative Thymocyte Differentiation. *The Journal of Experimental Medicine*. 199 (12), 1719-1724.

Felix, N. J. & Allen, P. M. (2007) Specificity of T-cell alloreactivity. *Nat Rev Immunol*. 7 (12), 942-953.

Feng, D., Bond, C. J., Ely, L. K., Maynard, J. & Garcia, K. C. (2007) Structural evidence for a germline-encoded T cell receptor-major histocompatibility complex interaction 'codon'. *Nature Immunology*. 8 (9), 975-983.

Ferreira, C., Singh, Y., Furmanski, A. L., Wong, F. S., Garden, O. A. & Dyson, J. (2009) Non-obese diabetic mice select a low-diversity repertoire of natural regulatory T cells. *Proceedings of the National Academy of Sciences*. 106 (20), 8320-8325.

Ferrier, P., Krippel, B., Blackwell, T. K., Furley, A. J., Suh, H., Winoto, A., Cook, W. D., Hood, L., Costantini, F. & Alt, F. W. (1990) Separate elements control DJ and VDJ rearrangement in a transgenic recombination substrate. *The EMBO Journal*. 9 (1), 117-125.

Feyerabend, T. B., Terszowski, G., Tietz, A., Blum, C., Luche, H., Gossler, A., Gale, N. W., Radtke, F., Fehling, H. J. & Rodewald, H. (2009) Deletion of Notch1 Converts Pro-T Cells to Dendritic Cells and Promotes Thymic B Cells by Cell-Extrinsic and Cell-Intrinsic Mechanisms. *Immunity*. 30 (1), 67-79.

Freeman, J. D., Warren, R. L., Webb, J. R., Nelson, B. H. & Holt, R. A. (2009) Profiling the T-cell receptor beta-chain repertoire by massively parallel sequencing. *Genome Research*. 19 (10), 1817-1824.

Fugmann, S. D., Lee, A. I., Shockett, P. E., Villey, I. J. & Schatz, D. G. (2000) The RAG proteins and V(D)J recombination: complexes, ends, and transposition. *Annu Rev Immunol*. 18495-527.

Fugmann, S. D. & Schatz, D. G. (2001) Identification of Basic Residues in RAG2 Critical for DNA Binding by the RAG1-RAG2 Complex. *Molecular Cell*. 8 (4), 899-910.

Gakamsky, D. M., Luescher, I. F., Pramanik, A., Kopito, R. B., Lemonnier, F., Vogel, H., Bigler, R. & Pecht, I. (2005) CD8 kinetically promotes ligand binding to the T-cell antigen receptor. *Biophysical Journal*. 89 (3), 2121-2133.

Gallegos, A. M. & Bevan, M. J. (2006) Central tolerance: good but imperfect. *Immunological Reviews*. 209 (1), 290-296.

Gameiro, J., Nagib, P. & Verinaud, L. (2010) The thymus microenvironment in regulating thymocyte differentiation. *Cell Adhesion & Migration*. 4 (3), 382-390.

Gangadharan, D., Lambalez, F., Attinger, A., Wang-Zhu, Y., Sullivan, B. A. & Cheroutre, H. (2006) Identification of Pre- and Postselection TCR $\alpha\beta$ + Intraepithelial Lymphocyte Precursors in the Thymus. *Immunity*. 25 (4), 631-641.

Gangadharan, D. & Cheroutre, H. (2004) The CD8 isoform CD8 $\alpha\alpha$ is not a functional homologue of the TCR co-receptor CD8 $\alpha\beta$. *Current Opinion in Immunology*. 16 (3), 264-270.

- Gao, G. F., Tormo, J., Gerth, U. C., Wyer, J. R., McMichael, A. J., Stuart, D. I., Bell, J. I., Jones, E. Y. & Jakobsen, B. K. (1997) Crystal structure of the complex between human CD8 α - α and HLA-A2. *Nature*. 387 (6633), 630-634.
- Garboczi, D. N., Ghosh, P., Utz, U., Fan, Q. R., Biddison, W. E. & Wiley, D. C. (1996) Structure of the complex between human T-cell receptor, viral peptide and HLA-A2. *Nature*. 384 (6605), 134-141.
- Garcia, K. C., Degano, M., Stanfield, R. L., Brunmark, A., Jackson, M. R., Peterson, P. A., Teyton, L. & Wilson, I. A. (1996a) An $\alpha\beta$ T cell receptor structure at 2.5 Å and its orientation in the TCR-MHC complex. *Science*. 274 (5285), 209-219.
- Garcia, K. C., Gapin, L., Adams, J. J., Birnbaum, M. E., Scott-Browne, J., Kappler, J. W. & Marrack, P. (2012) A Closer Look at TCR Germline Recognition. *Immunity*. 36 (6), 887-888.
- Garcia, K. C., Scott, C. A., Brunmark, A., Carbone, F. R., Peterson, P. A., Wilson, I. A. & Teyton, L. (1996b) CD8 enhances formation of stable T-cell receptor/MHC class I molecule complexes. *Nature*. 384 (6609), 577-581.
- Garcia, K. C., Teyton, L. & Wilson, I. A. (1999) STRUCTURAL BASIS OF T CELL RECOGNITION. *Annual Review of Immunology*. 17 (1), 369-397.
- Garman, R. D., Ko, J. -, Vulpe, C. D. & Raulet, D. H. (1986) T-cell receptor variable region gene usage in T-cell populations. *Proceedings of the National Academy of Sciences of the United States of America*. 83 (11), 3987-3991.
- Gattinoni, L., Powell Jr., D. J., Rosenberg, S. A. & Restifo, N. P. (2006) Adoptive immunotherapy for cancer: Building on success. *Nature Reviews Immunology*. 6 (5), 383-393.
- Germain, R. N. (2002) T-cell development and the CD4-CD8 lineage decision. *Nat Rev Immunol*. 2 (5), 309-322.
- Germain, R. N., Stefanova, I. & Dorfelan, J. (2002) Self-Recognition and the Regulation of Cd4+ T Cell Survival. In: Gupta, S., Butcher, E. & Paul, W. (eds.). *Lymphocyte Activation and Immune Regulation IX: Homeostasis and Lymphocyte Traffic*. Boston, MA, Springer US. pp. 97-105.
- Gerondakis, S., Fulford, T. S., Messina, N. L. & Grumont, R. J. (2014) NF-kappa]B control of T cell development. *Nature Immunology*. 15 (1), 15-25.
- Godfrey, D. I., Kennedy, J., Suda, T. & Zlotnik, A. (1993) A developmental pathway involving four phenotypically and functionally distinct subsets of CD3-CD4-CD8- triple-negative adult mouse thymocytes defined by CD44 and CD25 expression. *The Journal of Immunology*. 150 (10), 4244-4252.
- Godfrey, D. I., Rossjohn, J. & McCluskey, J. (2008) The Fidelity, Occasional Promiscuity, and Versatility of T Cell Receptor Recognition. *Immunity*. 28 (3), 304-314.
- Goldrath, A. W. & Bevan, M. J. (1999) Selecting and maintaining a diverse T-cell repertoire. *Nature*. 402 (6759), 255-262.
- Goodarzi, A. A., Yu, Y., Riballo, E., Douglas, P., Walker, S. A., Ye, R., Harer, C., Marchetti, C., Morrice, N., Jeggo, P. A. & Lees-Miller, S. (2006) DNA-PK autophosphorylation facilitates Artemis endonuclease activity. *The EMBO Journal*. 25 (16), 3880-3889.

- Grandjean, I., Duban, L., Bonney, E. A., Corcuff, E., Di Santo, J. P., Matzinger, P. & Lantz, O. (2003) Are Major Histocompatibility Complex Molecules Involved in the Survival of Naive CD4+ T Cells? *The Journal of Experimental Medicine*. 198 (7), 1089-1102.
- Gras, S., Burrows, S. R., Turner, S. J., Sewell, A. K., McCluskey, J. & Rossjohn, J. (2012) A structural voyage toward an understanding of the MHC-I-restricted immune response: Lessons learned and much to be learned. *Immunological Reviews*. 250 (1), 61-81.
- Grawunder, U., Zimmer, D., Fugmann, S., Schwarz, K. & Lieber, M. R. (1998) DNA Ligase IV Is Essential for V(D)J Recombination and DNA Double-Strand Break Repair in Human Precursor Lymphocytes. *Molecular Cell*. 2 (4), 477-484.
- Gu, J., Li, S., Zhang, X., Wang, L., Niewolik, D., Schwarz, K., Legerski, R. J., Zandi, E. & Lieber, M. R. (2010) DNA-PKcs regulates a single-stranded DNA endonuclease activity of Artemis. *DNA Repair*. 9 (4), 429-437.
- Gu, J., Lu, H., Tippin, B., Shimazaki, N., Goodman, M. F. & Lieber, M. R. (2006) XRCC4:DNA ligase IV can ligate incompatible DNA ends and can ligate across gaps. *The EMBO Journal*. 26 (4), 1010-1023.
- Guo, H. -, Jardetzky, T. S., Garrett, T. P. J., Lane, W. S., Strominger, J. L. & Wiley, D. C. (1992) Different length peptides bind to HLA-Aw68 similarly at their ends but bulge out in the middle. *Nature*. 360 (6402), 364-366.
- Haga-Friedman, A., Horovitz-Fried, M. & Cohen, C. J. (2012) Incorporation of Transmembrane Hydrophobic Mutations in the TCR Enhance Its Surface Expression and T Cell Functional Avidity. *The Journal of Immunology*. 188 (11), 5538-5546.
- Hamad, A. R. A., O'Herrin, S. M., Lebowitz, M. S., Srikrishnan, A., Bieler, J., Schneck, J. & Pardoll, D. (1998) Potent T Cell Activation with Dimeric Peptide-Major Histocompatibility Complex Class II Ligand: The Role of CD4 Coreceptor. *The Journal of Experimental Medicine*. 188 (9), 1633-1640.
- Hanabuchi, S., Ito, T., Park, W., Watanabe, N., Shaw, J. L., Roman, E., Arima, K., Wang, Y., Voo, K. S., Cao, W. & Liu, Y. (2010) Thymic Stromal Lymphopoietin-Activated Plasmacytoid Dendritic Cells Induce the Generation of FOXP3+ Regulatory T Cells in Human Thymus. *The Journal of Immunology*. 184 (6), 2999-3007.
- Hansen, T. H. & Bouvier, M. (2009) MHC class I antigen presentation: learning from viral evasion strategies. *Nat Rev Immunol*. 9 (7), 503-513.
- Harwood, N. E. & Batista, F. D. (2010) Early Events in B Cell Activation. *Annual Review of Immunology*. 28 (1), 185-210.
- Hatada, M. H., Lu, X., Laird, E. R., Green, J., Morgenstern, J. P., Lou, M., Marr, C. S., Phillips, T. B., Ram, M. K., Theriault, K., Zoller, M. J. & Karas, J. L. (1995) Molecular basis for interaction of the protein tyrosine kinase ZAP-70 with the T-cell receptor. *Nature*. 377 (6544), 32-38.
- Hawse, W. F., Champion, M. M., Joyce, M. V., Hellman, L. M., Hossain, M., Ryan, V., Pierce, B. G., Weng, Z. & Baker, B. M. (2012) Cutting Edge: Evidence for a Dynamically Driven T Cell Signaling Mechanism. *The Journal of Immunology*. 188 (12), 5819-5823.

- Hayes, S. M. & Love, P. E. (2006) Strength of signal: a fundamental mechanism for cell fate specification. *Immunological Reviews*. 209 (1), 170-175.
- He, X., Park, K., Wang, H., He, X., Zhang, Y., Hua, X., Li, Y. & Kappes, D. J. (2008) CD4-CD8 Lineage Commitment Is Regulated by a Silencer Element at the ThPOK Transcription-Factor Locus. *Immunity*. 28 (3), 346-358.
- He, X., He, X., Dave, V. P., Zhang, Y., Hua, X., Nicolas, E., Xu, W., Roe, B. A. & Kappes, D. J. (2005) The zinc finger transcription factor Th-POK regulates CD4 versus CD8 T-cell lineage commitment. *Nature*. 433 (7028), 826-833.
- Heemskerk, M. H. M. (2010) T-cell receptor gene transfer for the treatment of leukemia and other tumors. *Haematologica*. 95 (1), 15-19.
- Helmink, B. A. & Sleckman, B. P. (2012) The Response to and Repair of RAG-Mediated DNA Double-Strand Breaks. *Annual Review of Immunology*. 30 (1), 175-202.
- Hinterberger, M., Aichinger, M., da Costa, O. P., Voehringer, D., Hoffmann, R. & Klein, L. (2010) Autonomous role of medullary thymic epithelial cells in central CD4+ T cell tolerance. *Nature Immunology*. 11 (6), 512-519.
- Hiom, K. & Gellert, M. (1998) Assembly of a 12/23 paired signal complex: A critical control point in V(D)J recombination. *Molecular Cell*. 1 (7), 1011-1019.
- Ho, W. Y., Blattman, J. N., Dossett, M. L., Yee, C. & Greenberg, P. D. (2003) Adoptive immunotherapy: Engineering T cell responses as biologic weapons for tumor mass destruction. *Cancer Cell*. 3 (5), 431-437.
- Hoeijmakers, J. H. J. (2001) Genome maintenance mechanisms for preventing cancer. *Nature*. 411 (6835), 366-374.
- Holland, S. J., Bartok, I., Attaf, M., Genolet, R., Luescher, I. F., Kotsiou, E., Richard, A., Wang, E., White, M., Coe, D. J., Chai, J., Ferreira, C. & Dyson, J. (2012) The T-cell receptor is not hardwired to engage MHC ligands. *Proceedings of the National Academy of Sciences*. 109 (45), E3111-E3118.
- Holler, P. D., Holman, P. O., Shusta, E. V., O'Herrin, S., Wittrup, K. D. & Kranz, D. M. (2000) In vitro evolution of a T cell receptor with high affinity for peptide/MHC. *Proceedings of the National Academy of Sciences of the United States of America*. 97 (10), 5387-5392.
- Holst, J., Vignali, K. M., Burton, A. R. & Vignali, D. A. A. (2006) Rapid analysis of T-cell selection in vivo using T cell-receptor retrogenic mice. *Nat Meth*. 3 (3), 191-197.
- Huang, F. & Nau, W. M. (2003) A Conformational Flexibility Scale for Amino Acids in Peptides. *Angewandte Chemie International Edition*. 42 (20), 2269-2272.
- Hubert, F., Kinkel, S. A., Davey, G. M., Phipson, B., Mueller, S. N., Liston, A., Proietto, A. I., Cannon, P. Z. F., Forehan, S., Smyth, G. K., Wu, L., Goodnow, C. C., Carbone, F. R., Scott, H. S. & Heath, W. R. (2011) Aire regulates the transfer of antigen from mTECs to dendritic cells for induction of thymic tolerance. *Blood*. 118 (9), 2462-2472.

- Hudson, L. L., Markert, M. L., Devlin, B. H., Haynes, B. F. & Sempowski, G. D. (2007) Human T Cell Reconstitution in DiGeorge Syndrome and HIV-1 Infection. *Seminars in Immunology*. 19 (5), 297-309.
- Hughes, M. M., Yassai, M., Sedy, J. R., Wehrly, T. D., Huang, C., Kanagawa, O., Gorski, J. & Sleckman, B. P. (2003) T cell receptor CDR3 loop length repertoire is determined primarily by features of the V(D)J recombination reaction. *European Journal of Immunology*. 33 (6), 1568-1575.
- Huppa, J. B., Axmann, M., Mortelmaier, M. A., Lillemeier, B. F., Newell, E. W., Brameshuber, M., Klein, L. O., Schutz, G. J. & Davis, M. M. (2010) TCR-peptide-MHC interactions in situ show accelerated kinetics and increased affinity. *Nature*. 463 (7283), 963-967.
- Huseby, E. S., White, J., Crawford, F., Vass, T., Becker, D., Pinilla, C., Marrack, P. & Kappler, J. W. (2005) How the T Cell Repertoire Becomes Peptide and MHC Specific. *Cell*. 122 (2), 247-260.
- Im, E. J., Bais, A. J., Yang, W., Ma, Q., Guo, X., Sepe, S. M. & Junghans, R. P. (2014) Recombination-deletion between homologous cassettes in retrovirus is suppressed via a strategy of degenerate codon substitution. *Molecular Therapy Methods & Clinical Development*. 114022.
- Itano, A., Salmon, P., Kioussis, D., Tolaini, M., Corbella, P. & Robey, E. (1996) The cytoplasmic domain of CD4 promotes the development of CD4 lineage T cells. *The Journal of Experimental Medicine*. 183 (3), 731-741.
- Jameson, S. C., Kaye, J. & Gascoigne, N. R. J. (1990) A T cell receptor Va region selectively expressed in CD4+ cells. *Journal of Immunology*. 145 (5), 1324-1331.
- Janeway, C. A., Travers, P., Walport, M. & Capra, J. D. (2005) Immunobiology: the immune system in health and disease.
- Janeway, C. A. & Medzhitov, R. (2002) INNATE IMMUNE RECOGNITION. *Annual Review of Immunology*. 20 (1), 197-216.
- Johnson, G. & Wu, T. T. (1999) Random length assortment of human and mouse T cell receptor for antigen agr] and bgr] chain CDR3. *Immunology and Cell Biology*. 77 (5), 391-394.
- Jones, J. M. & Gellert, M. (2002) Ordered assembly of the V(D)J synaptic complex ensures accurate recombination. *The EMBO Journal*. 21 (15), 4162-4171.
- Jorgensen, J. L., Esser, U., De St. Groth, B. F., Reay, P. A. & Davis, M. M. (1992) Mapping T-cell receptor-peptide contacts by variant peptide immunization of single-chain transgenics. *Nature*. 355 (6357), 224-230.
- Jung, D. & Alt, F. W. (2004) Unraveling V(D)J Recombination: Insights into Gene Regulation. *Cell*. 116 (2), 299-311.
- Kaiko, G. E., Horvat, J. C., Beagley, K. W. & Hansbro, P. M. (2007) Immunological decision-making: how does the immune system decide to mount a helper T-cell response? *Immunology*. 123 (3), 326-338.
- Kappes, D. J., He, X. & He, X. (2005) CD4-CD8 lineage commitment: an inside view. *Nature Immunology*. 6 (8), 761-766.

- Kappler, J. W., Roehm, N. & Marrack, P. (1987) T cell tolerance by clonal elimination in the thymus. *Cell*. 49 (2), 273-280.
- Kawakami, Y., Eliyahu, S., Delgado, C. H., Robbins, P. F., Sakaguchi, K., Appella, E., Yannelli, J. R., Adema, G. J., Miki, T. & Rosenberg, S. A. (1994) Identification of a human melanoma antigen recognized by tumor-infiltrating lymphocytes associated with in vivo tumor rejection. *Proceedings of the National Academy of Sciences of the United States of America*. 91 (14), 6458-6462.
- Kawamoto, H., Ohmura, K., Fujimoto, S. & Katsura, Y. (1999) Emergence of T Cell Progenitors Without B Cell or Myeloid Differentiation Potential at the Earliest Stage of Hematopoiesis in the Murine Fetal Liver. *The Journal of Immunology*. 162 (5), 2725-2731.
- Kelly, B. T., Tam, J. S., Verbsky, J. W. & Routes, J. M. (2013) Screening for severe combined immunodeficiency in neonates. *Clinical Epidemiology*. 5363-369.
- Kern, P., Hussey, R. E., Spoerl, R., Reinherz, E. L. & Chang, H. -. (1999) Expression, purification, and functional analysis of murine ectodomain fragments of CD8 $\alpha\alpha$ and CD8 $\alpha\beta$ dimers. *Journal of Biological Chemistry*. 274 (38), 27237-27243.
- Kessels, H. W. H. G., van den Boom, M. D., Spits, H., Hooijberg, E. & Schumacher, T. N. M. (2000) Changing T cell specificity by retroviral T cell receptor display. *Proceedings of the National Academy of Sciences*. 97 (26), 14578-14583.
- Kieke, M. C., Shusta, E. V., Boder, E. T., Teyton, L., Wittrup, K. D. & Kranz, D. M. (1999) Selection of functional T cell receptor mutants from a yeast surface-display library. *Proceedings of the National Academy of Sciences*. 96 (10), 5651-5656.
- Kim, J. H., Lee, S., Li, L., Park, H., Park, J., Lee, K. Y., Kim, M., Shin, B. A. & Choi, S. (2011) High Cleavage Efficiency of a 2A Peptide Derived from Porcine Teschovirus-1 in Human Cell Lines, Zebrafish and Mice. *PLoS ONE*. 6 (4), e18556.
- Kjer-Nielsen, L., Patel, O., Corbett, A. J., Le Nours, J., Meehan, B., Liu, L., Bhati, M., Chen, Z., Kostenko, L., Reantragoon, R., Williamson, N. A., Purcell, A. W., Dudek, N. L., McConville, M. J., O'Hair, R. A. J., Khairallah, G. N., Godfrey, D. I., Fairlie, D. P., Rossjohn, J. & McCluskey, J. (2012) MR1 presents microbial vitamin B metabolites to MAIT cells. *Nature*. 491 (7426), 717-723.
- Kjer-Nielsen, L., Dunstone, M. A., Kostenko, L., Ely, L. K., Beddoe, T., Mifsud, N. A., Purcell, A. W., Brooks, A. G., McCluskey, J. & Rossjohn, J. (2004) Crystal structure of the human T cell receptor CD3 $\epsilon\gamma$ heterodimer complexed to the therapeutic mAb OKT3. *Proceedings of the National Academy of Sciences of the United States of America*. 101 (20), 7675-7680.
- Klein, L., Kyewski, B., Allen, P. M. & Hogquist, K. A. (2014) Positive and negative selection of the T cell repertoire: what thymocytes see (and don't see). *Nat Rev Immunol*. 14 (6), 377-391.
- Koch, U. & Radtke, F. (2011) Mechanisms of T Cell Development and Transformation. *Annual Review of Cell and Developmental Biology*. 27 (1), 539-562.
- Koop, B. F., Wilson, R. K., Wang, K., Vernooij, B., Zaller, D., Kuo, C. L., Seto, D., Toda, M. & Hood, L. (1992) Organization, structure, and function of 95 kb of DNA spanning the murine T-cell receptor Ca Cd region. *Genomics*. 13 (4), 1209-1230.

- Kretschmer, K., Apostolou, I., Hawiger, D., Khazaie, K., Nussenzweig, M. C. & von Boehmer, H. (2005) Inducing and expanding regulatory T cell populations by foreign antigen. *Nature Immunology*. 6 (12), 1219-1227.
- Kronenberg, M. & Zajonc, D. M. (2013) A 'GEM' of a cell. *Nature Immunology*. 14 (7), 694-695.
- Kuhns, M. S. & Badgandi, H. B. (2012) Piecing together the family portrait of TCR-CD3 complexes. *Immunological Reviews*. 250 (1), 120-143.
- Kuhns, M. S. & Davis, M. M. (2007) Disruption of Extracellular Interactions Impairs T Cell Receptor-CD3 Complex Stability and Signaling. *Immunity*. 26 (3), 357-369.
- Kuhns, M. S., Davis, M. M. & Garcia, K. C. (2006) Deconstructing the Form and Function of the TCR/CD3 Complex. *Immunity*. 24 (2), 133-139.
- Kulski, J. K., Shiina, T., Anzai, T., Kohara, S. & Inoko, H. (2002) Comparative genomic analysis of the MHC: the evolution of class I duplication blocks, diversity and complexity from shark to man. *Immunological Reviews*. 190 (1), 95-122.
- Kumar, R. K., Cristan, H. & Paul, S. (2008) *The "Classical" Ovalbumin Challenge Model of Asthma in Mice*.
- Kunjibettu, S., Fuller-Espie, S., Carey, G. B. & Spain, L. M. (2001) Conserved transmembrane tyrosine residues of the TCR β chain are required for TCR expression and function in primary T cells and hybridomas. *International Immunology*. 13 (2), 211-222.
- Kurioka, A., Ussher, J. E., Cosgrove, C., Clough, C., Fergusson, J. R., Smith, K., Kang, Y., Walker, L. J., Hansen, T. H., Willberg, C. B. & Klenerman, P. (2015) MAIT cells are licensed through granzyme exchange to kill bacterially sensitized targets. *Mucosal Immunol*. 8 (2), 429-440.
- Kyewski, B. & Klein, L. (2006) A CENTRAL ROLE FOR CENTRAL TOLERANCE. *Annual Review of Immunology*. 24 (1), 571-606.
- Lacorazza, H. D., Tuček-Szabo, C., Vasović, L. V., Remus, K. & Nikolich-Žugich, J. (2001) Premature TCR $\alpha\beta$ Expression and Signaling in Early Thymocytes Impair Thymocyte Expansion and Partially Block Their Development. *The Journal of Immunology*. 166 (5), 3184-3193.
- Landolfi, N. F., Thakur, A. B., Fu, H., Vásquez, M., Queen, C. & Tsurushita, N. (2001) The Integrity of the Ball-and-Socket Joint Between V and C Domains Is Essential for Complete Activity of a Humanized Antibody. *The Journal of Immunology*. 166 (3), 1748-1754.
- Laugel, B., van den Berg, H. A., Gostick, E., Cole, D. K., Wooldridge, L., Boulter, J., Milicic, A., Price, D. A. & Sewell, A. K. (2007) Different T Cell Receptor Affinity Thresholds and CD8 Coreceptor Dependence Govern Cytotoxic T Lymphocyte Activation and Tetramer Binding Properties. *Journal of Biological Chemistry*. 282 (33), 23799-23810.
- Lauritsen, J. P. H., Wong, G. W., Lee, S., Lefebvre, J. M., Ciofani, M., Rhodes, M., Kappes, D. J., Zúñiga-Pflücker, J. C. & Wiest, D. L. (2009) Differential induction of Id3 signals lineage divergence, Notch-independent differentiation, and functional maturation of gamma delta T cells. *Immunity*. 31 (4), 565-575.

Laydon, D. J., Bangham, C. R. M. & Asquith, B. (2015) Estimating T-cell repertoire diversity: limitations of classical estimators and a new approach. *Philosophical Transactions of the Royal Society B: Biological Sciences*. 370 (1675), 20140291.

Lee, G. S., Neiditch, M. B., Salus, S. S. & Roth, D. B. (2004) RAG Proteins Shepherd Double-Strand Breaks to a Specific Pathway, Suppressing Error-Prone Repair, but RAG Nicking Initiates Homologous Recombination. *Cell*. 117 (2), 171-184.

Lee, K. -, Huang, J., Takeda, Y. & Dynan, W. S. (2000) DNA ligase IV and XRCC4 form a stable mixed tetramer that functions synergistically with other repair factors in a cell-free end-joining system. *Journal of Biological Chemistry*. 275 (44), 34787-34796.

Lefranc, M. (2005) IMGT, the international ImMunoGeneTics information system[®]: a standardized approach for immunogenetics and immunoinformatics. *Immunome Research*. 13-3.

Lefranc, M., Giudicelli, V., Ginestoux, C., Jabado-Michaloud, J., Folch, G., Bellahcene, F., Wu, Y., Gemrot, E., Brochet, X., Lane, J., Regnier, L., Ehrenmann, F., Lefranc, G. & Duroux, P. (2009) IMGT[®], the international ImMunoGeneTics information system[®]. *Nucleic Acids Research*. 37 (suppl 1), D1006-D1012.

Lesk, A. M. & Chothia, C. (1988) Elbow motion in the immunoglobulins involves a molecular ball-and-socket joint. *Nature*. 335 (6186), 188-190.

Li, Q., Dinner, A. R., Qi, S., Irvine, D. J., Huppa, J. B., Davis, M. M. & Chakraborty, A. K. (2004) CD4 enhances T cell sensitivity to antigen by coordinating Lck accumulation at the immunological synapse. *Nature Immunology*. 5 (8), 791-799.

Li, S., Chang, H. H., Niewolik, D., Hedrick, M. P., Pinkerton, A. B., Hassig, C. A., Schwarz, K. & Lieber, M. R. (2014) Evidence That the DNA Endonuclease ARTEMIS also Has Intrinsic 5'-Exonuclease Activity. *Journal of Biological Chemistry*. 289 (11), 7825-7834.

Li, Y., Moysey, R., Molloy, P. E., Vuidepot, A., Mahon, T., Baston, E., Dunn, S., Liddy, N., Jacob, J., Jakobsen, B. K. & Boulter, J. M. (2005) Directed evolution of human T-cell receptors with picomolar affinities by phage display. *Nat Biotech*. 23 (3), 349-354.

Liddy, N., Bossi, G., Adams, K. J., Lissina, A., Mahon, T. M., Hassan, N. J., Gavarret, J., Bianchi, F. C., Pumphrey, N. J., Ladell, K., Gostick, E., Sewell, A. K., Lissin, N. M., Harwood, N. E., Molloy, P. E., Li, Y., Cameron, B. J., Sami, M., Baston, E. E., Todorov, P. T., Paston, S. J., Dennis, R. E., Harper, J. V., Dunn, S. M., Ashfield, R., Johnson, A., McGrath, Y., Plesa, G., June, C. H., Kalos, M., Price, D. A., Vuidepot, A., Williams, D. D., Sutton, D. H. & Jakobsen, B. K. (2012) Monoclonal TCR-redirectioned tumor cell killing. *Nature Medicine*. 18 (6), 980-987.

Lieberman, J. (2003) The ABCs of granule-mediated cytotoxicity: new weapons in the arsenal. *Nat Rev Immunol*. 3 (5), 361-370.

Linette, G. P., Stadtmauer, E. A., Maus, M. V., Rapoport, A. P., Levine, B. L., Emery, L., Litzky, L., Bagg, A., Carreno, B. M., Cimino, P. J., Binder-Scholl, G., Smethurst, D. P., Gerry, A. B., Pumphrey, N. J., Bennett, A. D., Brewer, J. E., Dukes, J., Harper, J., Tayton-Martin, H., Jakobsen, B. K., Hassan, N. J., Kalos, M. & June, C. H. (2013) Cardiovascular toxicity and titin cross-reactivity of affinity-enhanced T cells in myeloma and melanoma. *Blood*. 122 (6), 863-871.

- Lio, C. J., Dodson, L. F., Deppong, C. M., Hsieh, C. & Green, J. M. (2010) CD28 Facilitates the Generation of Foxp3- Cytokine Responsive Regulatory T Cell Precursors. *The Journal of Immunology*. 184 (11), 6007-6013.
- Lio, C. J. & Hsieh, C. (2008) A Two-Step Process for Thymic Regulatory T Cell Development. *Immunity*. 28 (1), 100-111.
- Liston, A., Nutsch, K. M., Farr, A. G., Lund, J. M., Rasmussen, J. P., Koni, P. A. & Rudensky, A. Y. (2008) Differentiation of regulatory Foxp3+ T cells in the thymic cortex. *Proceedings of the National Academy of Sciences*. 105 (33), 11903-11908.
- Liu, Y., Zhang, P., Li, J., Kulkarni, A. B., Perruche, S. & Chen, W. (2008) A critical function for TGF-beta] signaling in the development of natural CD4+CD25+Foxp3+ regulatory T cells. *Nature Immunology*. 9 (6), 632-640.
- Livák, F., Tourigny, M., Schatz, D. G. & Petrie, H. T. (1999) Characterization of TCR Gene Rearrangements During Adult Murine T Cell Development. *The Journal of Immunology*. 162 (5), 2575-2580.
- Lu, H., Schwarz, K. & Lieber, M. R. (2007) Extent to which hairpin opening by the Artemis:DNA-PKcs complex can contribute to junctional diversity in V(D)J recombination. *Nucleic Acids Research*. 35 (20), 6917-6923.
- Lu, M., Tayu, R., Ikawa, T., Masuda, K., Matsumoto, I., Mugishima, H., Kawamoto, H. & Katsura, Y. (2005) The Earliest Thymic Progenitors in Adults Are Restricted to T, NK, and Dendritic Cell Lineage and Have a Potential to Form More Diverse TCR β Chains than Fetal Progenitors. *The Journal of Immunology*. 175 (9), 5848-5856.
- Luckey, M. A., Kimura, M. Y., Waickman, A. T., Feigenbaum, L., Singer, A. & Park, J. (2014) The transcription factor ThPOK suppresses Runx3 and imposes CD4+ lineage fate by inducing the SOCS suppressors of cytokine signaling. *Nature Immunology*. 15 (7), 638-645.
- Luescher, I. F., Vivier, E., Layer, A., Mahiou, J., Godeau, F., Malissen, B. & Romero, P. (1995) CD8 modulation of T-cell antigen receptor-ligand interactions on living cytotoxic T lymphocytes. *Nature*. 373 (6512), 353-356.
- Lynch, G. W., Slaytor, E. K., Elliott, F. D., Saurajen, A., Turville, S. G., Sloane, A. J., Cameron, P. U., Cunningham, A. L. & Halliday, G. M. (2003) CD4 is expressed by epidermal Langerhans' cells predominantly as covalent dimers. *Experimental Dermatology*. 12 (5), 700-711.
- Ma, Y., Pannicke, U., Schwarz, K. & Lieber, M. R. (2002) Hairpin Opening and Overhang Processing by an Artemis/DNA-Dependent Protein Kinase Complex in Nonhomologous End Joining and V(D)J Recombination. *Cell*. 108 (6), 781-794.
- Ma, Y., Schwarz, K. & Lieber, M. R. (2005) The Artemis:DNA-PKcs endonuclease cleaves DNA loops, flaps, and gaps. *DNA Repair*. 4 (7), 845-851.
- Machida, K. & Mayer, B. J. (2005) The SH2 domain: versatile signaling module and pharmaceutical target. *Biochimica Et Biophysica Acta (BBA) - Proteins and Proteomics*. 1747 (1), 1-25.

- Madura, F., Rizkallah, P. J., Holland, C. J., Fuller, A., Bulek, A., Godkin, A. J., Schauenburg, A. J., Cole, D. K. & Sewell, A. K. (2015) Structural basis for ineffective T-cell responses to MHC anchor residue-improved "heteroclitic" peptides. *European Journal of Immunology*. 45 (2), 584-591.
- Maekawa, A., Schmidt, B., Fazekas de St. Groth, B., Sanejouand, Y. & Hogg, P. J. (2006) Evidence for a Domain-Swapped CD4 Dimer as the Coreceptor for Binding to Class II MHC. *The Journal of Immunology*. 176 (11), 6873-6878.
- Mahaney, B. L., Meek, K. & Lees-Miller, S. (2009) Repair of ionizing radiation-induced DNA double strand breaks by non-homologous end-joining. *The Biochemical Journal*. 417 (3), 639-650.
- Maillard, I., Tu, L., Sambandam, A., Yashiro-Ohtani, Y., Millholland, J., Keeshan, K., Shestova, O., Xu, L., Bhandoola, A. & Pear, W. S. (2006) The requirement for Notch signaling at the β -selection checkpoint in vivo is absolute and independent of the pre-T cell receptor. *The Journal of Experimental Medicine*. 203 (10), 2239-2245.
- Malecek, K., Zhong, S., McGary, K., Yu, C., Huang, K., Johnson, L. A., Rosenberg, S. A. & Krogsgaard, M. (2013) Engineering improved T cell receptors using an alanine-scan guided T cell display selection system. *Journal of Immunological Methods*. 392 (0), 1-11.
- Markert, M. L., Hummell, D. S., Rosenblatt, H. M., Schiff, S. E., Harville, T. O., Williams, L. W., Schiff, R. I. & Buckley, R. H. (1998) Complete DiGeorge syndrome: Persistence of profound immunodeficiency. *The Journal of Pediatrics*. 132 (1), 15-21.
- Marrack, P. & Kappler, J. (1988) T cells can distinguish between allogeneic major histocompatibility complex products on different cell types. *Nature*. 332 (6167), 840-843.
- Marrack, P., Scott-Browne, J., Dai, S., Gapin, L. & Kappler, J. W. (2008) Evolutionarily Conserved Amino Acids That Control TCR-MHC Interaction. *Annual Review of Immunology*. 26 (1), 171-203.
- Mason, D. (1998) A very high level of crossreactivity is an essential feature of the T-cell receptor. *Immunology Today*. 19 (9), 395-404.
- Mathis, D. & Benoist, C. (2009) Aire. *Annual Review of Immunology*. 27 (1), 287-312.
- Matthias, L. J., Yam, P. T. W., Jiang, X., Vandegraaff, N., Li, P., Pombourios, P., Donoghue, N. & Hogg, P. J. (2002) Disulfide exchange in domain 2 of CD4 is required for entry of HIV-1. *Nature Immunology*. 3 (8), 727-732.
- Mazza, C. & Malissen, B. (2007) What guides MHC-restricted TCR recognition? *Seminars in Immunology*. 19 (4), 225-235.
- McCarthy, M. K. & Weinberg, J. B. (2015) The immunoproteasome and viral infection: a complex regulator of inflammation. *Frontiers in Microbiology*. 621.
- Metzger, T. C. & Anderson, M. S. (2011) Control of central and peripheral tolerance by Aire. *Immunological Reviews*. 241 (1), 89-103.
- Michie, A. M. & Zúñiga-Pflücker, J. C. (2002) Regulation of thymocyte differentiation: pre-TCR signals and β -selection. *Seminars in Immunology*. 14 (5), 311-323.

- Miles, J. J., Douek, D. C. & Price, D. A. (2011) Bias in the alpha beta T-cell repertoire: implications for disease pathogenesis and vaccination. *Immunology and Cell Biology*. 89 (3), 375-387.
- Miles, J. J., Elhassen, D., Borg, N. A., Silins, S. L., Tynan, F. E., Burrows, J. M., Purcell, A. W., Kjer-Nielsen, L., Rossjohn, J., Burrows, S. R. & McCluskey, J. (2005) CTL Recognition of a Bulged Viral Peptide Involves Biased TCR Selection. *The Journal of Immunology*. 175 (6), 3826-3834.
- Miles, J. J., McCluskey, J., Rossjohn, J. & Gras, S. (2015) Understanding the complexity and malleability of T-cell recognition. *Immunology and Cell Biology*. 93 (5), 433-441.
- Modesti, M., Hesse, J. E. & Gellert, M. (1999) DNA binding of Xrcc4 protein is associated with V(D)J recombination but not with stimulation of DNA ligase IV activity. *The EMBO Journal*. 18 (7), 2008-2018.
- Modesti, M., Junop, M. S., Ghirlando, R., van de Rakt, M., Gellert, M., Yang, W. & Kanaar, R. (2003) Tetramerization and DNA Ligase IV Interaction of the DNA Double-strand Break Repair Protein XRCC4 are Mutually Exclusive. *Journal of Molecular Biology*. 334 (2), 215-228.
- Moldovan, M., Yachou, A., Lévesque, K., Wu, H., Hendrickson, W. A., Cohen, E. A. & Sékaly, R. (2002) CD4 Dimers Constitute the Functional Component Required for T Cell Activation. *The Journal of Immunology*. 169 (11), 6261-6268.
- Mombaerts, P., Clarke, A. R., Rudnicki, M. A., Iacomini, J., Itohara, S., Lafaille, J. J., Wang, L., Ichikawa, Y., Jaenisch, R., Hooper, M. L. & Tonegawa, S. (1992) Mutations in T-cell antigen receptor genes alpha and beta block thymocyte development at different stages. *Nature*. 360 (6401), 225-231.
- Morgan, R. A., Dudley, M. E., Wunderlich, J. R., Hughes, M. S., Yang, J. C., Sherry, R. M., Royal, R. E., Topalian, S. L., Kammula, U. S., Restifo, N. P., Zheng, Z., Nahvi, A., de Vries, C., Rogers-Freezer, L., Mavroukakis, S. A. & Rosenberg, S. A. (2006) Cancer Regression in Patients After Transfer of Genetically Engineered Lymphocytes. *Science (New York, N.Y.)*. 314 (5796), 126-129.
- Moss, P. A. H. & Bell, J. I. (1996) Comparative sequence analysis of the human T cell receptor TCRA and TCRB CDR3 regions. *Human Immunology*. 48 (1-2), 32-38.
- Motea, E. A. & Berdis, A. J. (2010) Terminal deoxynucleotidyl transferase: The story of a misguided DNA polymerase. *Biochimica Et Biophysica Acta (BBA) - Proteins and Proteomics*. 1804 (5), 1151-1166.
- Mundy, C. L., Patenge, N., Matthews, A. G. W. & Oettinger, M. A. (2002) Assembly of the RAG1/RAG2 Synaptic Complex. *Molecular and Cellular Biology*. 22 (1), 69-77.
- Münz, C. (2012) Antigen Processing for MHC Class II Presentation via Autophagy. *Frontiers in Immunology*. 39.
- Neefjes, J. (1999) CIIV, MIIC and other compartments for MHC class II loading. *European Journal of Immunology*. 29 (5), 1421-1425.
- Neefjes, J., Jongsma, M. L. M., Paul, P. & Bakke, O. (2011) Towards a systems understanding of MHC class I and MHC class II antigen presentation. *Nat Rev Immunol*. 11 (12), 823-836.
- Nika, K., Soldani, C., Salek, M., Paster, W., Gray, A., Etzensperger, R., Fugger, L., Polzella, P., Cerundolo, V., Dushek, O., Höfer, T., Viola, A. & Acuto, O. (2010) Constitutively Active Lck Kinase in T Cells Drives Antigen Receptor Signal Transduction. *Immunity*. 32 (6), 766-777.

- Nishana, M. & Raghavan, S. C. (2012) Role of recombination activating genes in the generation of antigen receptor diversity and beyond. *Immunology*. 137 (4), 271-281.
- Noris, M., Casiraghi, F., Todeschini, M., Cravedi, P., Cugini, D., Monteferrante, G., Aiello, S., Cassis, L., Gotti, E., Gaspari, F., Cattaneo, D., Perico, N. & Remuzzi, G. (2007) Regulatory T Cells and T Cell Depletion: Role of Immunosuppressive Drugs. *Journal of the American Society of Nephrology*. 18 (3), 1007-1018.
- Novotný, J., Tonegawa, S., Saito, H., Kranz, D. M. & Eisen, H. N. (1986) Secondary, tertiary, and quaternary structure of T-cell-specific immunoglobulin-like polypeptide chains. *Proceedings of the National Academy of Sciences of the United States of America*. 83 (3), 742-746.
- Oh, J. & Shin, J. (2015) The Role of Dendritic Cells in Central Tolerance. *Immune Network*. 15 (3), 111-120.
- Ohnmacht, C., Pullner, A., King, S. B. S., Drexler, I., Meier, S., Brocker, T. & Voehringer, D. (2009) Constitutive ablation of dendritic cells breaks self-tolerance of CD4 T cells and results in spontaneous fatal autoimmunity. *The Journal of Experimental Medicine*. 206 (3), 549-559.
- Okazaki, K. & Sakano, H. (1988) Thymocyte circular DNA excised from T cell receptor alpha-delta gene complex. *EMBO Journal*. 7 (6), 1669-1674.
- Olaru, A., Petrie, H. T. & Livák, F. (2005) Beyond the 12/23 Rule of VDJ Recombination Independent of the Rag Proteins. *The Journal of Immunology*. 174 (10), 6220-6226.
- Ouyang, W., Beckett, O., Ma, Q. & Li, M. O. (2010) Transforming Growth Factor- β Signaling Curbs Thymic Negative Selection Promoting Regulatory T Cell Development. *Immunity*. 32 (5), 642-653.
- Ouyang, W., Kolls, J. K. & Zheng, Y. (2008) The Biological Functions of T Helper 17 Cell Effector Cytokines in Inflammation. *Immunity*. 28 (4), 454-467.
- Pace, C. N. & Scholtz, J. M. (1998) A helix propensity scale based on experimental studies of peptides and proteins. *Biophysical Journal*. 75 (1), 422-427.
- Pang, S. S., Berry, R., Chen, Z., Kjer-Nielsen, L., Perugini, M. A., King, G. F., Wang, C., Chew, S. H., La Gruta, N. L., Williams, N. K., Beddoe, T., Tiganis, T., Cowieson, N. P., Godfrey, D. I., Purcell, A. W., Wilce, M. C. J., McCluskey, J. & Rossjohn, J. (2010) The structural basis for autonomous dimerization of the pre-T-cell antigen receptor. *Nature*. 467 (7317), 844-848.
- Pannetier, C., Cochet, M., Darche, S., Casrouge, A., Zöller, M. & Kourilsky, P. (1993) The sizes of the CDR3 hypervariable regions of the murine T-cell receptor beta chains vary as a function of the recombined germ-line segments. *Proceedings of the National Academy of Sciences*. 90 (9), 4319-4323.
- Park, K., He, X., Lee, H., Hua, X., Li, Y., Wiest, D. & Kappes, D. J. (2010) TCR-mediated ThPOK induction promotes development of mature (CD24-) $\gamma\delta$ thymocytes. *The EMBO Journal*. 29 (14), 2329-2341.
- Pear, W. S., Miller, J. P., Xu, L., Pui, J. C., Soffer, B., Quackenbush, R. C., Pendergast, A. M., Bronson, R., Aster, J. C., Scott, M. L. & Baltimore, D. (1998) Efficient and Rapid Induction of a Chronic Myelogenous Leukemia-Like Myeloproliferative Disease in Mice Receiving P210 bcr/abl-Transduced Bone Marrow. *Blood*. 92 (10), 3780-3792.

- Pecht, I. & Gakamsky, D. M. (2005) Spatial coordination of CD8 and TCR molecules controls antigen recognition by CD8+ T-cells. *FEBS Letters*. 579 (15), 3336-3341.
- Pereira, P., Boucontet, L. & Cumano, A. (2012) Temporal Predisposition to $\alpha\beta$ and $\gamma\delta$ T Cell Fates in the Thymus. *The Journal of Immunology*. 188 (4), 1600-1608.
- Perez-Diez, A., Joncker, N. T., Choi, K., Chan, W. F. N., Anderson, C. C., Lantz, O. & Matzinger, P. (2007) CD4 cells can be more efficient at tumor rejection than CD8 cells. *Blood*. 109 (12), 5346-5354.
- Petrie, H. T. & Zúñiga-Pflücker, J. C. (2007) Zoned Out: Functional Mapping of Stromal Signaling Microenvironments in the Thymus. *Annual Review of Immunology*. 25 (1), 649-679.
- Plasilova, M., Risitano, A. & Maciejewski, J. P. (2003) Application of the Molecular Analysis of the T-Cell Receptor Repertoire in the Study of Immune-Mediated Hematologic Diseases. *Hematology*. 8 (3), 173-181.
- Probst-Kepper, M., Hecht, H., Herrmann, H., Janke, V., Ocklenburg, F., Klemmner, J., van den Eynde, B. J. & Weiss, S. (2004) Conformational Restraints and Flexibility of 14-Meric Peptides in Complex with HLA-B*3501. *The Journal of Immunology*. 173 (9), 5610-5616.
- Proietto, A. I., van Dommelen, S., Zhou, P., Rizzitelli, A., D'Amico, A., Steptoe, R. J., Naik, S. H., Lahoud, M. H., Liu, Y., Zheng, P., Shortman, K. & Wu, L. (2008) Dendritic cells in the thymus contribute to T-regulatory cell induction. *Proceedings of the National Academy of Sciences of the United States of America*. 105 (50), 19869-19874.
- Purbhoo, M. A., Boulter, J. M., Price, D. A., Vuidepot, A., Hourigan, C. S., Dunbar, P. R., Olson, K., Dawson, S. J., Phillips, R. E., Jakobsen, B. K., Bell, J. I. & Sewell, A. K. (2001) The Human CD8 Coreceptor Effects Cytotoxic T Cell Activation and Antigen Sensitivity Primarily by Mediating Complete Phosphorylation of the T Cell Receptor ζ Chain. *Journal of Biological Chemistry*. 276 (35), 32786-32792.
- Quigley, M., Greenaway, H. Y., Venturi, V., Lindsay, R., Quinn, K. M., Seder, R. A., Douek, D. C., Davenport, M. P. & Price, D. A. (2010) Convergent recombination shapes the clonotypic landscape of the naive T-cell repertoire. *Proceedings of the National Academy of Sciences of the United States of America*. 107 (45), 19414-19419.
- Radauer, C., Nandy, A., Ferreira, F., Goodman, R. E., Larsen, J. N., Lidholm, J., Pomés, A., Raulf-Heimsoth, M., Rozynek, P., Thomas, W. R. & Breiteneder, H. (2014) Update of the WHO/IUIS Allergen Nomenclature Database based on analysis of allergen sequences. *Allergy*. 69 (4), 413-419.
- Raman, M. C. C., Rizkallah, P. J., Simmons, R., Donnellan, Z., Dukes, J., Bossi, G., Le Provost, G., S., Todorov, P., Baston, E., Hickman, E., Mahon, T., Hassan, N., Vuidepot, A., Sami, M., Cole, D. K. & Jakobsen, B. K. (2015) Direct molecular mimicry enables off-target cardiovascular toxicity by an enhanced affinity TCR designed for cancer immunotherapy. *Scientific Reports*. 618851.
- Rangarajan, S. & Mariuzza, R. A. (2014) T cell receptor bias for MHC: co-evolution or co-receptors? *Cellular and Molecular Life Sciences*. 71 (16), 3059-3068.
- Reith, W., LeibundGut-Landmann, S. & Waldburger, J. (2005) Regulation of MHC class II gene expression by the class II transactivator. *Nat Rev Immunol*. 5 (10), 793-806.

- Richman, S. A., Aggen, D. H., Dossett, M. L., Donermeyer, D. L., Allen, P. M., Greenberg, P. D. & Kranz, D. M. (2009) Structural features of T cell receptor variable regions that enhance domain stability and enable expression as single-chain V α V β fragments. *Molecular Immunology*. 46 (5), 902-916.
- Rist, M., Smith, C., Bell, M. J., Burrows, S. R. & Khanna, R. (2009) Cross-recognition of HLA DR4 alloantigen by virus-specific CD8+ T cells: a new paradigm for self-/nonself-recognition. *Blood*. 114 (11), 2244-2253.
- Rivera-Calzada, A., Spagnolo, L., Pearl, L. H. & Llorca, O. (2006) Structural model of full-length human Ku70-Ku80 heterodimer and its recognition of DNA and DNA-PKcs. *EMBO Reports*. 8 (1), 56-62.
- Robins, H. S., Srivastava, S. K., Campregher, P. V., Turtle, C. J., Andriesen, J., Riddell, S. R., Carlson, C. S. & Warren, E. H. (2010) Overlap and effective size of the human CD8(+) T-cell receptor repertoire. *Science Translational Medicine*. 2 (47), 47ra64-47ra64.
- Robinson, J., Mistry, K., McWilliam, H., Lopez, R., Parham, P. & Marsh, S. G. E. (2011) The IMGT/HLA database. *Nucleic Acids Research*. 39 (1), D1171-D1176.
- Roche, P. A. & Furuta, K. (2015) The ins and outs of MHC class II-mediated antigen processing and presentation. *Nat Rev Immunol*. 15 (4), 203-216.
- Rock, E. P., Sibbald, P. R., Davis, M. M. & Chien, Y. H. (1994) CDR3 length in antigen-specific immune receptors. *The Journal of Experimental Medicine*. 179 (1), 323-328.
- Rosenberg, S. A., Restifo, N. P., Yang, J. C., Morgan, R. A. & Dudley, M. E. (2008) Adoptive cell transfer: a clinical path to effective cancer immunotherapy. *Nat Rev Cancer*. 8 (4), 299-308.
- Rossjohn, J., Gras, S., Miles, J. J., Turner, S. J., Godfrey, D. I. & McCluskey, J. (2015) T Cell Antigen Receptor Recognition of Antigen-Presenting Molecules. *Annual Review of Immunology*. 33 (1), 169-200.
- Rubtsova, K., Scott-Browne, J. P., Crawford, F., Dai, S., Marrack, P. & Kappler, J. W. (2009) Many different V β CDR3s can reveal the inherent MHC reactivity of germline-encoded TCR V regions. *Proceedings of the National Academy of Sciences of the United States of America*. 106 (19), 7951-7956.
- Rudd, C. E., Taylor, A. & Schneider, H. (2009) CD28 and CTLA-4 coreceptor expression and signal transduction. *Immunological Reviews*. 229 (1), 12-26.
- Rudolph, M. G., Stanfield, R. L. & Wilson, I. A. (2006) HOW TCRS BIND MHCS, PEPTIDES, AND CORECEPTORS. *Annual Review of Immunology*. 24 (1), 419-466.
- Rudolph, M. G. & Wilson, I. A. (2002) The specificity of TCR/pMHC interaction. *Current Opinion in Immunology*. 14 (1), 52-65.
- Ryan, M. D., FAU, K. A. & Thomas, G. P. (1991) Cleavage of foot-and-mouth disease virus polyprotein is mediated by residues located within a 19 amino acid sequence.
- Sakaguchi, S., Yamaguchi, T., Nomura, T. & Ono, M. (2008) Regulatory T Cells and Immune Tolerance. *Cell*. 133 (5), 775-787.

- Sasada, T., Touma, M., Chang, H., Clayton, L. K., Wang, J. & Reinherz, E. L. (2002) Involvement of the TCR C β FG Loop in Thymic Selection and T Cell Function. *The Journal of Experimental Medicine*. 195 (11), 1419-1431.
- Sato, T., Ohno, S., Hayashi, T., Sato, C., Kohu, K., Satake, M. & Habu, S. (2005) Dual Functions of Runx Proteins for Reactivating CD8 and Silencing CD4 at the Commitment Process into CD8 Thymocytes. *Immunity*. 22 (3), 317-328.
- Schamel, W. W. A., Arechaga, I., Risueño, R. M., van Santen, H. M., Cabezas, P., Risco, C., Valpuesta, J. M. & Alarcón, B. (2005) Coexistence of multivalent and monovalent TCRs explains high sensitivity and wide range of response. *The Journal of Experimental Medicine*. 202 (4), 493-503.
- Schatz, D. G. & Ji, Y. (2011) Recombination centres and the orchestration of V(D)J recombination. *Nat Rev Immunol*. 11 (4), 251-263.
- Scott-Browne, J., Crawford, F., Young, M. H., Kappler, J. W., Marrack, P. & Gapin, L. (2011) Evolutionarily conserved features contribute to $\alpha\beta$ T cell receptor specificity. *Immunity*. 35 (4), 526-535.
- Scott-Browne, J., White, J., Kappler, J. W., Gapin, L. & Marrack, P. (2009) Germline-encoded amino acids in the $\alpha\beta$ T-cell receptor control thymic selection. *Nature*. 458 (7241), 1043-1046.
- Seddon, B. & Zamoyska, R. (2002) TCR Signals Mediated by Src Family Kinases Are Essential for the Survival of Naive T Cells. *The Journal of Immunology*. 169 (6), 2997-3005.
- Setoguchi, R., Tachibana, M., Naoe, Y., Muroi, S., Akiyama, K., Tezuka, C., Okuda, T. & Taniuchi, I. (2008) Repression of the Transcription Factor Th-POK by Runx Complexes in Cytotoxic T Cell Development. *Science*. 319 (5864), 822-825.
- Sewell, A. K. (2012) Why must T cells be cross-reactive? *Nat Rev Immunol*. 12 (9), 669-677.
- Sharma, S. & Thomas, P. G. (2013) The two faces of heterologous immunity: protection or immunopathology. *Journal of Leukocyte Biology*. 95 (3), 405-416.
- Shevach, E. M. (2009) Mechanisms of Foxp3⁺ T Regulatory Cell-Mediated Suppression. *Immunity*. 30 (5), 636-645.
- Siegers, G. M., Swamy, M., Fernández-Malavé, E., Minguet, S., Rathmann, S., Guardo, A. C., Pérez-Flores, V., Regueiro, J. R., Alarcón, B., Fisch, P. & Schamel, W. W. A. (2007) Different composition of the human and the mouse $\gamma\delta$ T cell receptor explains different phenotypes of CD3 γ and CD3 δ immunodeficiencies. *The Journal of Experimental Medicine*. 204 (11), 2537-2544.
- Sim, B. -, Zerva, L., Greene, M. I. & Gascoigne, N. R. J. (1996) Control of MHC restriction by TCR V(a) CDR1 and CDR2. *Science*. 273 (5277), 963-966.
- Sinclair, C., Bains, I., Yates, A. J. & Seddon, B. (2013) Asymmetric thymocyte death underlies the CD4:CD8 T-cell ratio in the adaptive immune system. *Proceedings of the National Academy of Sciences of the United States of America*. 110 (31), E2905-E2914.
- Singer, A., Adoro, S. & Park, J. (2008) Lineage fate and intense debate: myths, models and mechanisms of CD4- versus CD8-lineage choice. *Nat Rev Immunol*. 8 (10), 788-801.

Singh, Y., Ferreira, C., Chan, A. C. Y., Dyson, J. & Garden, O. A. (2010) Restricted TCR- α CDR3 Diversity Disadvantages Natural Regulatory T Cell Development in the B6.2.16 β -Chain Transgenic Mouse. *The Journal of Immunology*. 185 (6), 3408-3416.

Sleckman, B. P., Bassing, C. H., Hughes, M. M., Okada, A., D'Auteuil, M., Wehrly, T. D., Woodman, B. B., Davidson, L., Chen, J. & Alt, F. W. (2000) Mechanisms that direct ordered assembly of T cell receptor β locus V, D, and J gene segments. *Proceedings of the National Academy of Sciences*. 97 (14), 7975-7980.

Smethurst, D. (2013) A pharmacologic perspective on newly emerging T-cell manipulation technologies. *British Journal of Clinical Pharmacology*. 76 (2), 173-187.

Smith-Garvin, J., Koretzky, G. A. & Jordan, M. S. (2009) T Cell Activation. *Annual Review of Immunology*. 27 (1), 591-619.

Soetandyo, N., Wang, Q., Ye, Y. & Li, L. (2010) Role of intramembrane charged residues in the quality control of unassembled T-cell receptor alpha-chains at the endoplasmic reticulum. *Journal of Cell Science*. 123 (7), 1031-1038.

Speir, J. A., Stevens, J., Joly, E., Butcher, G. W. & Wilson, I. A. (2001) Two Different, Highly Exposed, Bulged Structures for an Unusually Long Peptide Bound to Rat MHC Class I RT1-Aa. *Immunity*. 14 (1), 81-92.

Stadinski, B. D., Trenh, P., Duke, B., Huseby, P. G., Li, G., Stern, L. J. & Huseby, E. S. (2014) Effect of CDR3 Sequences and Distal V Gene Residues in Regulating TCR-MHC Contacts and Ligand Specificity. *The Journal of Immunology*. 192 (12), 6071-6082.

Stadinski, B., Trenh, P., Smith, R., Bautista, B., Huseby, P., Li, G., Stern, L. & Huseby, E. (2011) A Role for Differential Variable Gene Pairing in Creating T Cell Receptors Specific for Unique Major Histocompatibility Ligands. *Immunity*. 35 (5), 694-704.

Stern, L. J., Brown, J. H., Jardetzky, T. S., Gorga, J. C., Urban, R. G., Strominger, J. L. & Wiley, D. C. (1994) Crystal structure of the human class II MHC protein HLA-DR1 complexed with an influenza virus peptide. *Nature*. 368 (6468), 215-221.

Stewart, J. J., Lee, C. Y., Ibrahim, S., Watts, P., Shlomchik, M., Weigert, M. & Litwin, S. (1997) A Shannon entropy analysis of immunoglobulin and T cell receptor. *Molecular Immunology*. 34 (15), 1067-1082.

Stewart-Jones, G., McMichael, A. J., Bell, J. I., Stuart, D. I. & Jones, E. Y. (2003) A structural basis for immunodominant human T cell receptor recognition. *Nature Immunology*. 4 (7), 657-663.

Stockinger, B. (1999) T lymphocyte tolerance: From thymic deletion to peripheral control mechanisms. *Advances in Immunology*. 71 229-265.

Stoller, J. Z. & Epstein, J. A. (2005) Identification of a novel nuclear localization signal in Tbx1 that is deleted in DiGeorge syndrome patients harboring the 1223delC mutation. *Human Molecular Genetics*. 14 (7), 885-892.

Stoltze, L., Schirle, M., Schwarz, G., Schröter, C., Thompson, M. W., Hersh, L. B., Kalbacher, H., Stevanovic, S., Rammensee, H. G. & Schild, H. (2000) Two new proteases in the MHC class I processing pathway. *Nature Immunology*. 1 (5), 413-418.

Štros, M. (2010) HMGB proteins: Interactions with DNA and chromatin. *Biochimica Et Biophysica Acta (BBA) - Gene Regulatory Mechanisms*. 1799 (1–2), 101-113.

Summerhayes, I. C. & Franks, L. M. (1979) Effects of donor age on neoplastic transformation of adult mouse bladder epithelium in vitro. *Journal of the National Cancer Institute*. 62 (4), 1017-1023.

Sun, G., Liu, X., Mercado, P., Jenkinson, S. R., Kyriiotou, M., Feigenbaum, L., Galera, P. & Bosselut, R. (2005) The zinc finger protein cKrox directs CD4 lineage differentiation during intrathymic T cell positive selection. *Nature Immunology*. 6 (4), 373-381.

Sun, Z. - J., Kim, K. S., Wagner, G. & Reinherz, E. L. (2001) Mechanisms contributing to T cell receptor signaling and assembly revealed by the solution structure of an ectodomain fragment of the CD3 ϵ heterodimer. *Cell*. 105 (7), 913-923.

Sun, Z. - J., Sun, T. K., II, C. K., Fahmy, A., Reinherz, E. L. & Wagner, G. (2004) Solution structure of the CD3 ϵ ectodomain and comparison with CD3 ϵ as a basis for modeling T cell receptor topology and signaling. *Proceedings of the National Academy of Sciences of the United States of America*. 101 (48), 16867-16872.

Swanson, P. C. (2004) The bounty of RAGs: recombination signal complexes and reaction outcomes. *Immunological Reviews*. 200 (1), 90-114.

Szymczak, A. L. & Vignali, D. A. A. (2005) Development of 2A peptide-based strategies in the design of multicistronic vectors. *Expert Opinion on Biological Therapy*. 5 (5), 627-638.

Szymczak, A. L., Workman, C. J., Wang, Y., Vignali, K. M., Dilioglou, S., Vanin, E. F. & Vignali, D. A. A. (2004) Correction of multi-gene deficiency in vivo using a single 'self-cleaving' 2A peptide-based retroviral vector. *Nat Biotech*. 22 (5), 589-594.

Tagaya, Y., Maeda, Y., Mitsui, A., Kondo, N., Matsui, H., Hamuro, J., Brown, N., Arai, K., Yokota, T. & Wakasugi, H. (1989) ATL-derived factor (ADF), an IL-2 receptor/Tac inducer homologous to thioredoxin; possible involvement of dithiol-reduction in the IL-2 receptor induction. *The EMBO Journal*. 8 (3), 757-764.

Tai, X., Cowan, M., Feigenbaum, L. & Singer, A. (2005) CD28 costimulation of developing thymocytes induces Foxp3 expression and regulatory T cell differentiation independently of interleukin 2. *Nature Immunology*. 6 (2), 152-162.

Tan, M. P., Gerry, A. B., Brewer, J. E., Melchiori, L., Bridgeman, J. S., Bennett, A. D., Pumphrey, N. J., Jakobsen, B. K., Price, D. A., Ladell, K. & Sewell, A. K. (2015) T cell receptor binding affinity governs the functional profile of cancer-specific CD8+ T cells. *Clinical & Experimental Immunology*. 180 (2), 255-270.

Taniuchi, I. (2009) Transcriptional regulation in helper versus cytotoxic-lineage decision. *Current Opinion in Immunology*. 21 (2), 127-132.

Taniuchi, I., Osato, M., Egawa, T., Sunshine, M. J., Bae, S., Komori, T., Ito, Y. & Littman, D. R. (2002) Differential Requirements for Runx Proteins in CD4 Repression and Epigenetic Silencing during T Lymphocyte Development. *Cell*. 111 (5), 621-633.

- Theodossis, A., Guillonneau, C., Welland, A., Ely, L. K., Clements, C. S., Williamson, N. A., Webb, A. I., Wilce, J. A., Mulder, R. J., Dunstone, M. A., Doherty, P. C., McCluskey, J., Purcell, A. W., Turner, S. J. & Rossjohn, J. (2010) Constraints within major histocompatibility complex class I restricted peptides: Presentation and consequences for T-cell recognition. *Proceedings of the National Academy of Sciences*. 107 (12), 5534-5539.
- Tikhonova, A., Van Laethem, F., Hanada, K., Lu, J., Pobezinsky, L., Hong, C., Ginter, T., Jeurling, S., Bernhardt, G., Park, J., Yang, J., Sun, P. & Singer, A. (2012) $\alpha\beta$ T Cell Receptors that Do Not Undergo Major Histocompatibility Complex-Specific Thymic Selection Possess Antibody-like Recognition Specificities. *Immunity*. 36 (1), 79-91.
- Tonegawa, S. (1983) Somatic generation of antibody diversity. *Nature*. 302 (5909), 575-581.
- Touma, M., Chang, H. C., Sasada, T., Handley, M., Clayton, L. K. & Reinherz, E. L. (2006) The TCR C β FG loop regulates $\alpha\beta$ T cell development. *Journal of Immunology*. 176 (11), 6812-6823.
- Trapani, J. A. & Smyth, M. J. (2002) Functional significance of the perforin/granzyme cell death pathway. *Nat Rev Immunol*. 2 (10), 735-747.
- Treiner, E. & Lantz, O. (2006) CD1d- and MR1-restricted invariant T cells: of mice and men. *Current Opinion in Immunology*. 18 (5), 519-526.
- Trombetta, E. S. & Mellman, I. (2005) CELL BIOLOGY OF ANTIGEN PROCESSING IN VITRO AND IN VIVO. *Annual Review of Immunology*. 23 (1), 975-1028.
- Trop, S., Rhodes, M., Wiest, D. L., Hugo, P. & Zúñiga-Pflücker, J. C. (2000) Competitive Displacement of pTa by TCR- α During TCR Assembly Prevents Surface Coexpression of Pre-TCR and $\alpha\beta$ TCR. *The Journal of Immunology*. 165 (10), 5566-5572.
- Turner, S. J., Doherty, P. C., McCluskey, J. & Rossjohn, J. (2006) Structural determinants of T-cell receptor bias in immunity. *Nat Rev Immunol*. 6 (12), 883-894.
- Tynan, F. E., Borg, N. A., Miles, J. J., Beddoe, T., El-Hassen, D., Silins, S. L., van Zuylen, W. J. M., Purcell, A. W., Kjer-Nielsen, L., McCluskey, J., Burrows, S. R. & Rossjohn, J. (2005a) High Resolution Structures of Highly Bulged Viral Epitopes Bound to Major Histocompatibility Complex Class I: IMPLICATIONS FOR T-CELL RECEPTOR ENGAGEMENT AND T-CELL IMMUNODOMINANCE. *Journal of Biological Chemistry*. 280 (25), 23900-23909.
- Tynan, F. E., Burrows, S. R., Buckle, A. M., Clements, C. S., Borg, N. A., Miles, J. J., Beddoe, T., Whisstock, J. C., Wilce, M. C., Silins, S. L., Burrows, J. M., Kjer-Nielsen, L., Kostenko, L., Purcell, A. W., McCluskey, J. & Rossjohn, J. (2005b) T cell receptor recognition of a 'super-bulged' major histocompatibility complex class I-bound peptide. *Nature Immunology*. 6 (11), 1114-1122.
- Ueno, H., Banchereau, J. & Vinuesa, C. G. (2015) Pathophysiology of T follicular helper cells in humans and mice. *Nature Immunology*. 16 (2), 142-152.
- Valujskikh, A., Lantz, O., Celli, S., Matzinger, P. & Heeger, P. S. (2002) Cross-primed CD8⁺ T cells mediate graft rejection via a distinct effector pathway. *Nature Immunology*. 3 (9), 844-851.
- van den Berg, H. A., Wooldridge, L., Laugel, B. & Sewell, A. K. (2007) Coreceptor CD8-driven modulation of T cell antigen receptor specificity. *Journal of Theoretical Biology*. 249 (2), 395-408.

- Van Laethem, F., Sarafova, S. D., Park, J., Tai, X., Pobezinsky, L., Guinter, T., Adoro, S., Adams, A., Sharrow, S. O., Feigenbaum, L. & Singer, A. (2007) Deletion of CD4 and CD8 Coreceptors Permits Generation of $\alpha\beta$ T Cells that Recognize Antigens Independently of the MHC. *Immunity*. 27 (5), 735-750.
- Van Laethem, F., Tikhonova, A. N. & Singer, A. (2012) MHC restriction is imposed on a diverse TCR repertoire by CD4 and CD8 coreceptors during thymic selection. *Trends in Immunology*. 33 (9), 437-441.
- van Meerwijk, J.P.M., Marguerat, S., Lees, R. K., Germain, R. N., Fowlkes, B. J. & MacDonald, H. R. (1997) Quantitative Impact of Thymic Clonal Deletion on the T Cell Repertoire. *The Journal of Experimental Medicine*. 185 (3), 377-384.
- Vang, K. B., Yang, J., Mahmud, S. A., Burchill, M. A., Vegoe, A. L. & Farrar, M. A. (2008) IL-2, -7, and -15, but Not Thymic Stromal Lymphopoietin, Redundantly Govern CD4+Foxp3+ Regulatory T Cell Development. *The Journal of Immunology*. 181 (5), 3285-3290.
- Vantourout, P. & Hayday, A. (2013) Six-of-the-best: unique contributions of $\gamma\delta$ T cells to immunology. *Nat Rev Immunol*. 13 (2), 88-100.
- Veillette, A., Bookman, M. A., Horak, E. M. & Bolen, J. B. (1988) The CD4 and CD8 T cell surface antigens are associated with the internal membrane tyrosine-protein kinase p56lck. *Cell*. 55 (2), 301-308.
- Venturi, V., Kedzierska, K., Price, D. A., Doherty, P. C., Douek, D. C., Turner, S. J. & Davenport, M. P. (2006) Sharing of T cell receptors in antigen-specific responses is driven by convergent recombination. *Proceedings of the National Academy of Sciences*. 103 (49), 18691-18696.
- Voll, R. E., Jimi, E., Phillips, R. J., Barber, D. F., Rincon, M., Hayday, A. C., Flavell, R. A. & Ghosh, S. (2000) NF- κ B Activation by the Pre-T Cell Receptor Serves as a Selective Survival Signal in T Lymphocyte Development. *Immunity*. 13 (5), 677-689.
- von Boehmer, H. (2005) Unique features of the pre-T-cell receptor α -chain: not just a surrogate. *Nat Rev Immunol*. 5 (7), 571-577.
- von Boehmer, H. & Melchers, F. (2010) Checkpoints in lymphocyte development and autoimmune disease. *Nature Immunology*. 11 (1), 14-20.
- Walker, J. R., Corpina, R. A. & Goldberg, J. (2001) Structure of the Ku heterodimer bound to DNA and its implications for double-strand break repair. *Nature*. 412 (6847), 607-614.
- Walker, J. M. & Slifka, M. K. (2010) Longevity of T-Cell Memory following Acute Viral Infection. In: Zanetti, M. & Schoenberger, S. P. (eds.). *Memory T Cells*. New York, NY, Springer New York. pp. 96-107.
- Wang, Y., Ray, S. C., Laeyendecker, O., Ticehurst, J. R. & Thomas, D. L. (1998) Assessment of Hepatitis C Virus Sequence Complexity by Electrophoretic Mobilities of Both Single- and Double-Stranded DNAs. *Journal of Clinical Microbiology*. 36 (10), 2982-2989.
- Wang, Z., Song, J., Taichman, R. S. & Krebsbach, P. H. (2006) Ablation of Proliferating Marrow with 5-Fluorouracil Allows Partial Purification of Mesenchymal Stem Cells. *Stem Cells*. 24 (6), 1573-1582.

- Warren, R. L., Freeman, J. D., Zeng, T., Choe, G., Munro, S., Moore, R., Webb, J. R. & Holt, R. A. (2011) Exhaustive T-cell repertoire sequencing of human peripheral blood samples reveals signatures of antigen selection and a directly measured repertoire size of at least 1 million clonotypes. *Genome Research*. 21 (5), 790-797.
- Weber, K. S., Donermeyer, D. L., Allen, P. M. & Kranz, D. M. (2005) Class II-restricted T cell receptor engineered in vitro for higher affinity retains peptide specificity and function. *Proceedings of the National Academy of Sciences of the United States of America*. 102 (52), 19033-19038.
- Weiss, A. & Littman, D. R. (1994) Signal transduction by lymphocyte antigen receptors. *Cell*. 76 (2), 263-274.
- Welsh, R. M., Che, J., Brehm, M. A. & Selin, L. K. (2010) HETEROLOGOUS IMMUNITY BETWEEN VIRUSES. *Immunological Reviews*. 235 (1), 244-266.
- Welsh, R. M. & Selin, L. K. (2002) No one is naive: the significance of heterologous T-cell immunity. *Nat Rev Immunol*. 2 (6), 417-426.
- Werlen, G., Hausmann, B. & Palmer, E. (2000) A motif in the $\alpha\beta$ T-cell receptor controls positive selection by modulating ERK activity. *Nature*. 406 (6794), 422-426.
- Wilson, A., Maréchal, C. & MacDonald, H. R. (2001) Biased V β Usage in Immature Thymocytes Is Independent of DJ β Proximity and pTa Pairing. *The Journal of Immunology*. 166 (1), 51-57.
- Witte, T., Spoerl, R. & Chang, H. -. (1999) The CD8 β ectodomain contributes to the augmented coreceptor function of CD8 $\alpha\beta$ heterodimers relative to CD8 $\alpha\alpha$ homodimers. *Cellular Immunology*. 191 (2), 90-96.
- Wlodarski, M. W., O'Keefe, C., Howe, E. C., Risitano, A. M., Rodriguez, A., Warshawsky, I., Loughran, T. P. & Maciejewski, J. P. (2005) Pathologic clonal cytotoxic T-cell responses: nonrandom nature of the T-cell receptor restriction in large granular lymphocyte leukemia. *Blood*. 106 (8), 2769-2780.
- Wolfer, A., Wilson, A., Nemir, M., MacDonald, H. R. & Radtke, F. (2002) Inactivation of Notch1 Impairs VDJ β Rearrangement and Allows pre-TCR-Independent Survival of Early $\alpha\beta$ Lineage Thymocytes. *Immunity*. 16 (6), 869-879.
- Wong, G. W., Knowles, G. C., Mak, T. W., Ferrando, A. A. & Zúñiga-Pflücker, J. C. (2012) HES1 opposes a PTEN-dependent check on survival, differentiation, and proliferation of TCR β -selected mouse thymocytes. *Blood*. 120 (7), 1439-1448.
- Wooldridge, L. (2013) Individual MHCI-Restricted T-Cell Receptors are Characterized by a Unique Peptide Recognition Signature. *Frontiers in Immunology*. 4199.
- Wooldridge, L., Ekeruche-Makinde, J., van den Berg, H. A., Skowera, A., Miles, J. J., Tan, M. P., Dolton, G., Clement, M., Llewellyn-Lacey, S., Price, D. A., Peakman, M. & Sewell, A. K. (2012) A Single Autoimmune T Cell Receptor Recognizes More Than a Million Different Peptides. *Journal of Biological Chemistry*. 287 (2), 1168-1177.
- Wooldridge, L., van den Berg, H. A., Glick, M., Gostick, E., Laugel, B., Hutchinson, S. L., Milicic, A., Brenchley, J. M., Douek, D. C., Price, D. A. & Sewell, A. K. (2005) Interaction between the CD8

Coreceptor and Major Histocompatibility Complex Class I Stabilizes T Cell Receptor-Antigen Complexes at the Cell Surface. *Journal of Biological Chemistry*. 280 (30), 27491-27501.

Wouters, M. A., Lau, K. K. & Hogg, P. J. (2004) Cross-strand disulphides in cell entry proteins: poised to act. *BioEssays*. 26 (1), 73-79.

Wu, L. C., Tuot, D. S., Lyons, D. S., Garcia, K. C. & Davis, M. M. (2002) Two-step binding mechanism for T-cell receptor recognition of peptide-MHC. *Nature*. 418 (6897), 552-556.

Wucherpennig, K. W., Gagnon, E., Call, M. J., Huseby, E. S. & Call, M. E. (2010) Structural Biology of the T-cell Receptor: Insights into Receptor Assembly, Ligand Recognition, and Initiation of Signaling. *Cold Spring Harbor Perspectives in Biology*. 2 (4), a005140.

Wucherpennig, K. W. & Sethi, D. (2011) T cell receptor recognition of self and foreign antigens in the induction of autoimmunity. *Seminars in Immunology*. 23 (2), 84-91.

Wyman, C. & Kanaar, R. (2006) DNA Double-Strand Break Repair: All's Well that Ends Well. *Annual Review of Genetics*. 40 (1), 363-383.

Wynn, T. A. (2015) Type 2 cytokines: mechanisms and therapeutic strategies. *Nat Rev Immunol*. 15 (5), 271-282.

Xing, Y. & Hogquist, K. A. (2012) T-Cell Tolerance: Central and Peripheral. *Cold Spring Harbor Perspectives in Biology*. 4 (6), .

Yagi, H., Furutani, Y., Hamada, H., Sasaki, T., Asakawa, S., Minoshima, S., Ichida, F., Joo, K., Kimura, M., Imamura, S., Kamatani, N., Momma, K., Takao, A., Nakazawa, M., Shimizu, N. & Matsuoka, R. (2003) Role of *TBX1* in human del22q11.2 syndrome. *The Lancet*. 362 (9393), 1366-1373.

Yamasaki, S., Ishikawa, E., Sakuma, M., Ogata, K., Sakata-Sogawa, K., Hiroshima, M., Wiest, D. L., Tokunaga, M. & Saito, T. (2006) Mechanistic basis of pre-T cell receptor-mediated autonomous signaling critical for thymocyte development. *Nature Immunology*. 7 (1), 67-75.

Yancopoulos, G. D. & Alt, F. W. (1985) Developmentally controlled and tissue-specific expression of unrearranged VH gene segments. *Cell*. 40 (2), 271-281.

Yano, K., Morotomi-Yano, K., Wang, S., Uematsu, N., Lee, K., Asaithamby, A., Weterings, E. & Chen, D. J. (2007) Ku recruits XLF to DNA double-strand breaks. *EMBO Reports*. 9 (1), 91-96.

Yao, S., Zhu, Y., Zhu, G., Augustine, M., Zheng, L., Goode, D., Broadwater, M., Ruff, W., Flies, S., Xu, H., Flies, D., Luo, L., Wang, S. & Chen, L. (2011) B7-H2 Is a Costimulatory Ligand for CD28 in Human. *Immunity*. 34 (5), 729-740.

Yasutomo, K., Doyle, C., Miele, L. & Germain, R. N. (2000) The duration of antigen receptor signalling determines CD4+ versus CD8+ T-cell lineage fate. *Nature*. 404 (6777), 506-510.

Yin, L., Huseby, E., Scott-Browne, J., Rubtsova, K., Pinilla, C., Crawford, F., Marrack, P., Dai, S. & Kappler, J. (2011) A Single T Cell Receptor Bound to Major Histocompatibility Complex Class I and Class II Glycoproteins Reveals Switchable TCR Conformers. *Immunity*. 35 (1), 23-33.

- Yin, Y. & Mariuzza, R. A. (2009) The Multiple Mechanisms of T Cell Receptor Cross-reactivity. *Immunity*. 31 (6), 849-851.
- Yin, Y., Wang, X. X. & Mariuzza, R. A. (2012) Crystal structure of a complete ternary complex of T-cell receptor, peptide-MHC, and CD4. *Proceedings of the National Academy of Sciences of the United States of America*. 109 (14), 5405-5410.
- Yoo, S. & Dynan, W. S. (1999) Geometry of a complex formed by double strand break repair proteins at a single DNA end: Recruitment of DNA-PKcs induces inward translocation of Ku protein. *Nucleic Acids Research*. 27 (24), 4679-4686.
- Zarin, P., Wong, G. W., Mohtashami, M., Wiest, D. L. & Zúñiga-Pflücker, J. C. (2014) Enforcement of $\gamma\delta$ -lineage commitment by the pre-T-cell receptor in precursors with weak $\gamma\delta$ -TCR signals. *Proceedings of the National Academy of Sciences*. 111 (15), 5658-5663.
- Zerrahn, J., Held, W. & Raulet, D. H. (1997) The MHC Reactivity of the T Cell Repertoire Prior to Positive and Negative Selection. *Cell*. 88 (5), 627-636.
- Zhang, J. & Sapp, C. M. (1999) Recombination between Two Identical Sequences within the Same Retroviral RNA Molecule. *Journal of Virology*. 73 (7), 5912-5917.
- Zhao, Y., Bennett, A. D., Zheng, Z., Wang, Q. J., Robbins, P. F., Yu, L. Y. L., Li, Y., Molloy, P. E., Dunn, S. M., Jakobsen, B. K., Rosenberg, S. A. & Morgan, R. A. (2007) High-Affinity TCRs Generated by Phage Display Provide CD4+ T Cells with the Ability to Recognize and Kill Tumor Cell Lines. *The Journal of Immunology*. 179 (9), 5845-5854.
- Ziegler, S. F. (2006) FOXP3: Of Mice and Men. *Annual Review of Immunology*. 24 (1), 209-226.